New differential cross section measurements in the Higgs sector

Sagar Addepalli

Brandeis University | sagar@brandeis.edu

SLAC Fundamental Physics Directorate Seminar

14th September, 2023

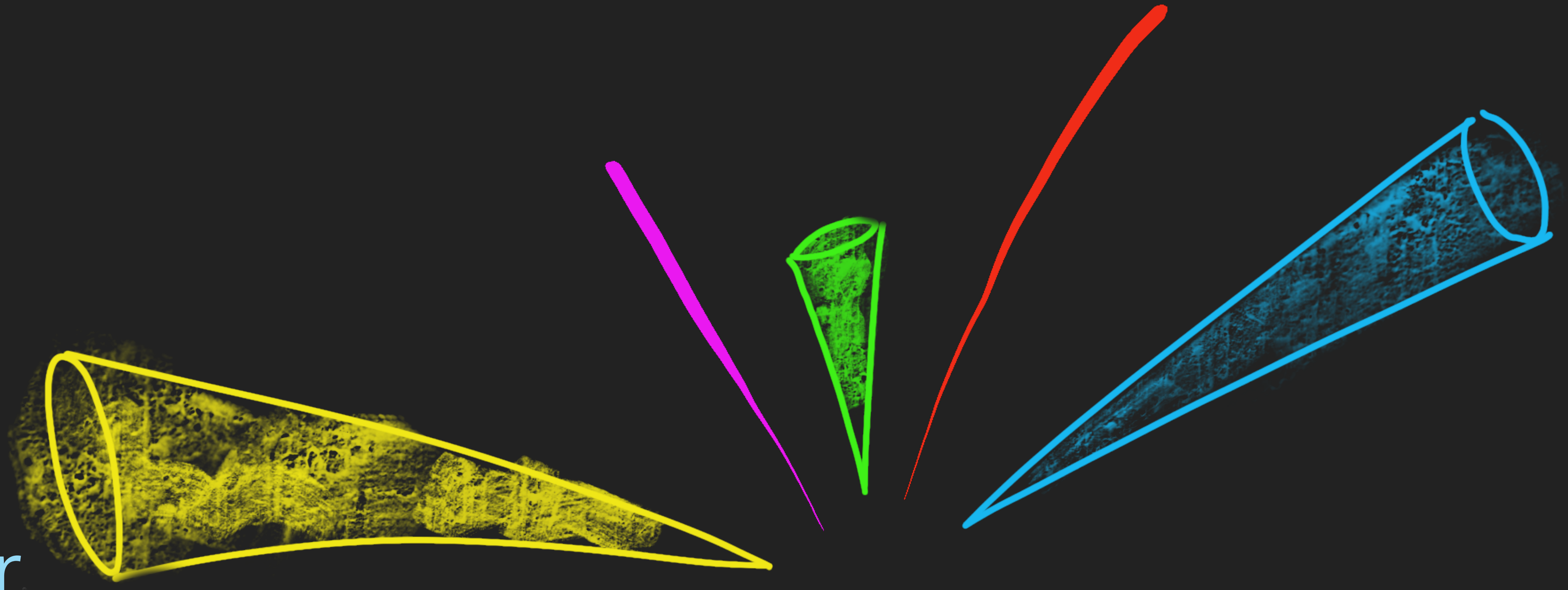

Joined Brandeis in August 2019 as a post-bac stationed at Brookhaven National Lab
Continuing as a PhD student (supervisor Gabriella Sciolla); expected graduation early 2024

Physics Analysis

Joined the effort to measure VBF H→WW cross-section
lead student towards completion (today's talk!)

Search for Heavy Neutral Leptons
(PhD thesis, not in today's talk)

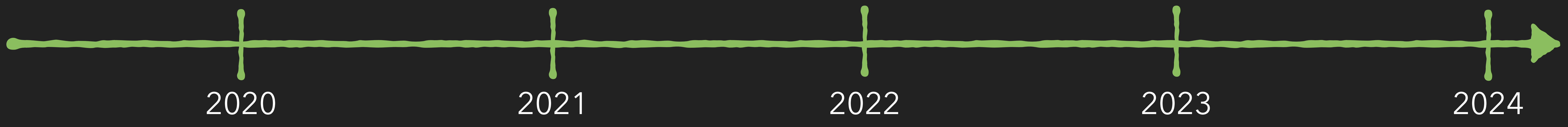

Detector hardware and Performance

ATLAS Inner Tracker upgrade at BNL
Detector assembly and testing

Muon Performance for displaced muons
Leading the activity for ATLAS

Cross Section measurements in the Higgs sector

- Introduction: Why do we do them?
- Strategy: How do we do them?
- Optimization: How well can we do them?
- Results and Interpretation: What do we learn from them?
- Future Projections: How good can we get at them?

Teaser: First fully fiducial measurement in the Vector Boson Fusion H→WW→$e\nu\mu\nu$ channel!

The Standard Model

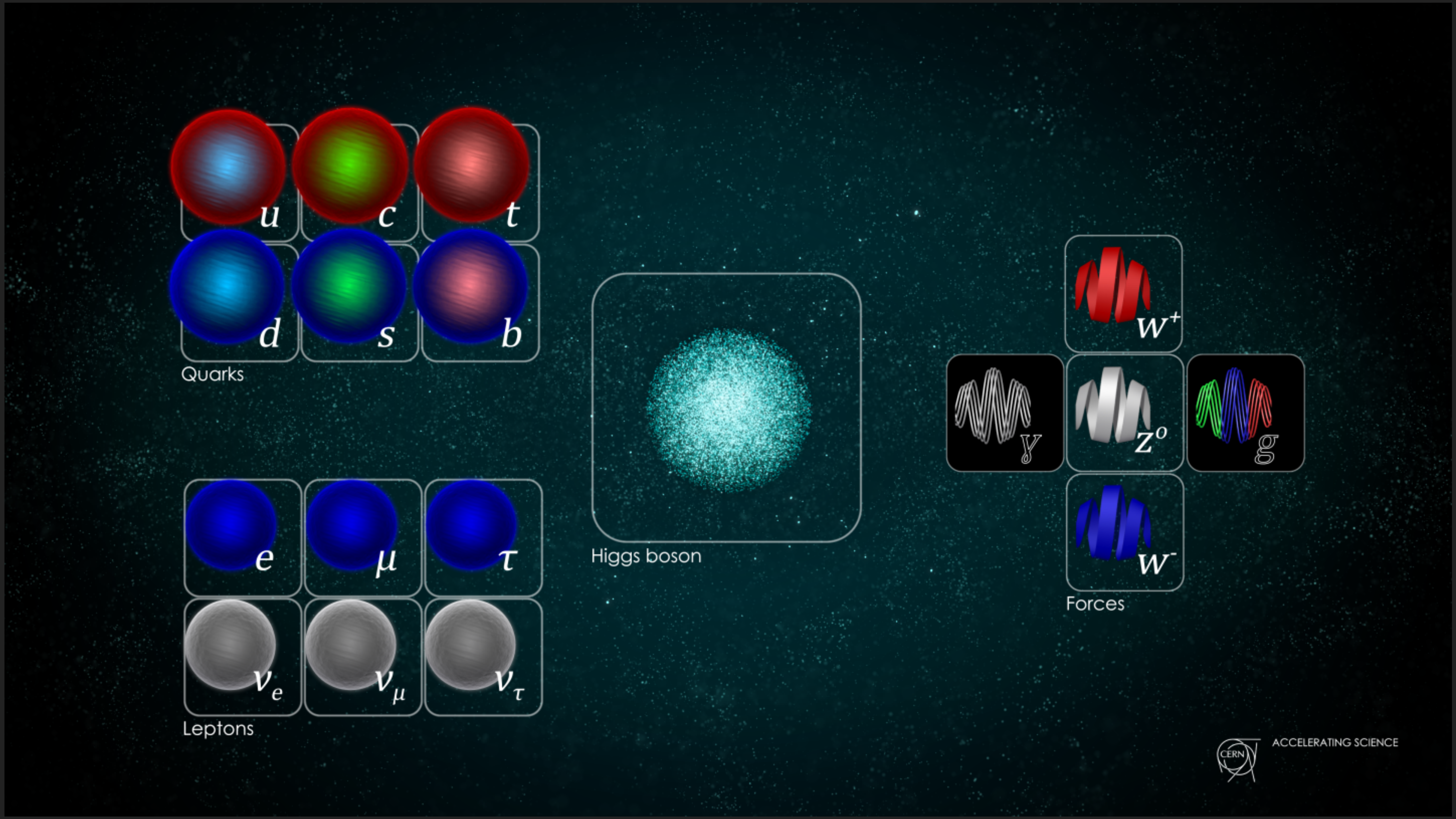

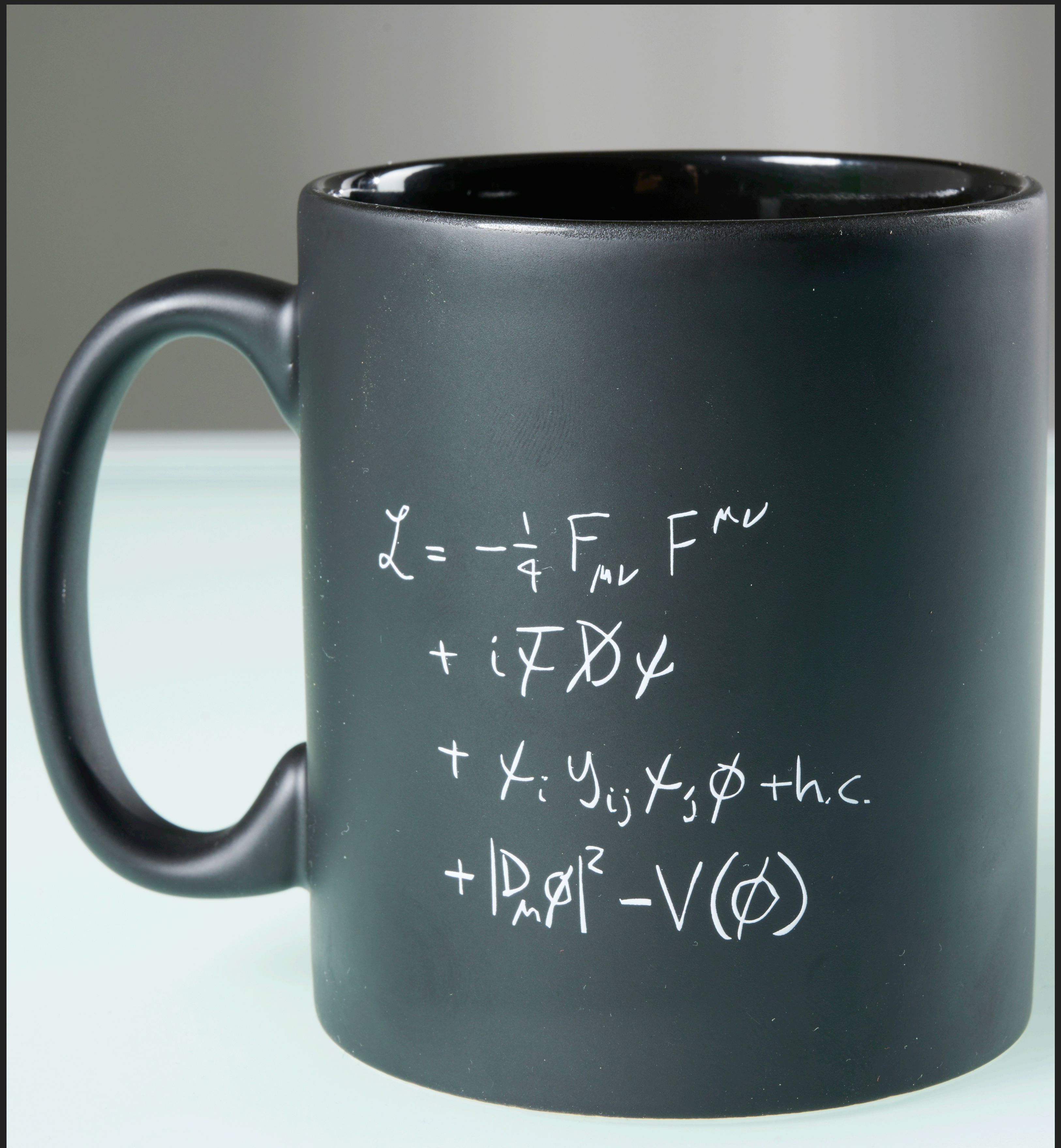

The Standard Model

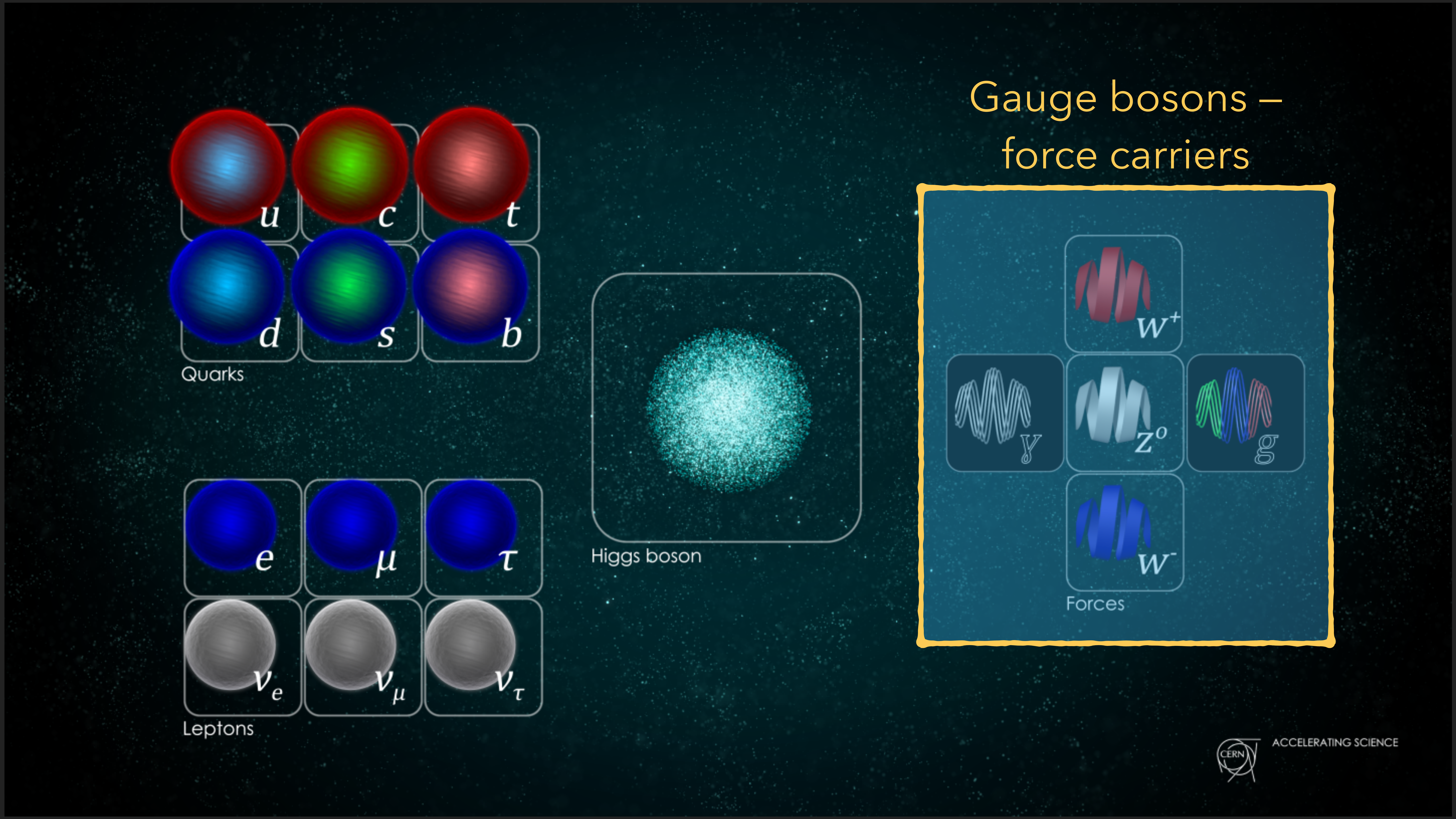

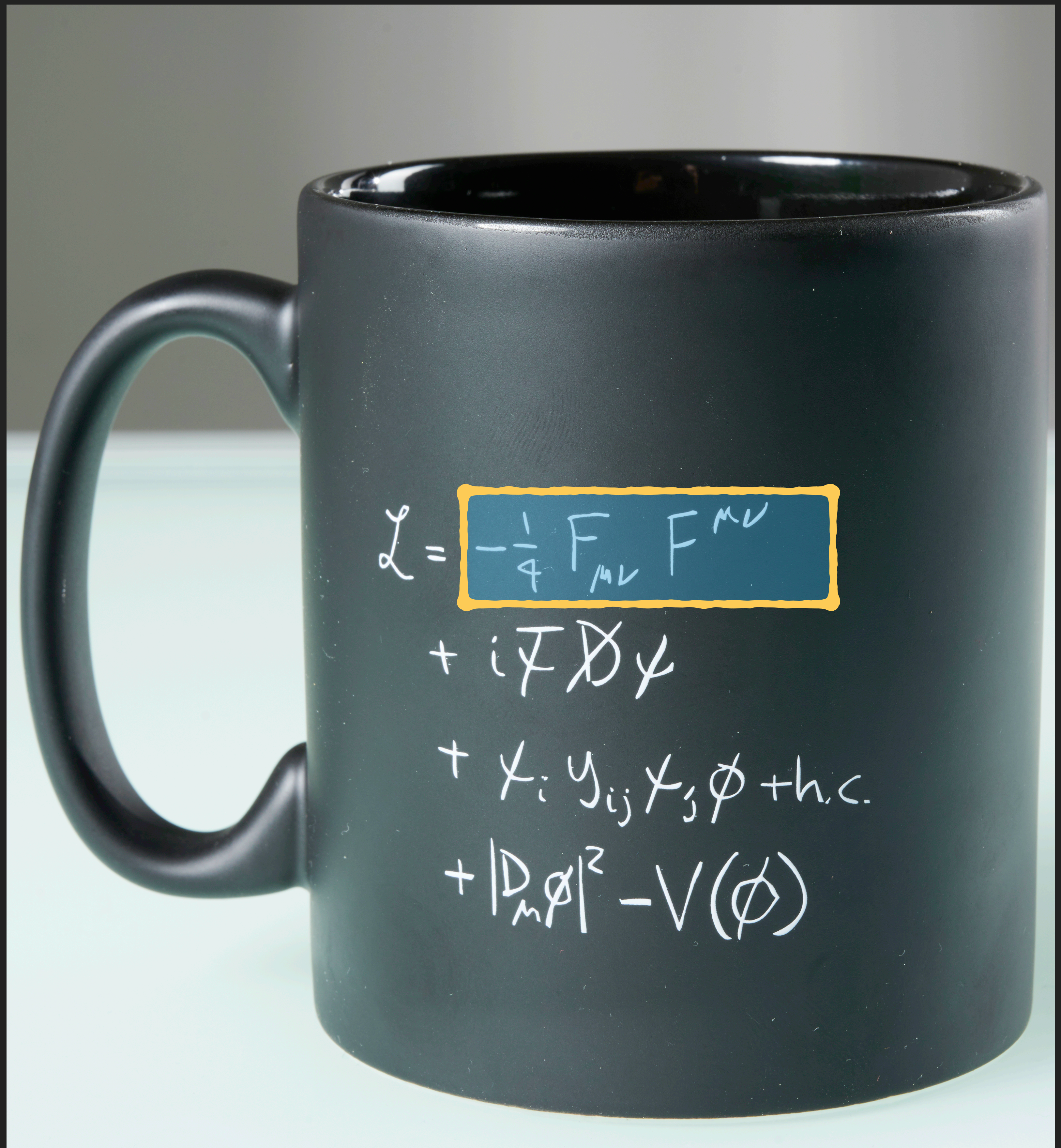

The Standard Model

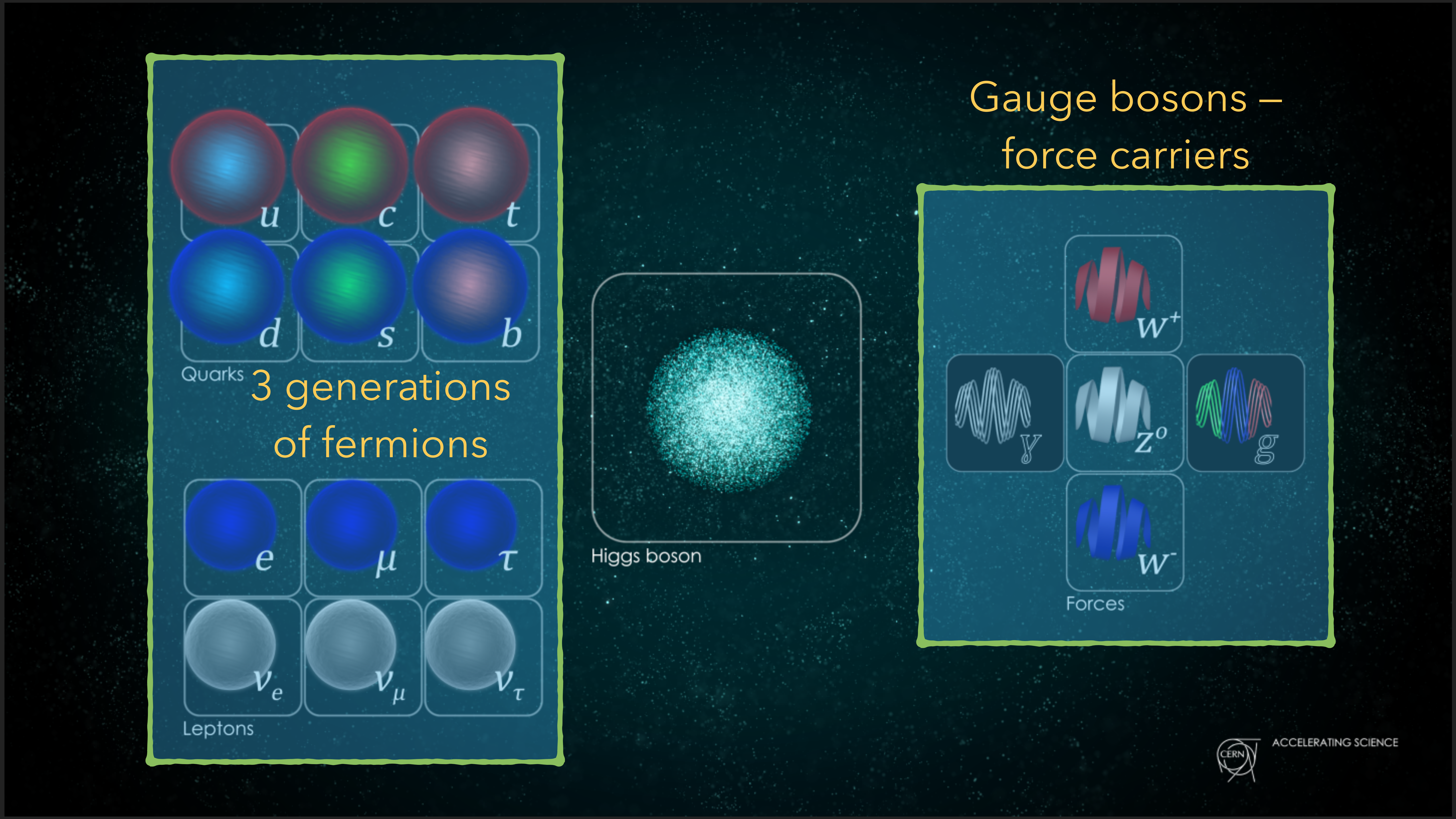

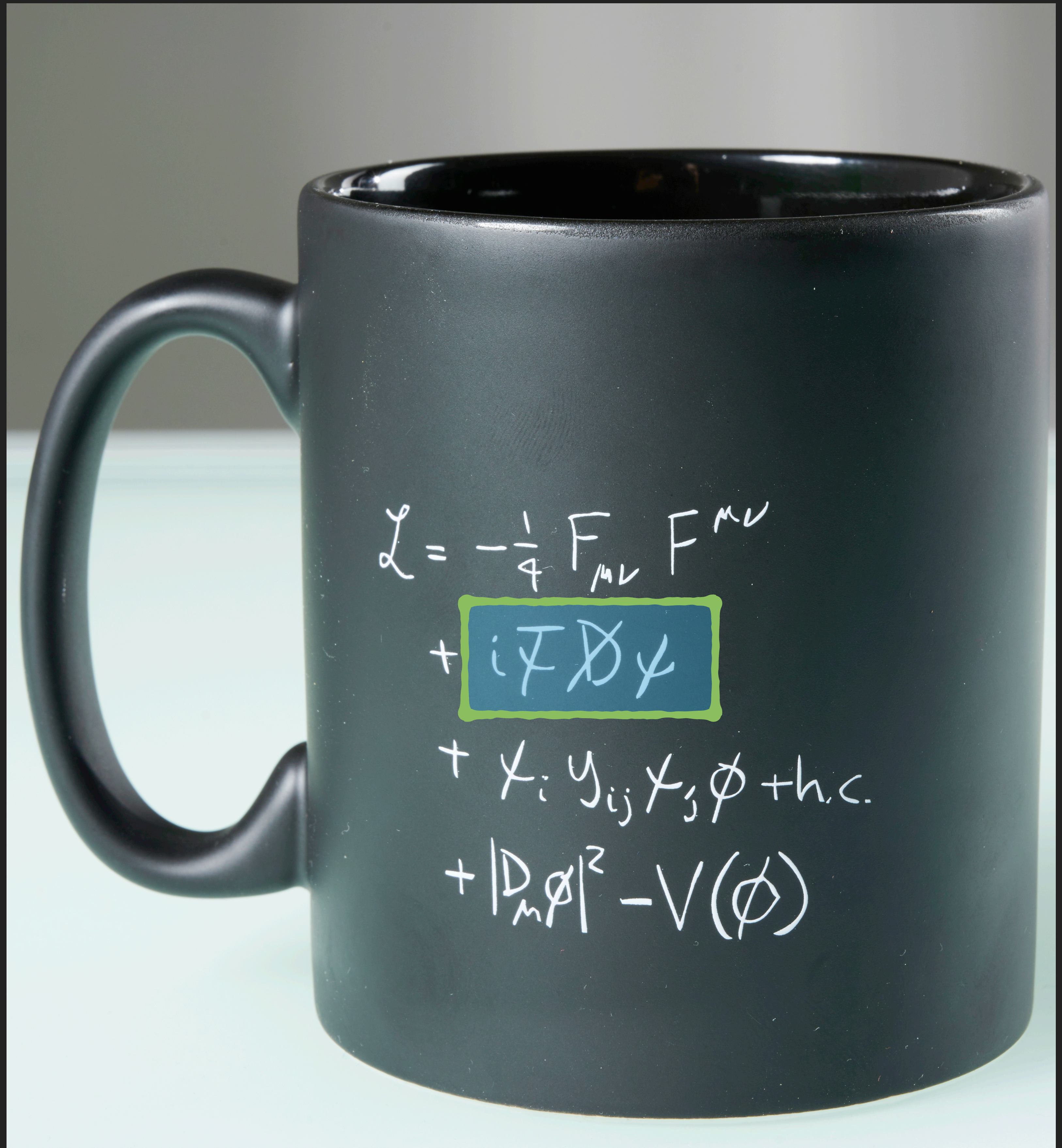

The Standard Model

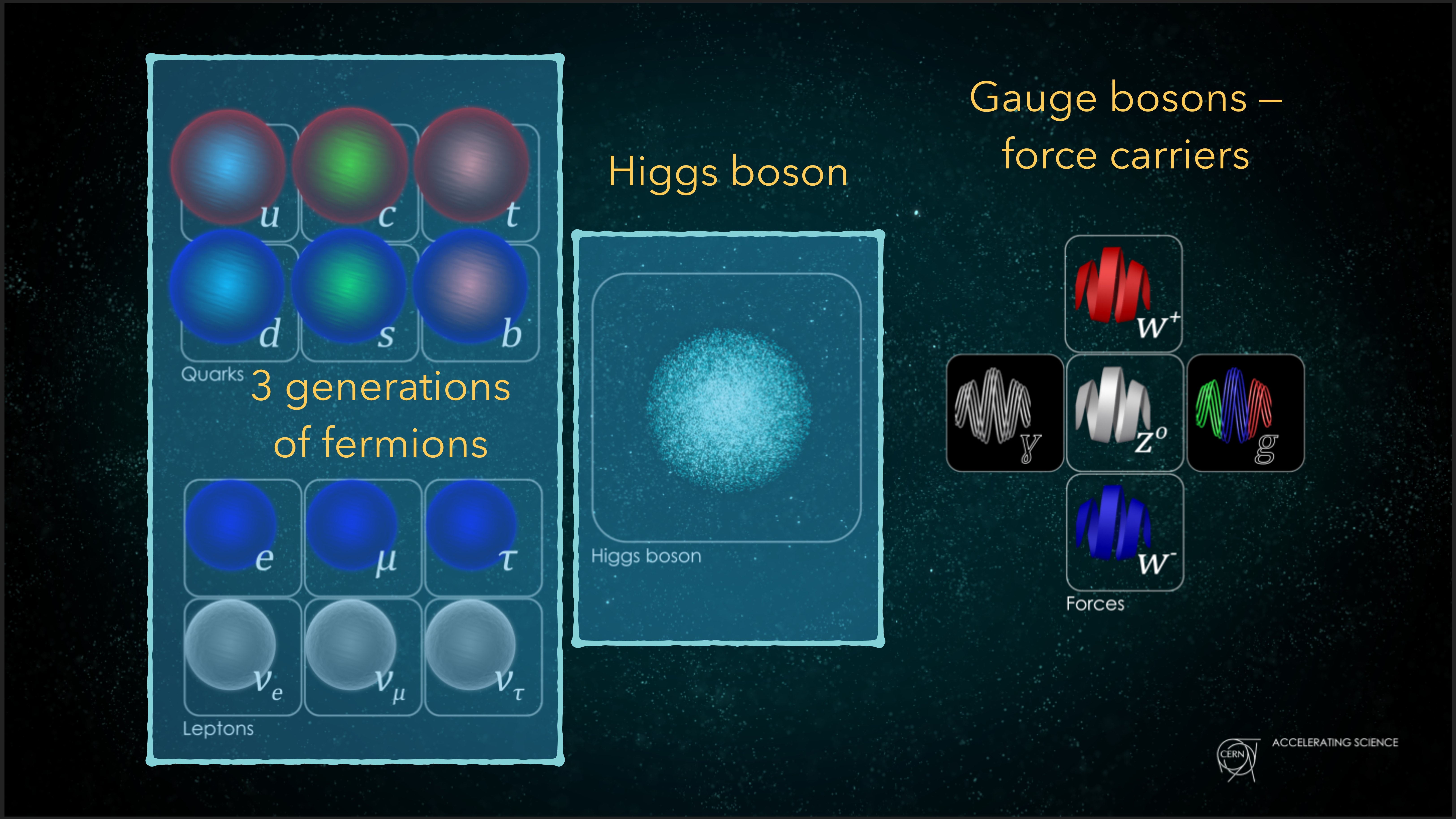

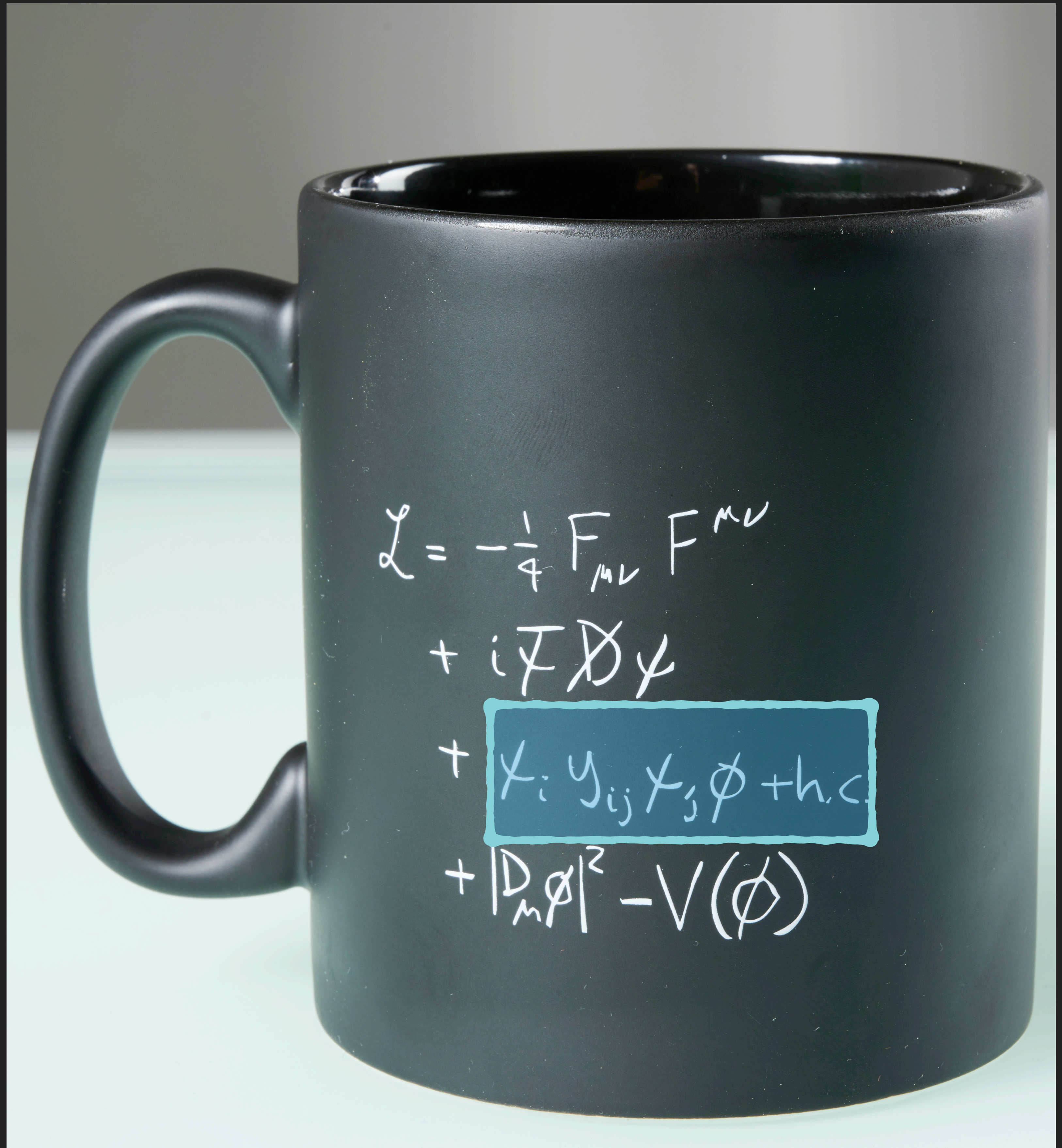

The Standard Model

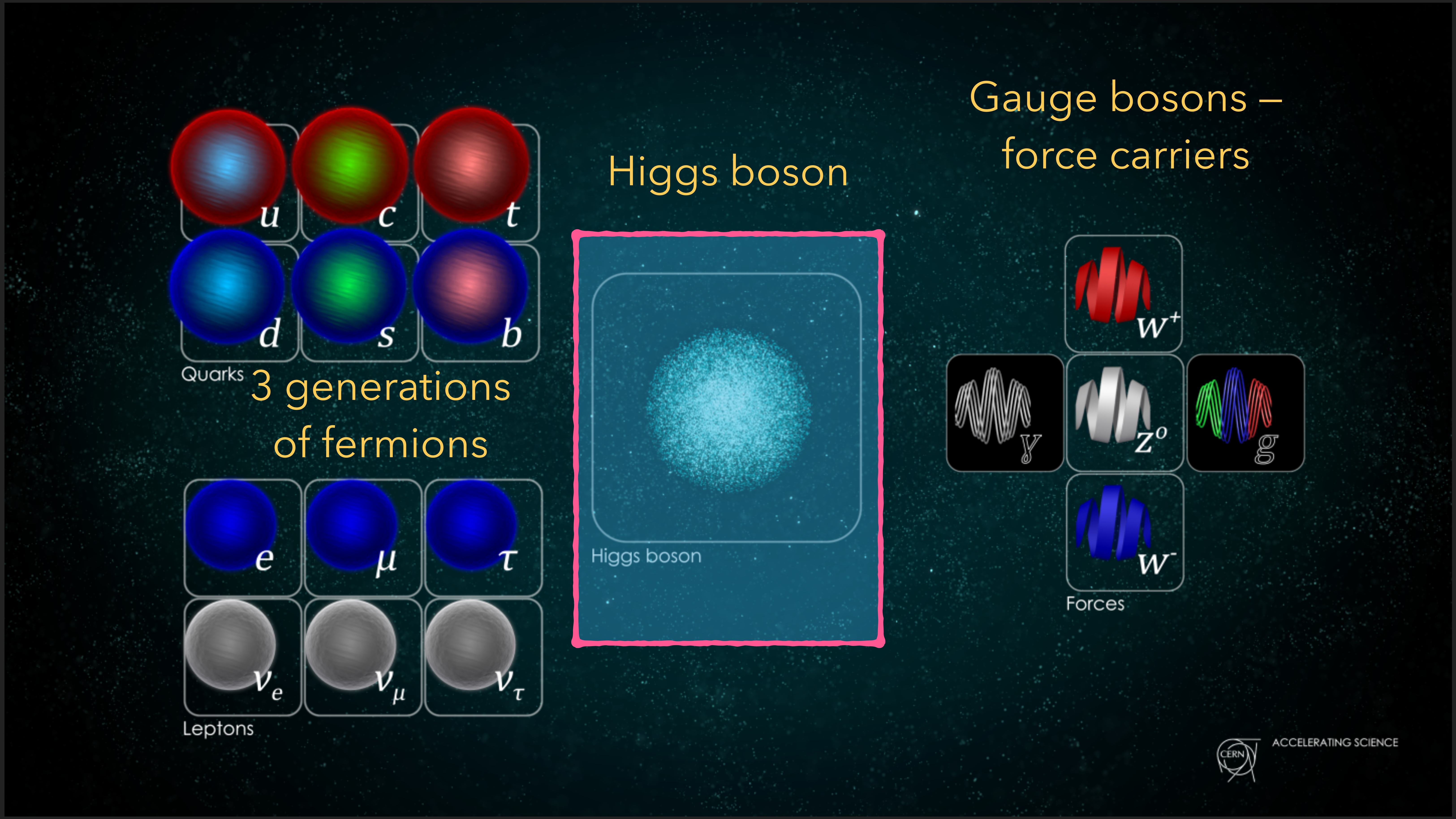

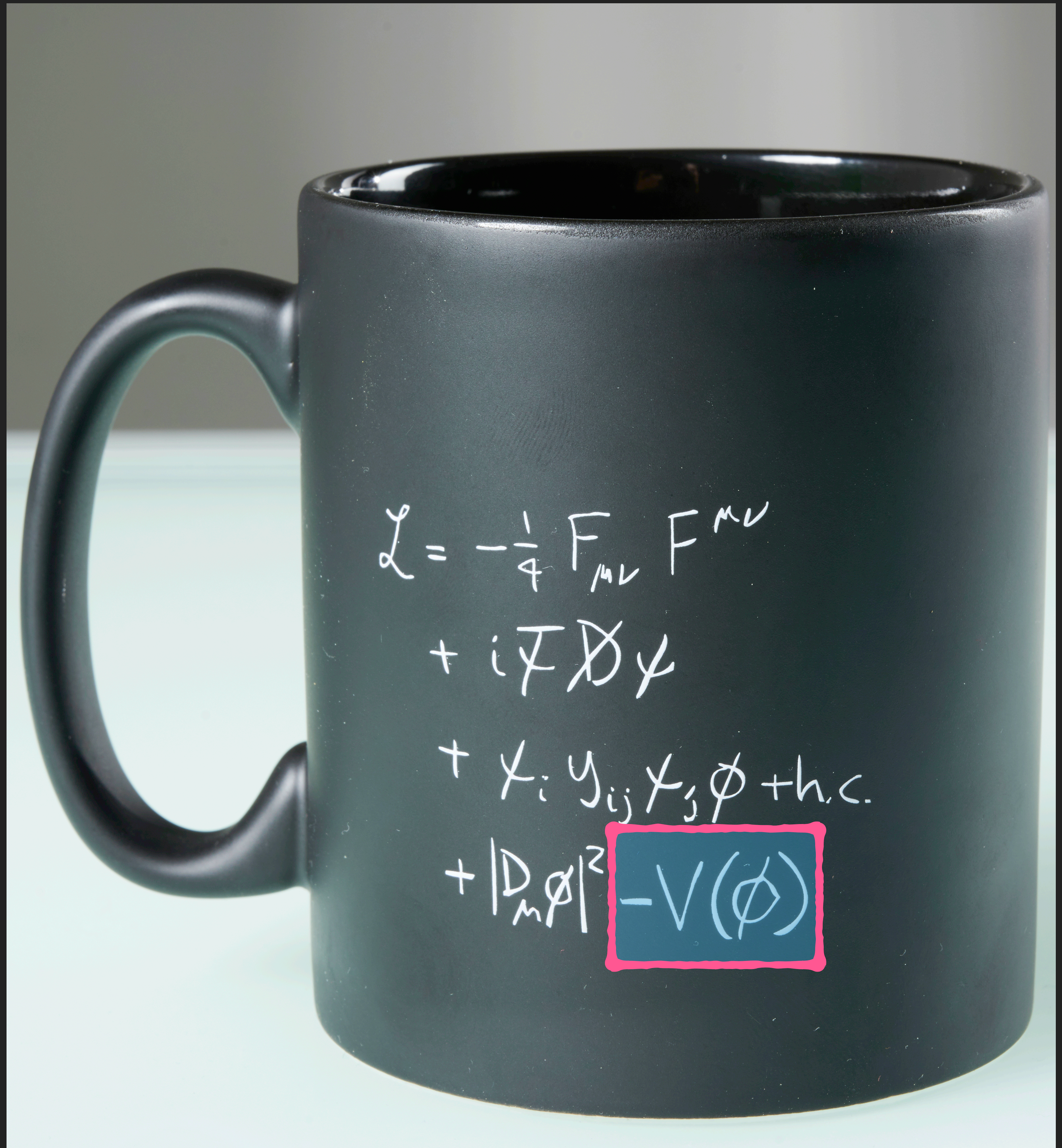

The Standard Model

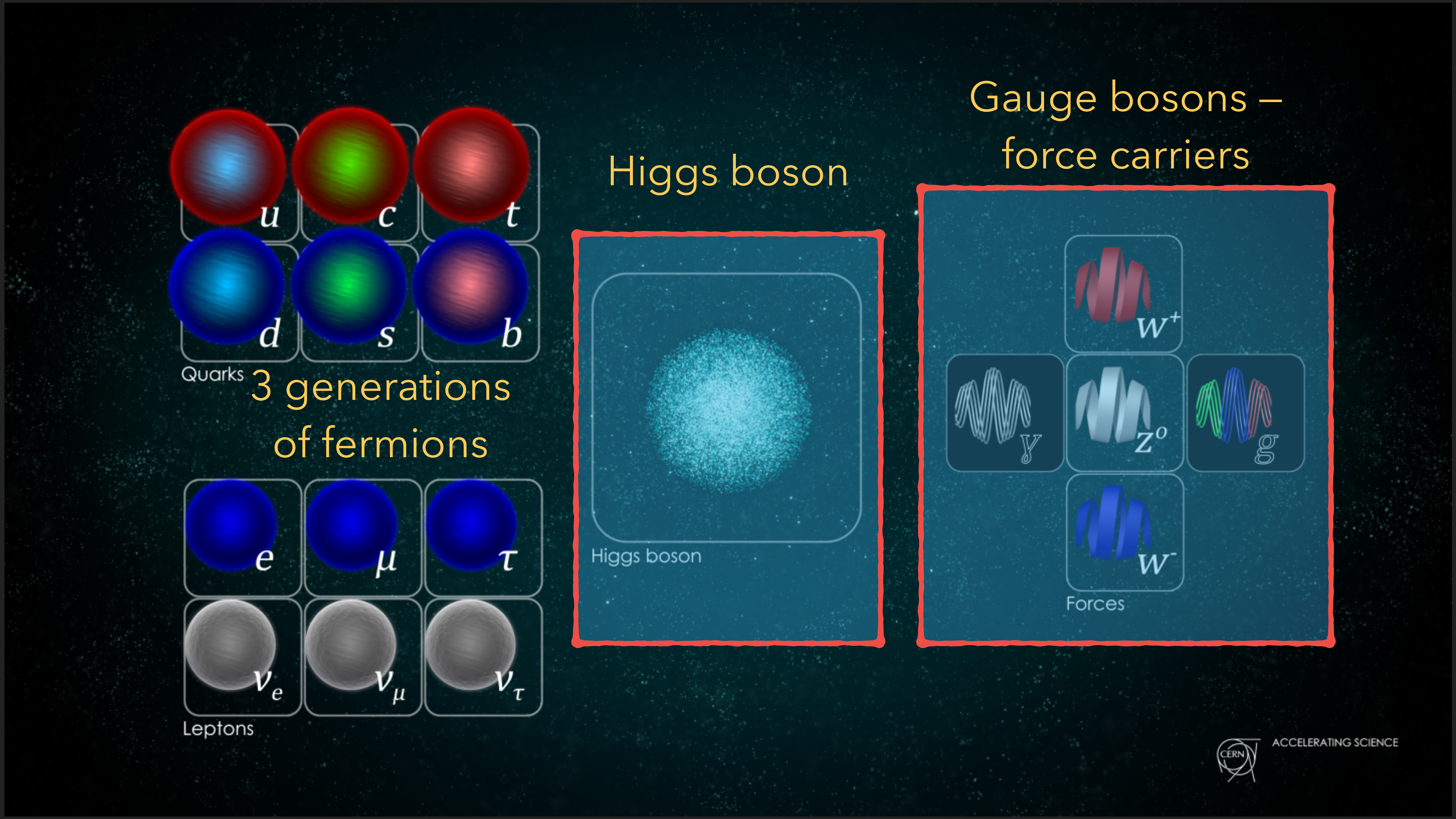

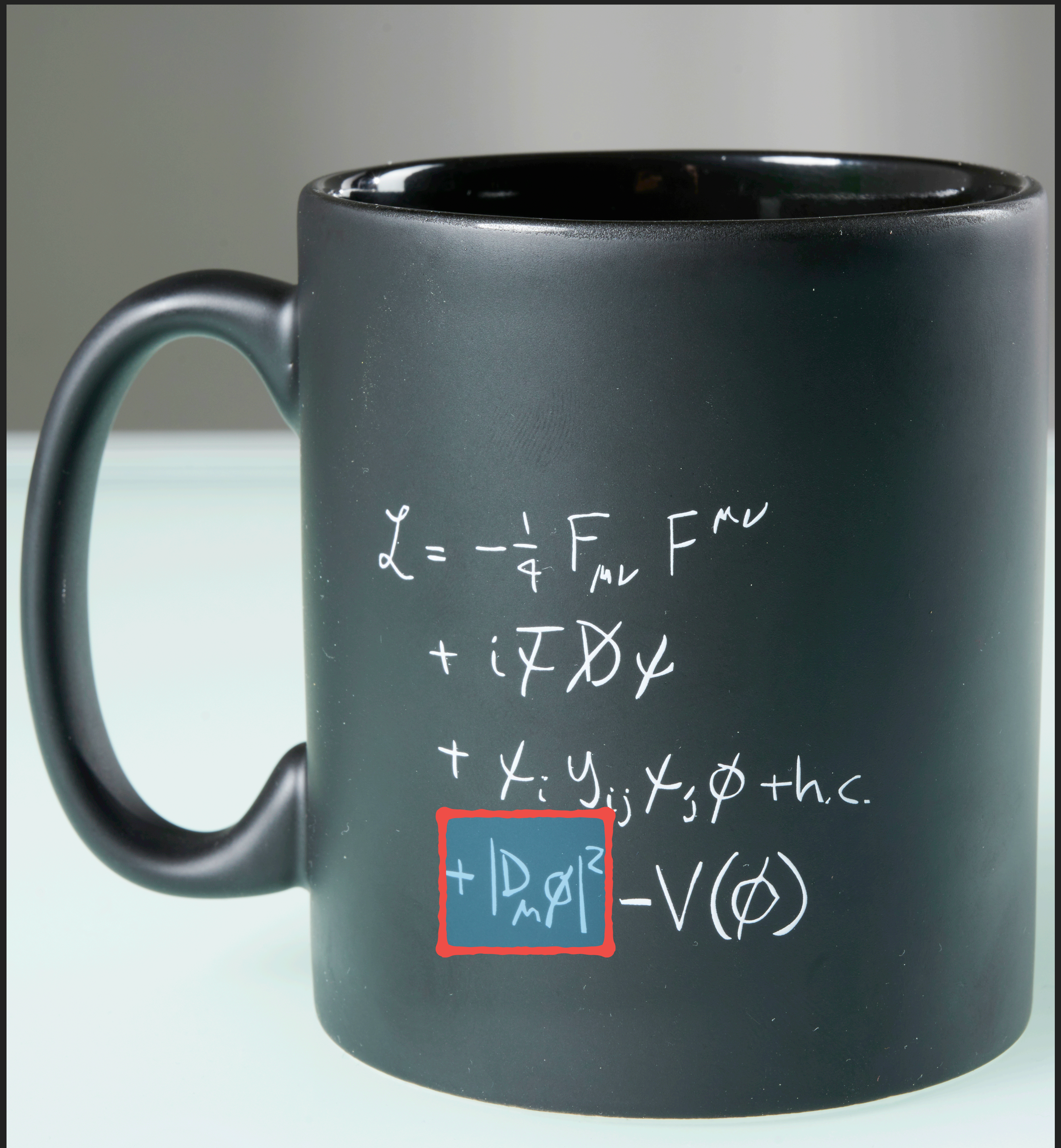

The Standard Model

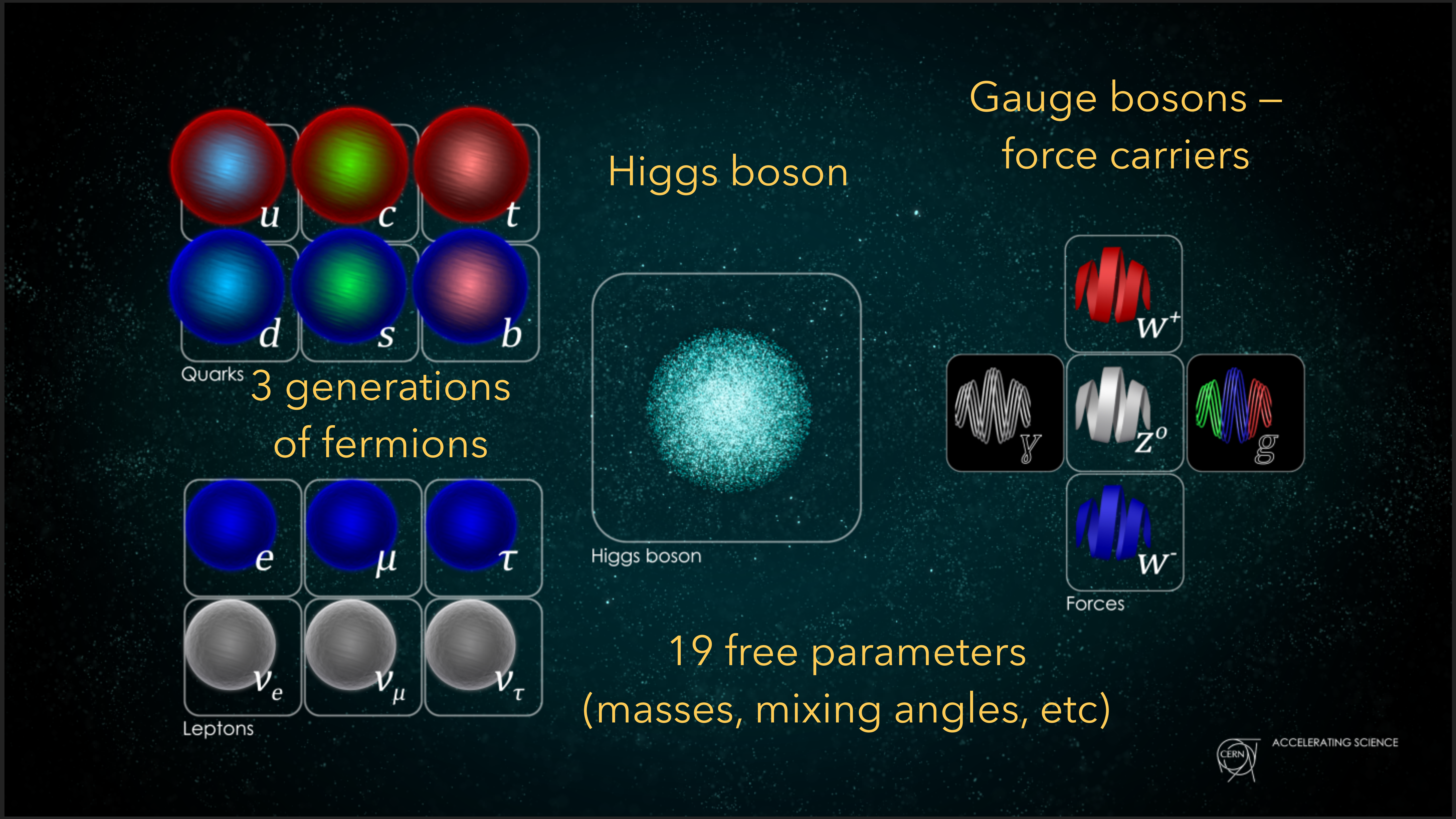

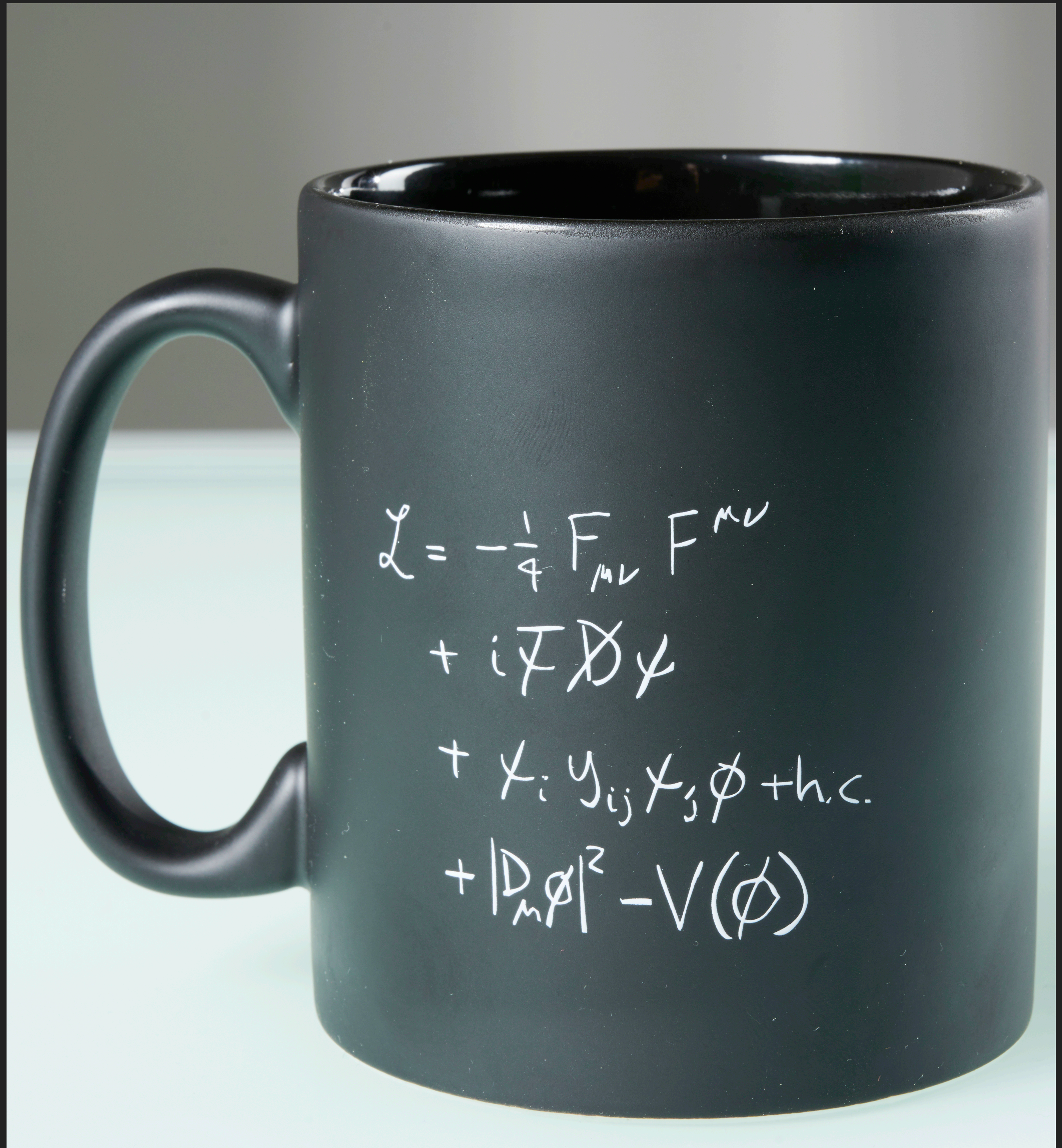

Current model of particle physics

The Standard Model

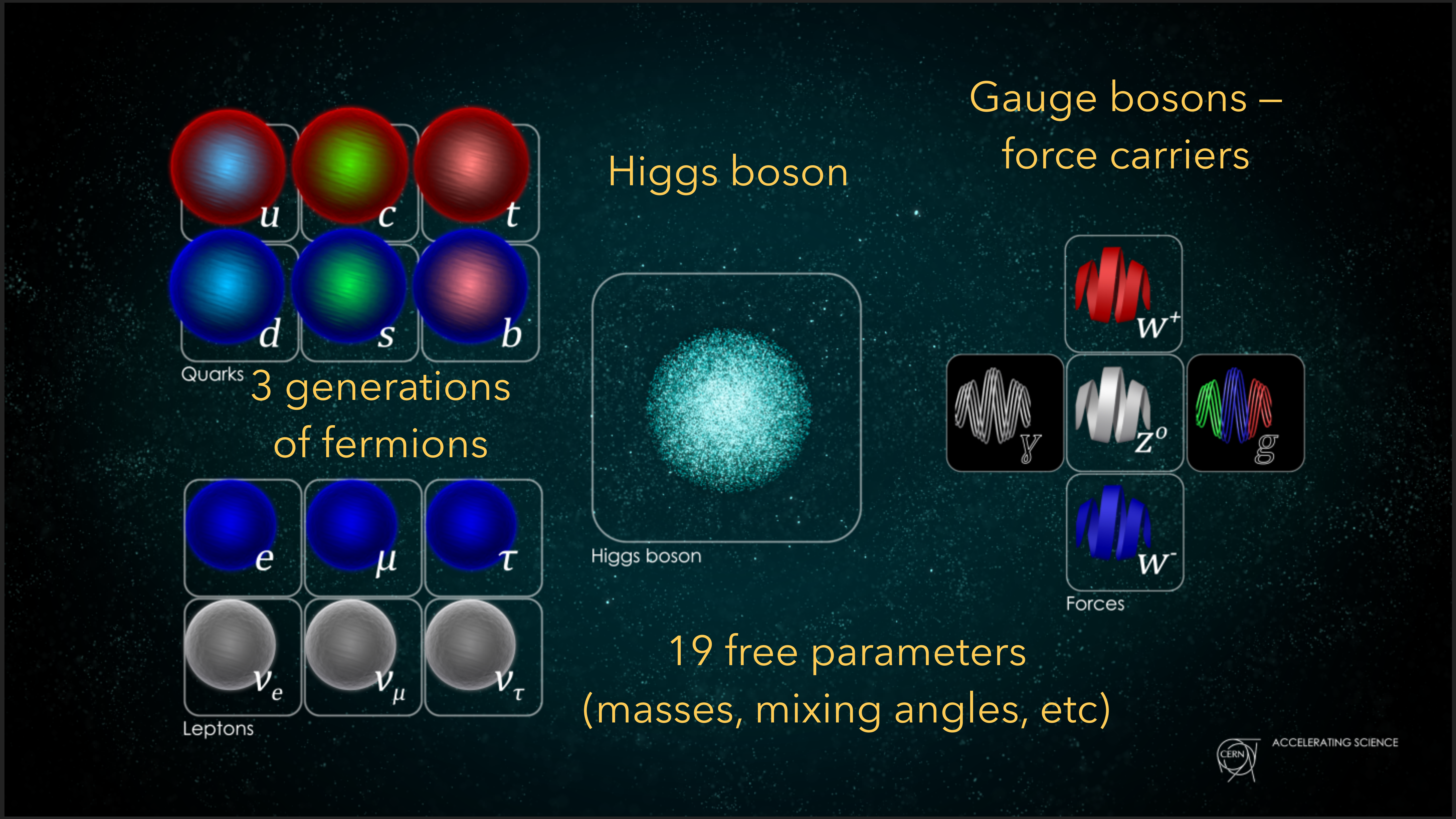

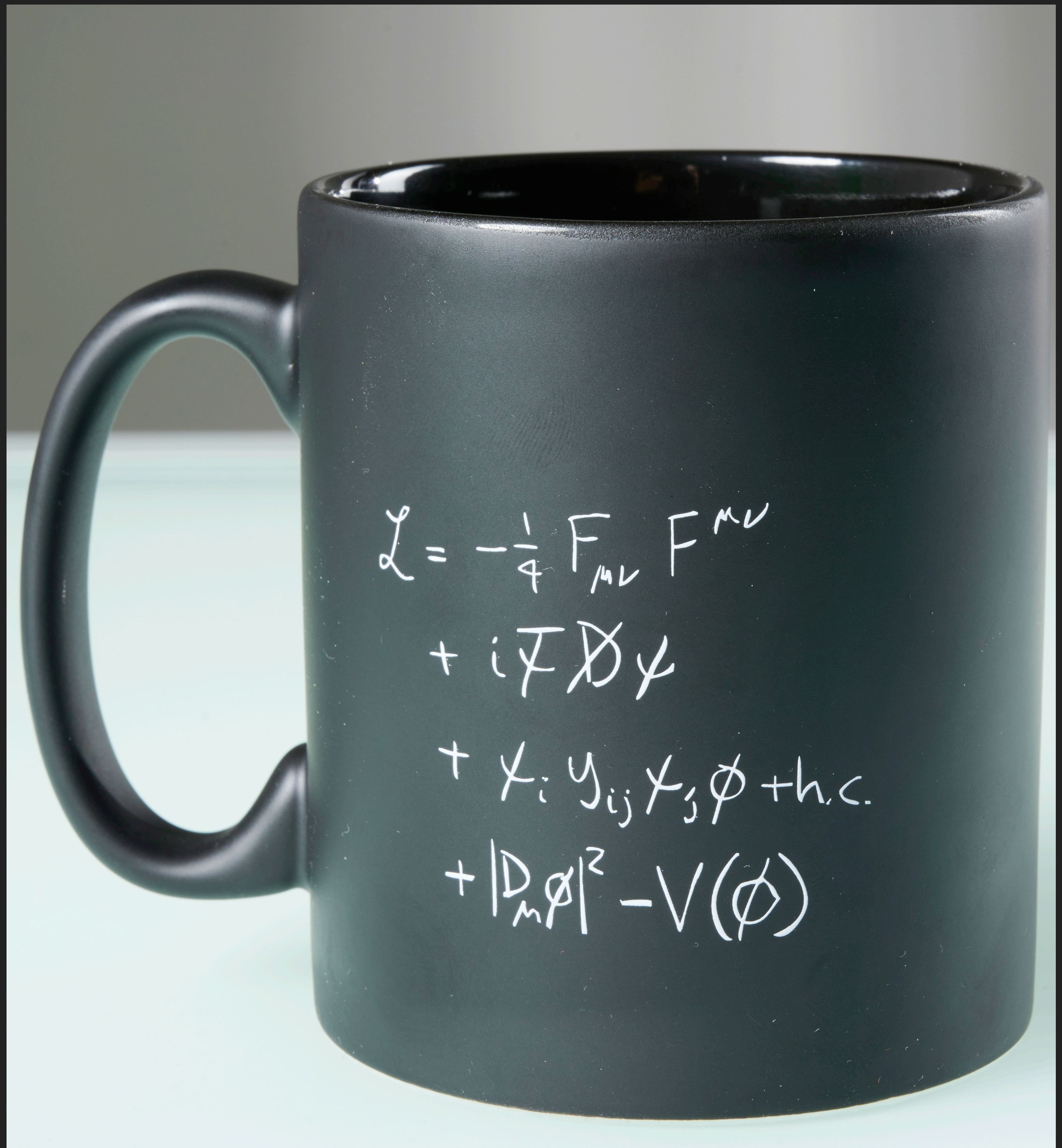

Current model of particle physics
Albeit incomplete…

Open Problems

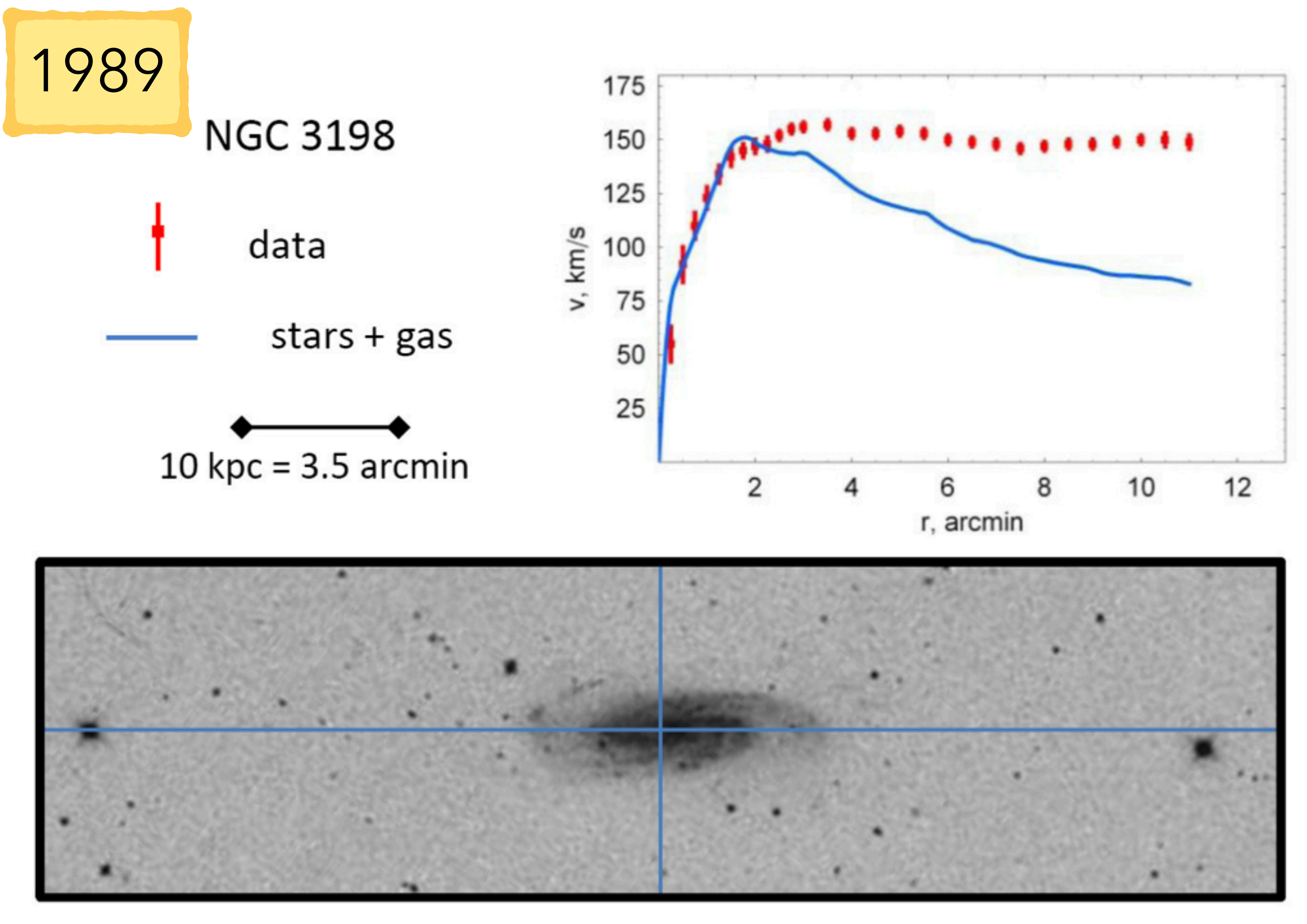

Begeman K G Astron. Astrophys. 223 47

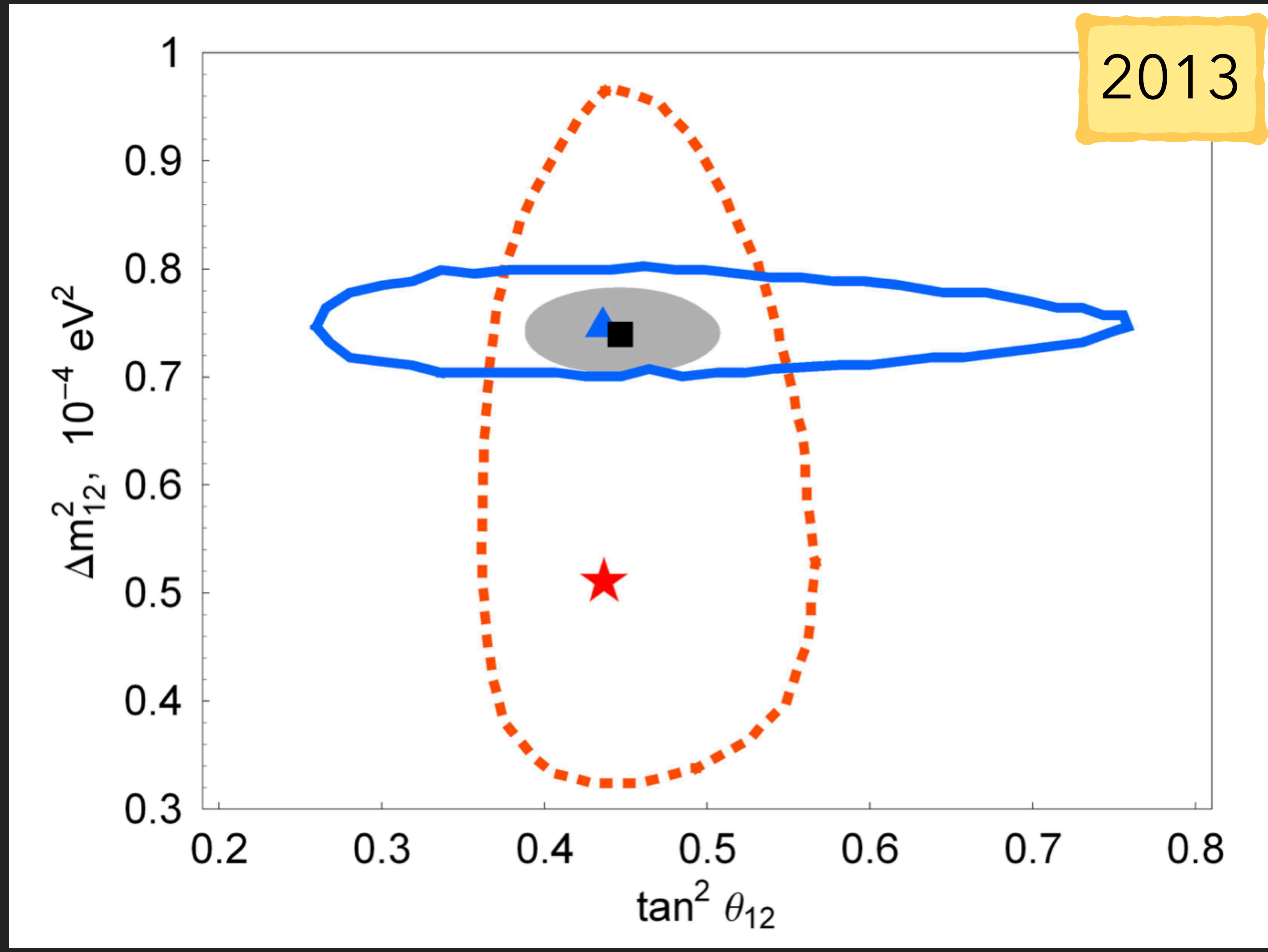

SNO Collaboration: Phys. Rev. C 88, 025501

Rotation curves of galaxies ⇒ dark matter

What is the nature of DM?

ν oscillations ⇒ ν have mass

What is the origin of ν mass?

Physicists try to tackle specific problems in two ways

- direct searches of their favourite particles in certain models
- **precision measurements** of Standard Model phenomena

Precision Measurements

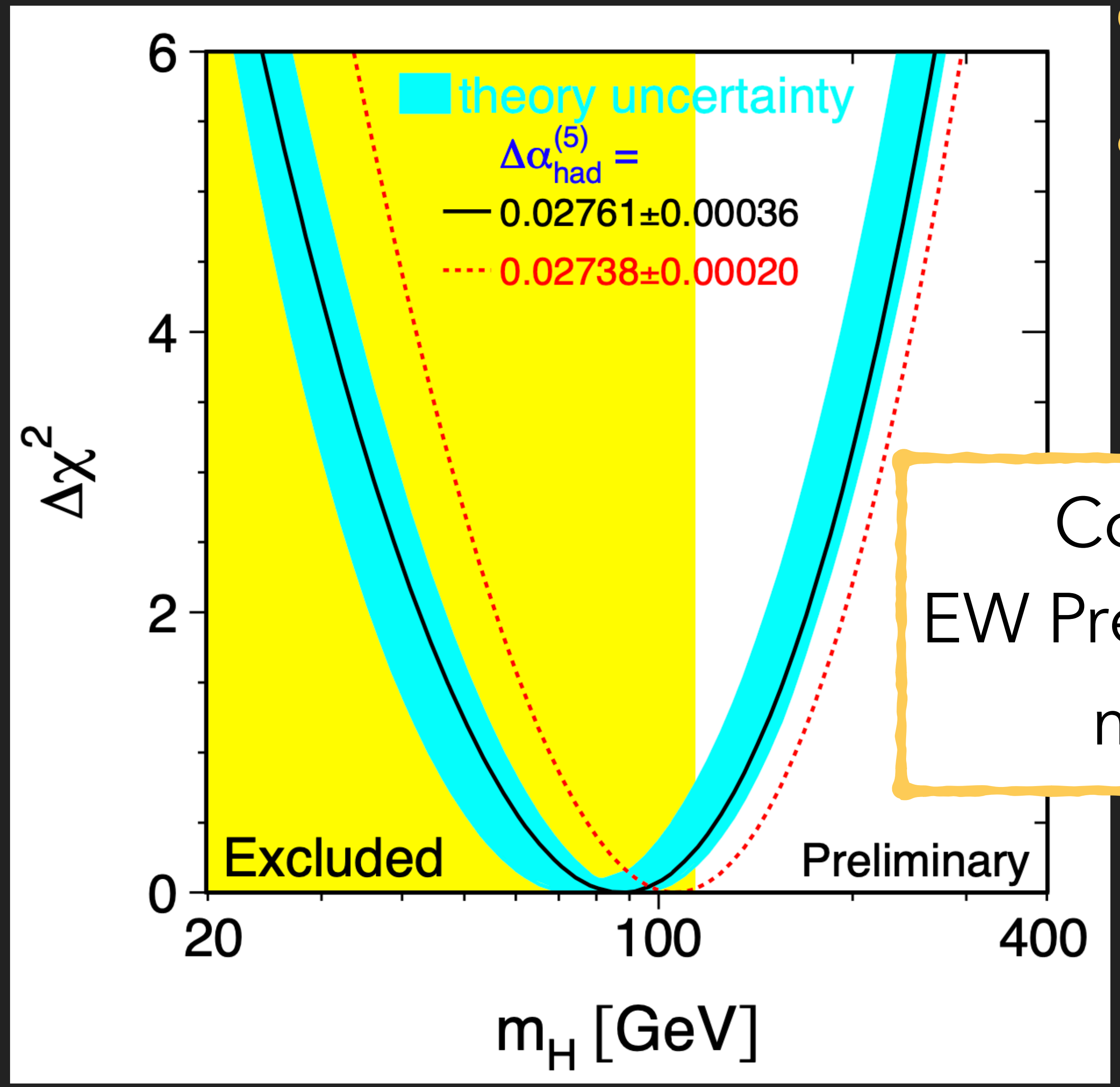

2002

Combination of LEP EW Precision measurements
$m(H) = 81^{+52}_{-33}$ GeV

LEP Collab.: arXiv:hep-ex/0112021

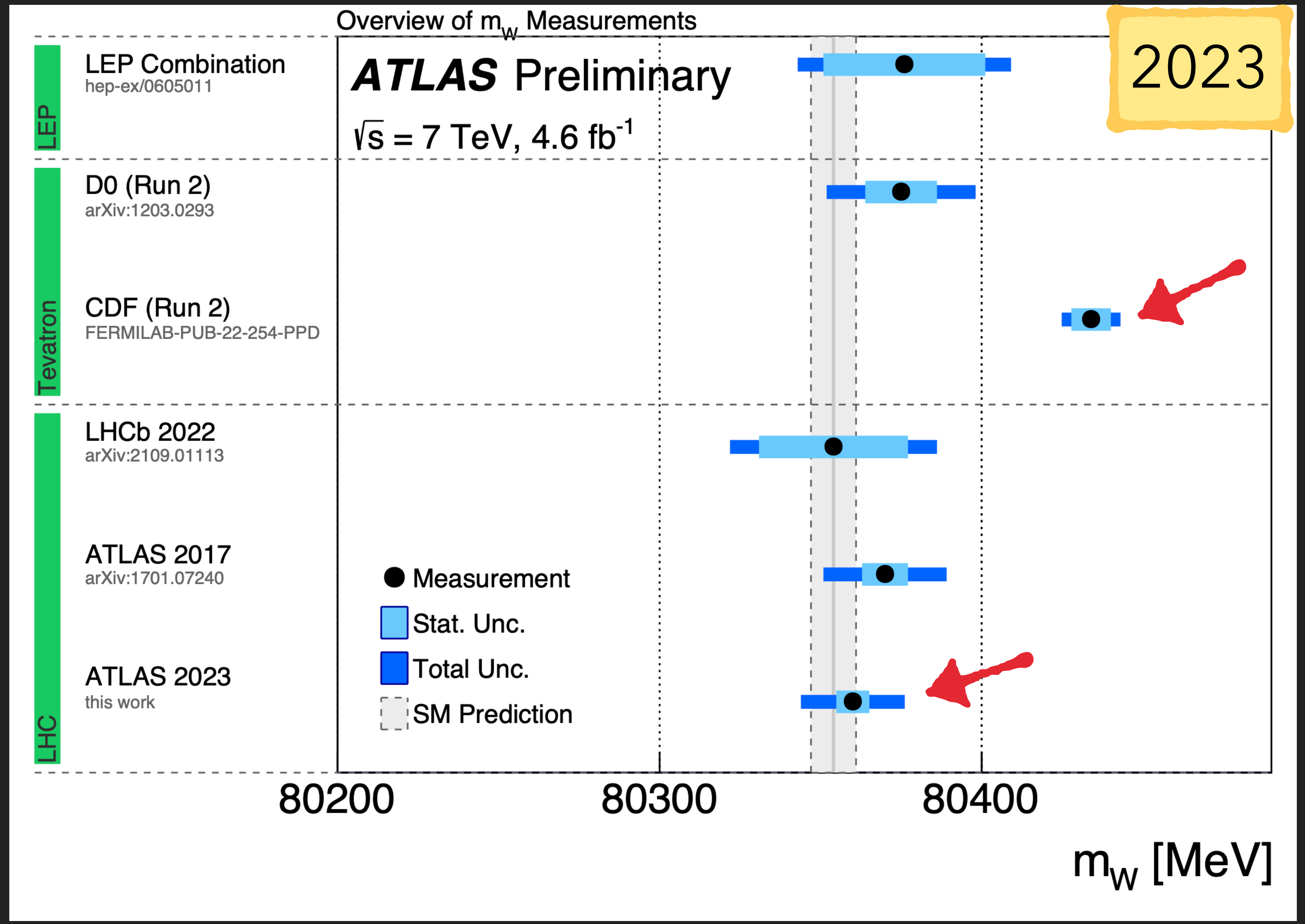

2023

ATLAS Collab.: ATLAS-CONF-2023-004

$$-\frac{(q/m)_p}{(q/m)_{\bar{p}}} = 1.000000000003(16)$$

2022

BASE Collab.: Nature 601, 53-57

Higgs Coupling to Electroweak Vector Bosons

- The gauge bosons *gain* mass through Electroweak Symmetry Breaking

- Post EWSB, the SM predicts HVV couplings at tree level

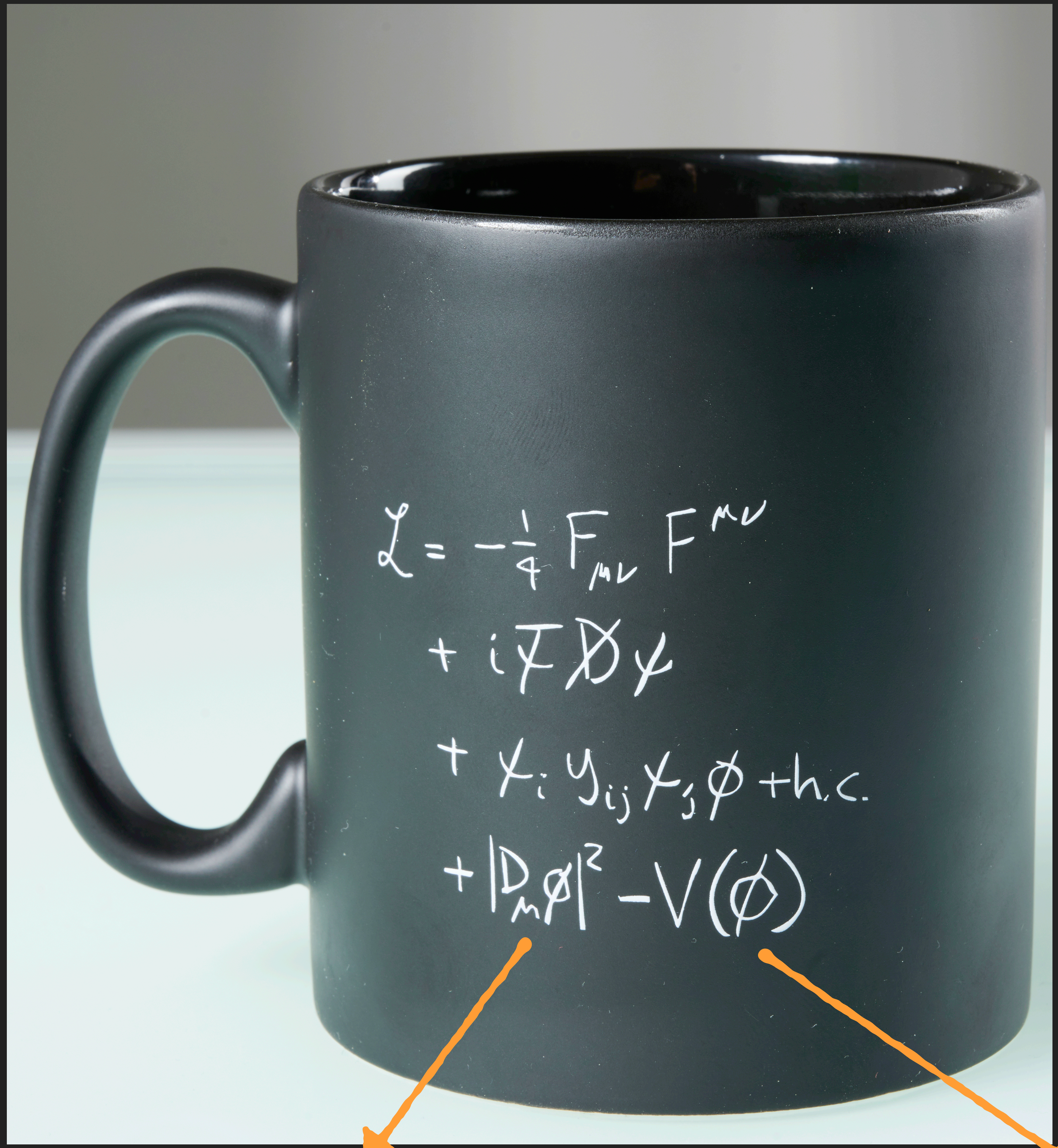

Higgs – gauge bosons interactions

Higgs potential

During interactions

$SU(2)_L \times U(1)_Y \rightarrow U(1)_{EM}$

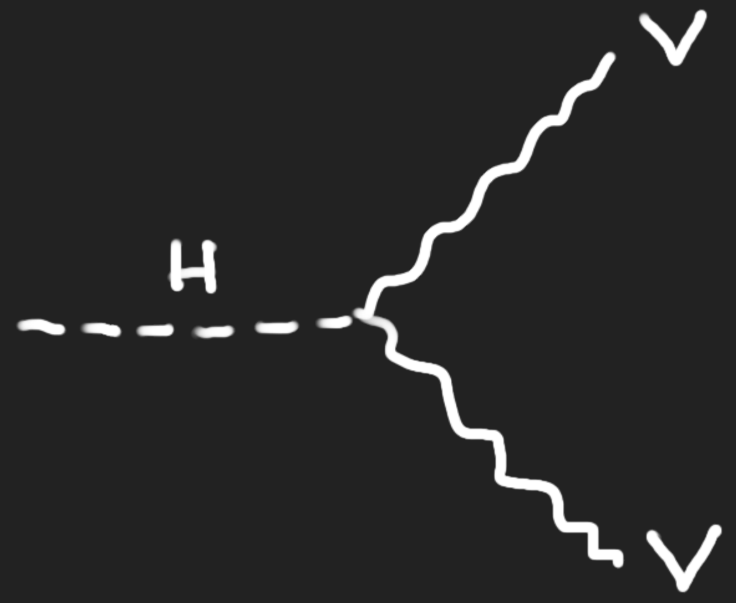

$$\frac{2iM_V^2}{v}\mathcal{O}_{HVV}$$

Higgs Coupling to Electroweak Vector Bosons

- The gauge bosons *gain* mass through Electroweak Symmetry Breaking
- Post EWSB, the SM predicts HVV couplings at tree level
- Precision measurements of the HVV coupling acts as a strong test to the structure of EWSB

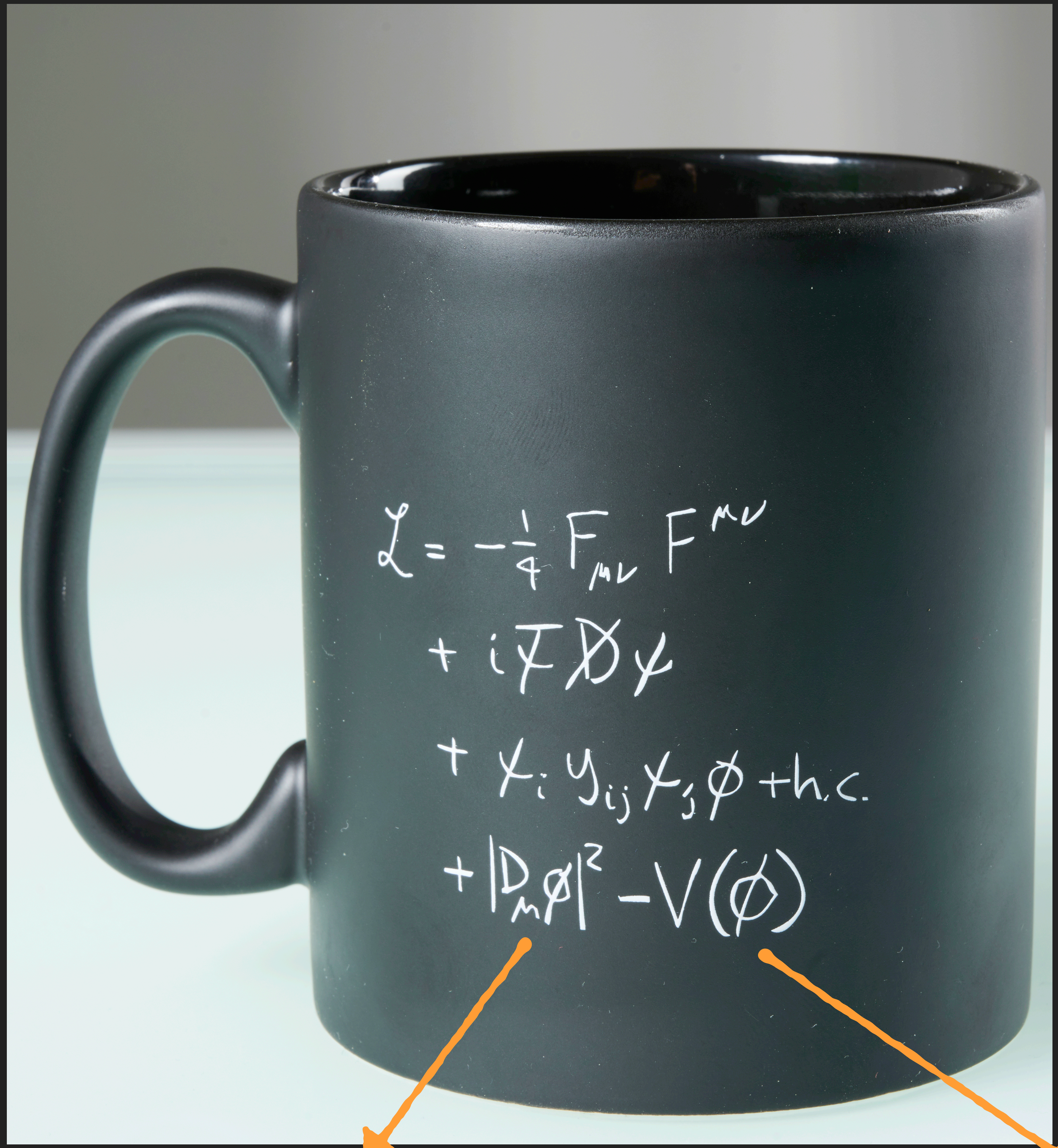

Higgs – gauge bosons interactions

Higgs potential

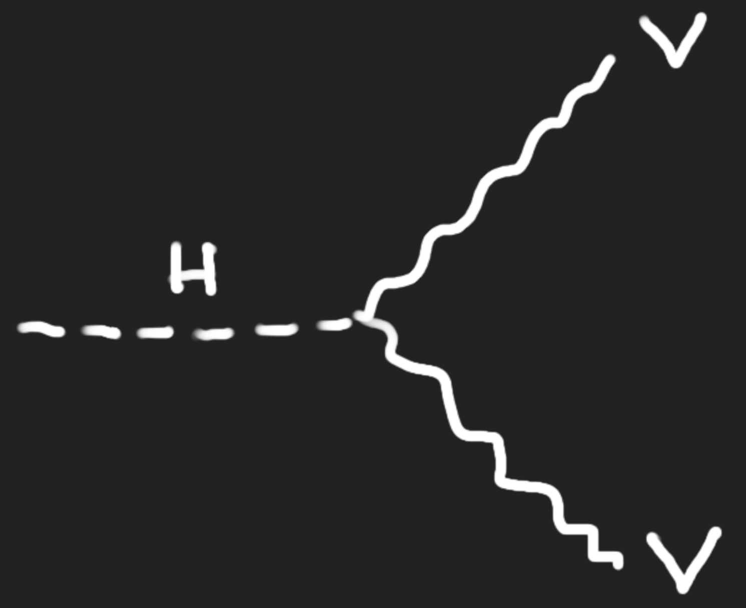

$$\frac{2iM_V^2}{v}\mathcal{O}_{HVV}$$

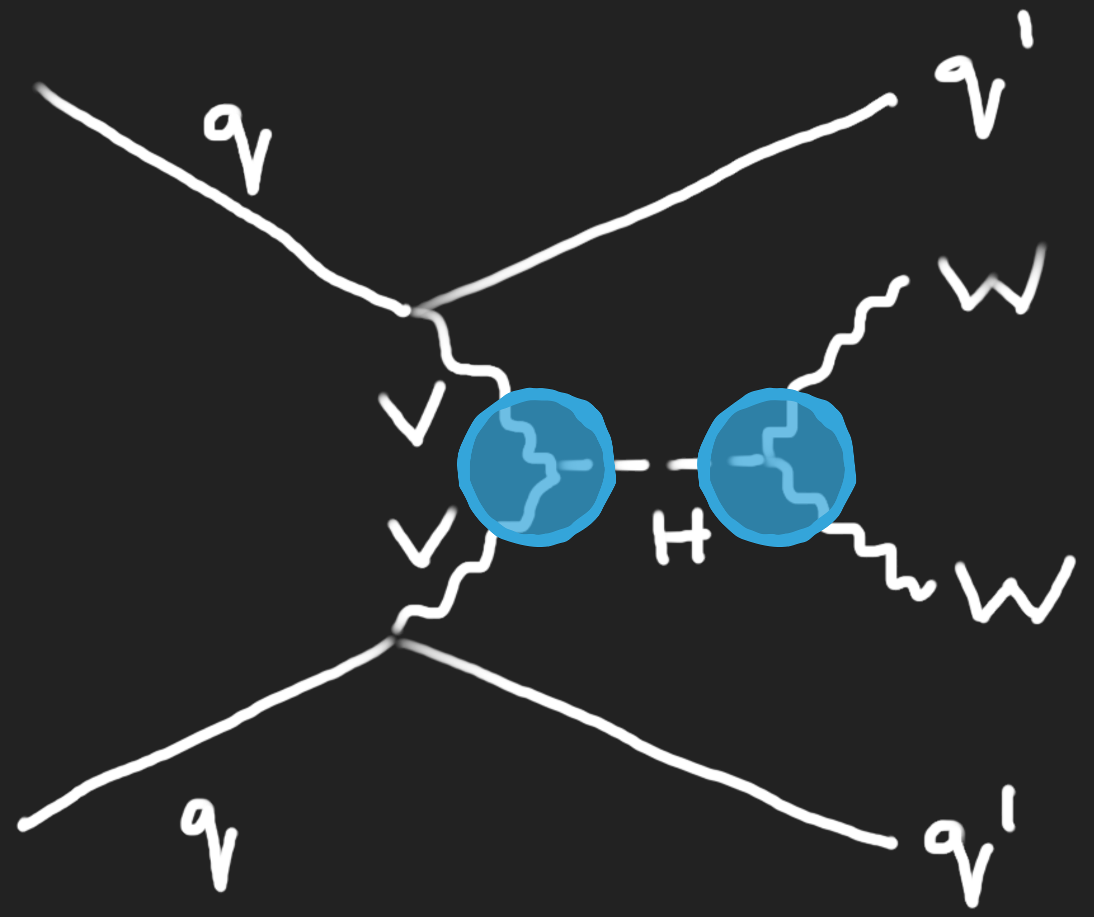

Vector Boson Fusion H → WW: HVV coupling in production as well as decay

ATLAS Experiment @ the LHC

pp collider at $\sqrt{s}$ = 13.6 TeV

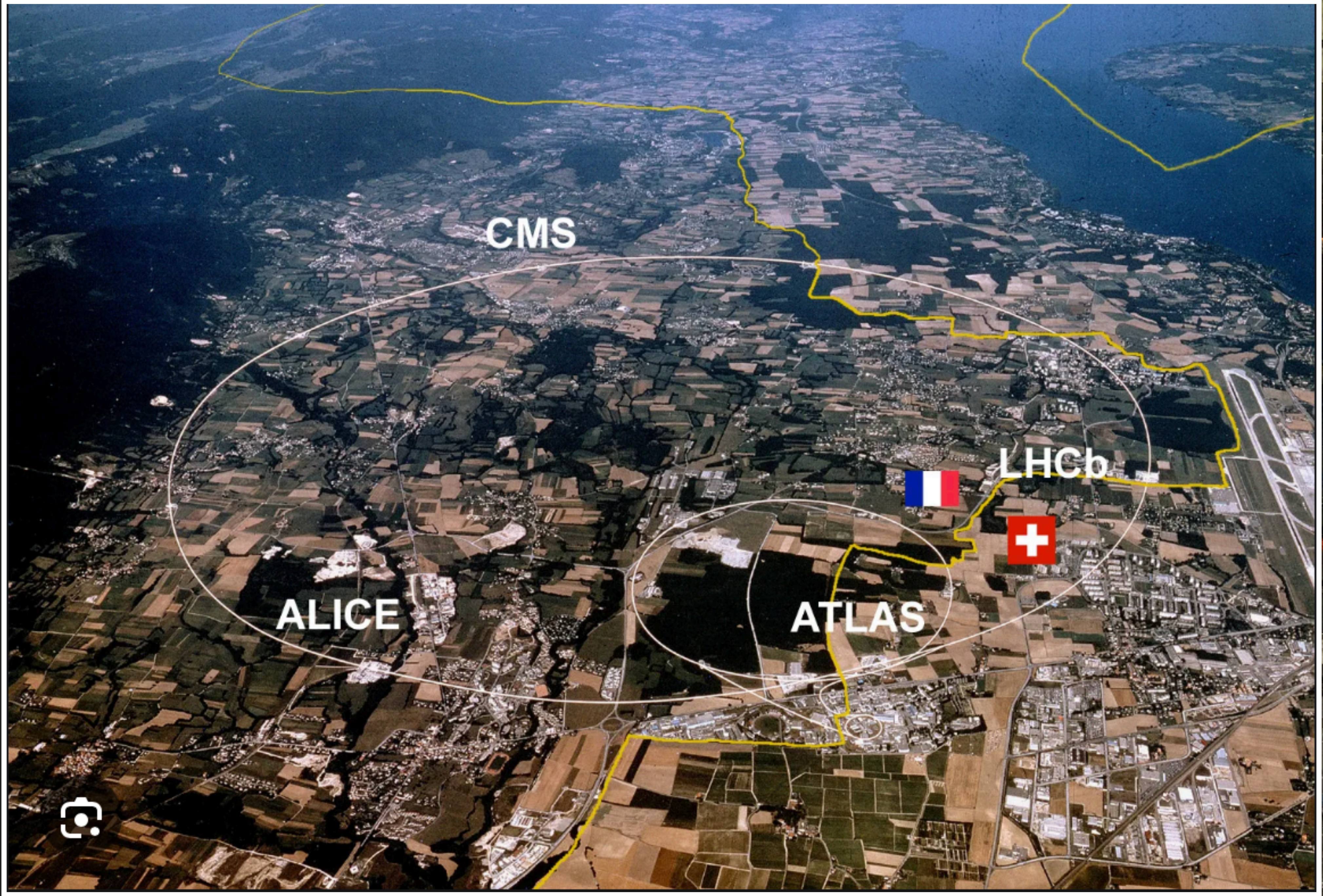

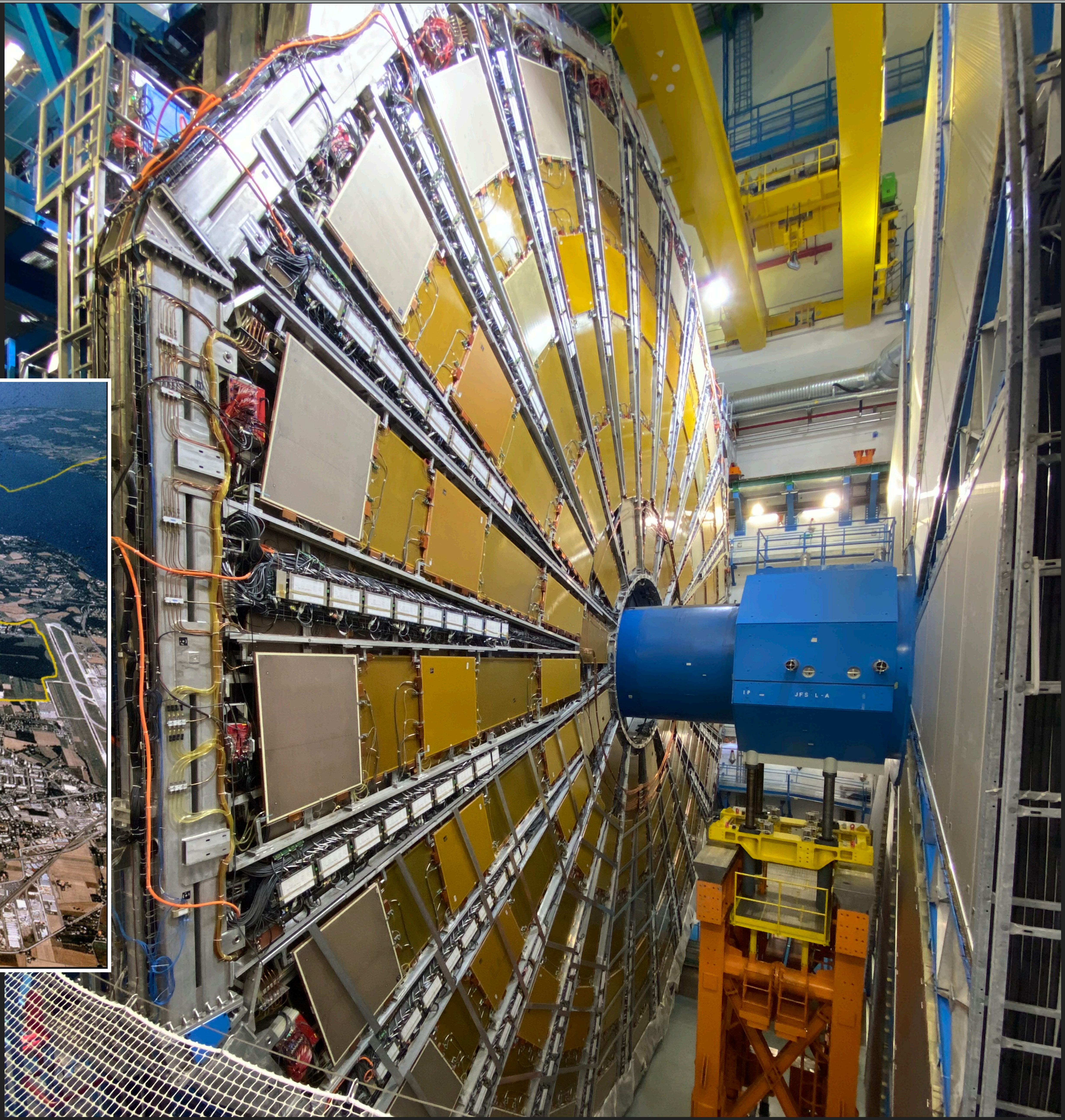

ATLAS Experiment @ the LHC

Run-2: $\sqrt{s}$ = 13 TeV
Data collected b/w 2015-2018

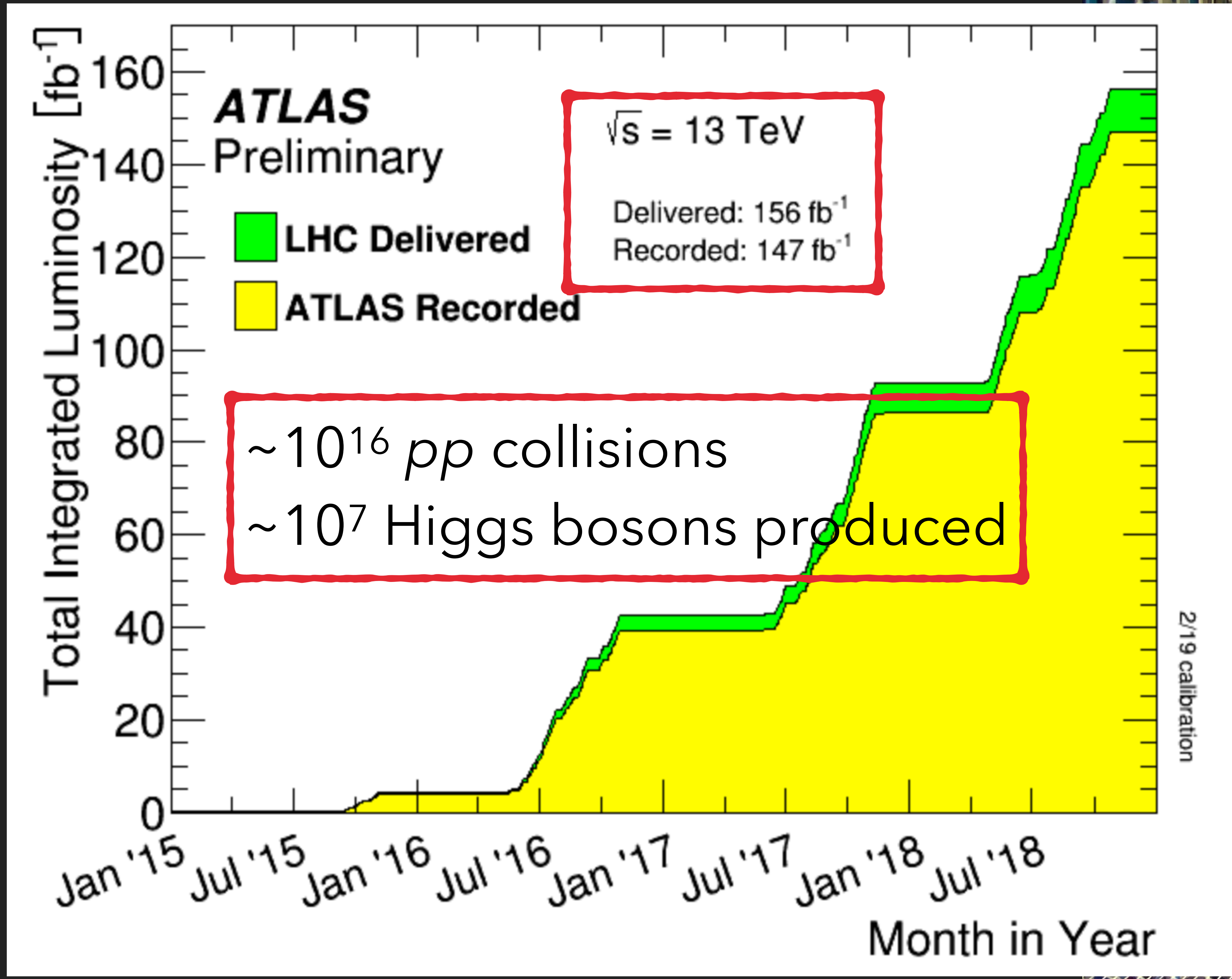

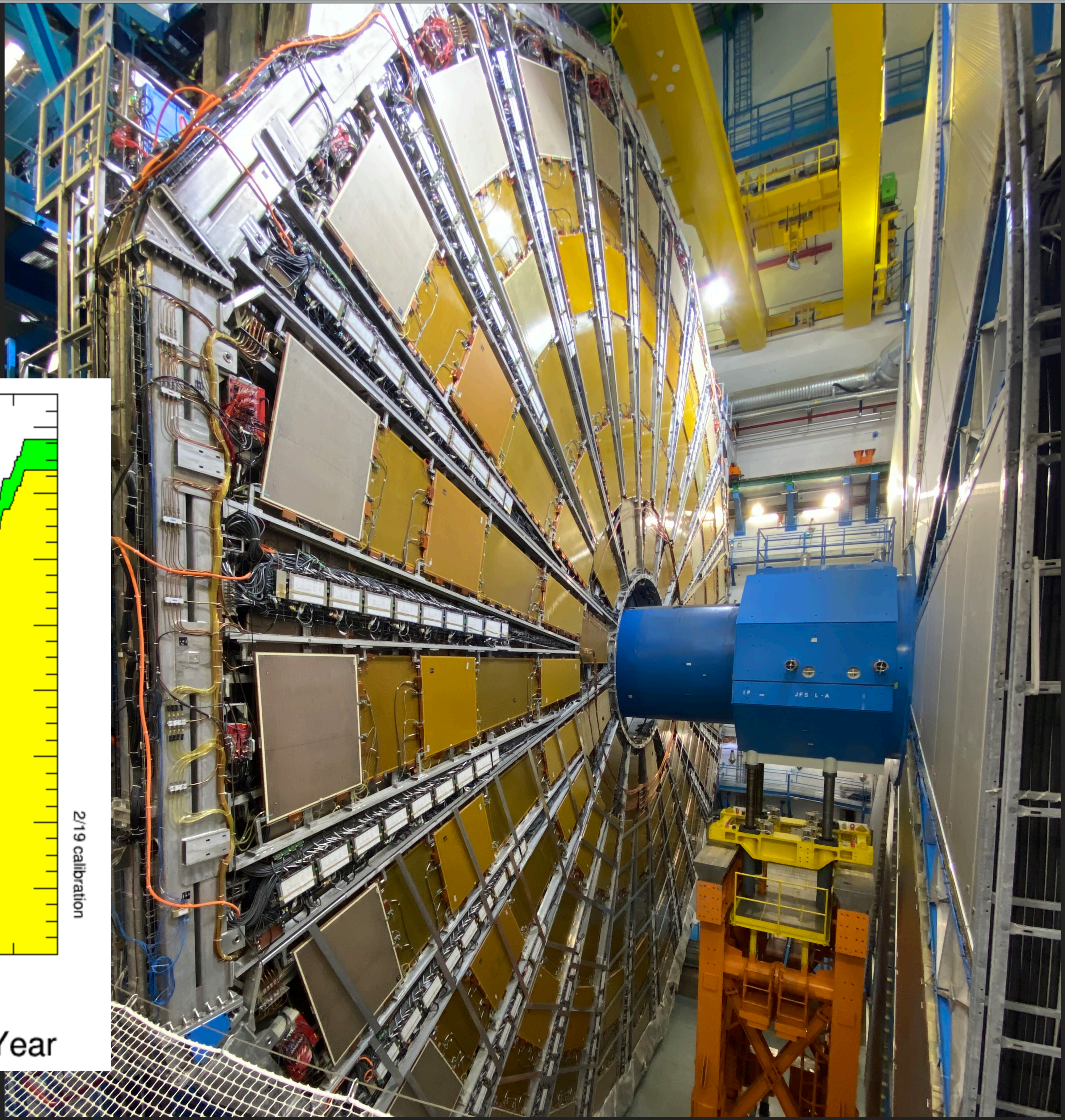

VBF H → WW at ATLAS

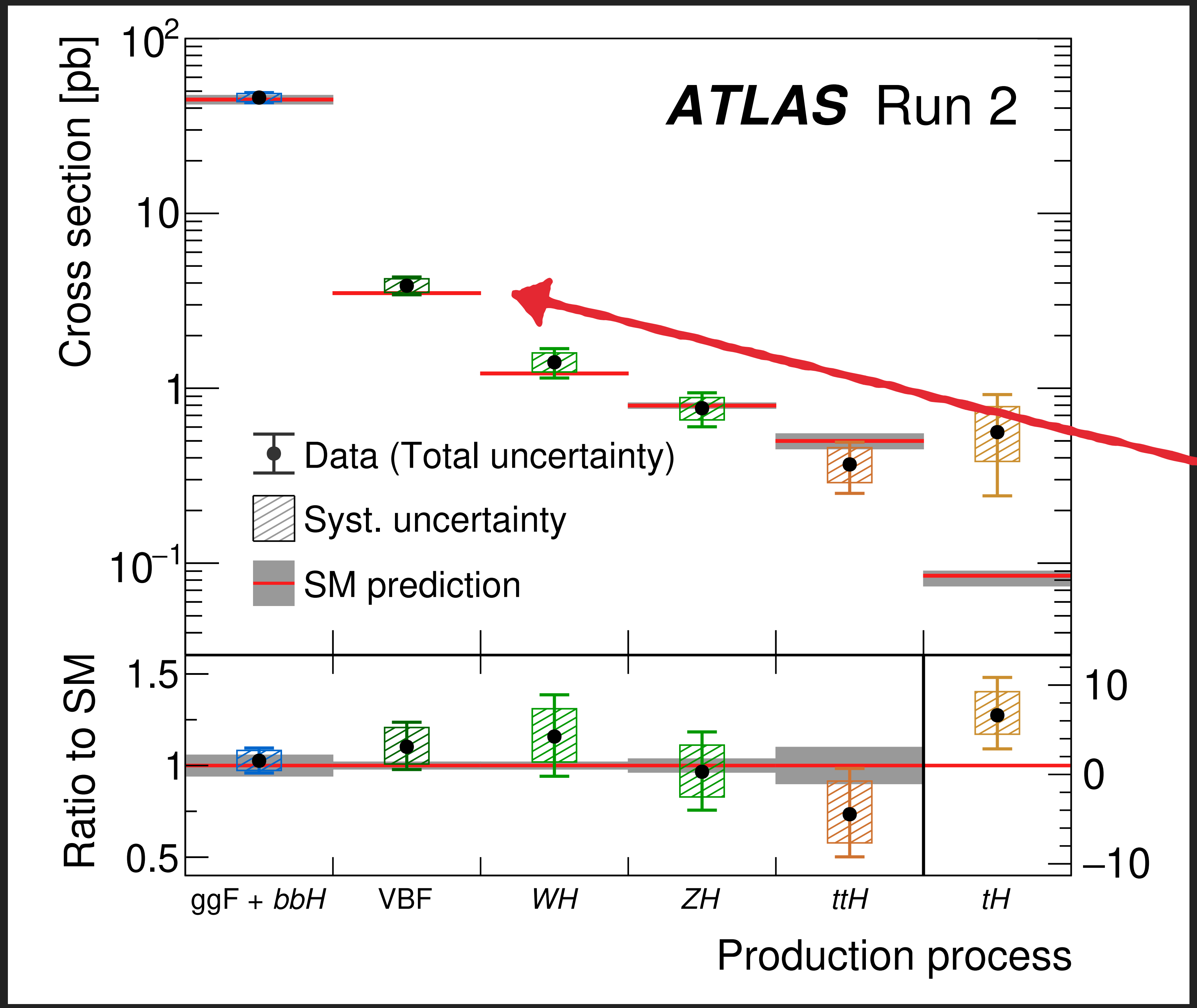

Nature **607**, 52–59 (2022)

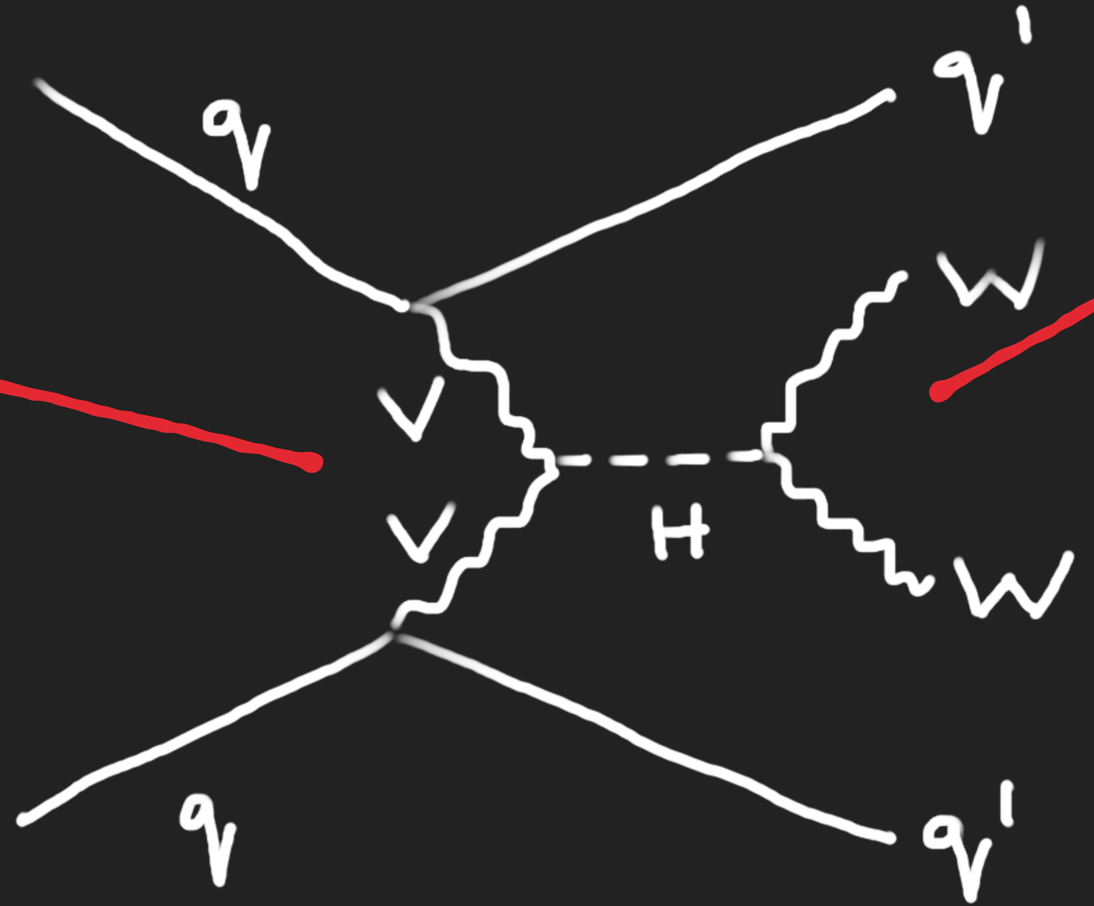

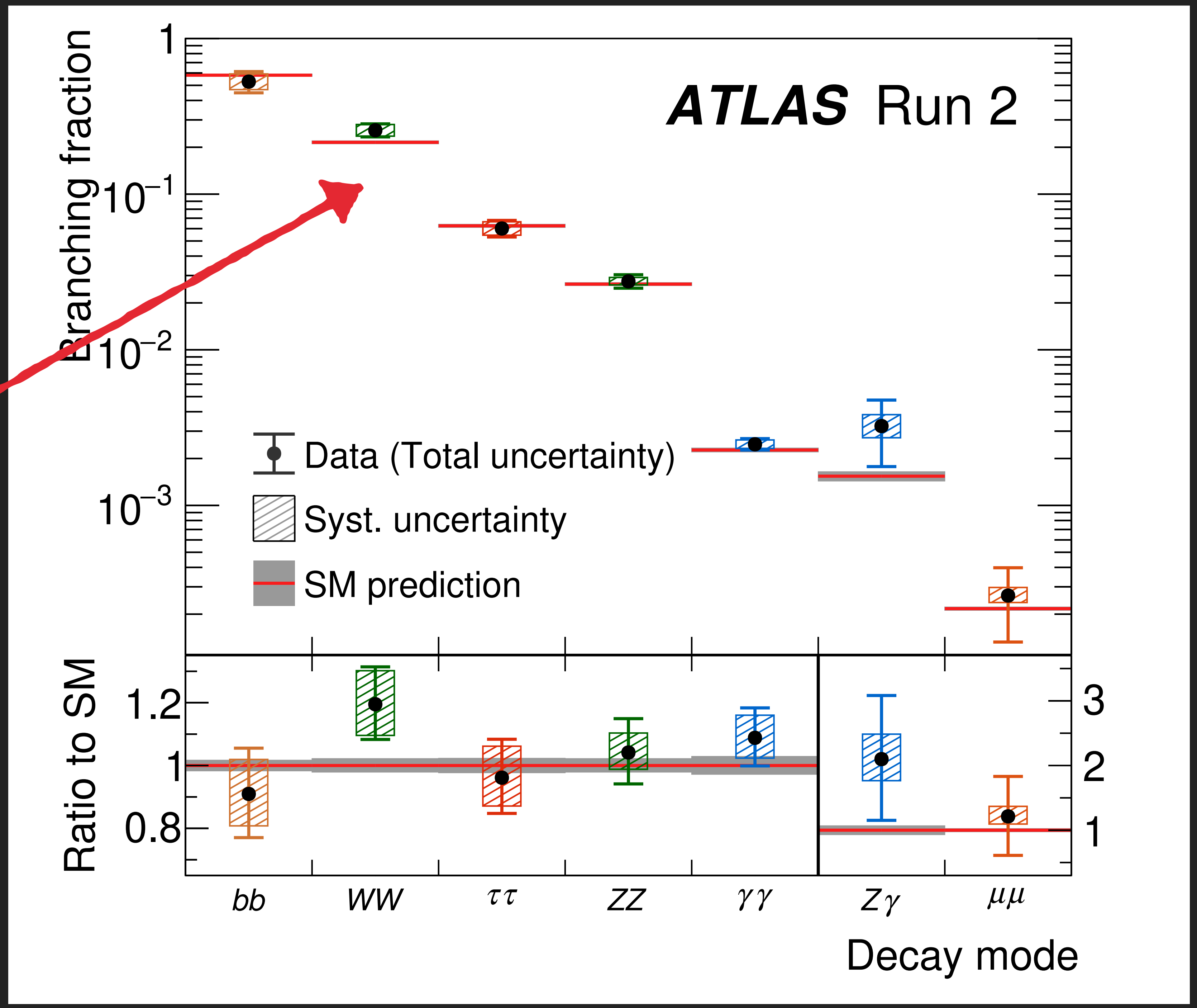

Nature **607**, 52–59 (2022)

$$N_{events} = \sigma_{VBF} \cdot BR_{H\to WW} \cdot \mathscr{L}_{Run-2} \cdot \text{W decay choice} = O(1000)$$

Within the statistical reach for differential measurements

Signal Signature

2 highly energetic, separated ***jets*** with no high energy jet activity between them

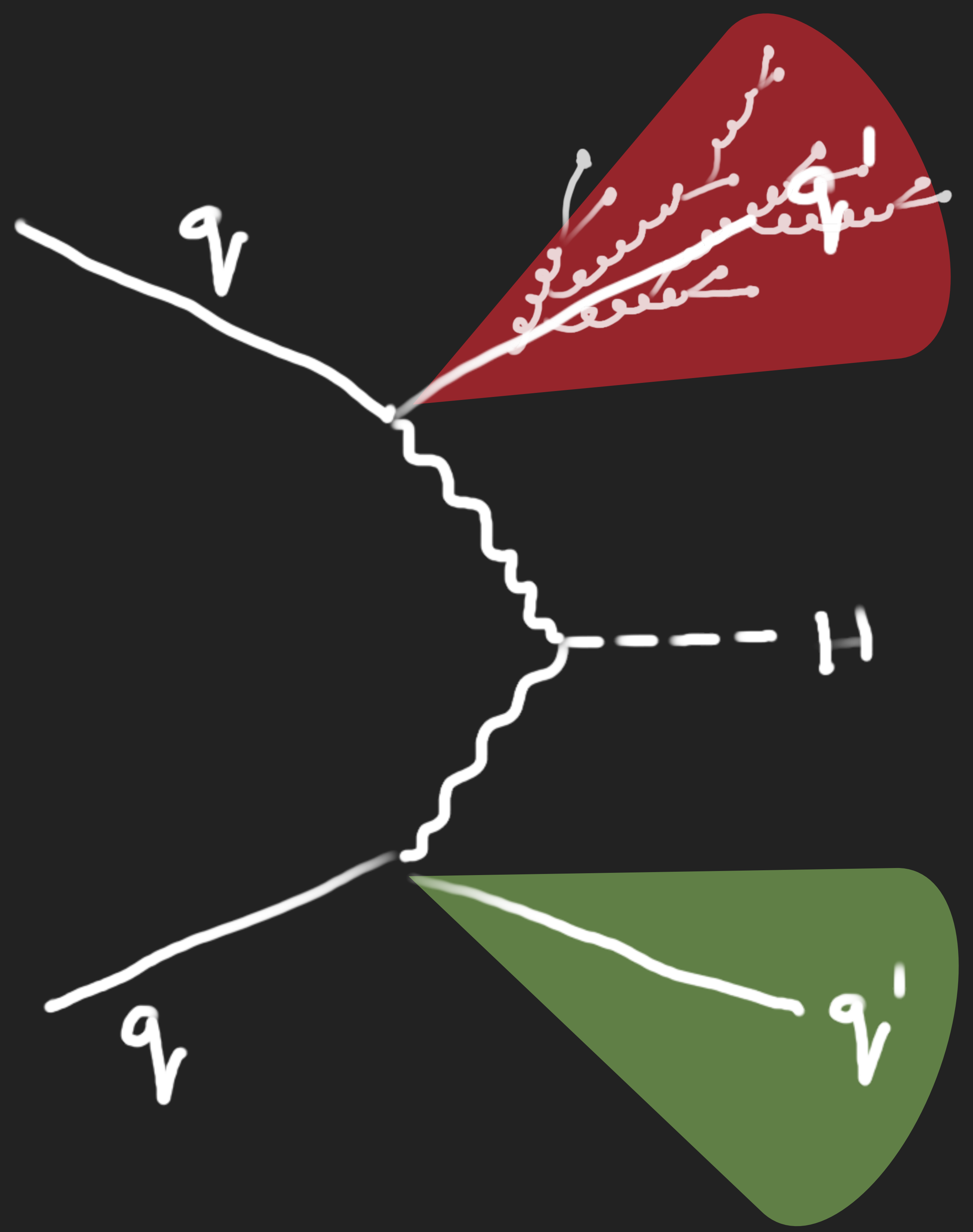

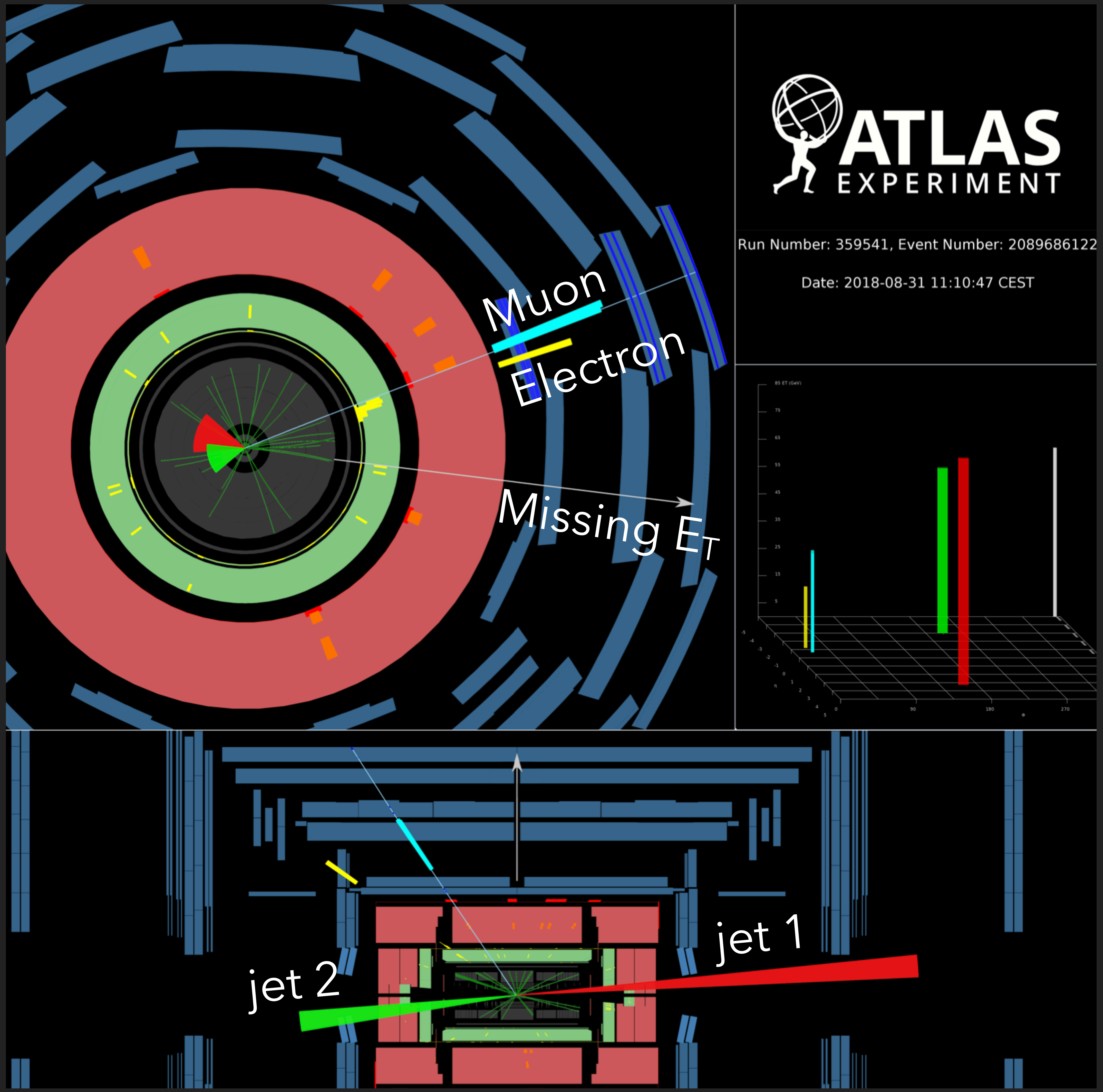

Decay products have a small opening angle

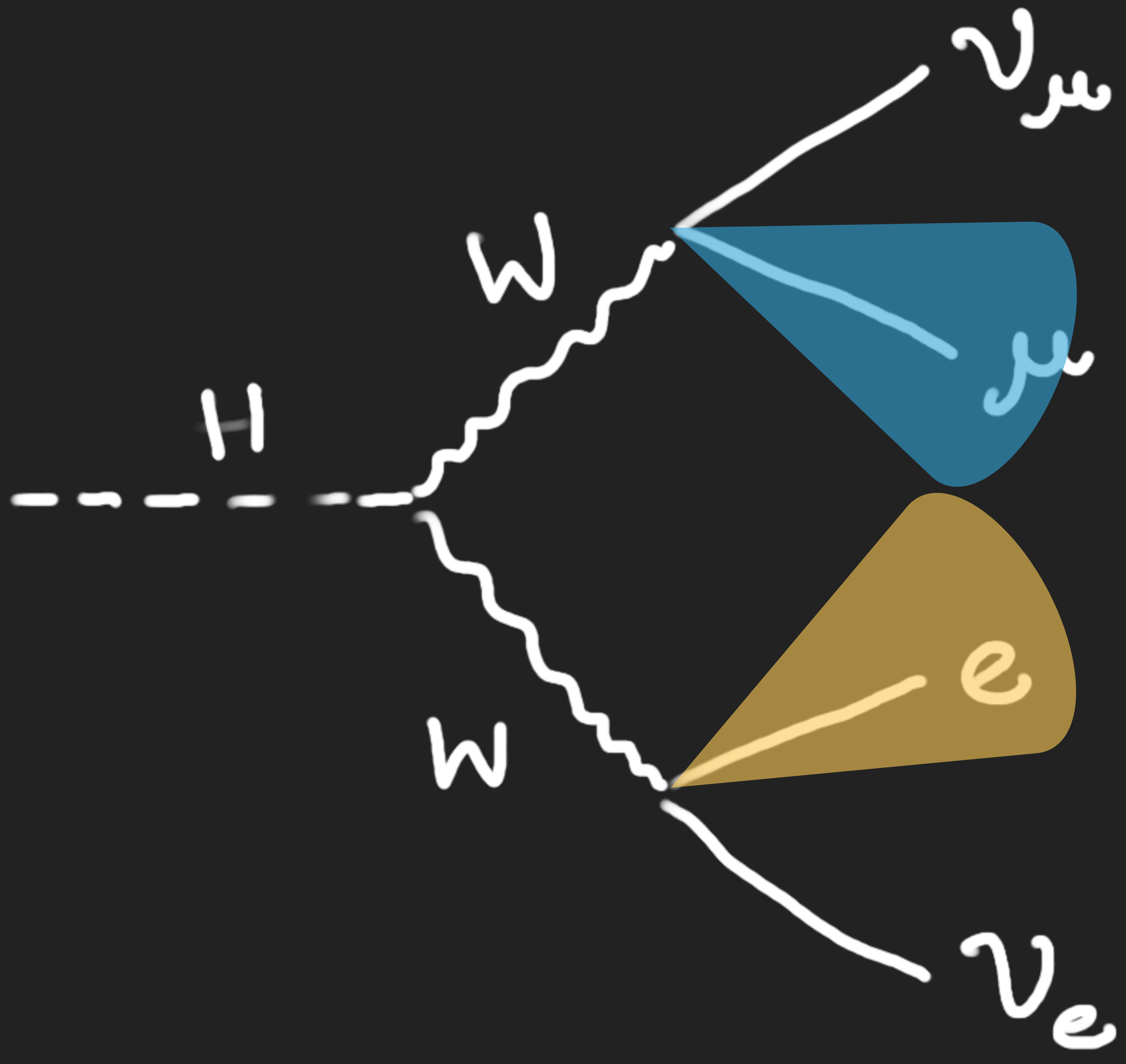

Fiducial Phase Space

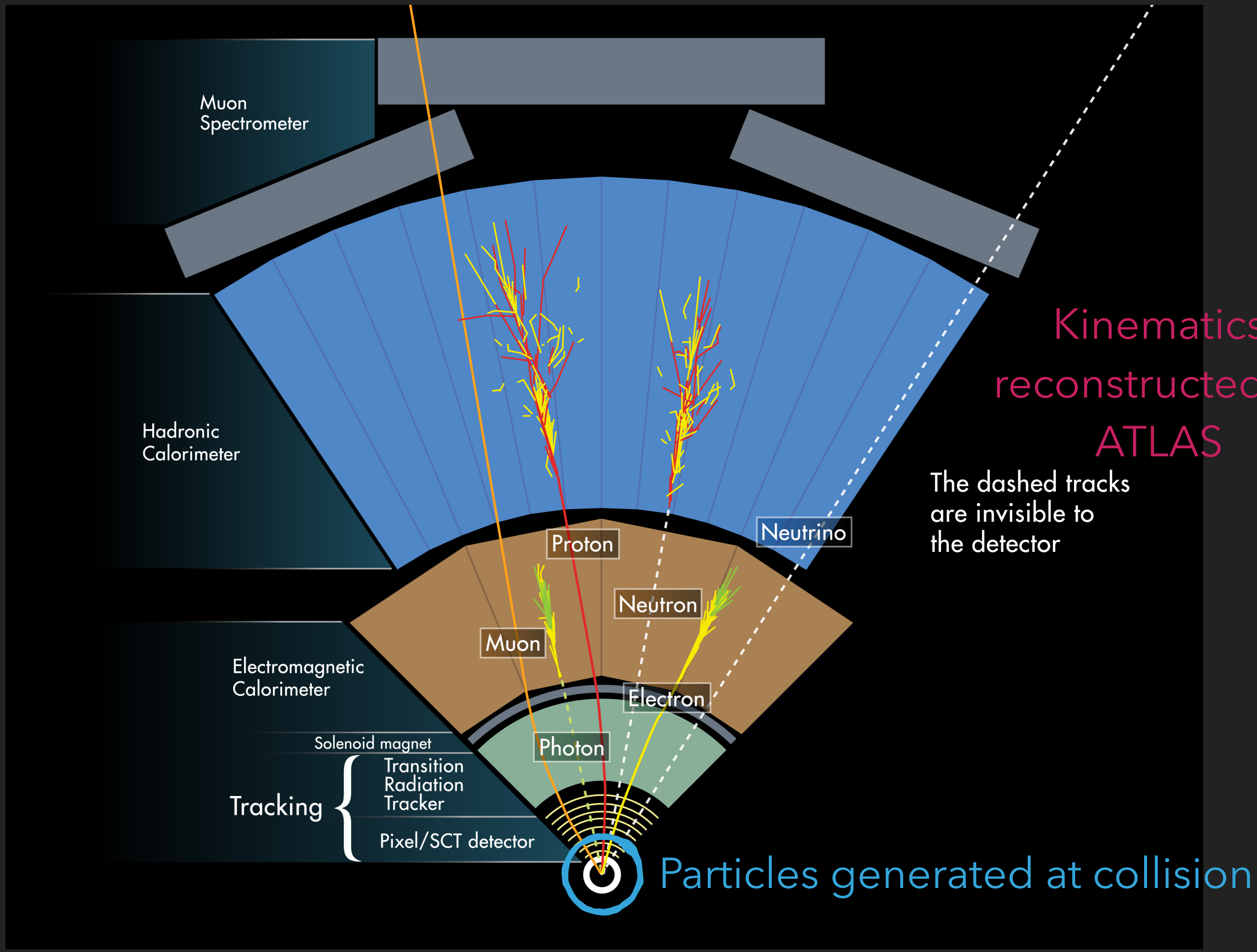

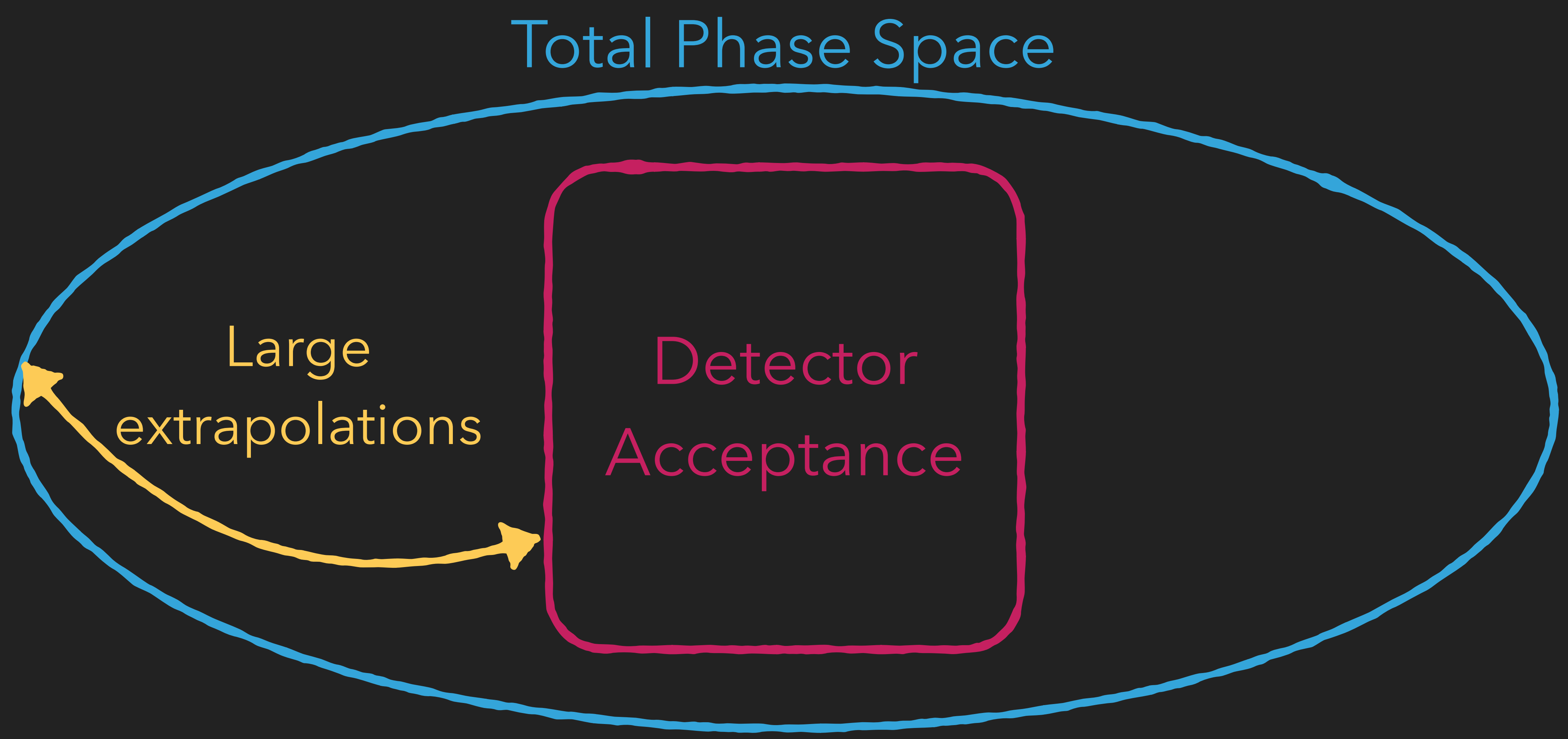

Measurements *lossy*: finite resolution, < 100% kinematic acceptance, kinematic cuts to isolate signal

Using Monte Carlo to go from the measured space to the total space adds large extrapolations due to limitations in the event generator and parton shower models

Fiducial Phase Space

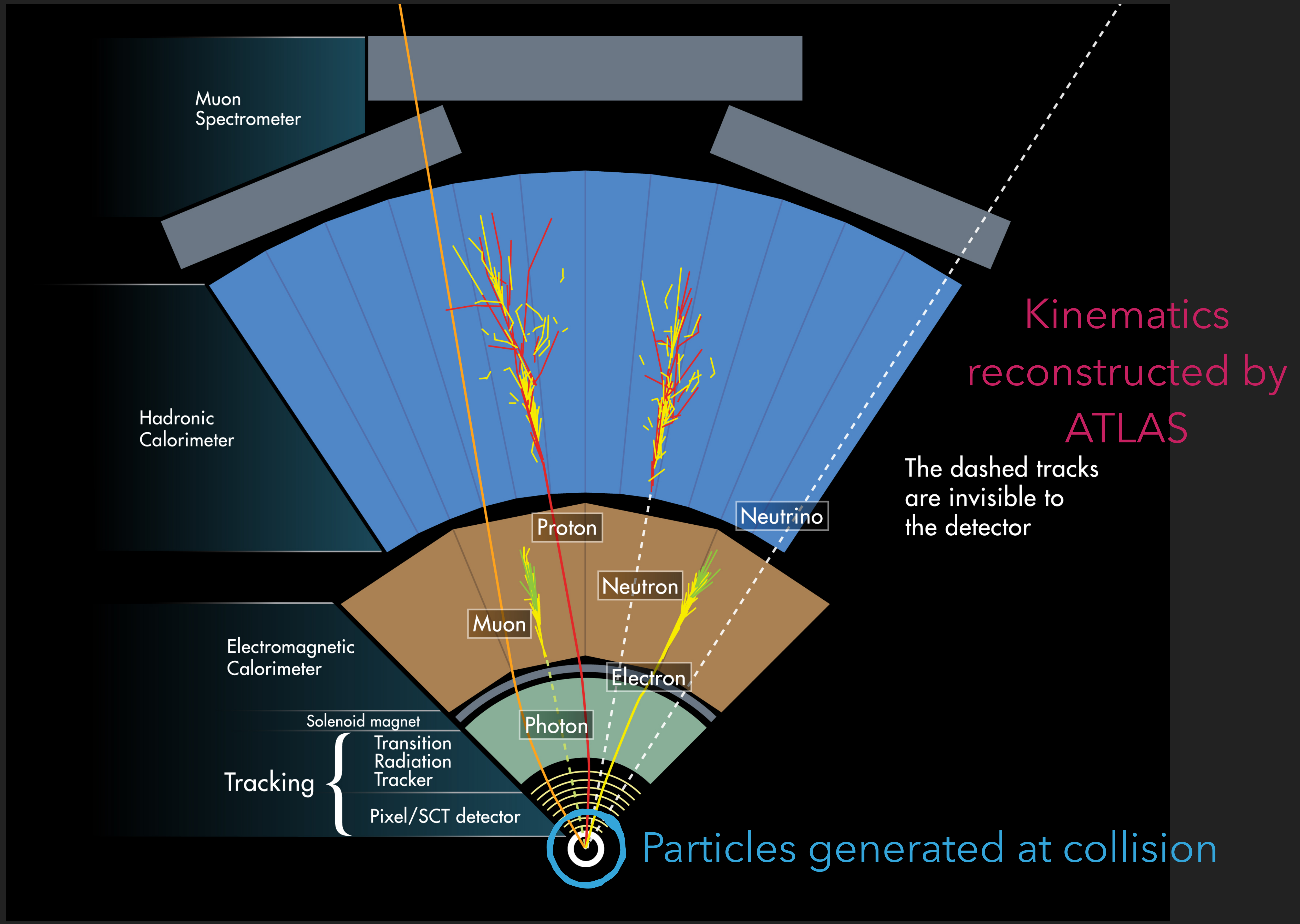

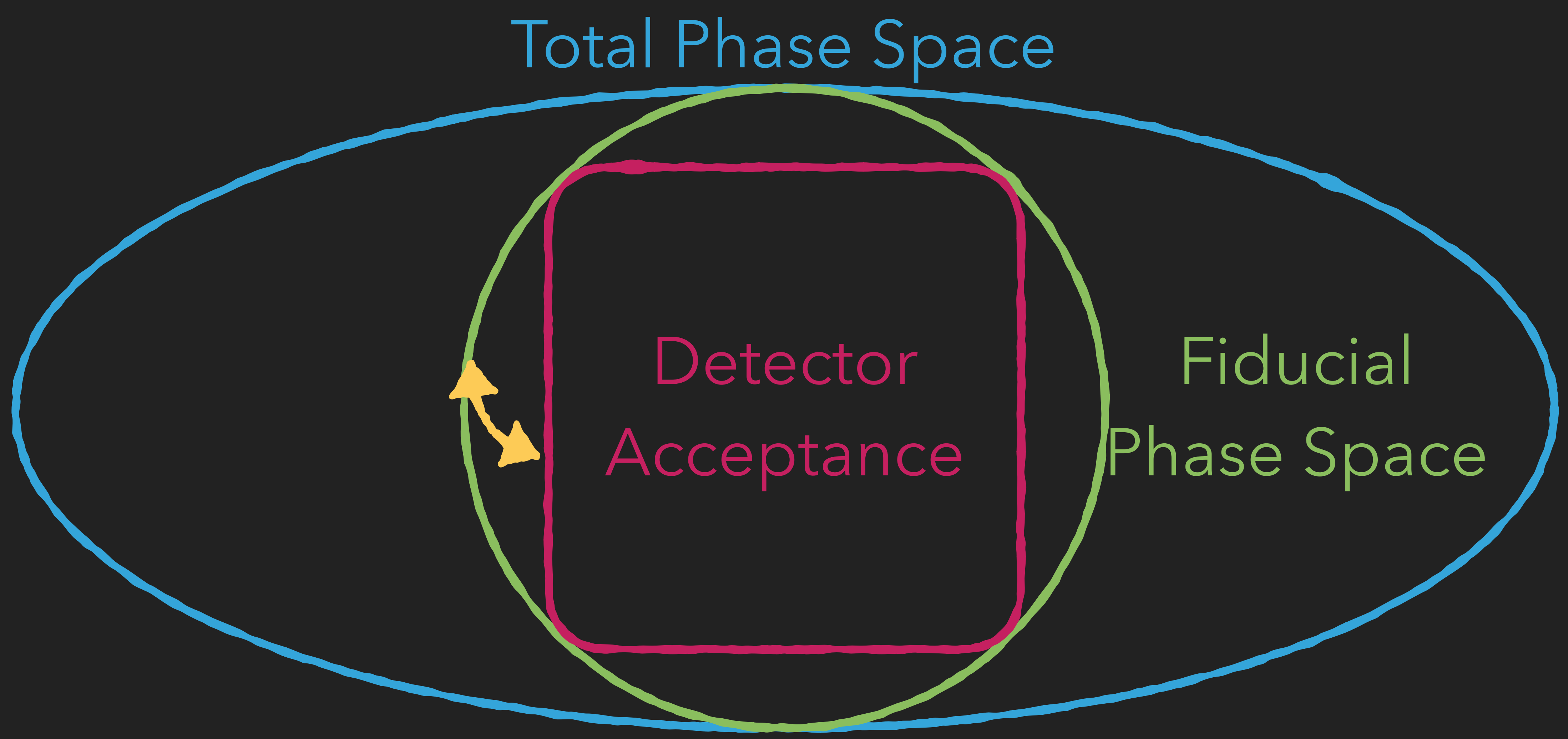

Fiducial region: defined by kinematics of particle-level final states close to detector level definition

Minimal extrapolations from the detector phase space to the fiducial.
Fiducial cross sections are the most model independent way to make measurements

Analysis Goals

- **Differential** fiducial cross-section of VBF production of Higgs in the WW ($\rightarrow \mu + e + E_T^{miss}$)+2jets final state
- Remove detector effects: go from the measurement phase space to the fiducial phase space. Report cross-section as functions of particle-level kinematics.
- Interpret the measurements to search for anomalous couplings of the Higgs boson

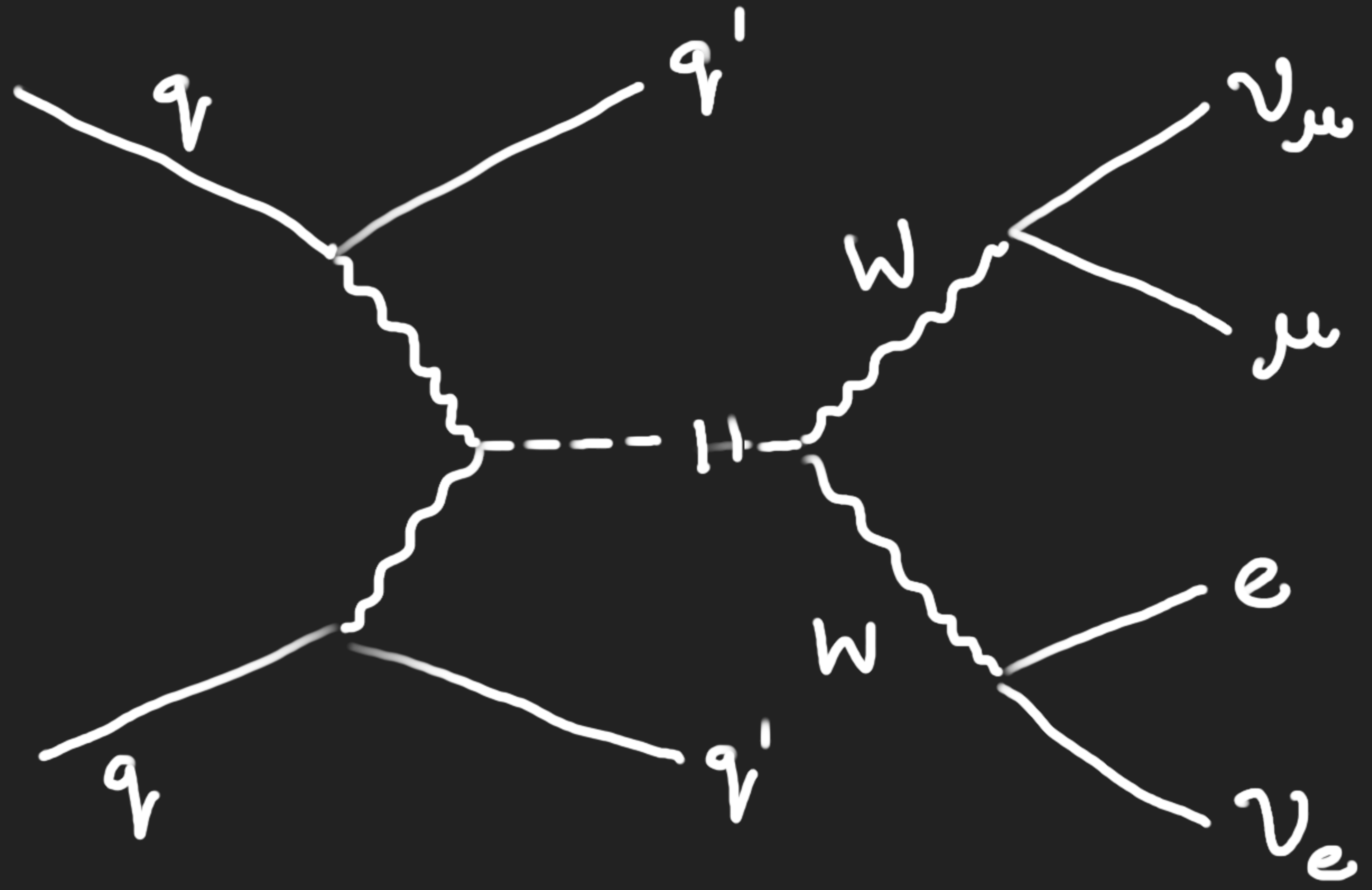

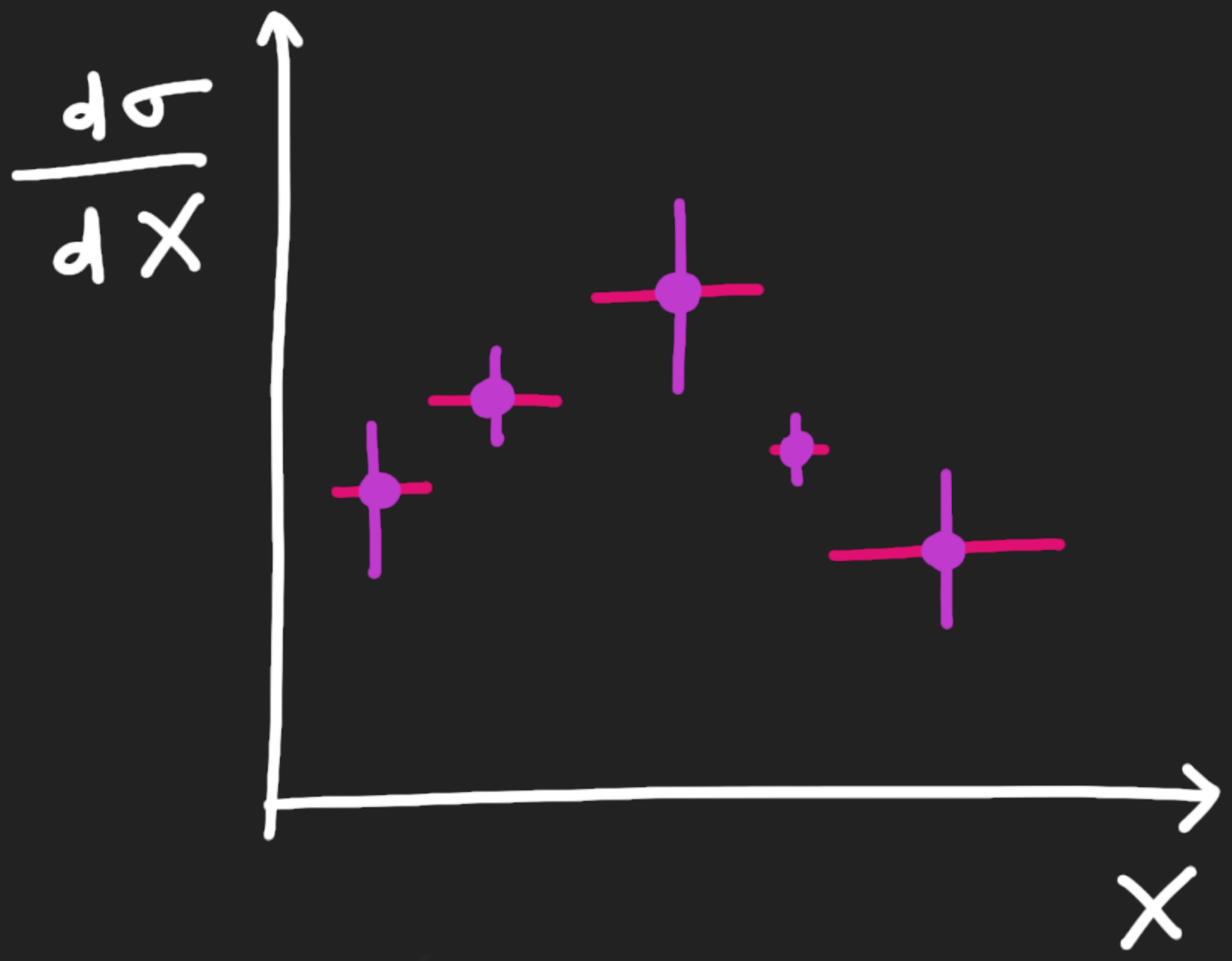

Analysis Challenges

- Final state not fully reconstructed – non-resonant signal
- Many SM processes with multi-lepton+multi-jet final states

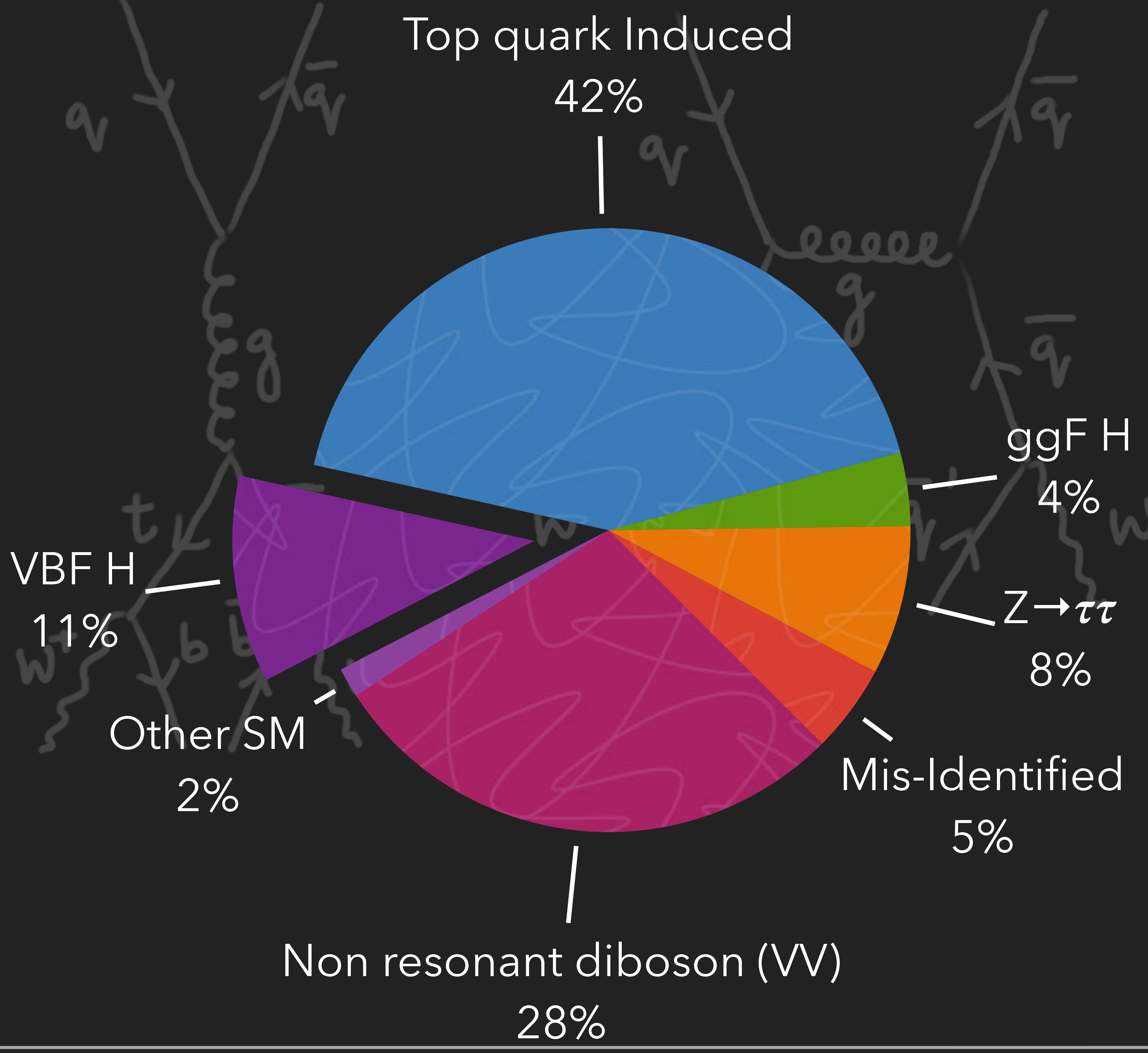

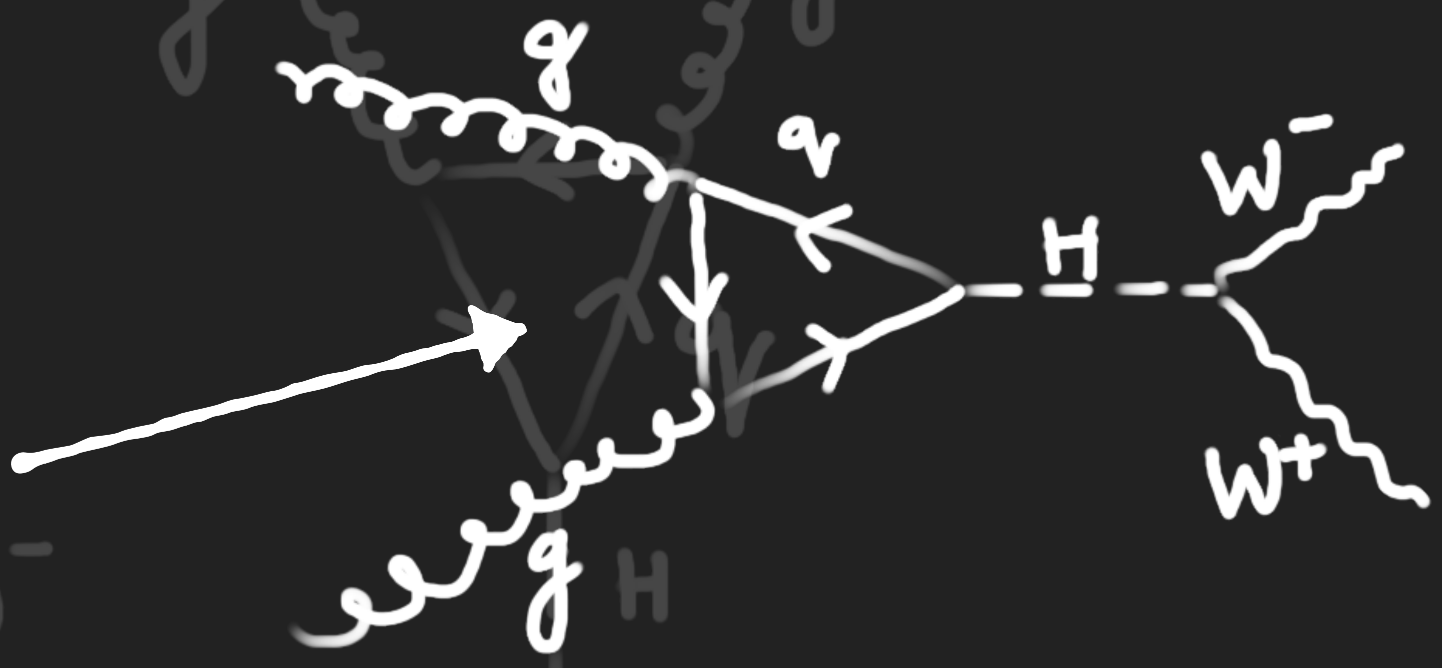

- Define a narrow signal rich phase space (Signal Region) to isolate the signal
- Estimate background contamination and the uncertainty on it
- Background subtracted data gives # signal events, N^{SR}_{signal}

Analysis Challenges

- Final state not fully reconstructed – non-resonant signal
- Many SM processes with multi-lepton+multi-jet final states

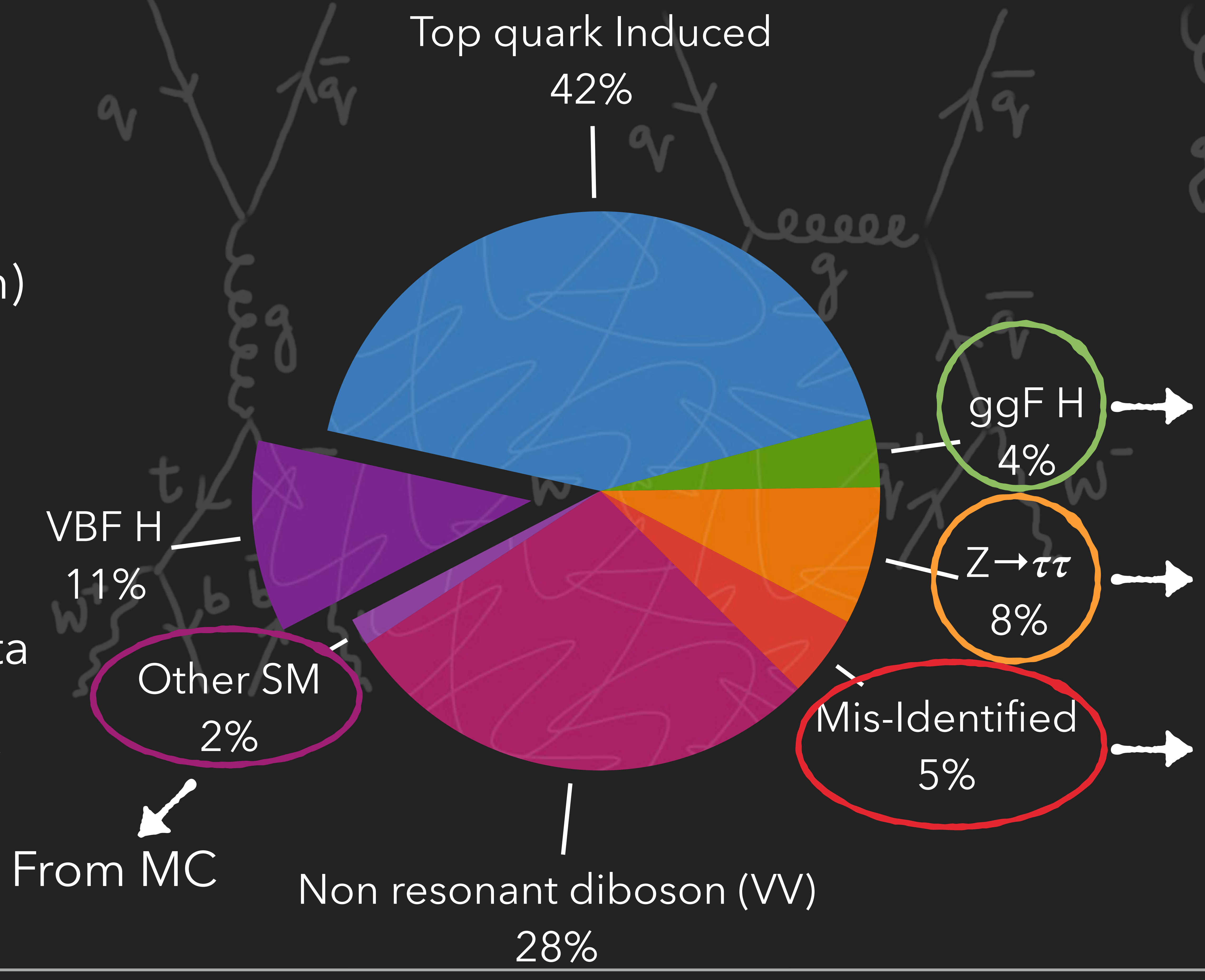

- Define a narrow signal rich phase space (Signal Region) to isolate the signal
- Estimate background contamination and the uncertainty on it
- Background subtracted data gives # signal events, N^{SR}_{signal}

- Define Control Regions orthogonal to the SR to isolate backgrounds
- CR allows data-driven estimation of background contamination in the SR

Biggest backgrounds – top induced and VV

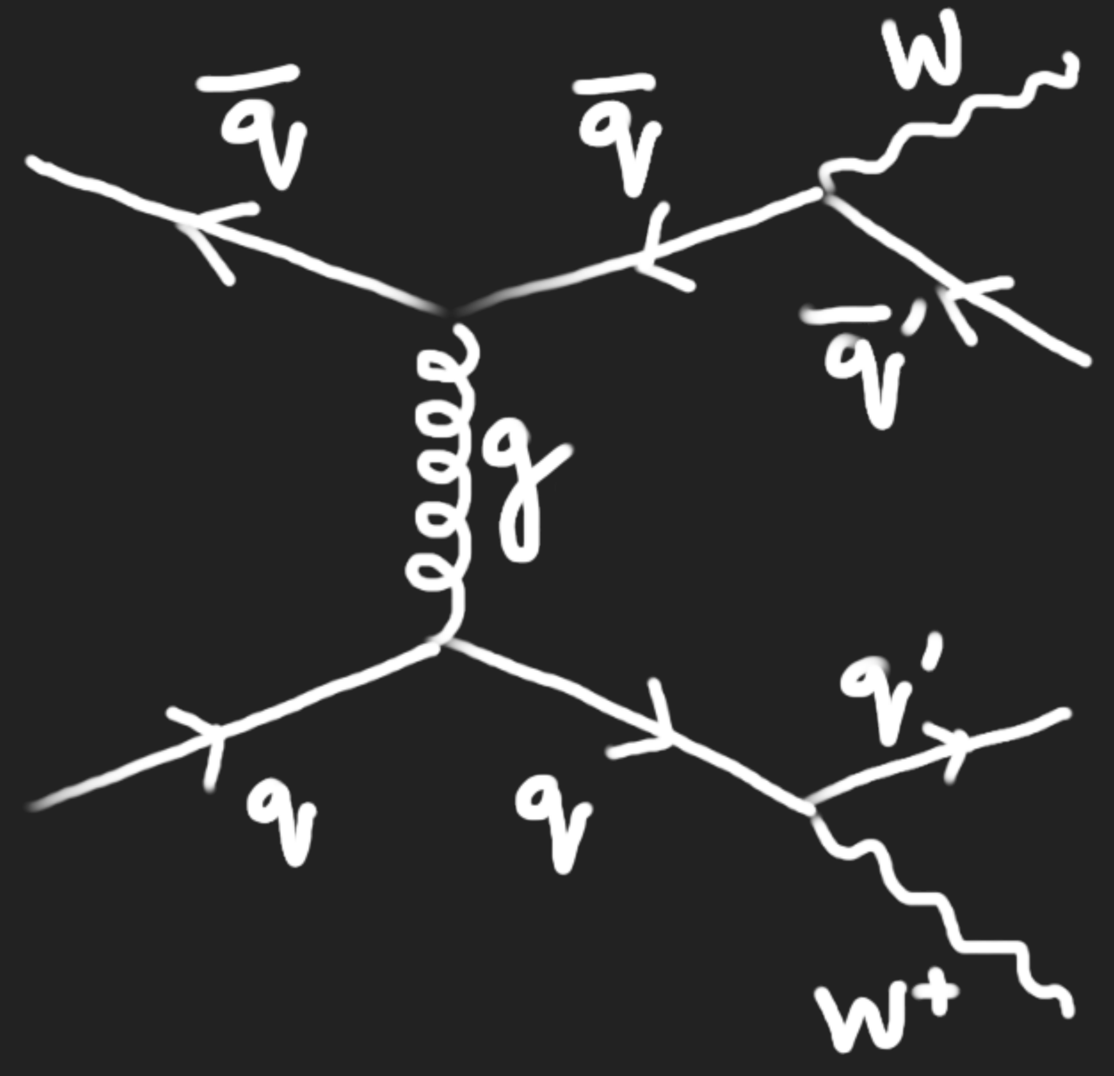

- SR is a **very narrow** VBF isolating phase space
- Raw modelling uncertainties comparable to the # signal events – need to be significantly reduced in a data-driven manner

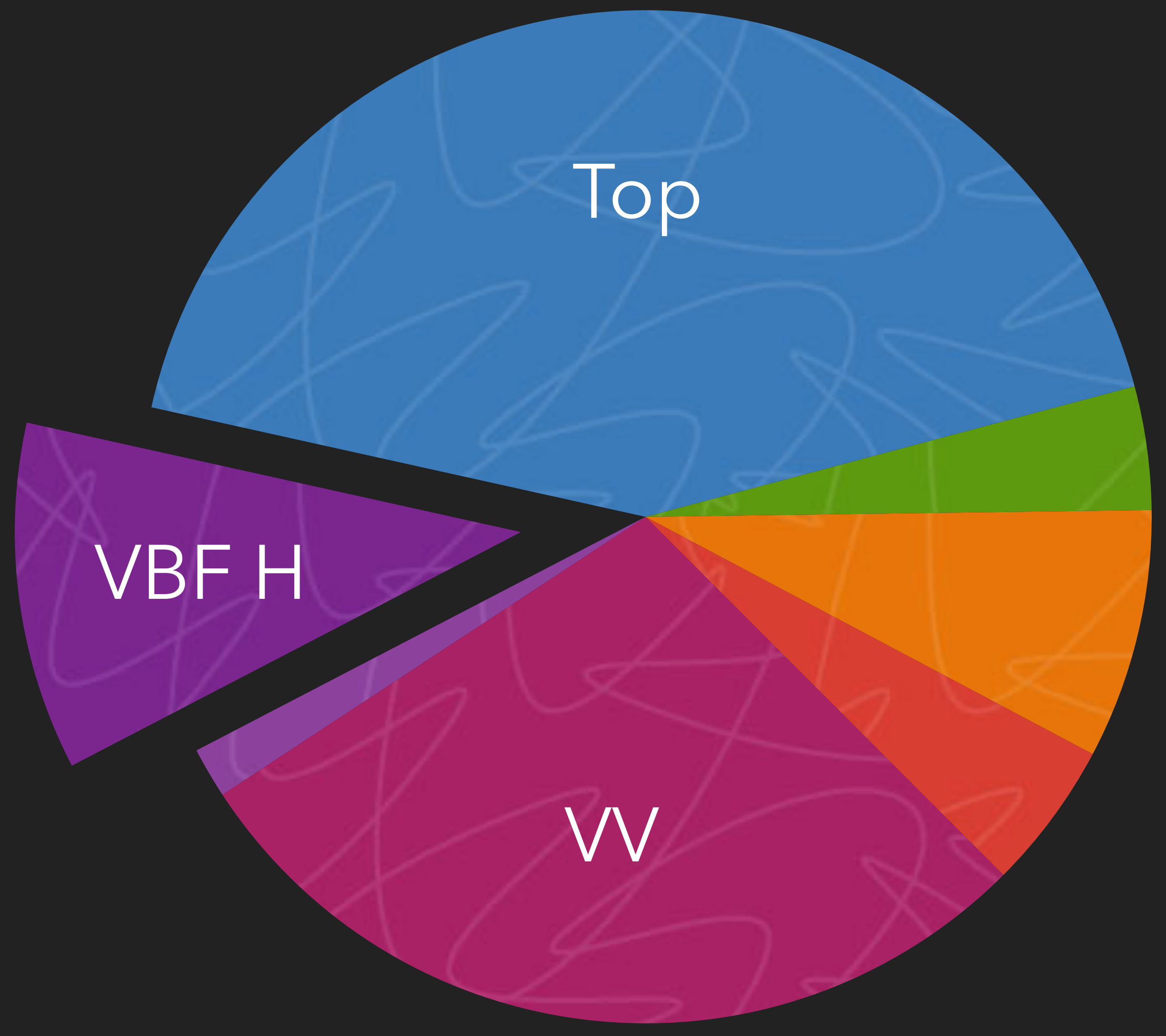

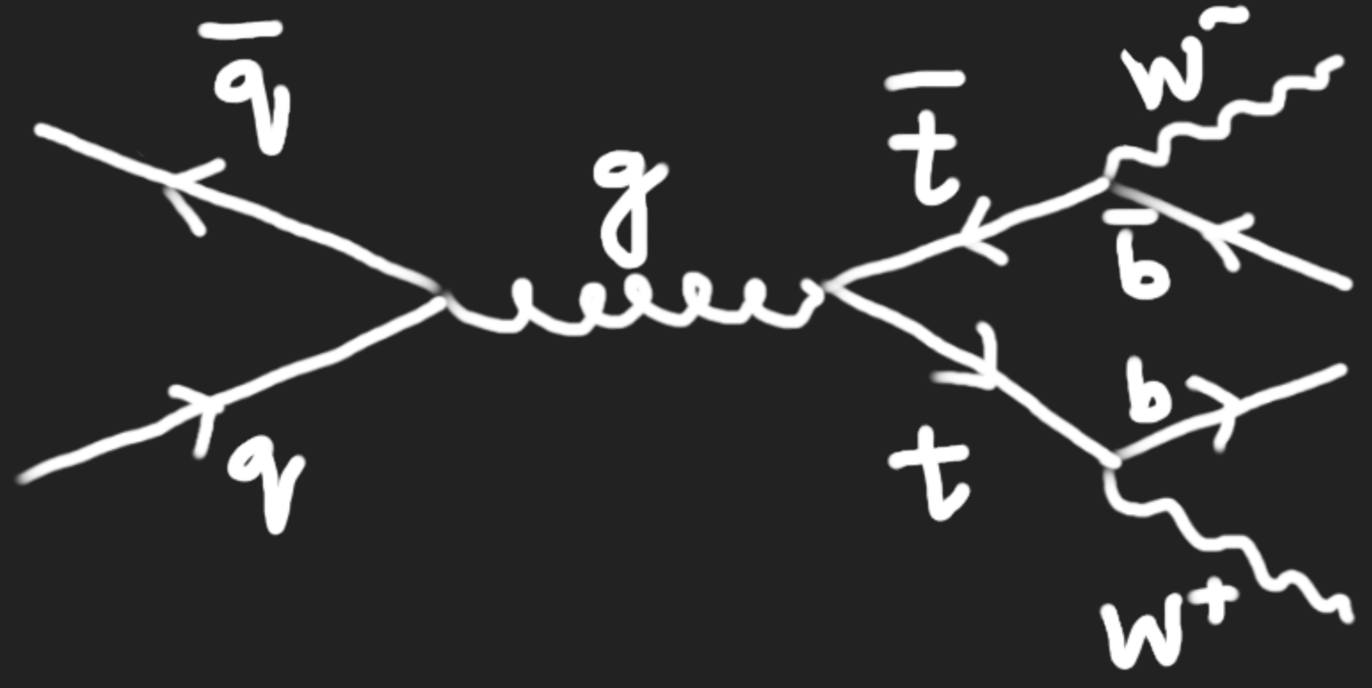

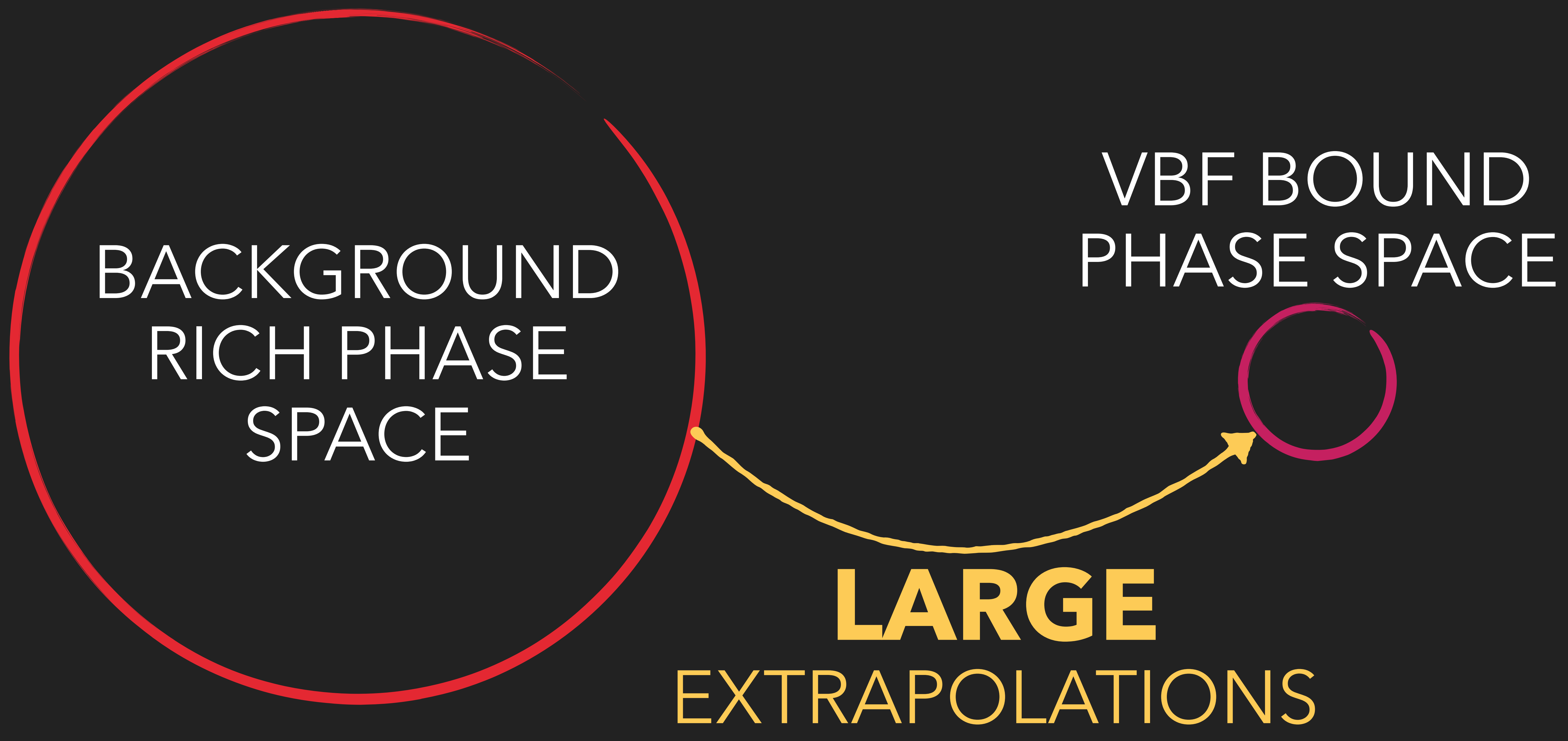

Biggest backgrounds – top induced and VV

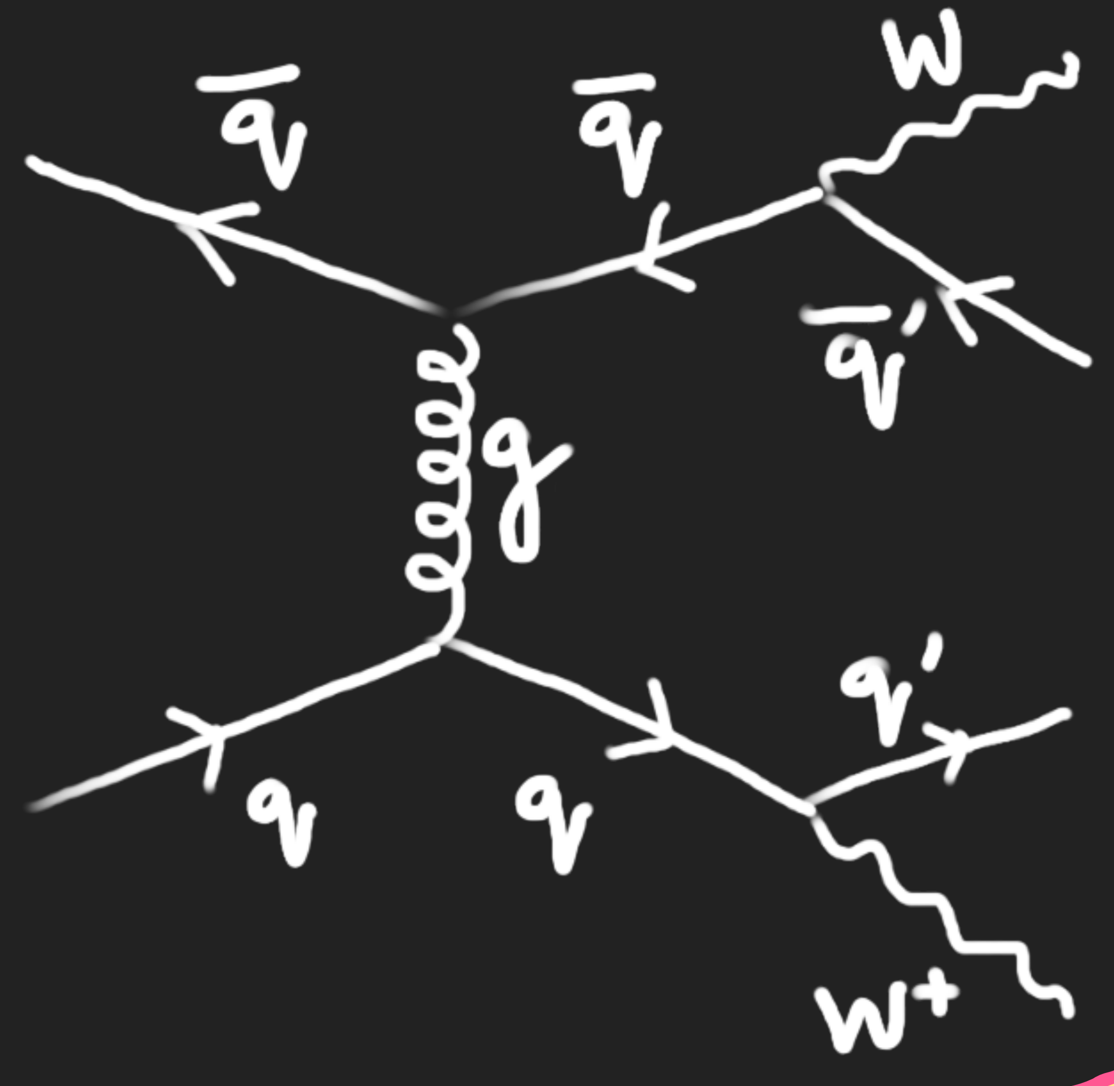

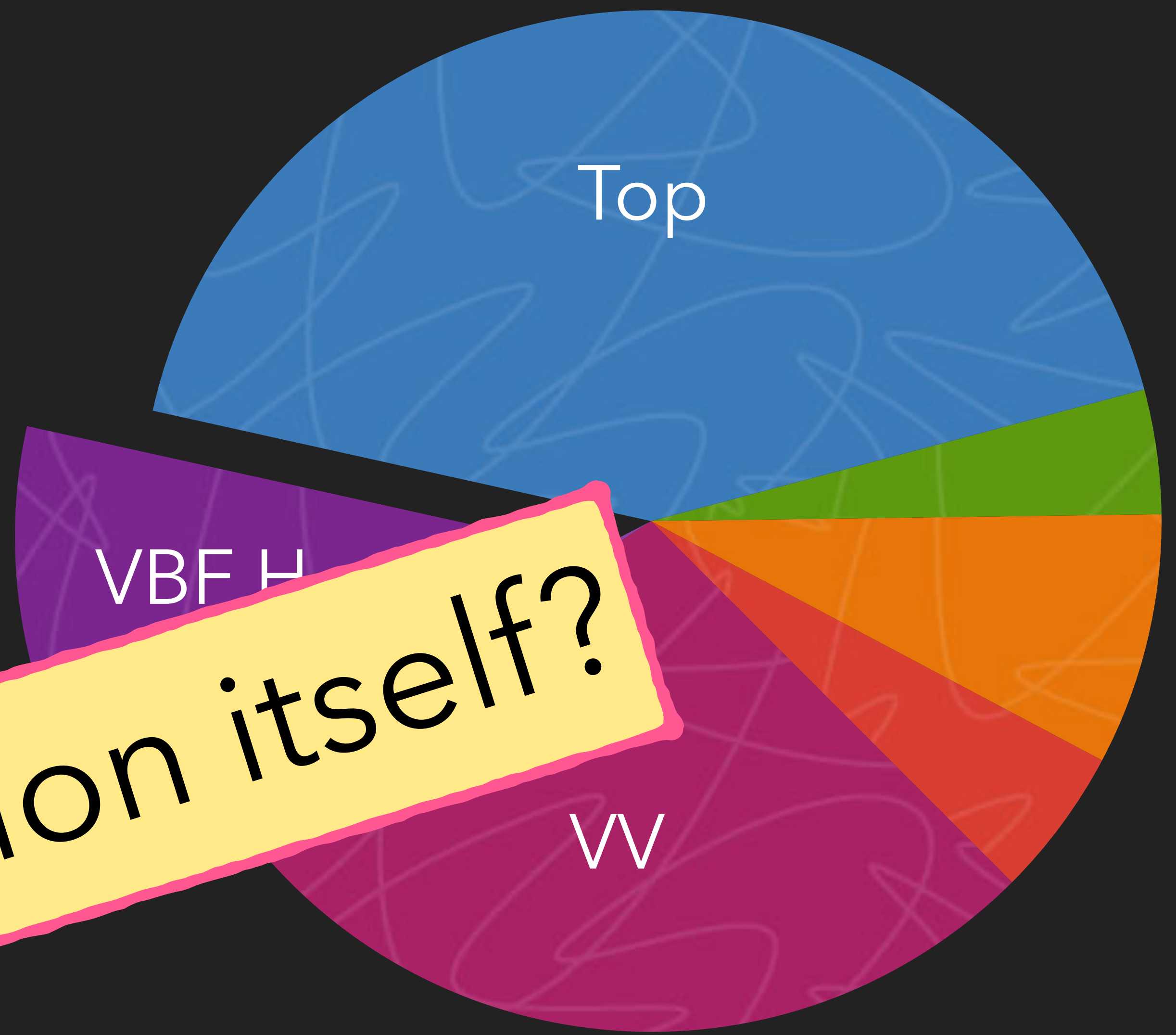

- SR is a **very narrow** VBF isolating phase space
- Raw modelling uncertainties comparable to th… # signal events – need to be signifi… reduced in a data-driven …

Can we estimate these from the Signal Region itself?

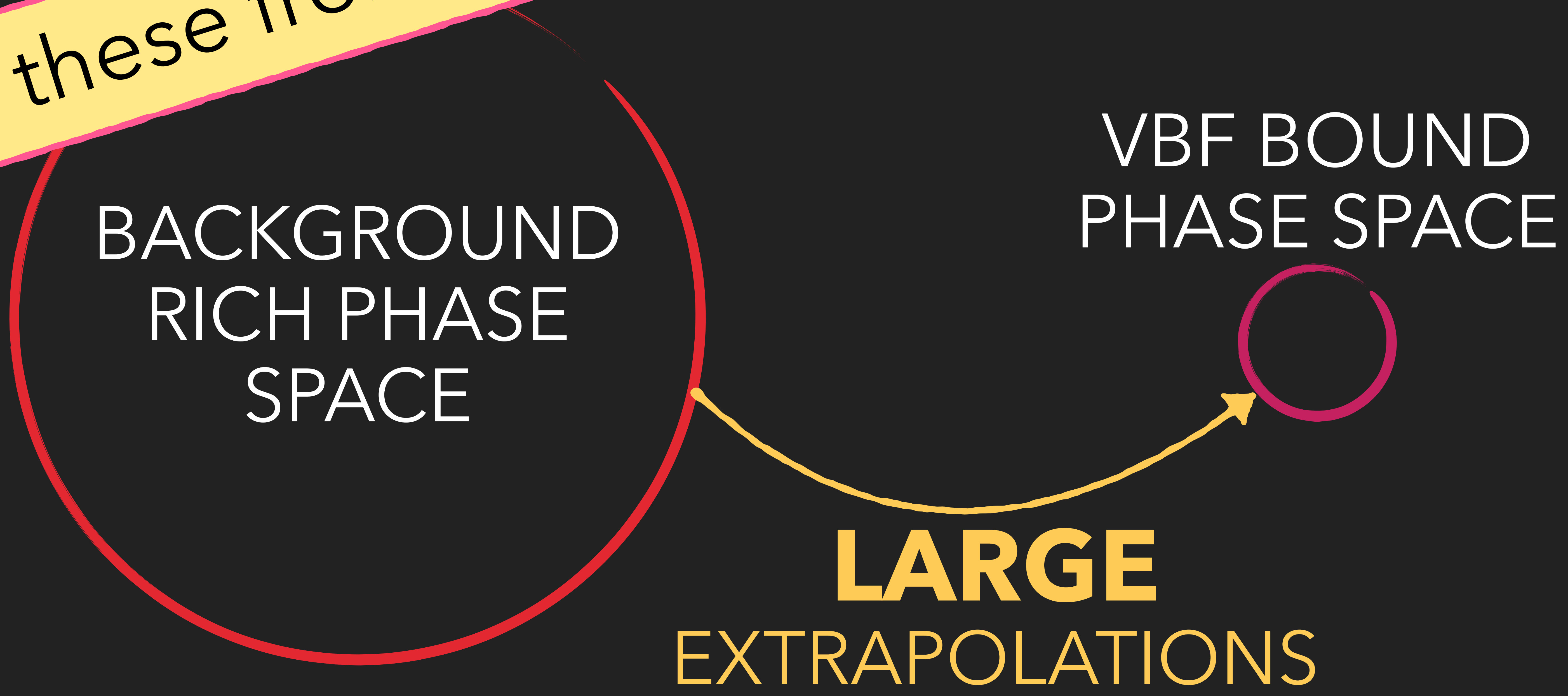

Signal-Background Classification

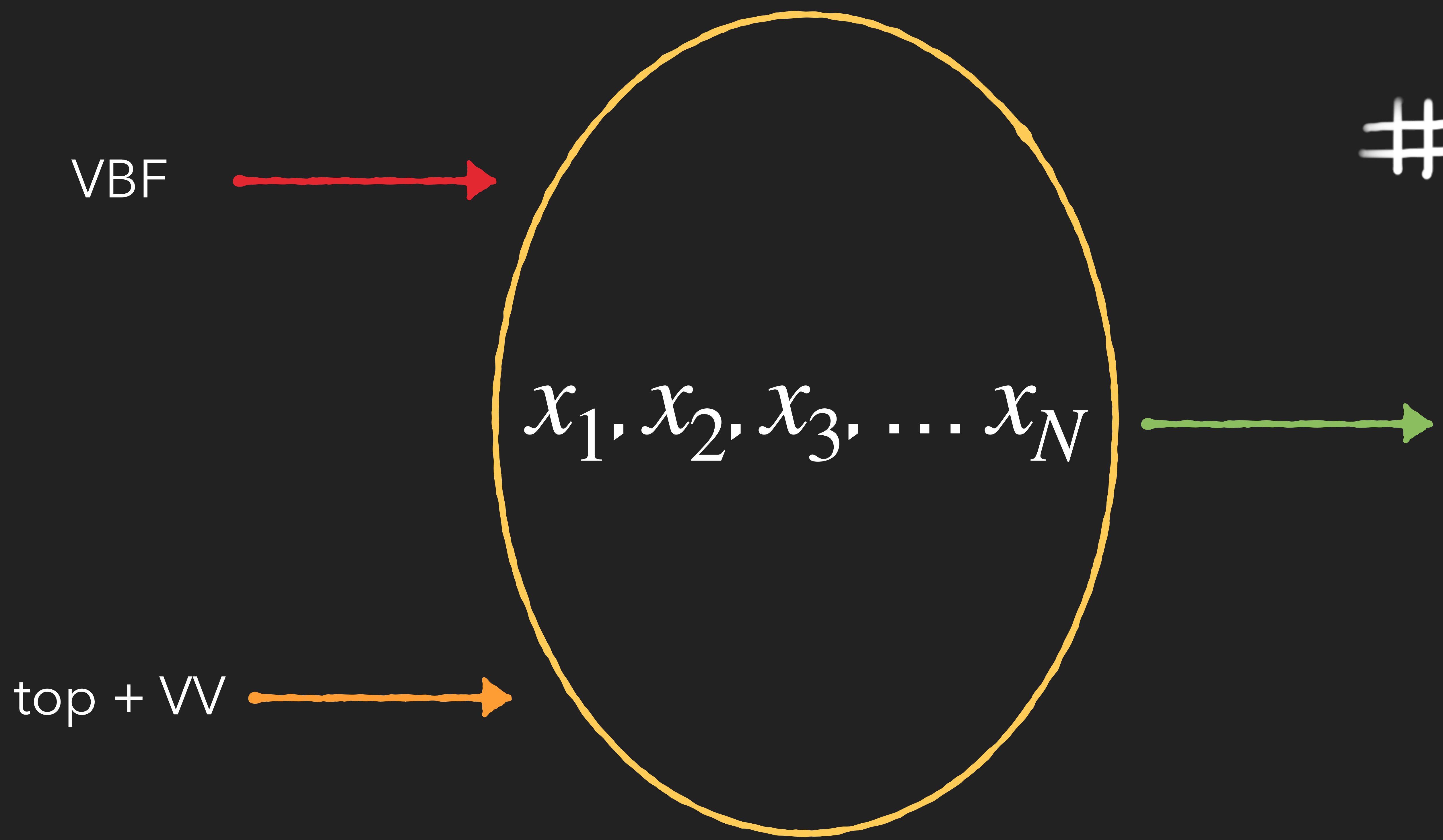

Boosted Decision Tree trained with
a **minimal** set of input variables
to classify VBF against top and VV

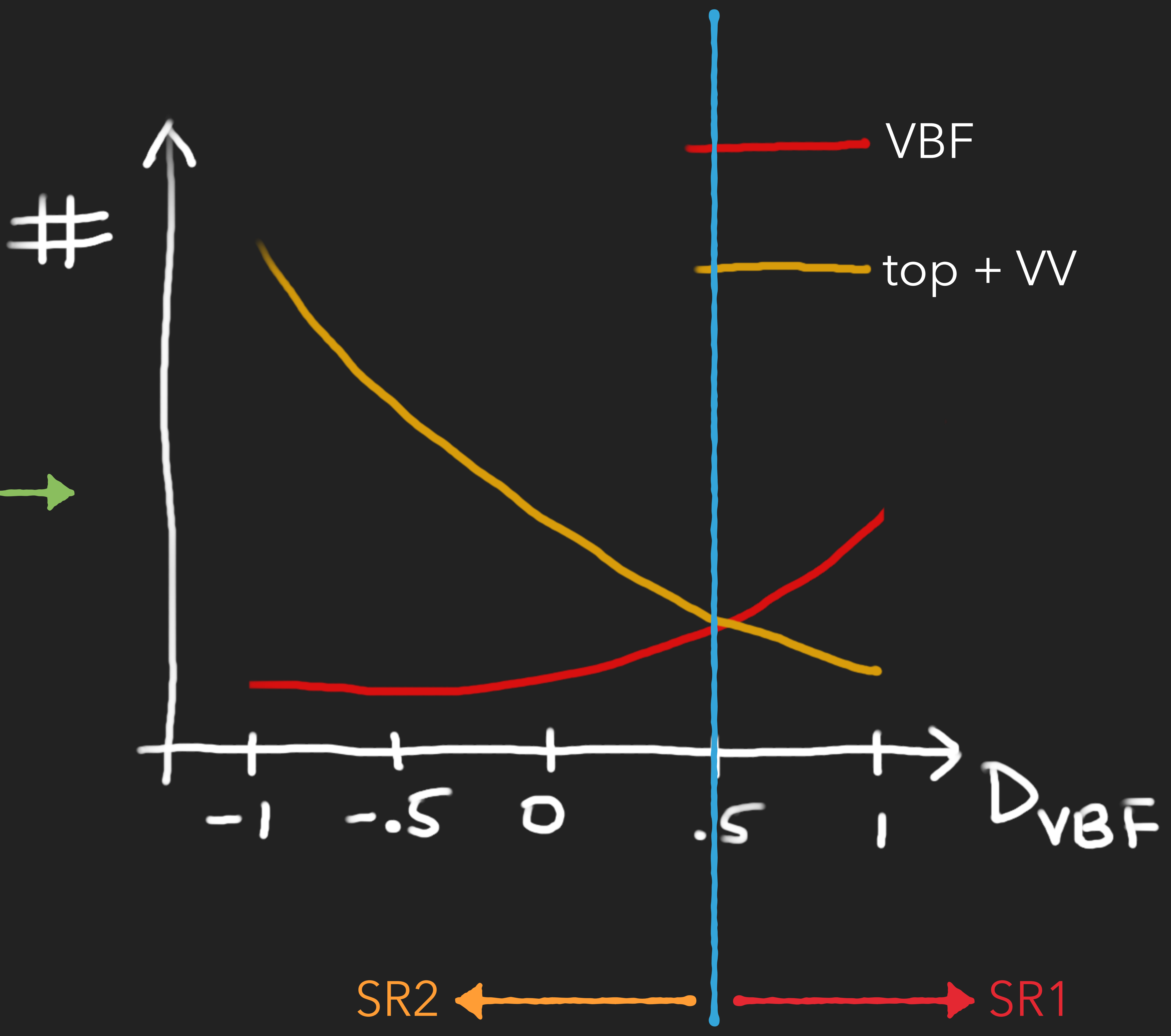

Signal Sensitivity

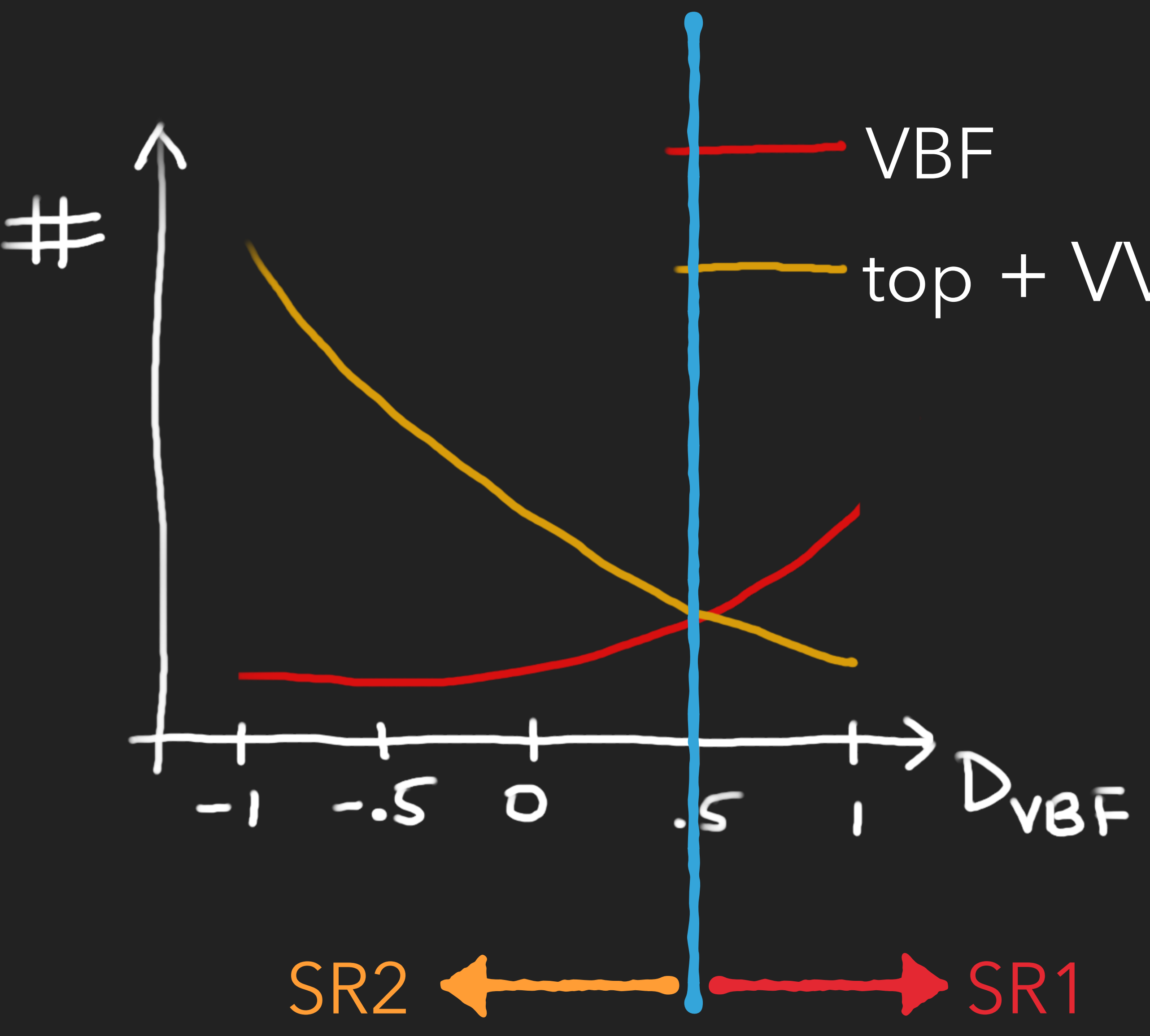

- D_{VBF} serves a two-fold purpose
  - Allows a data-driven estimation of the Top and VV bkgs from within the targeted phase space
  - Adds sensitivity to VBF signal
- No explicit cuts made on BDTs. SR1 and SR2 share signal and bkg norm factors in the simultaneous fit.
- All of SR is measured!

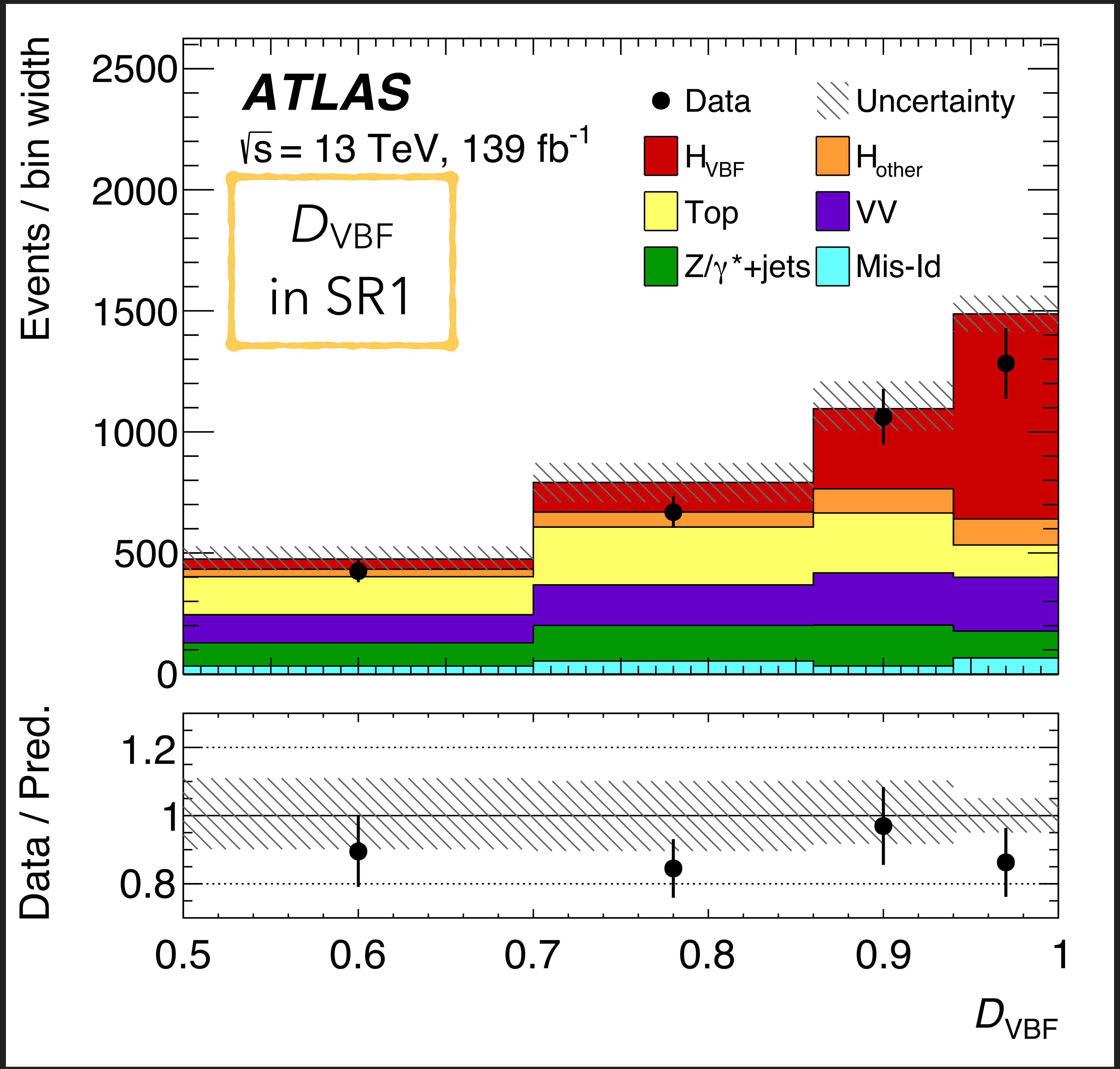

Background Sensitivity

D_{VBF} - VBF signal against Top+VV.

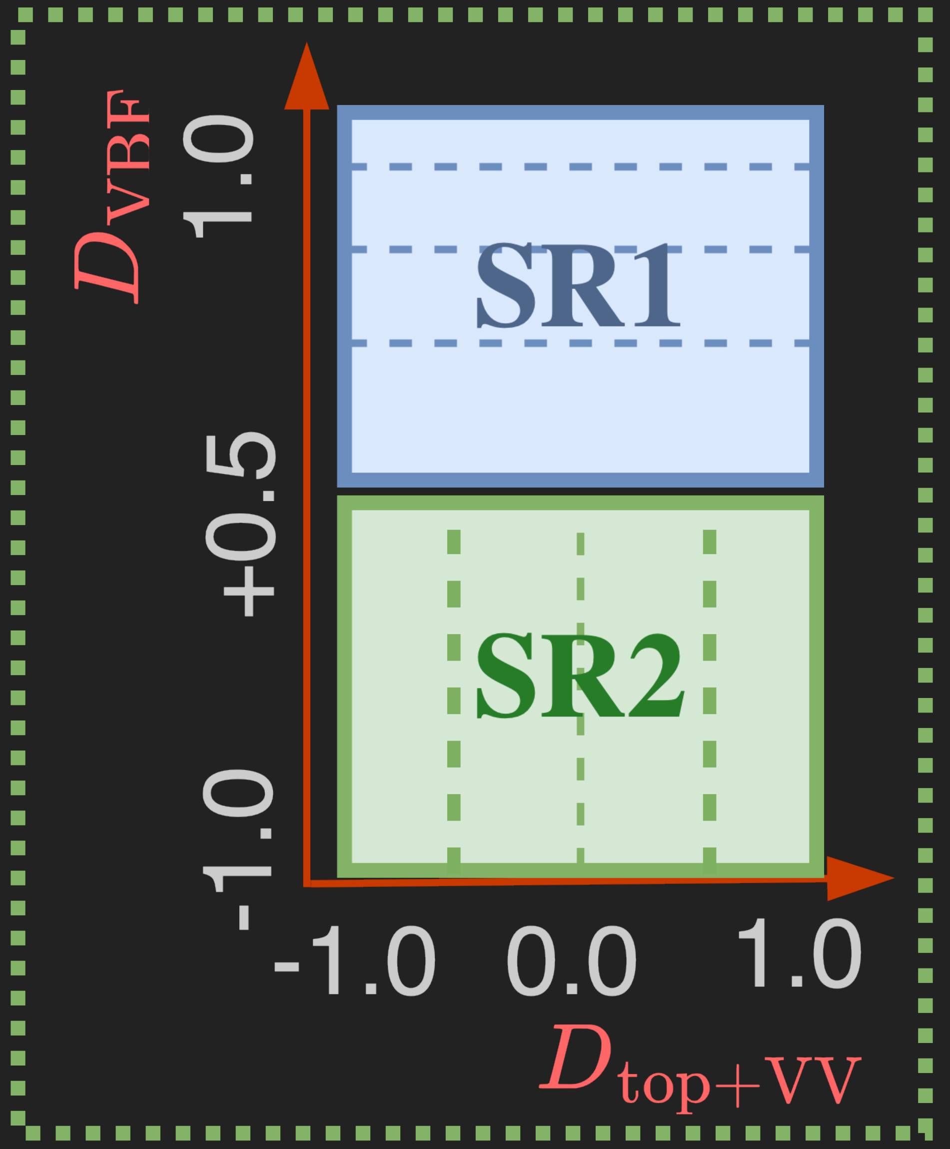

D_{top+VV} - Top+VV against all other processes.

- **Second BDT** trained in the SR to add sensitivity to top and VV estimation
- Top and VV estimated as a sum
- Similar kinematic properties for Top+VV in SR1 and SR2

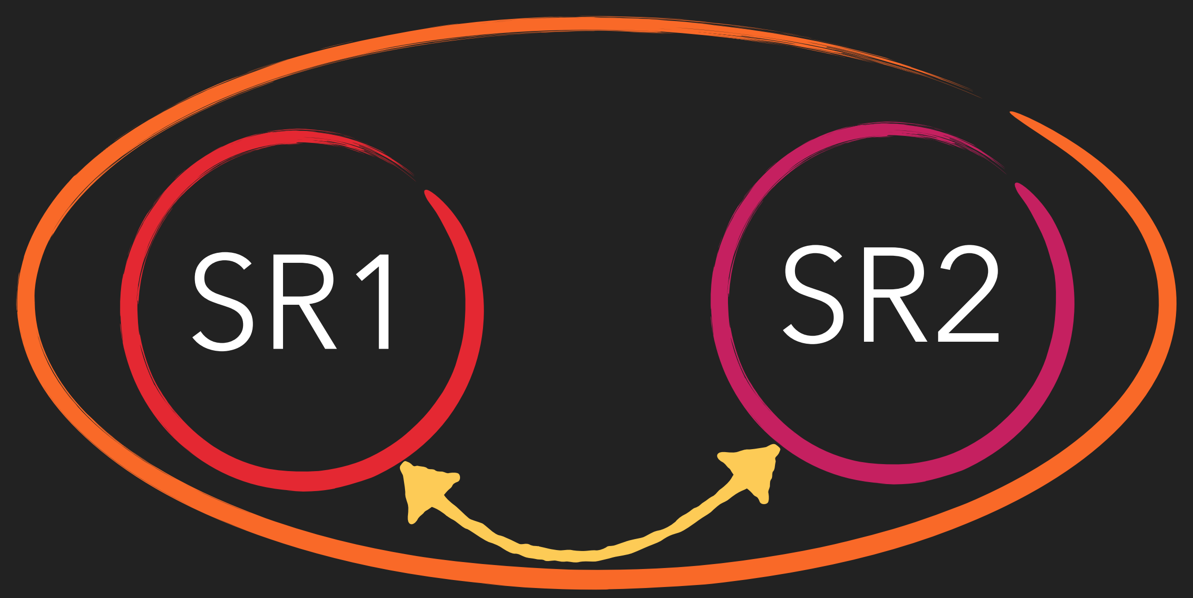

SMALL
EXTRAPOLATIONS

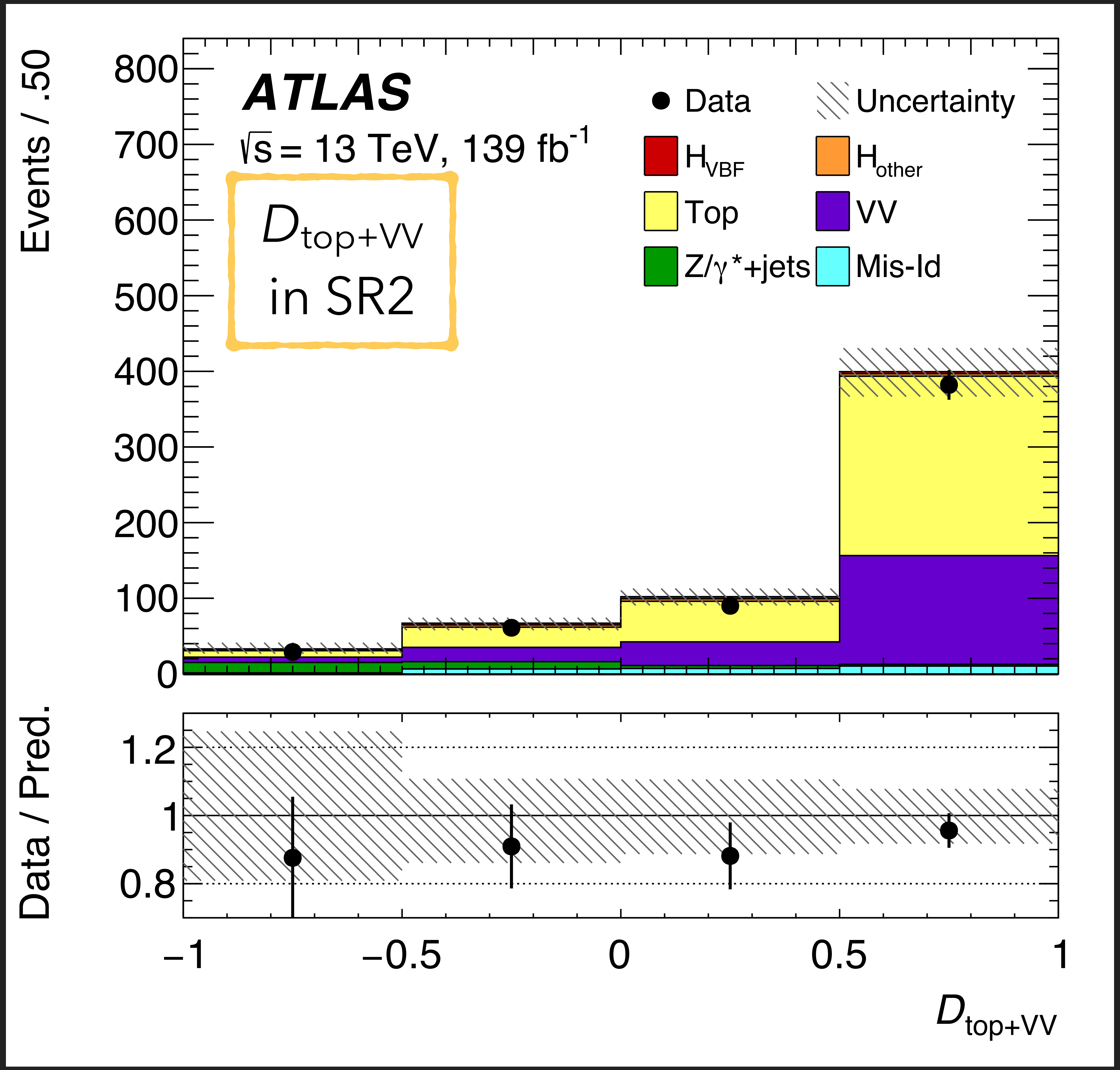

Simultaneous Fit Model

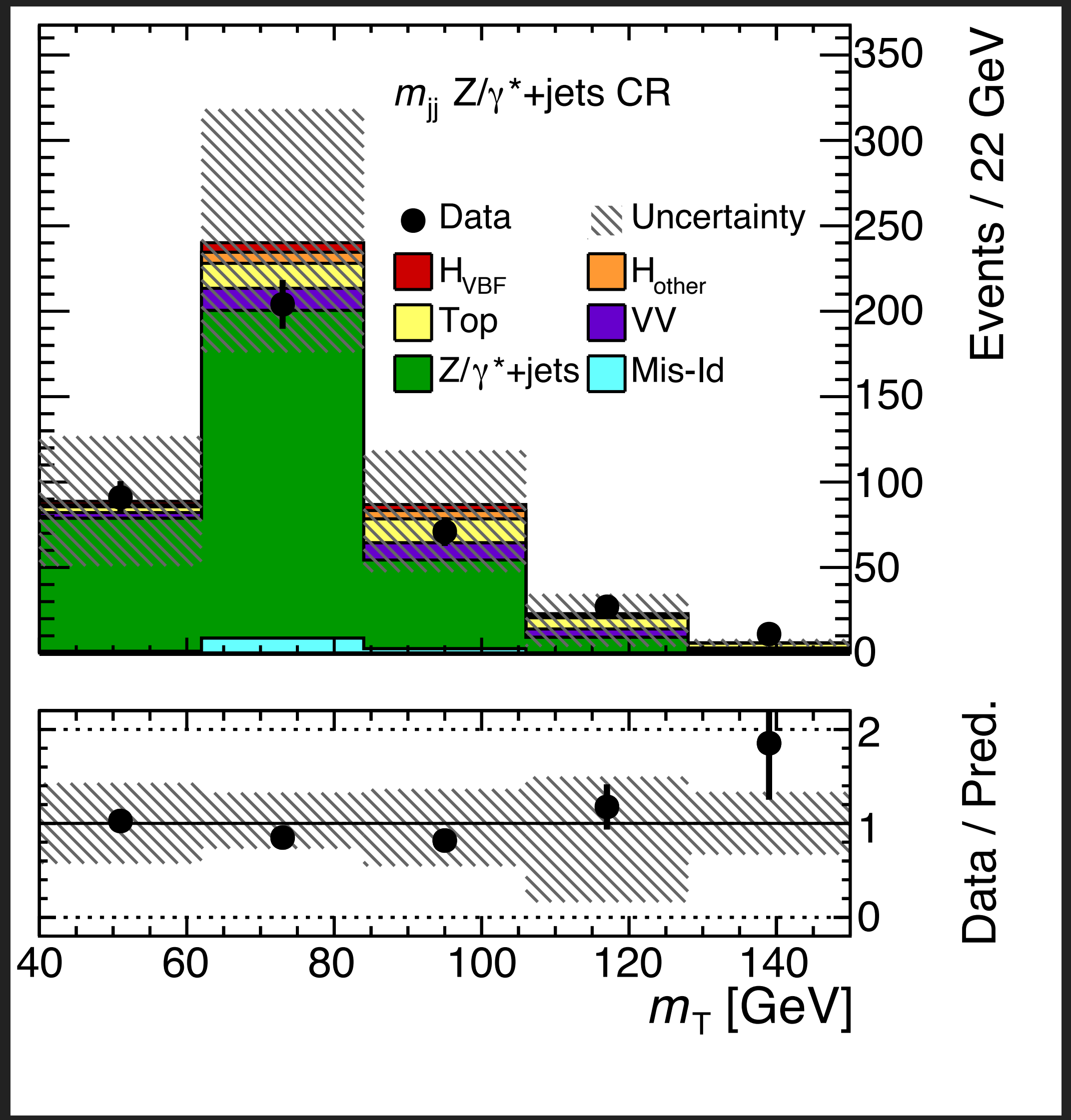

Z→ττ

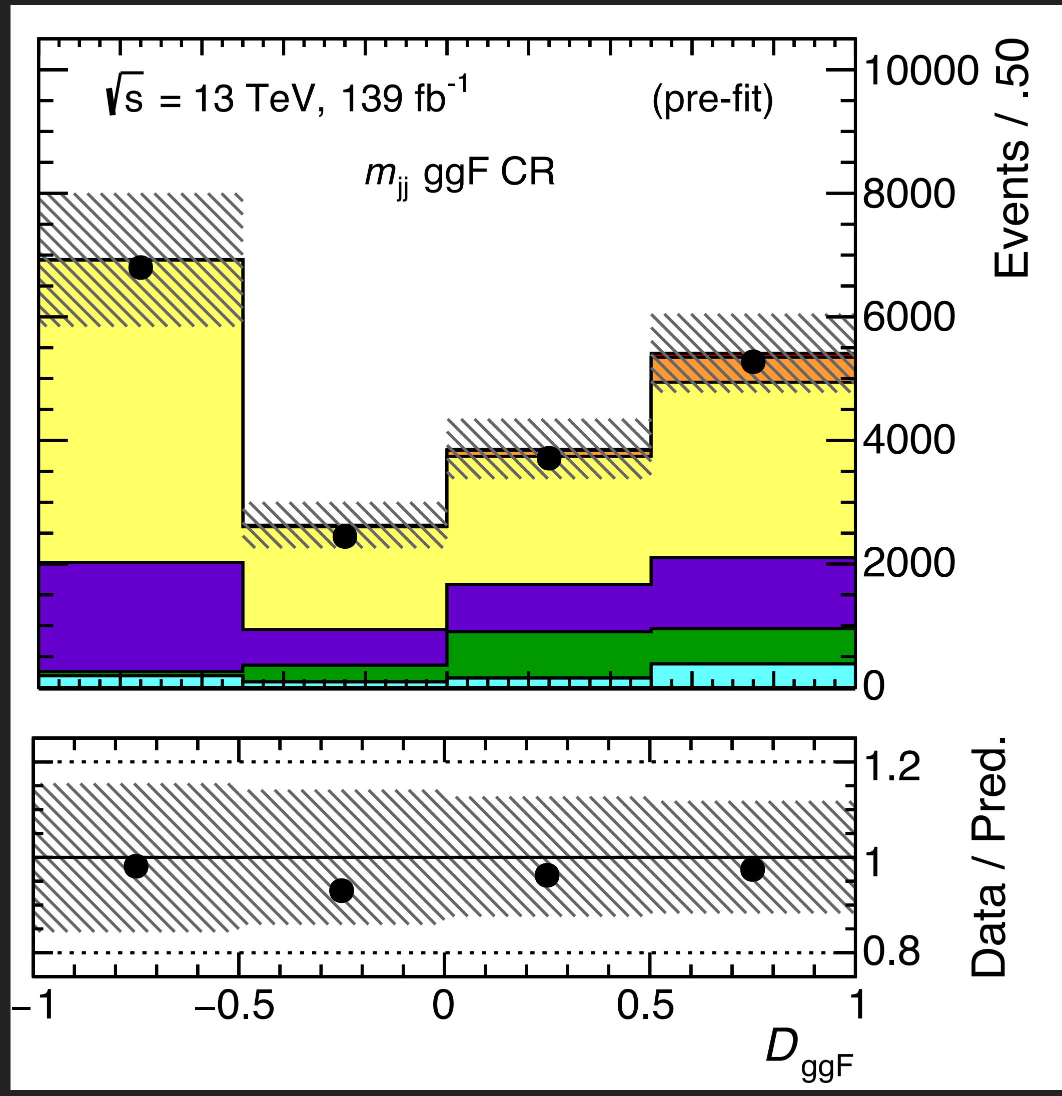

ggF Higgs

Signal Region

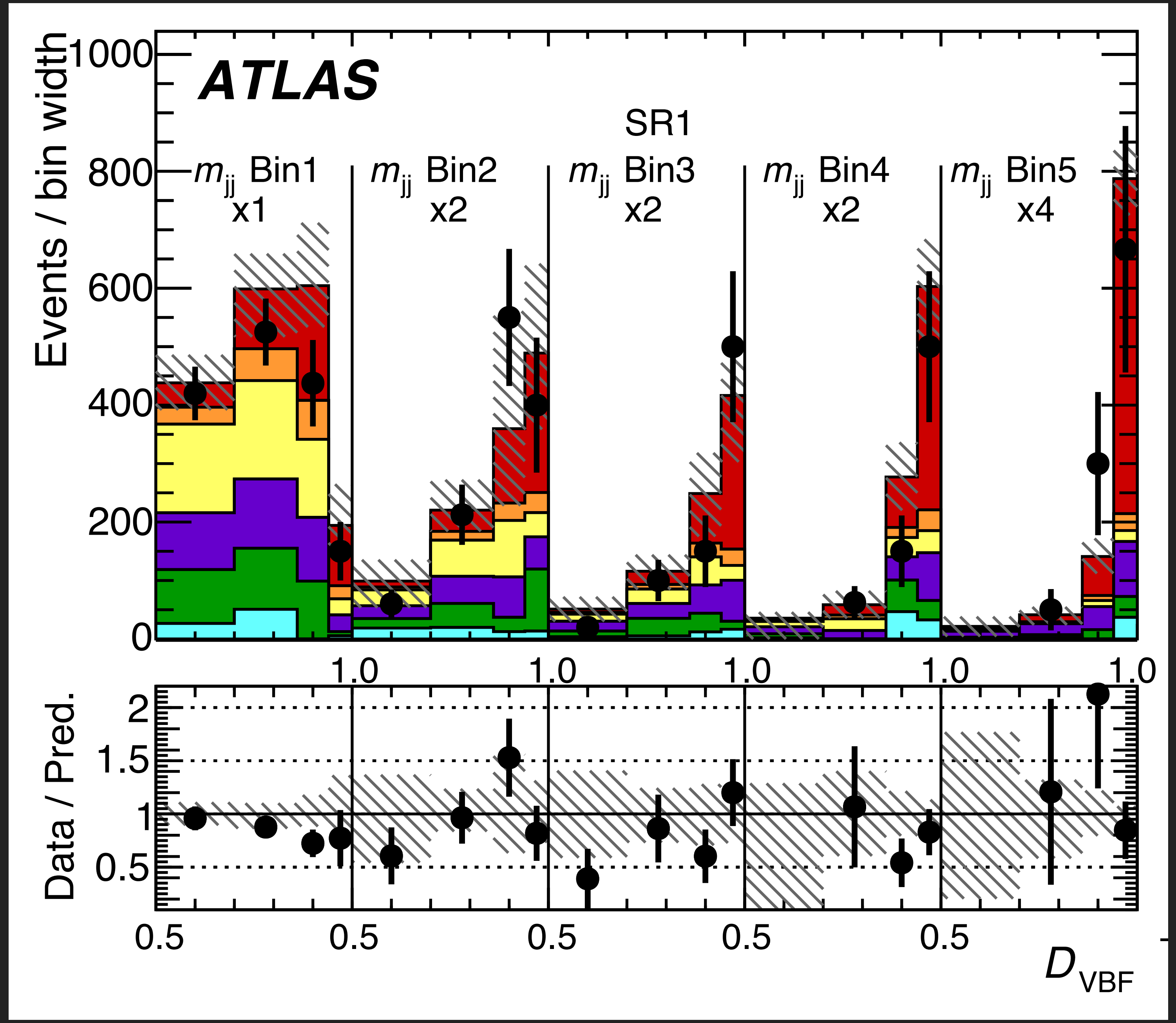

Signal Region 1

Top + VV

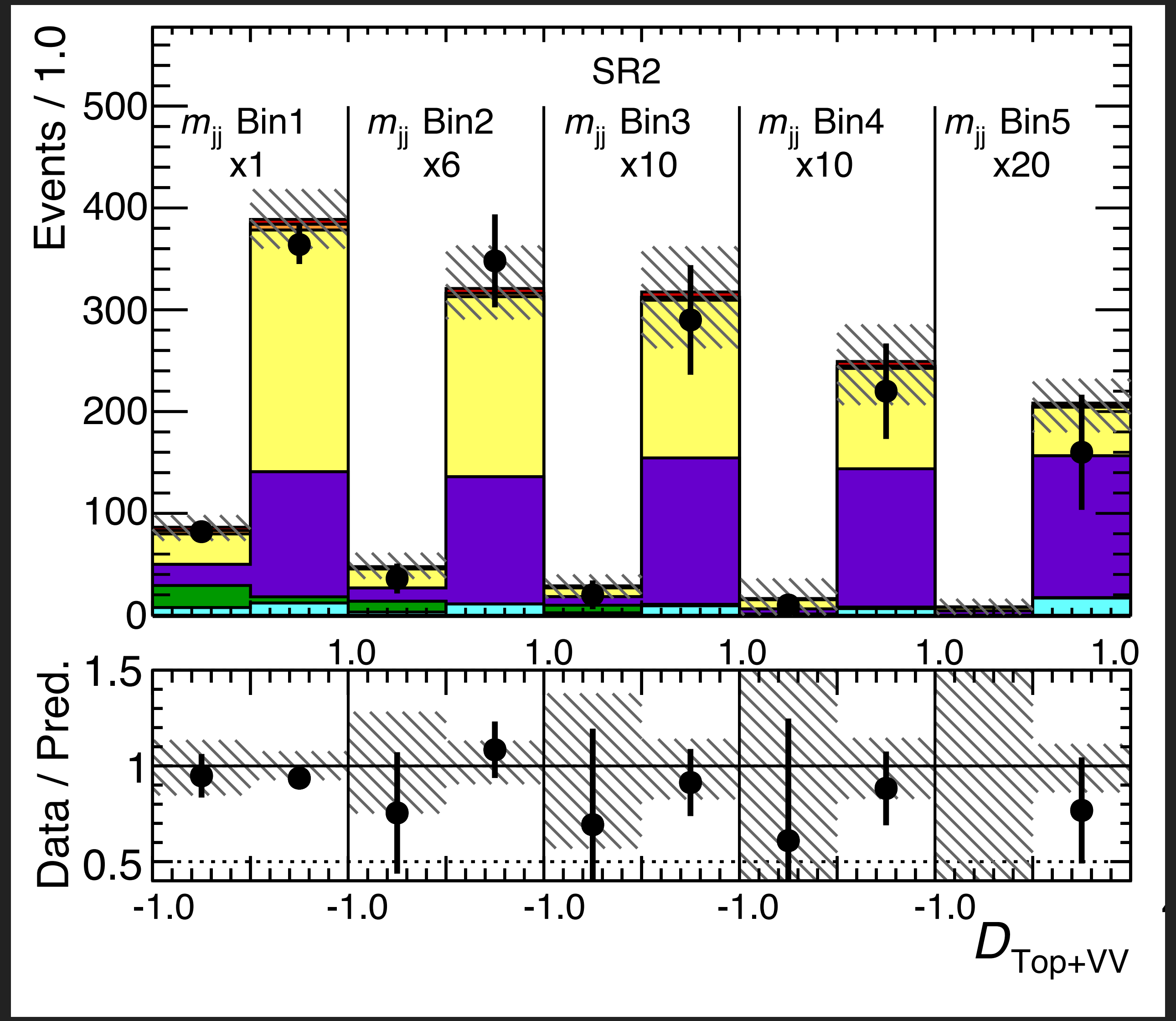

Signal Region 2

Removing Detector Effects – Unfolding

Unfolding done within the simultaneous fit by parametrizing the signal yield as fiducial XS

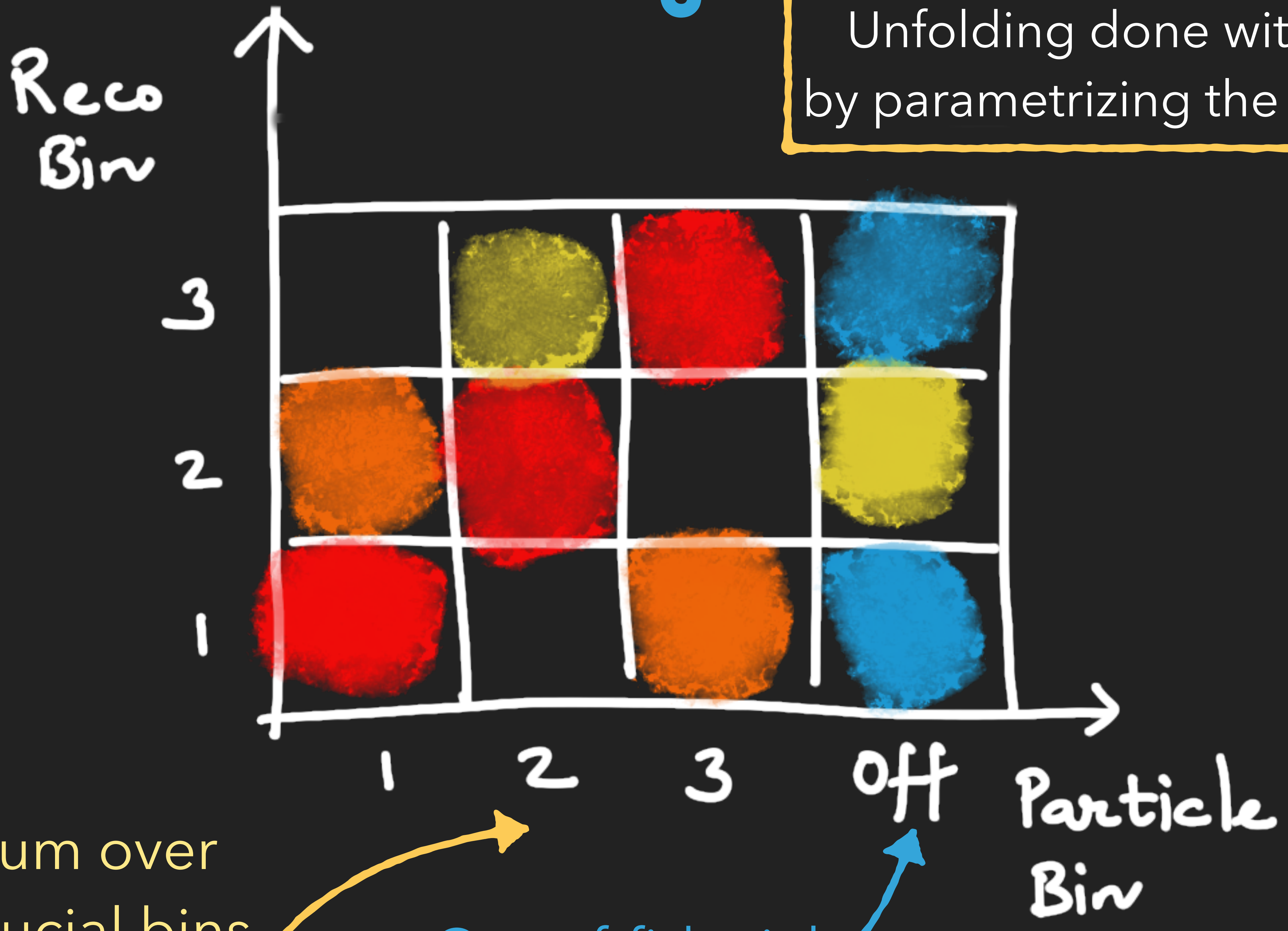

Observed signal events in reco bin

$\frac{d\sigma}{dX}$ **in fiducial bin**

Sum over fiducial bins

Out-of-fiducial

$$N^{\mathrm{SR}}_{\mathrm{signal},i} = \sum_j r_{ij} \cdot \left(1 + f_i^{\mathrm{nonfid}}\right) \cdot \mathscr{T}_i\left(D_{\mathrm{VBF}}, D_{\mathrm{top+VV}}\right) \cdot \mathscr{L} \cdot \sigma_j^{\mathrm{fid}}$$

signal PDF in reco bin

Integrated Luminosity

Reducing Model Dependence

- BDTs trained using SM Monte Carlo predictions – use maximal information from the model
- Necessary to penalize the BDT if it prefers a model

BDTs trained in a broader phase space than measured

$m_{\tau\tau}$	$< m_Z - 25$ GeV
Central jet veto	yes
Outside lepton veto	yes
m_{jj}	$>$ ~~450 GeV~~ 200
$\|\Delta y_{jj}\|$	> 2.1
$\|\Delta\phi_{\ell\ell}\|$	~~< 1.4 rad~~

SR Definition

$x_1, x_2, x_3, \ldots,$

$x_{i-1}, x_i, x_{i+1},$

$\ldots, x_N$

correlated

Training variables for D_{VBF} for integrated XS measurement

Remove x_i and correlated observables

$x_1, x_2, x_3, \ldots x_{i-2},$

$x_{i+2}, \ldots, x_N$

Training variables for D_{VBF} for x_i differential XS measurement

Tests of Model Independence

To test → How sensitive is the method of measurement to the modeling of the signal by the MC?

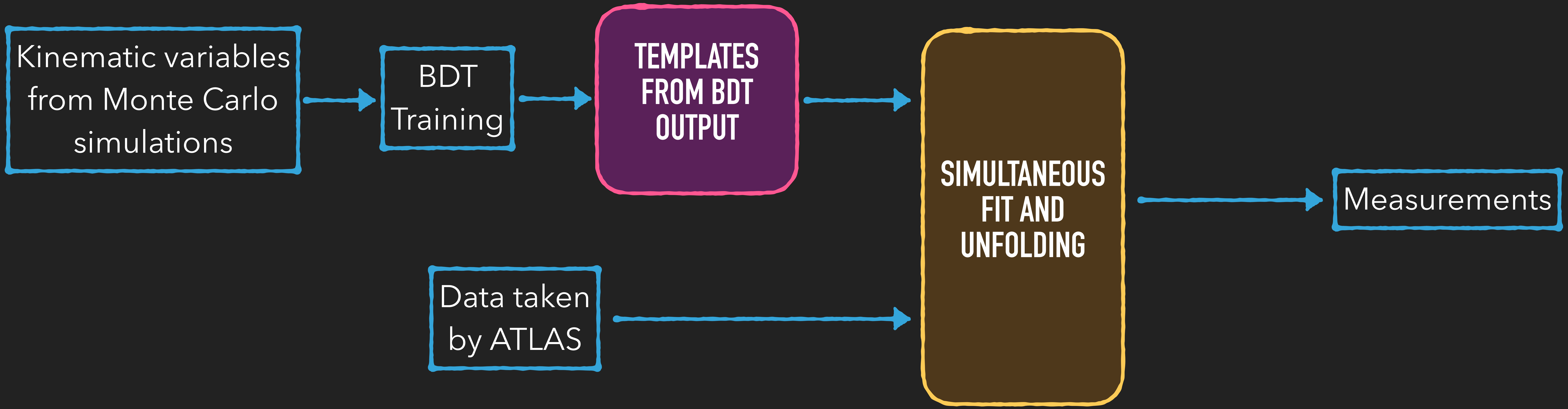

Tests of Model Independence – sensitivity to template shape

The template structure was modified by varying the kinematics used for BDT inputs in two independent tests

1. Re-weight variables the BDTs are sensitive to with BSM effects (physical effect)
2. Vary binned BDT shapes to $n\sigma_{\mathrm{stat}}$ deviations (statistical effect)

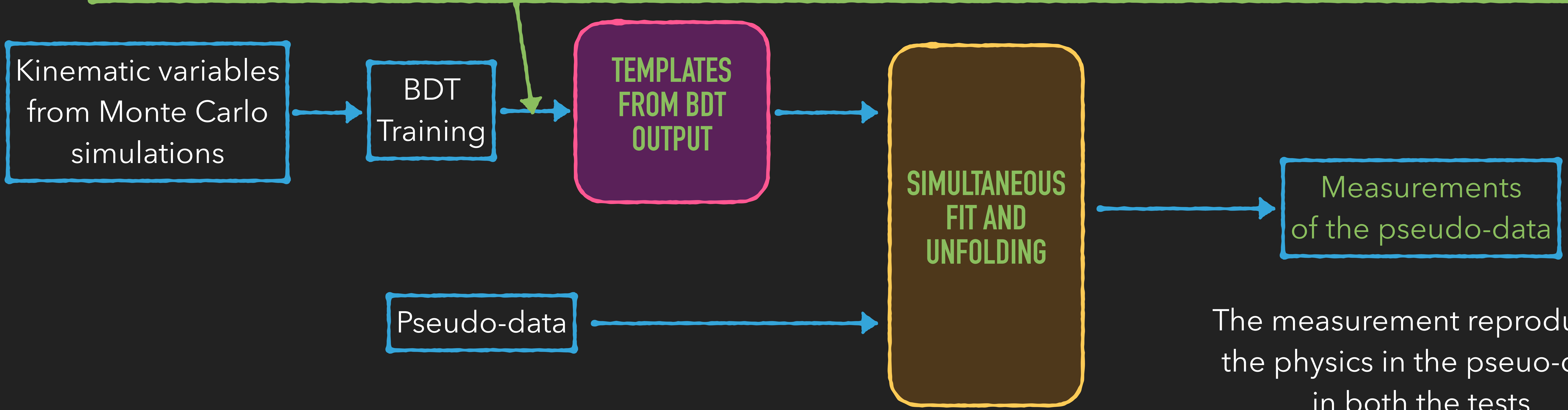

The measurement reproduced the physics in the pseudo-data in both the tests

Tests of Model Independence - accuracy of measurements

Multiple tests of the overall fit structure showed no bias towards the MC prediction used to train the BDTs and to build the fit templates. The measurement is model independent!

Integrated Fiducial Cross-Section

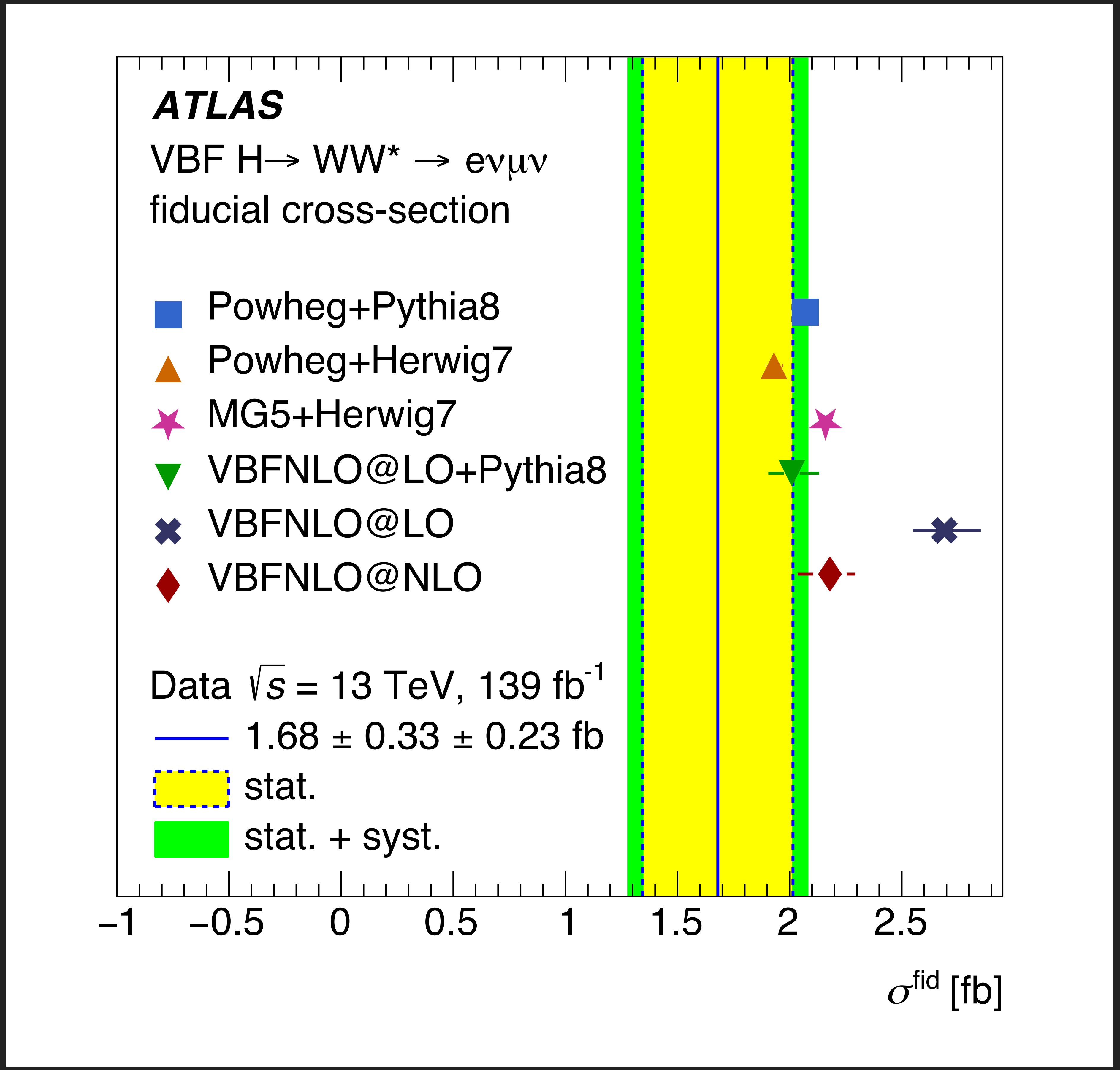

Integrated fiducial cross section measured with 23% error

Result limited by data statistics

Integrated Fiducial Cross-Section

Different Parton Shower models

EW and QCD @ LO vs NLO

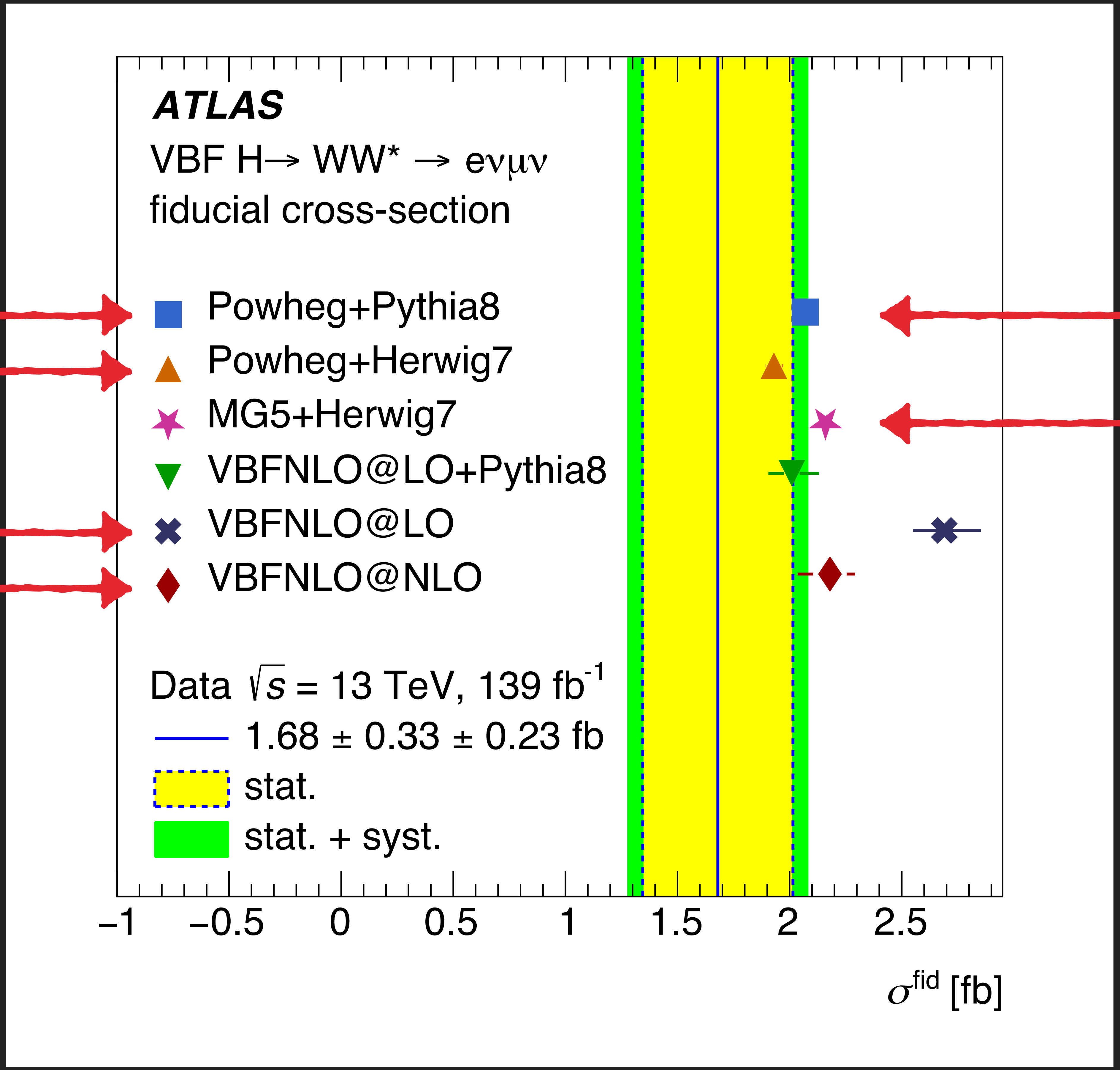

EW @ NLO vs LO

Different Parton Shower and Underlying Event models

Measured XS compared to theoretical predictions using different MC simulation models at varying orders of EW and QCD couplings

Integrated Fiducial Cross-Section

Eur. Phys. J. C (2023) 83:667

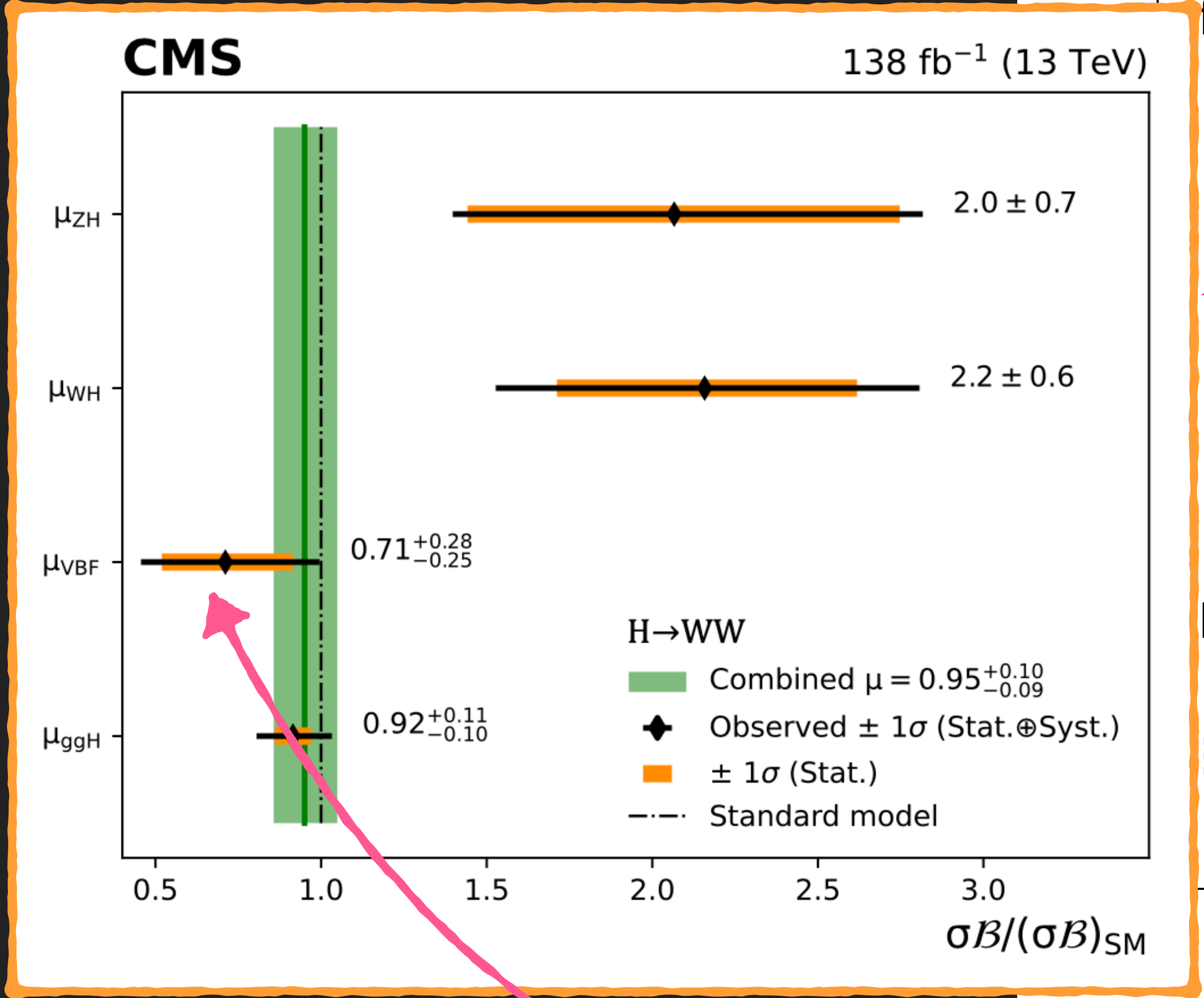

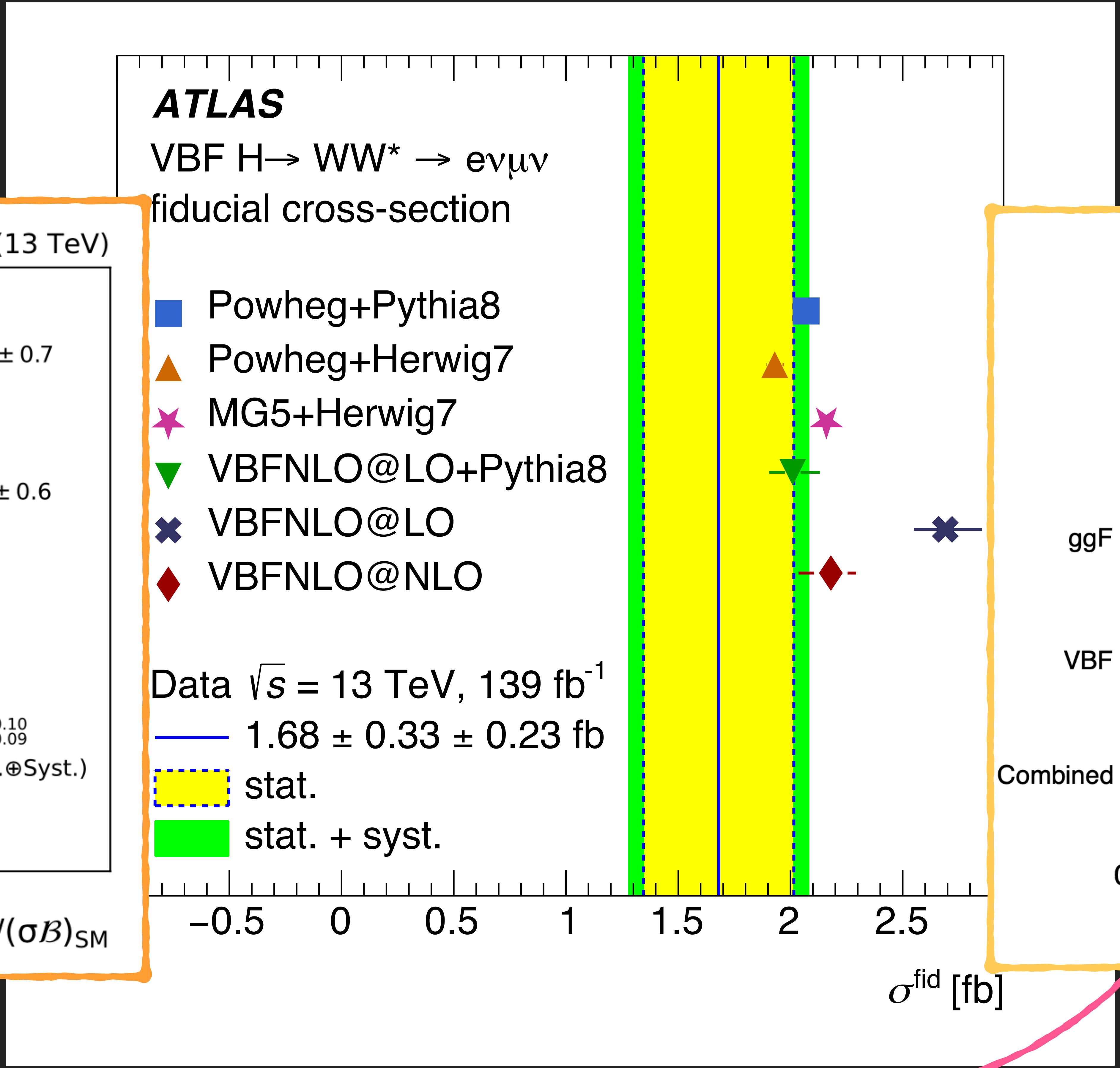

Phys. Rev. D **108**, 032005

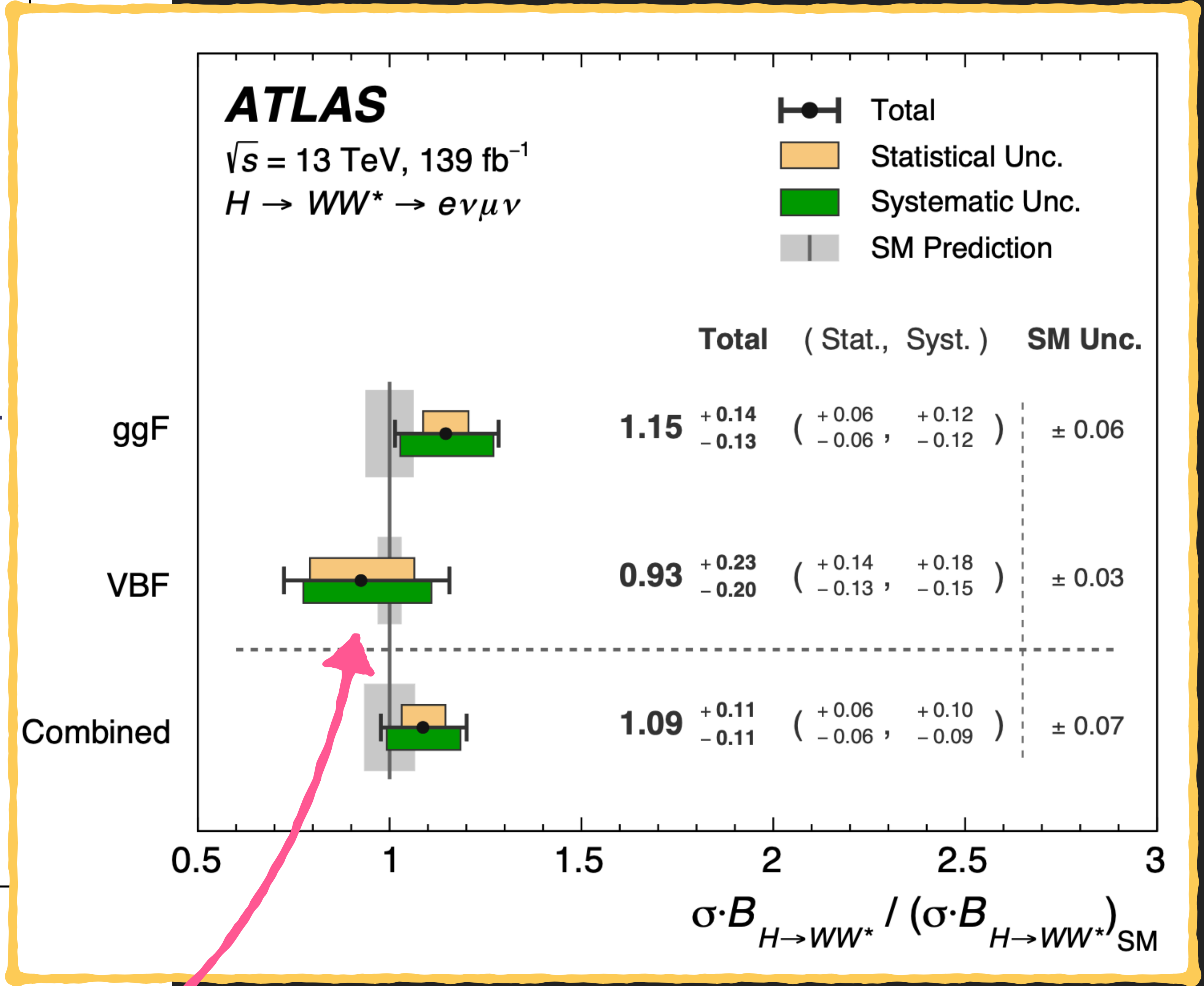

Measured XS smaller than predictions – consistent with independent measurements in similar phase spaces

Differential Cross-Sections

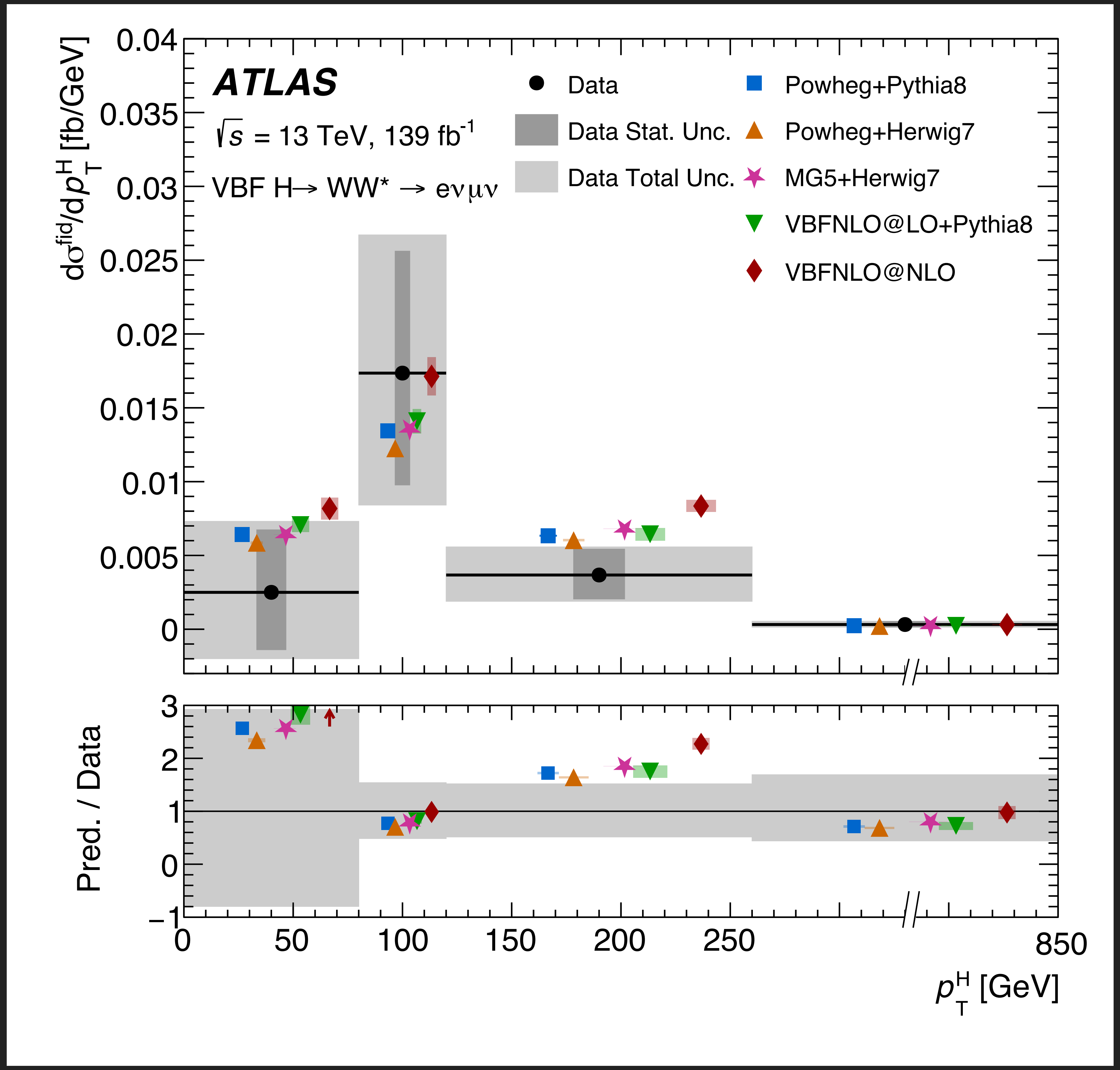

$$p_T^H = |\mathbf{p}_T^\mu + \mathbf{p}_T^e + \mathbf{p}_T^{miss}|$$

Observables unfolded:

1. m_{jj}
2. m_{ll}
3. $|\Delta Y_{jj}|$
4. $|\Delta Y_{ll}|$
5. $\Delta\phi_{jj}$
6. $|\Delta\phi_{ll}|$
7. Leading jet p_T
8. Sub-leading jet p_T
9. Leading lepton p_T
10. Sub-leading lepton p_T
11. p_T^{ll}
12. Higgs p_T
13. $\cos(\theta_\eta^*)$

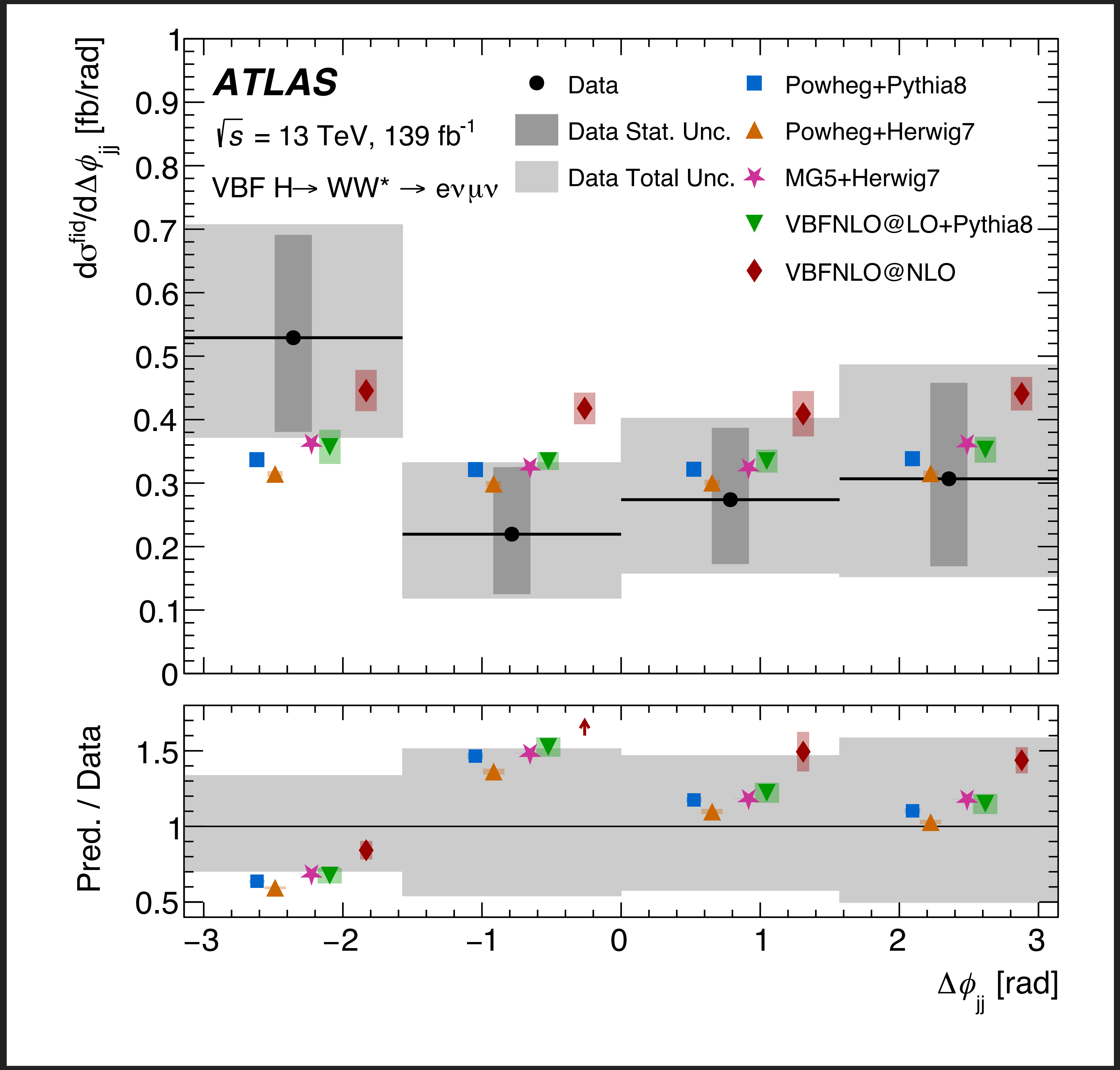

$$\Delta\phi_{jj} = \phi^{j_{\eta>}} - \phi^{j_{\eta<}}$$

13 observables measured in total! Both, lepton-like and jet-like

Uncertainties

- Unfolding keeps the signal modeling systematics under control
- Top induced and diboson modeling systematics sub-leading
- ggF estimated from data and modeling uncertainty under control
- Biggest detector systematic from jets and E_T^{miss} reconstruction
- Measurement precision limited by data statistics

Source	Uncertainty [%] σ^{fid}
Signal modeling	5
Signal parton shower	< 1
$t\bar{t}$ modeling	6
WW modeling	4
Z/γ^*+jets modeling	4
ggF modeling	5
Mis-Id background	< 1
Jets & Pile-up & E_T^{miss}	5
b-tagging	< 1
Leptons	1.5
Luminosity	1.5
MC statistics	5
Total systematics	13
Data statistics	20
Total uncertainty	23

Introduction to Effective Field Theory

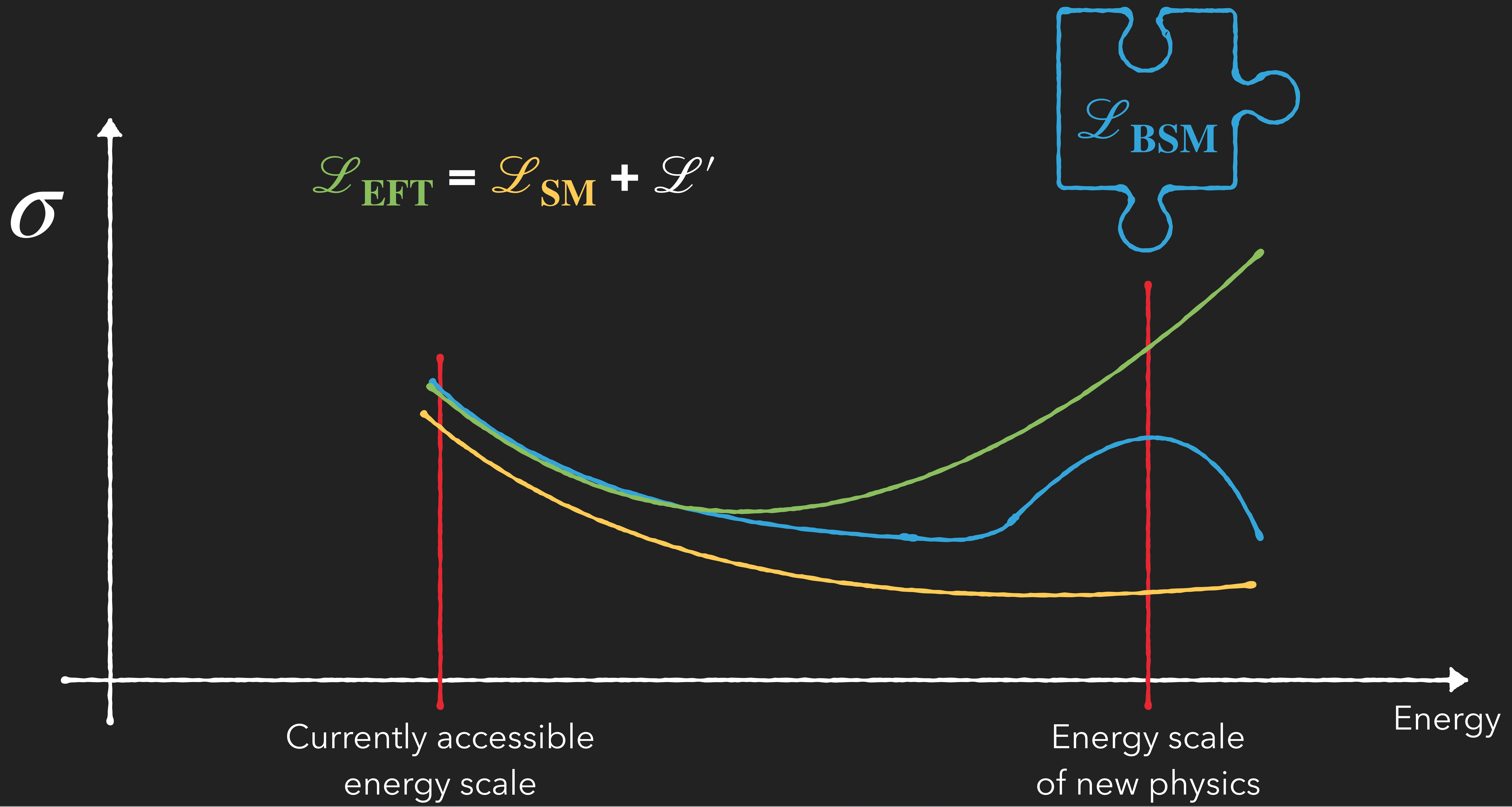

Introduction to Effective Field Theory

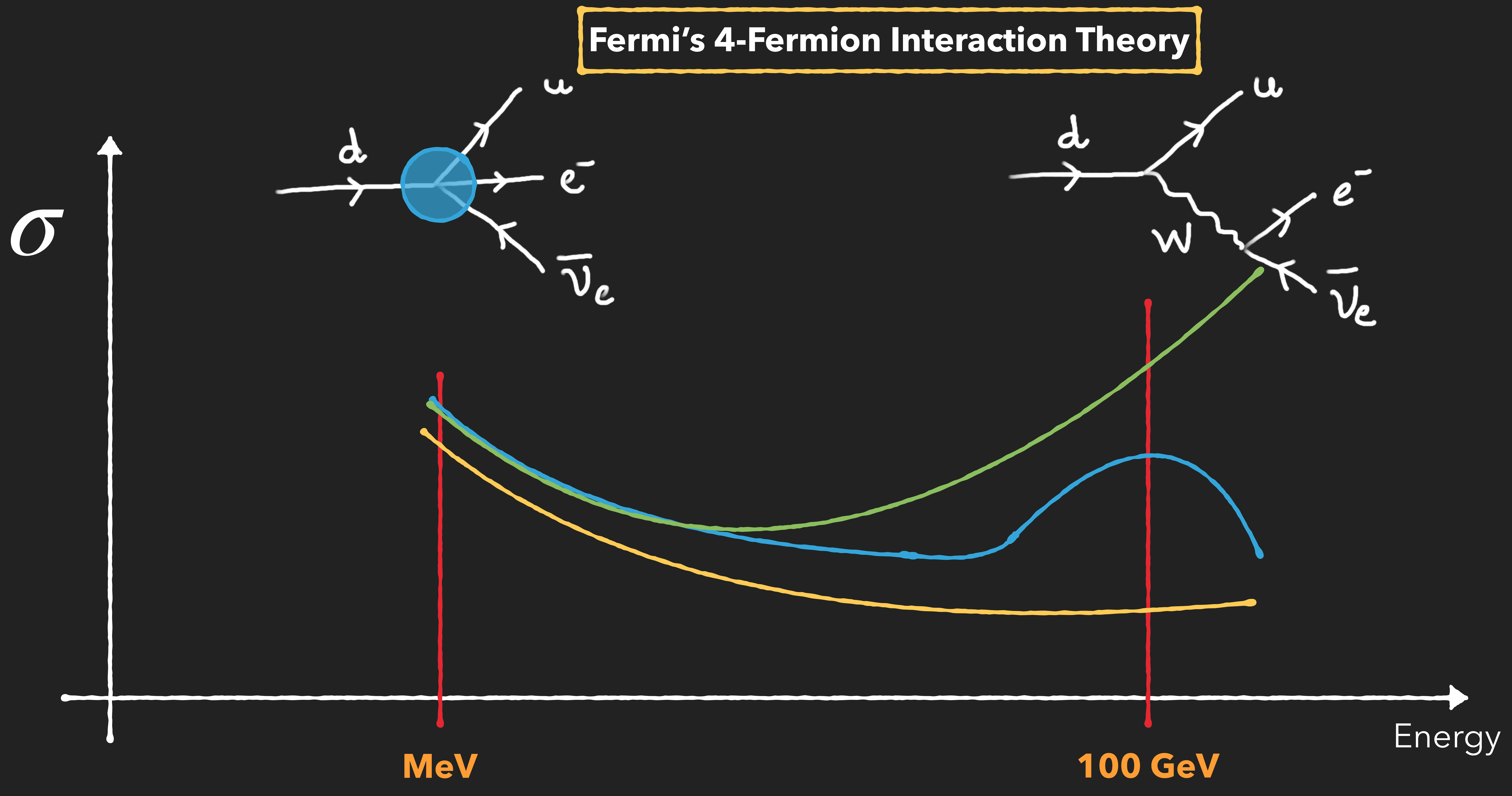

EFT Interpretation

- Interpreting the measurements in the formalism of Standard Model Effective Field Theory (arXiv:1709.06492)

Wilson coefficient
Strength of the operator

EFT Operator

$$\mathscr{L}_{\text{EFT}} = \mathscr{L}^{(4)}_{\text{SM}} + \sum_d \sum_i \frac{c_i^{(d)}}{\Lambda^{(d-4)}} O_i^{(d)}, \text{ for d > 4.}$$

Cut-off energy scale

$$\sigma - \sigma_{\text{SM}} \propto 2\frac{c}{\Lambda^2} \text{Re}\left(\mathscr{M}^*_{\text{SM}}\mathscr{M}\right) + \frac{c^2}{\Lambda^4} |\mathscr{M}^2|$$

Linear/Interference Term

Quadratic/Pure-BSM Term

EFT Interpretation

- Interpreting the measurements in the formalism of Standard Model Effective Field Theory (arXiv:1709.06492)
- Setting constraints on Wilson coefficients for both CP-even and CP-odd mass dimension-6 EFT operators

Wilson coefficient
Strength of the operator

EFT Operator

$$\mathscr{L}_{\mathrm{EFT}} = \mathscr{L}_{\mathrm{SM}}^{(4)} + \sum_d \sum_i \frac{c_i^{(d)}}{\Lambda^{(d-4)}} O_i^{(d)}, \text{ for d > 4.}$$

Cut-off energy scale

$$\sigma - \sigma_{\mathrm{SM}} \propto 2\frac{c}{\Lambda^2}\mathrm{Re}\left(\mathscr{M}_{\mathrm{SM}}^{*}\mathscr{M}\right) + \frac{c^2}{\Lambda^4}|\mathscr{M}^2|$$

Linear/Interference Term Quadratic/Pure-BSM Term

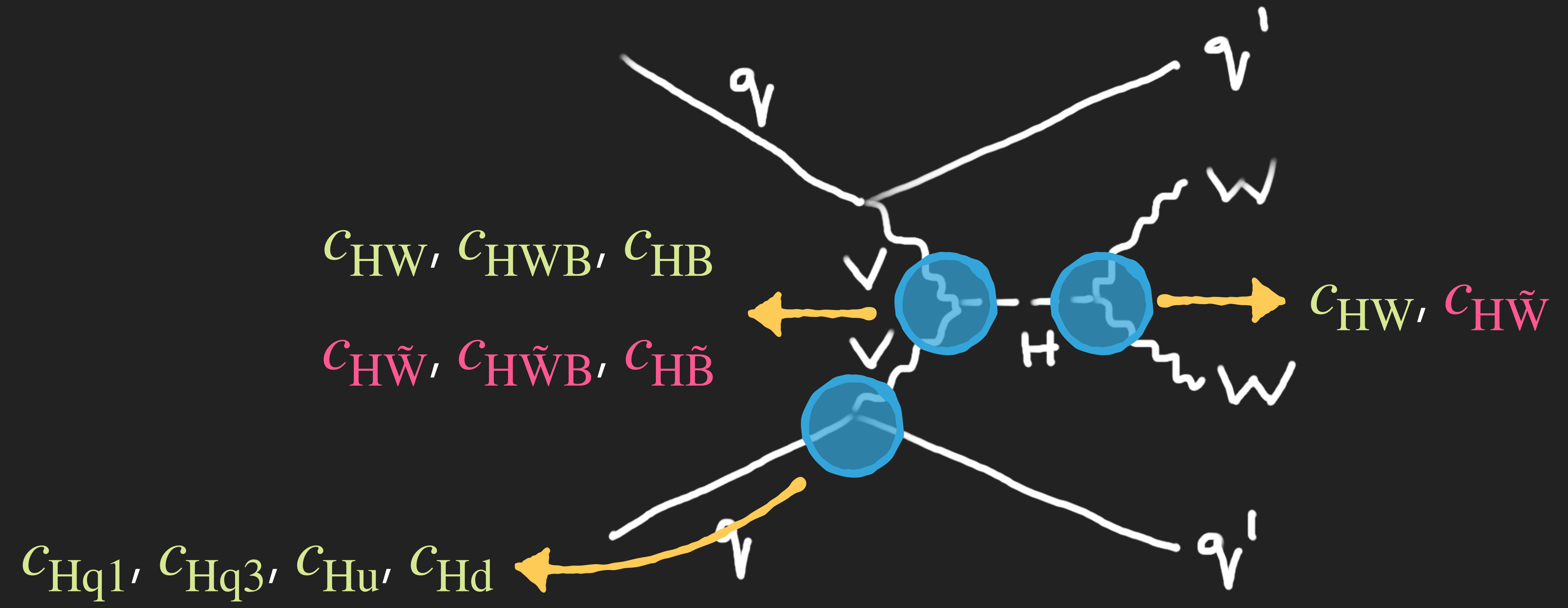

Can affect the VBF production…

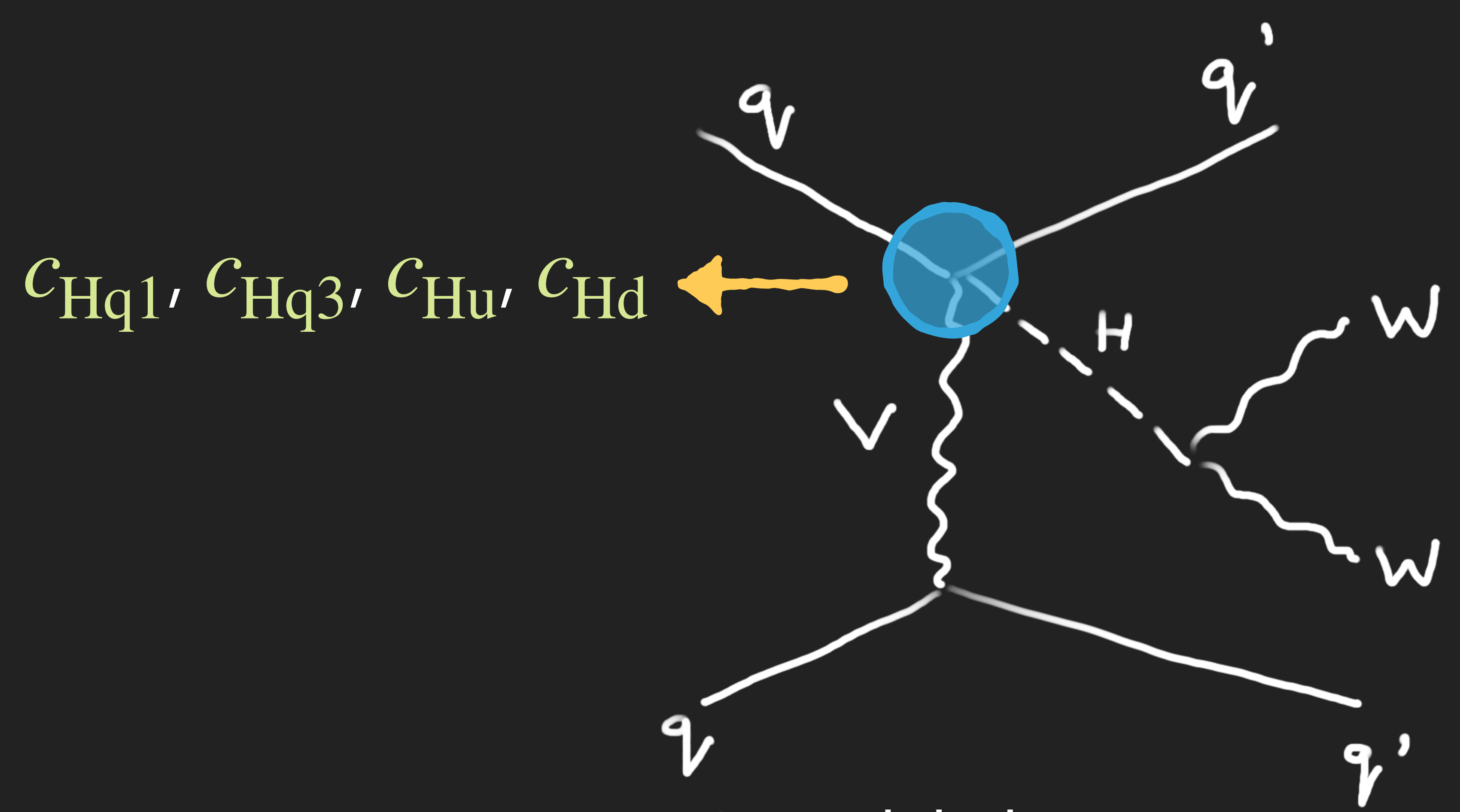

Or add diagrams!

Constraints on Wilson Coefficients

$$\sigma - \sigma_{SM} \propto c \cdot \sigma_{lin} + c^2 \cdot \sigma_{quad}$$

- All limits consistent with with the SM prediction
- Strongest limits on c_{HW}, $c_{H\tilde{W}}$ and c_{Hq3} from linear only parameterization
- Strongest limits on c_{HB}, $c_{H\tilde{B}}$, and c_{Hq3} from lin+quad parameterization
- Shows the impact of the quadratic term (and hence sensitivity to missing higher mass dimension terms)

$$\sigma - \sigma_{SM} \propto 2\frac{c_{dim-6}}{\Lambda^2} \cdot \mathrm{Re}\left(\mathcal{M}^*_{SM}\mathcal{M}_{dim-6}\right) + \frac{c^2_{dim-6}}{\Lambda^4}\left|\mathcal{M}_{dim-6}\right|^2 + 2\frac{c_{dim-8}}{\Lambda^4}\mathrm{Re}\left(\mathcal{M}^*_{SM}\mathcal{M}_{dim-8}\right)$$

same order of energy scale suppression

term **not** included in our parameterization

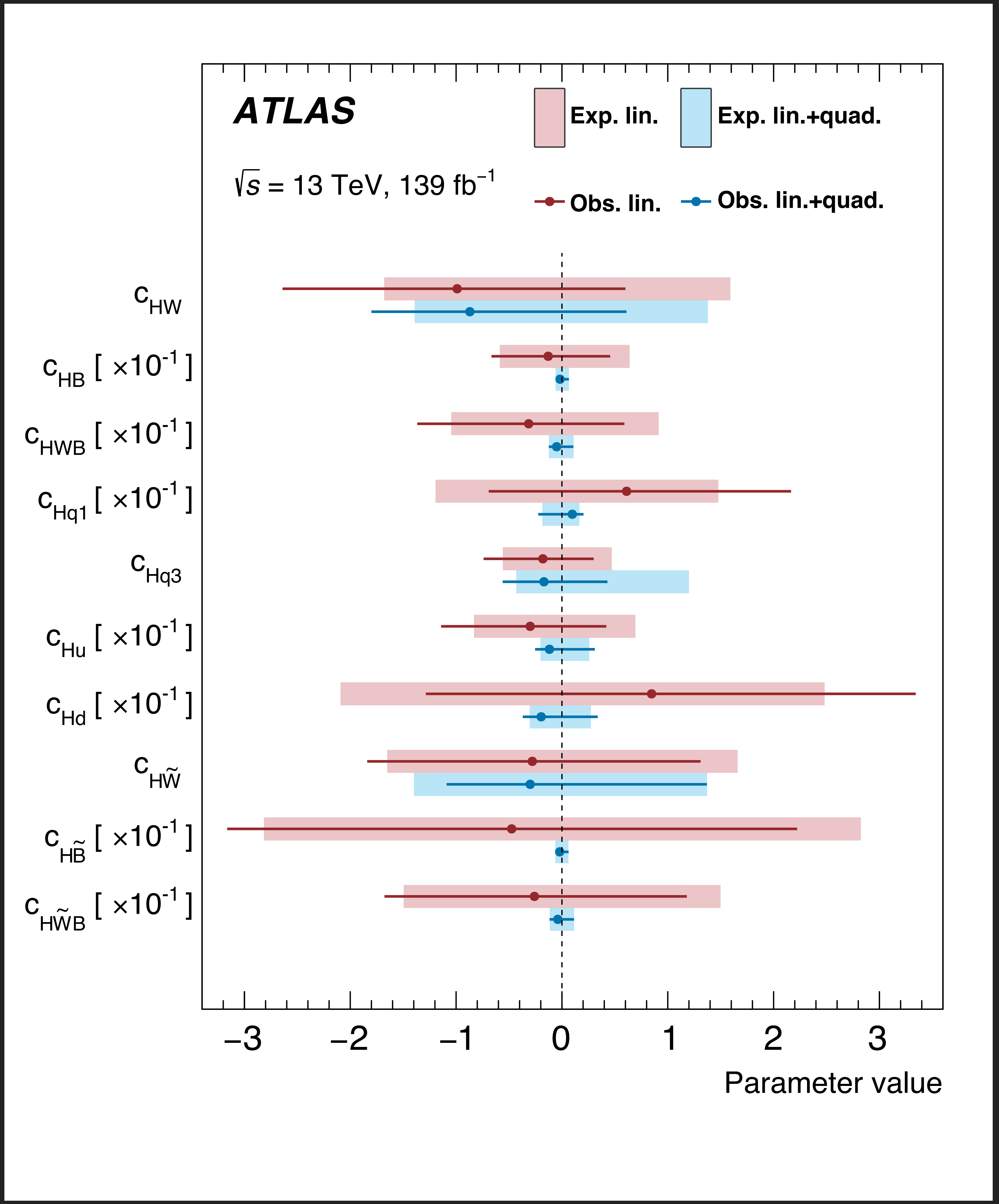

Analysis Method Highlights

- First fully fiducial XS in the VBF H→WW→$e\nu\mu\nu$ channel!
- Achieved a model independent result in a background dominated phase space
- Analysis strategy paves the way for such measurements with exotic signatures
- Indispensable while using large datasets when systematics will be the limiting factors

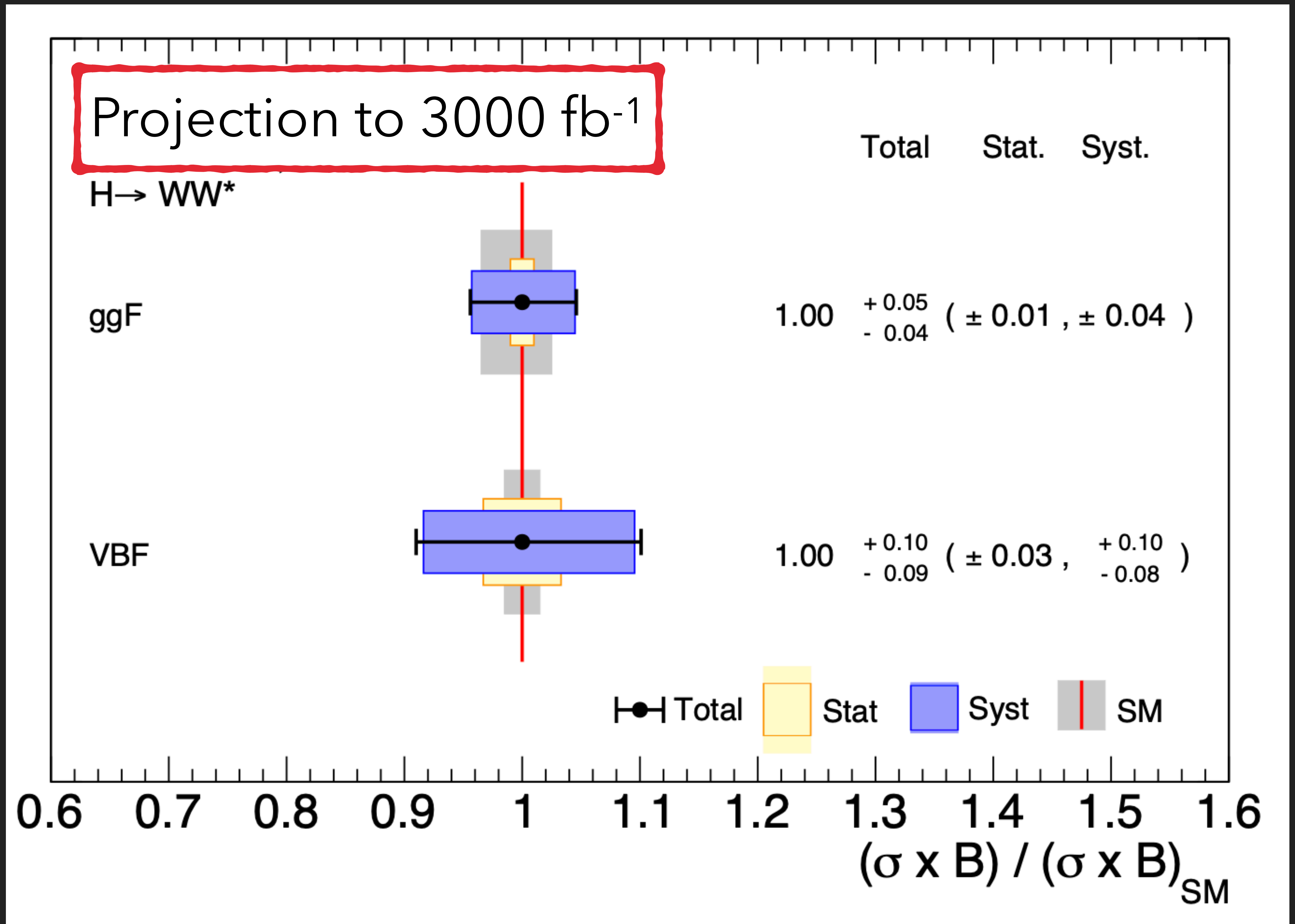

LHCWG2 Report: CERN-LPCC-2018-04

High Luminosity LHC

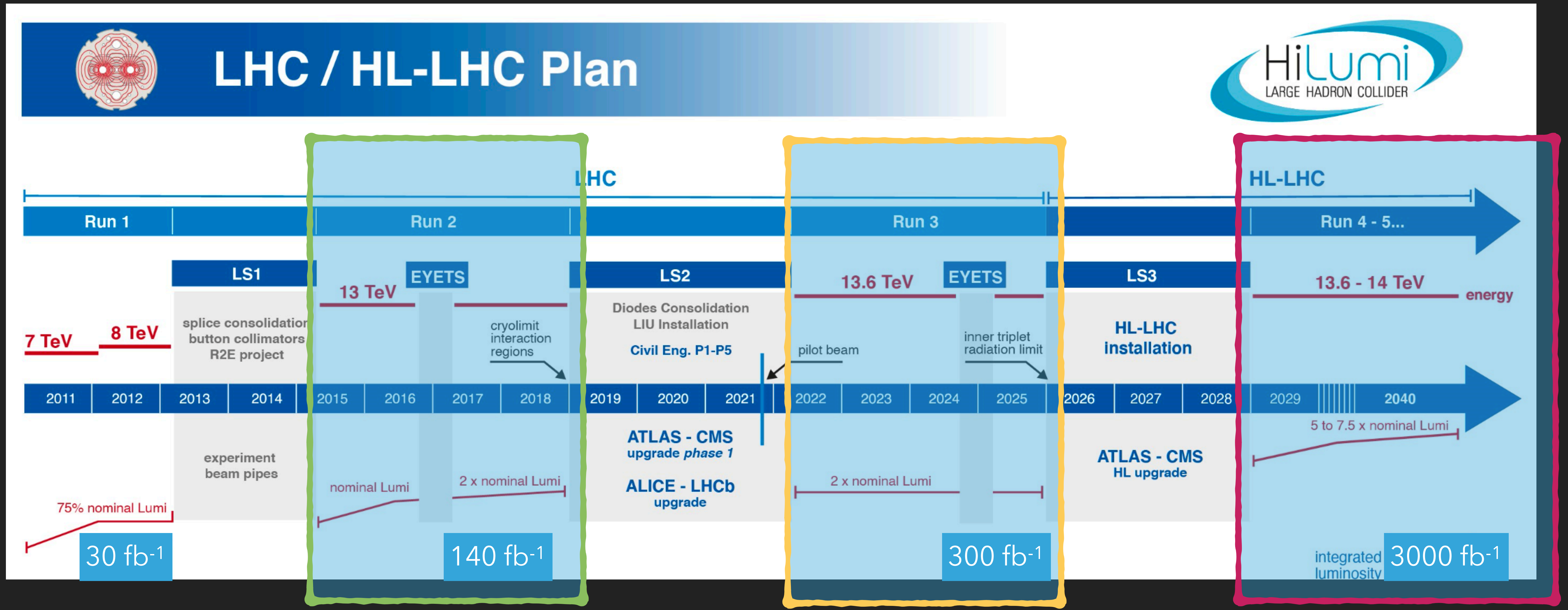

Statistics limited

Statistics limited

High precision era

$\text{Lumi}_{\text{HL-LHC}} = 3.5 \times \text{Lumi}_{\text{LHC}}$

5x data taking rate

10x Data Collected

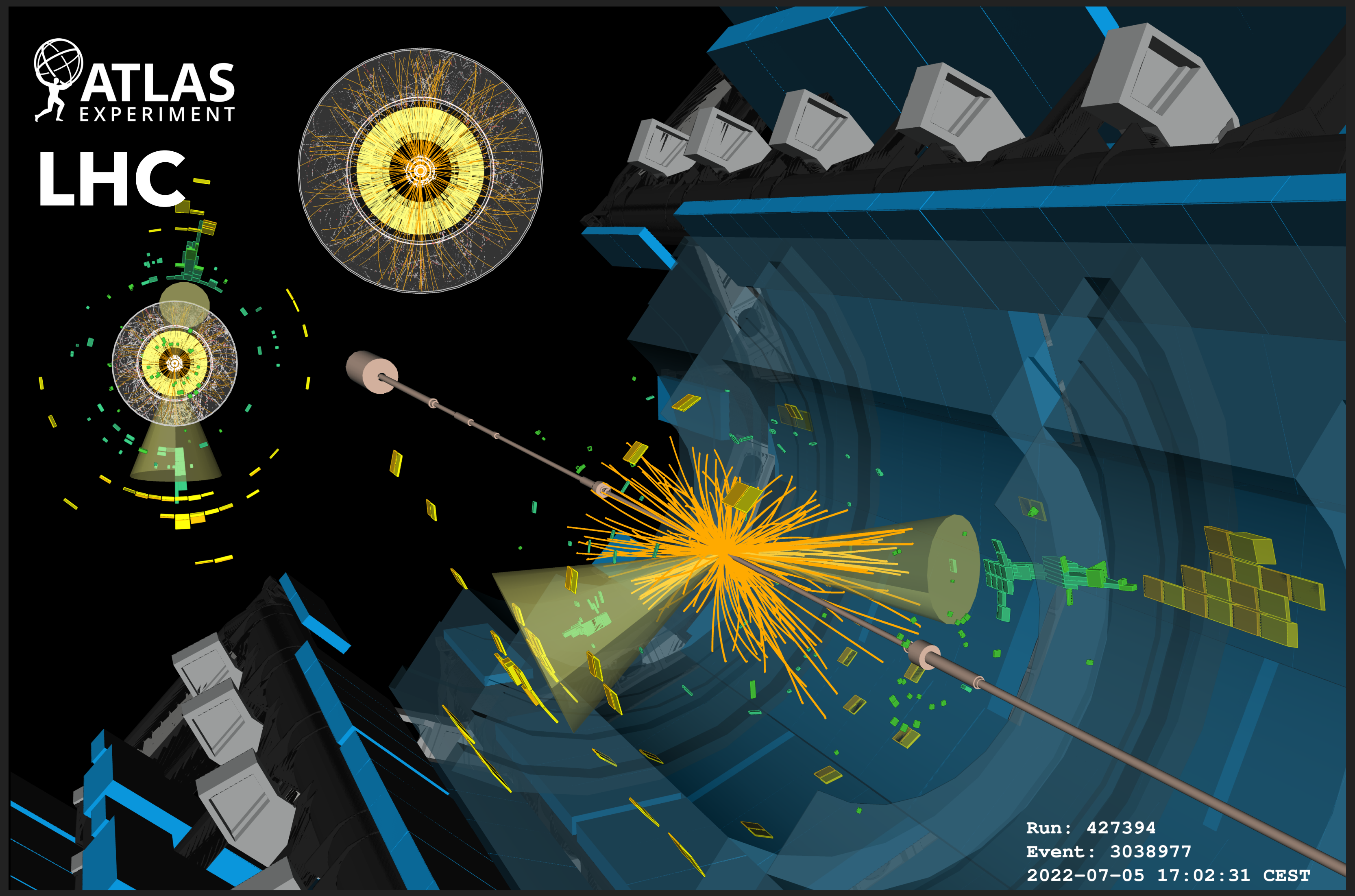

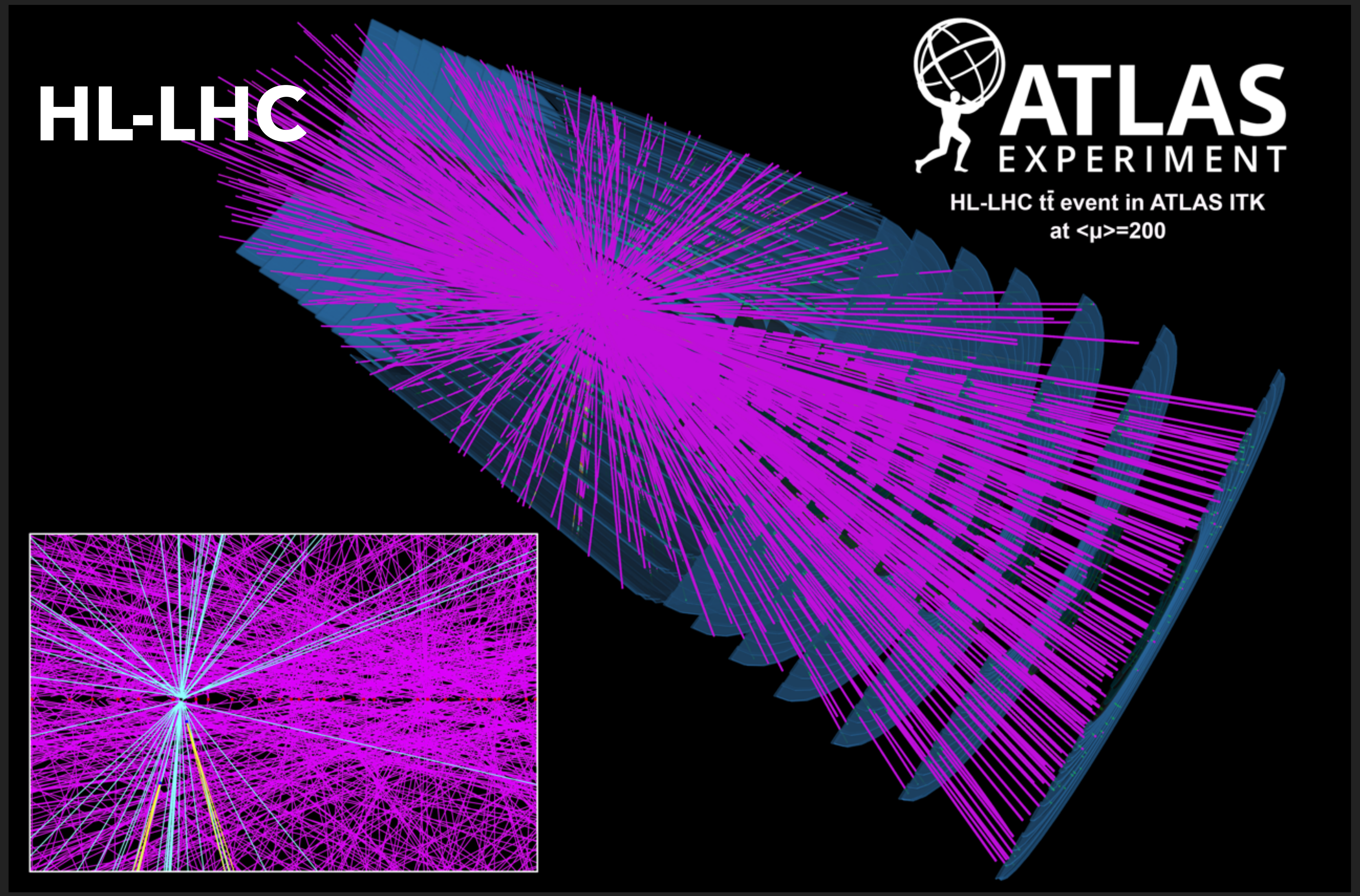

Inner Tracker (ITk) Upgrade

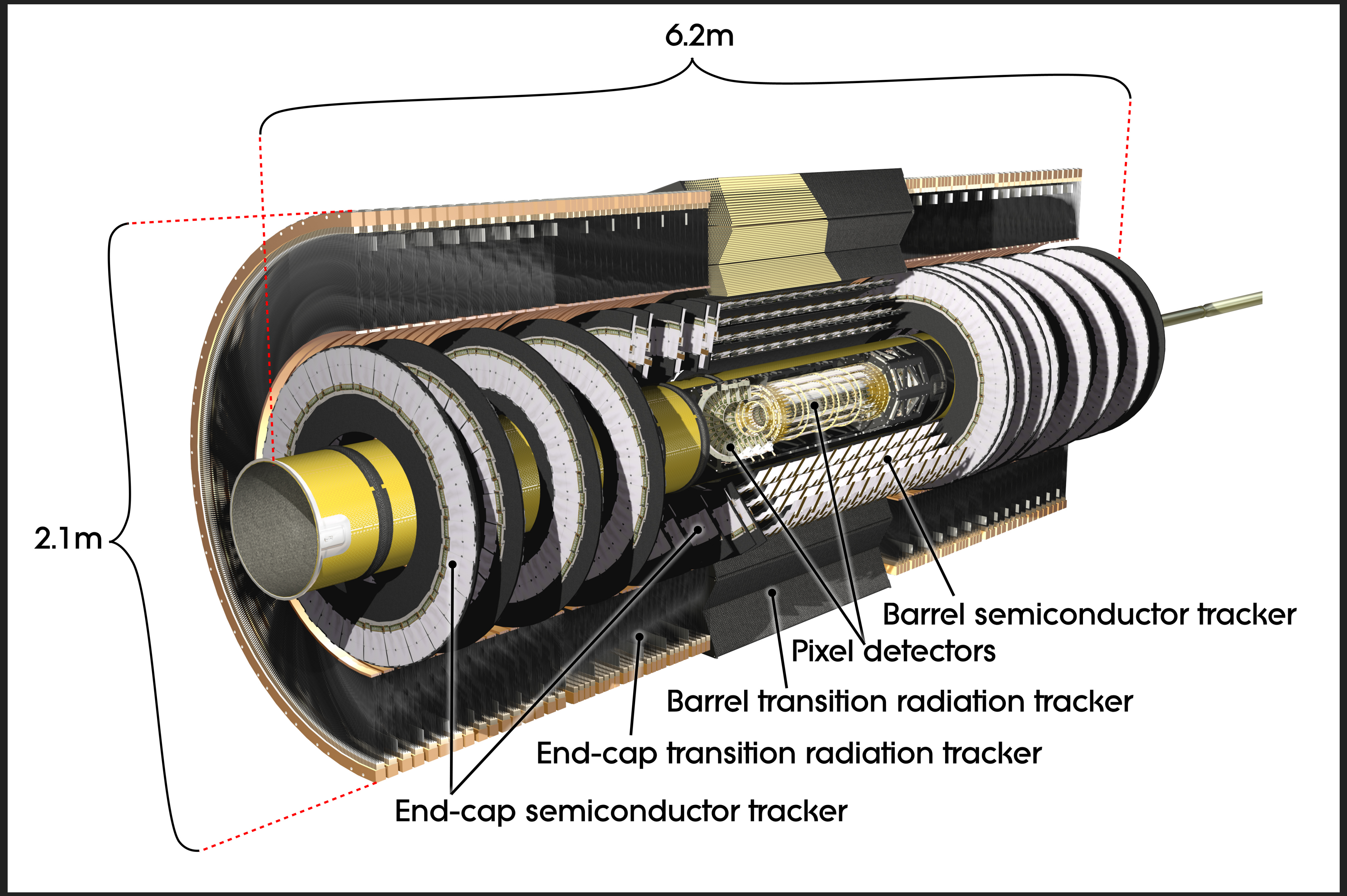

Inner Detector

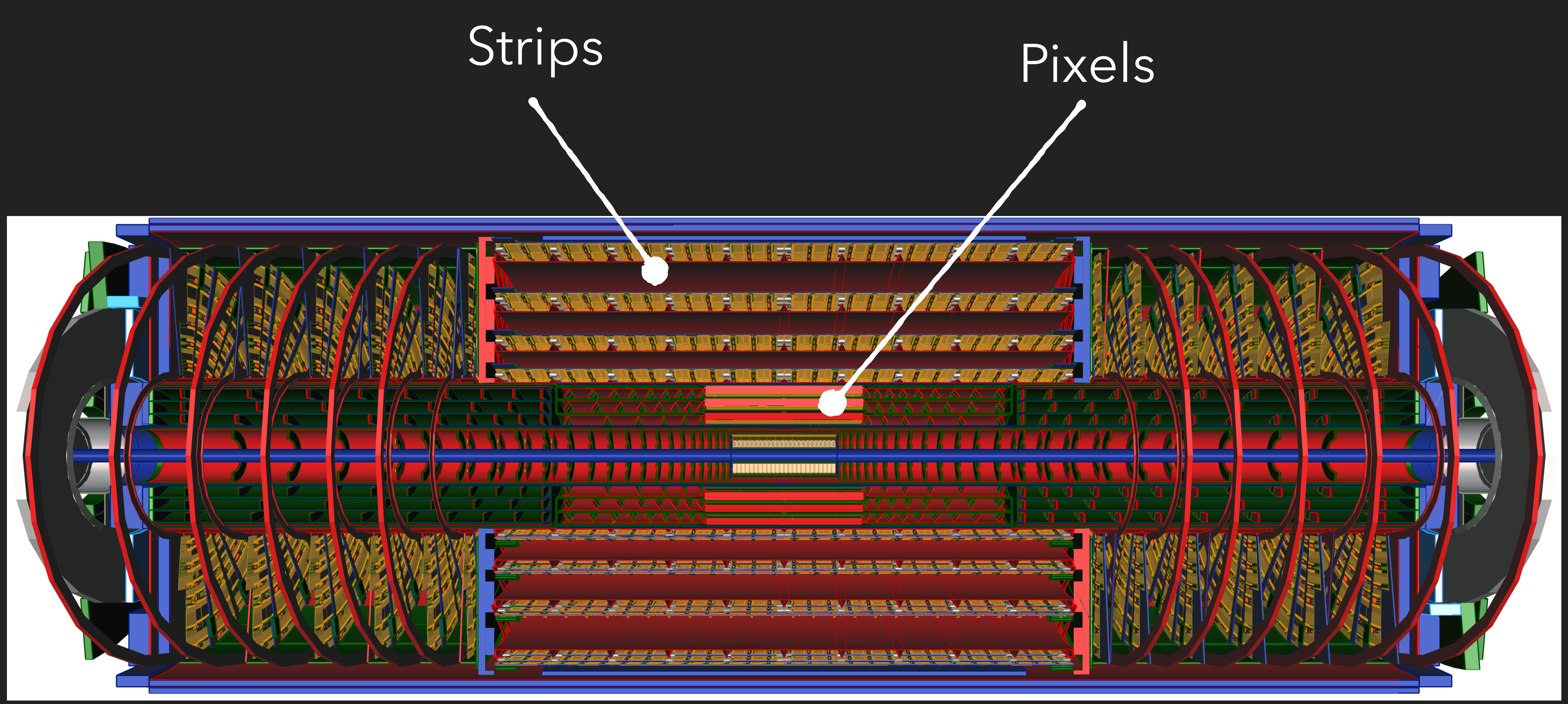

Inner Tracker

ITk is an all-silicon detector with **similar or better performance** as ID in harsher conditions

- More readout channels
- Higher resolution
- More radiation hard

Inner Tracker (ITk) Upgrade

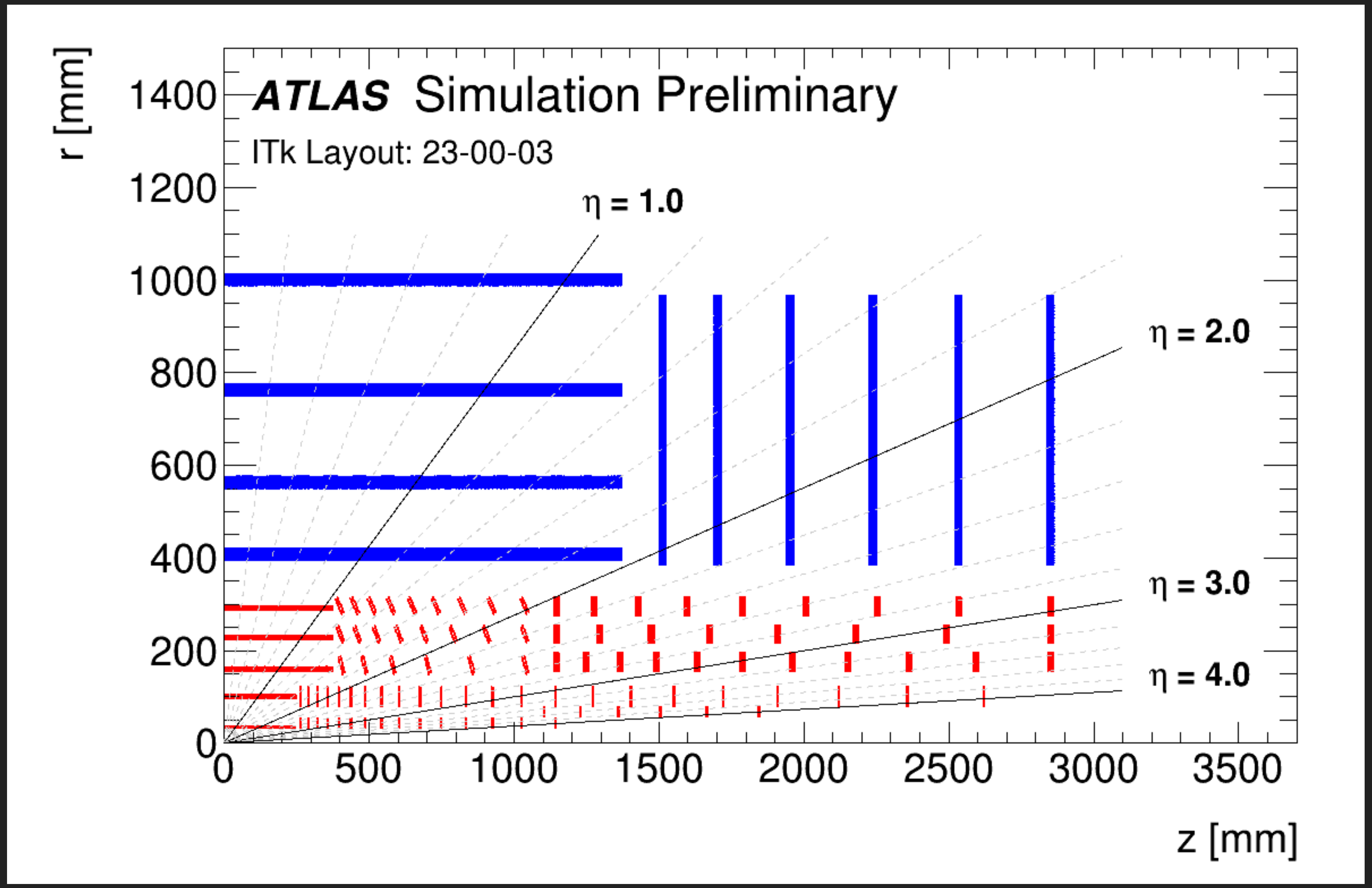

Tracker acceptance from 2.5 (ID) to 4.0 (ITk)
Adds track information for jets with $\eta > 2.5$ which is not available with the current Inner Detector

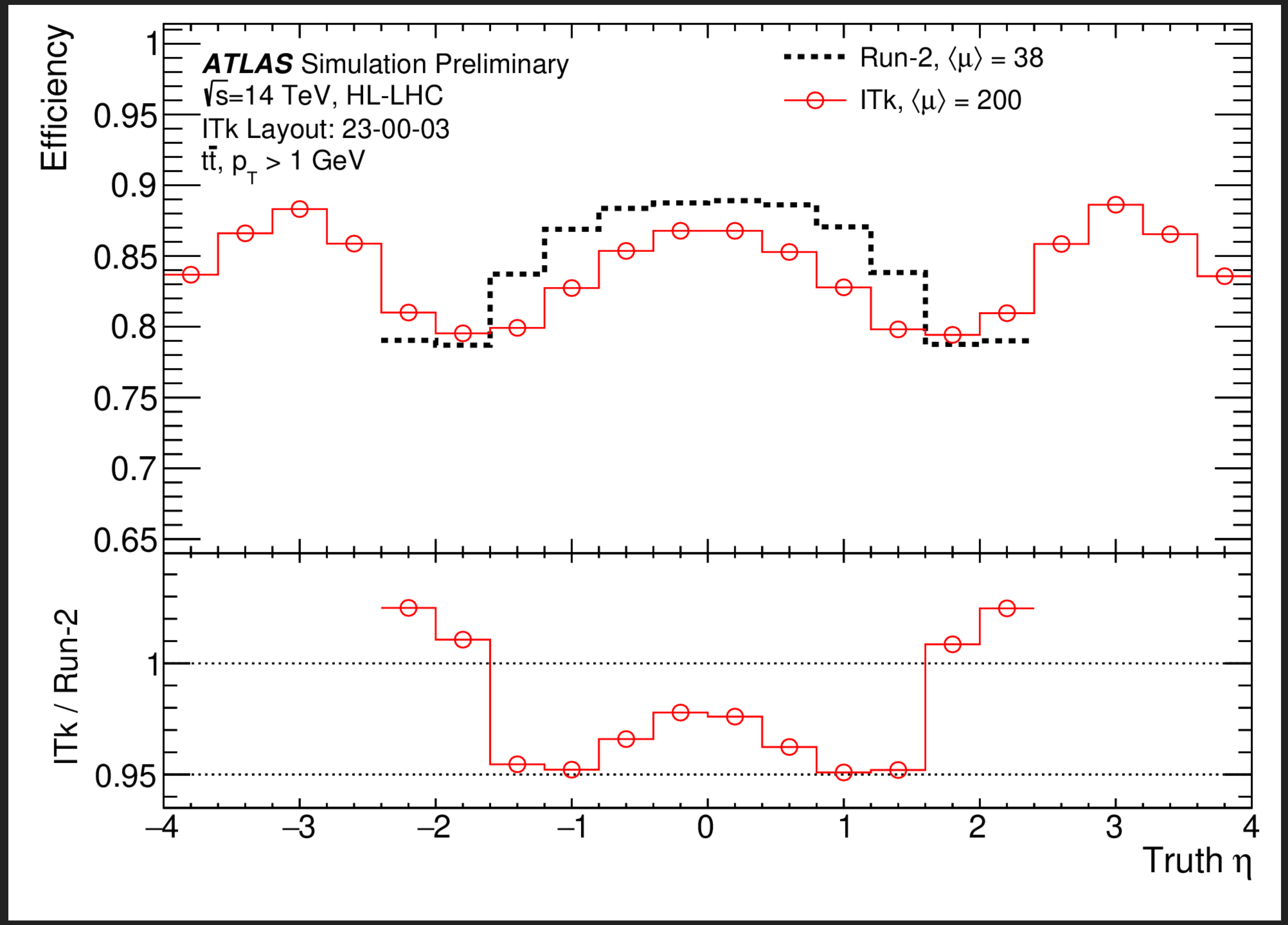

Allows for jet flavor identification, better jet-primary vertex tagging, and pileup jet rejection.
Significant background suppression in the VBF H→WW channel which has forward jets!

Stave Assembly

- Stationed at Brookhaven National Lab for 2 years as a key member of the stave assembly and testing team
- Built the first 28 module stave – critical prototype for the stave assembly step to pass the Final Design Review

Strip Module –
Smallest individual detector

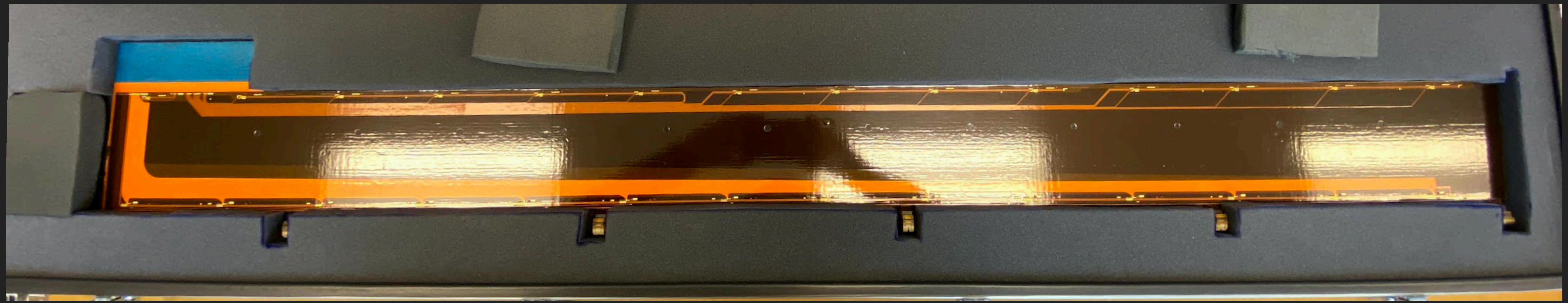

Stave Core – Mechanical and electrical support to the modules

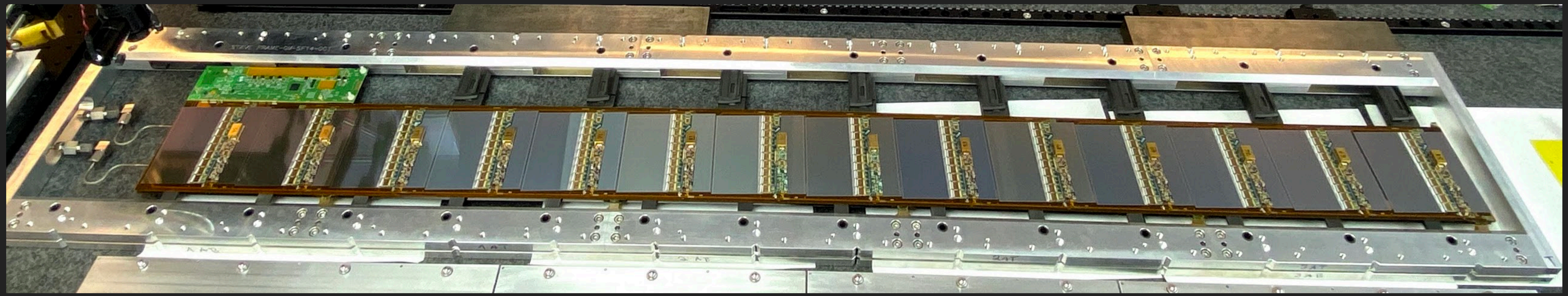

One side of the first 28 module **stave** prototype built with 50 μm accuracy

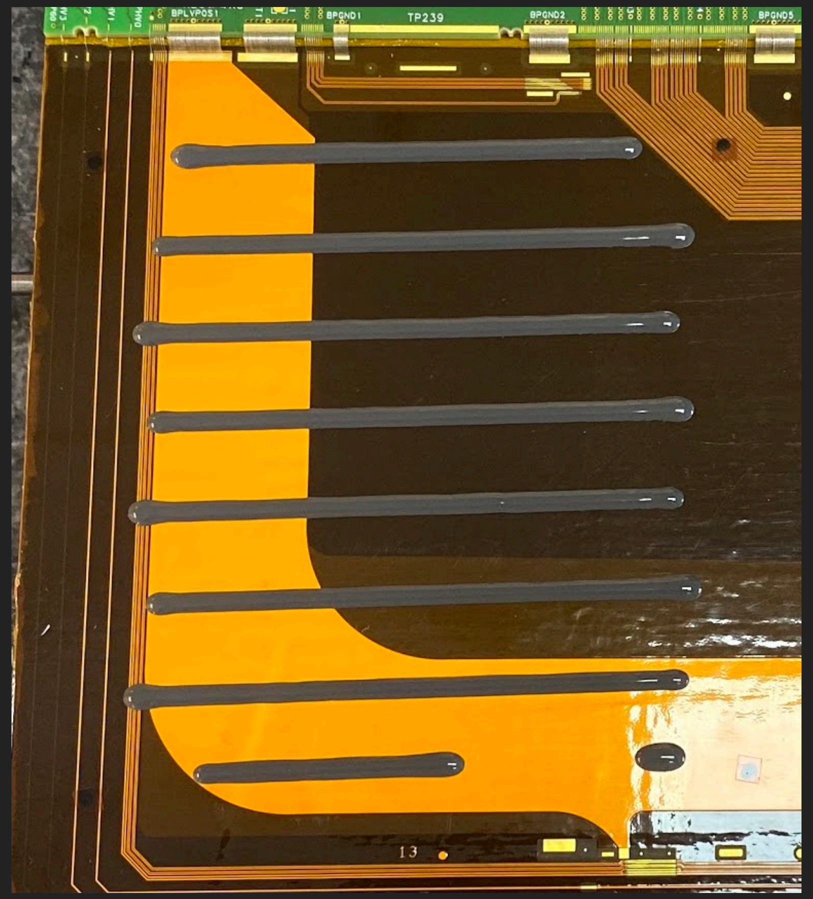

Radiation hard glue
(pattern since evolved)

Stave Metrology

- Set-up the first out-of-plane metrology apparatus for staves using a laser based measurement device
- Necessary quality control step to ensure stave insertion clearance and timely defect catching

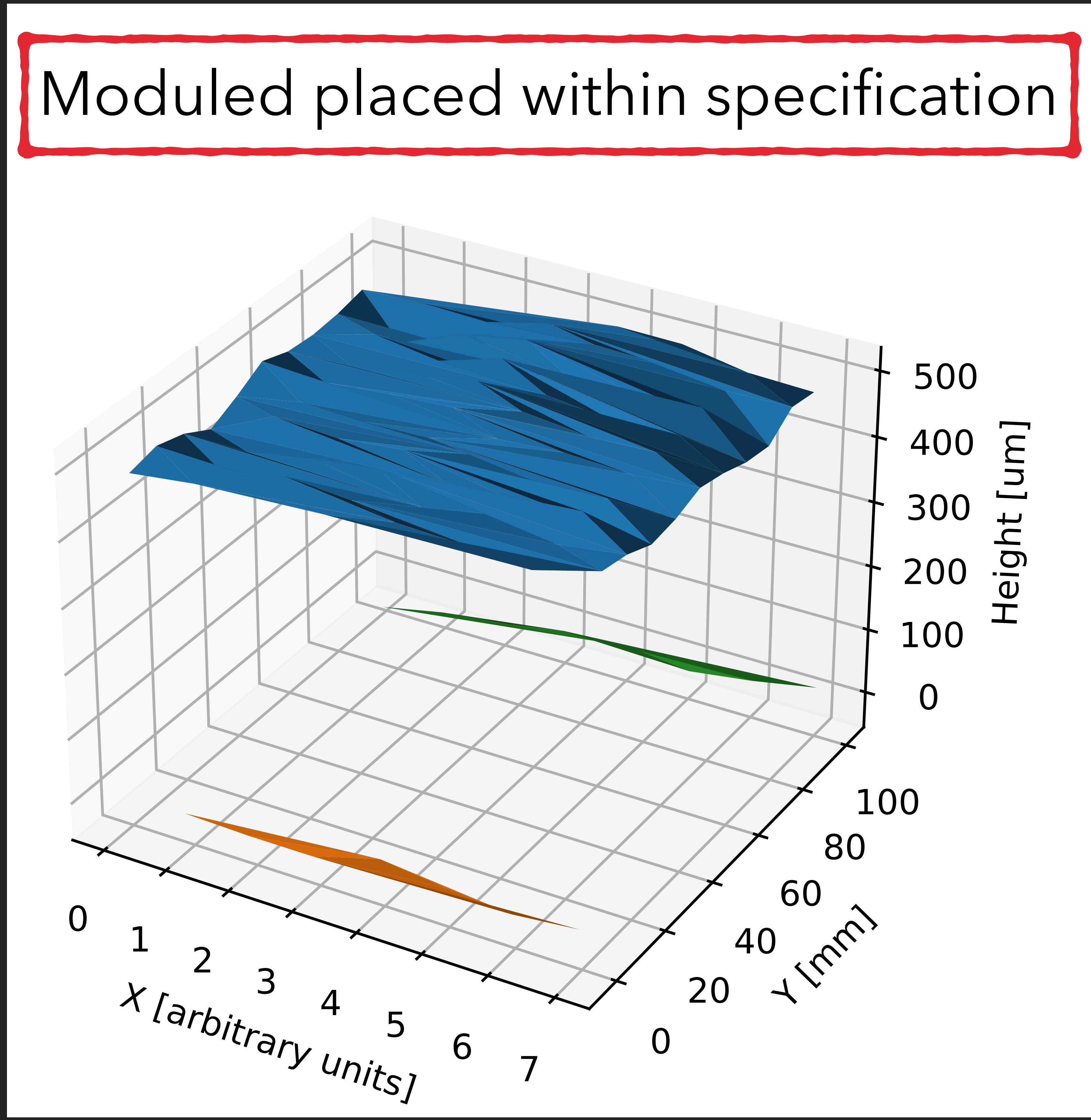

VBF H→WW Precision Measurements

- Strong probe of physics beyond the SM putting the structure of Electroweak Symmetry Breaking to test
- First fully fiducial differential cross section measurement in the *e* + μ + 2jets + E_T^{miss} final state
- Measured cross sections as functions of 13 kinematic observables and correlations
- Constrained Wilson coefficients for CP-even and CP-odd operators in an EFT framework
- Technique paves the way for future measurements of low cross section processes hidden under backgrounds

Phase-II of ATLAS

- 3000 fb^{-1} of *pp* collision data allows probing rare processes with extremely high precision putting SM to test
- Enhanced detector acceptance and reconstruction techniques add sensitivity to VBF H→WW measurement

Accepted Paper

arXiv:2304.03053

Integrated and differential fiducial cross-section measurements for the vector boson fusion production of the Higgs boson in the $H \to WW^* \to e\nu\mu\nu$ decay channel at 13 TeV with the ATLAS detector

Phys. Rev. D

ADDITIONAL MATERIAL

Higgs Mass Constraints from EW Precision Measurements

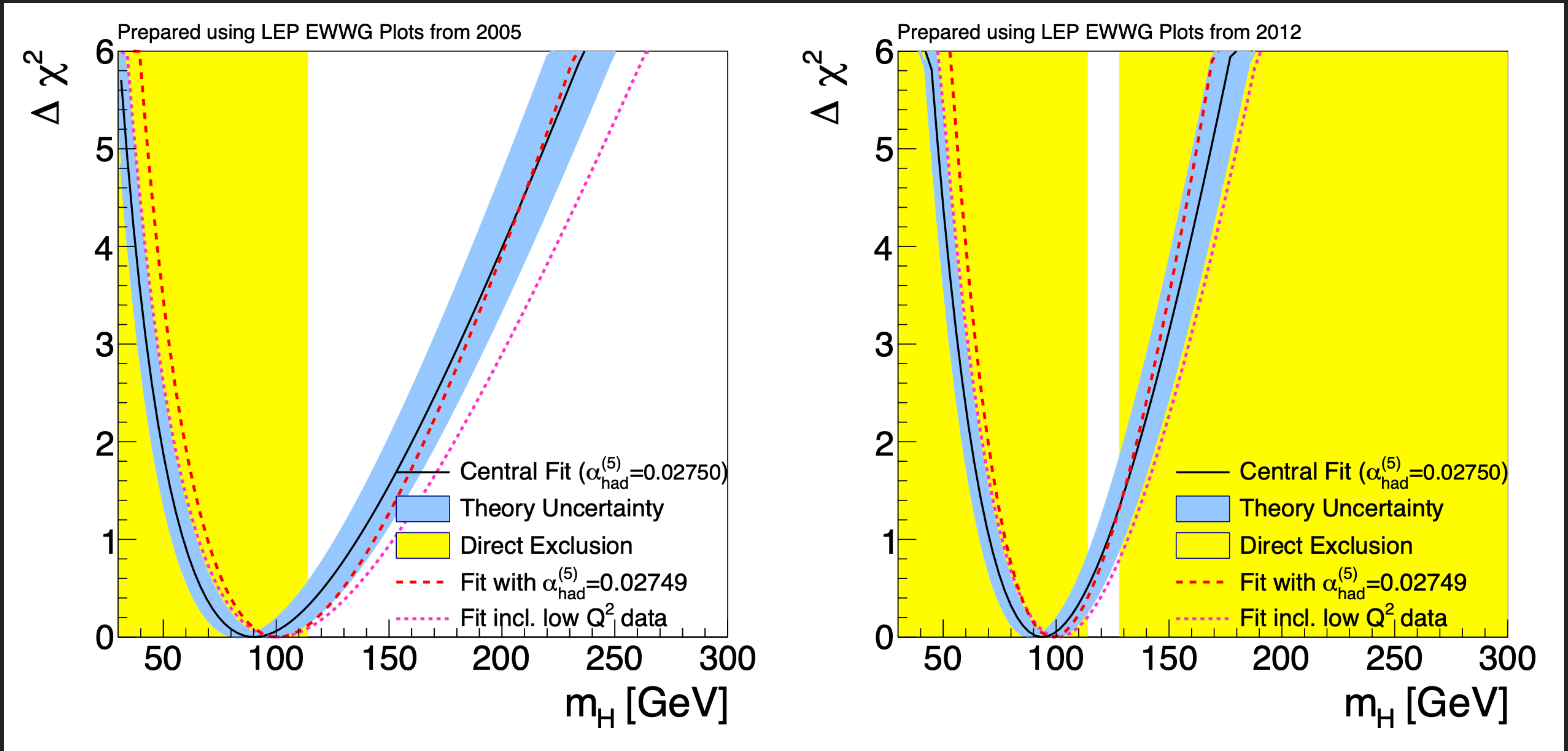

Model Independent Probe

Model independency ↔ low-model dependency

Sources of model dependency

- Phase space definition
- Profile-likelihood fit
- Machine learning methods relying on training models
- Extent of kinematic reconstruction

Reconstructing the kinematics of H is

- Robust, if the final state is fully reconstructed

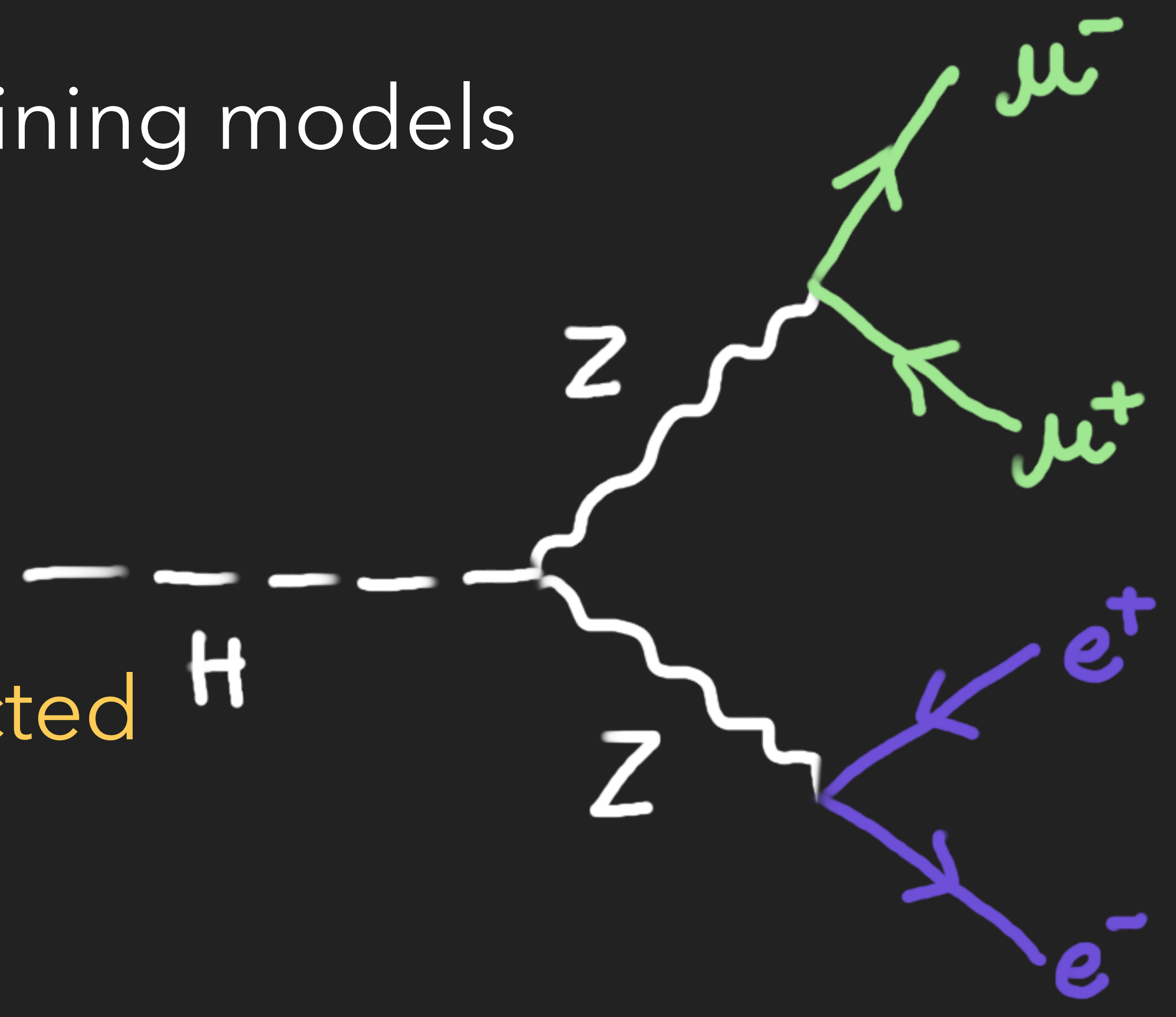

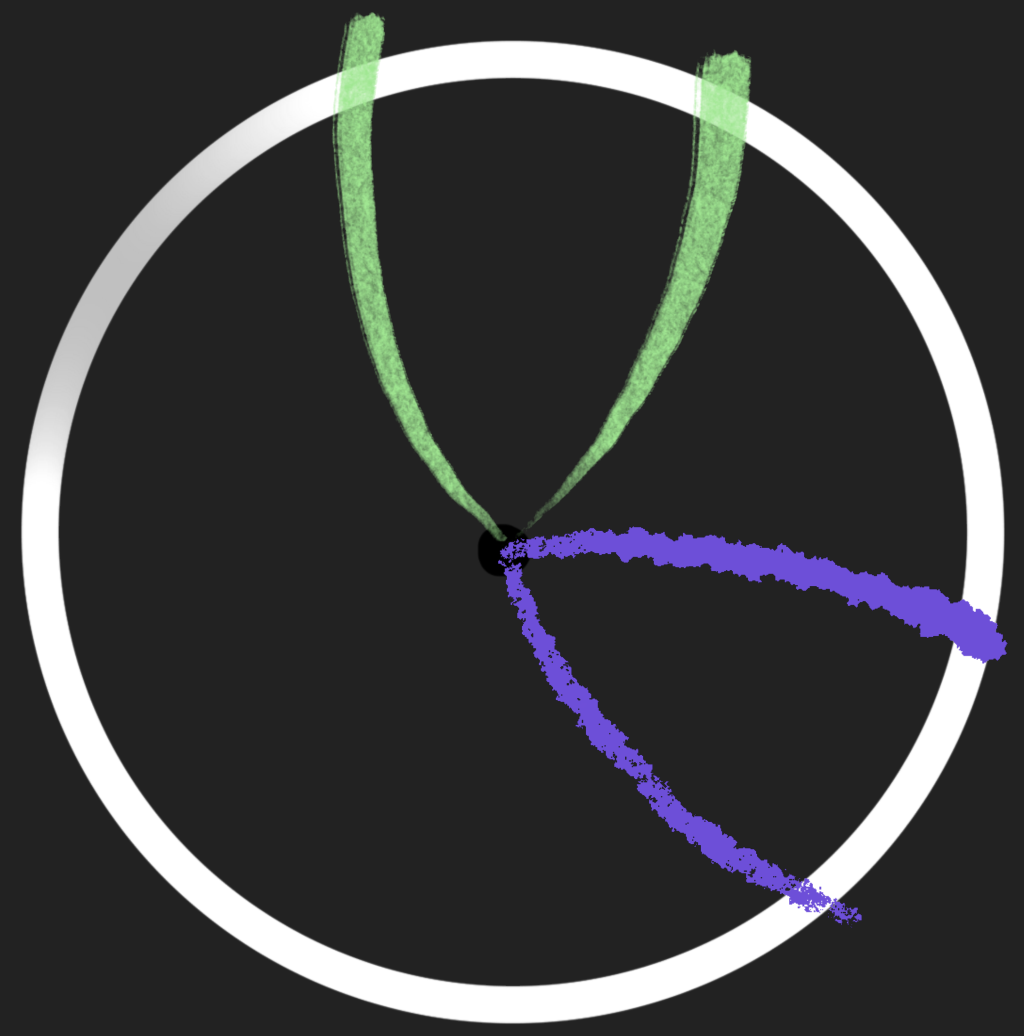

Fully reconstructible

Model Independent Probe

Model independency ↔ low-model dependency

Sources of model dependency

- Phase space definition
- Profile-likelihood fit
- Machine learning methods relying on training models
- Extent of kinematic reconstruction

Reconstructing the kinematics of H is

- Robust, if the final state is fully reconstructed
- Model driven, if not
  - Partial reconstruction – $\mathbf{E_T^{miss}}$
  - SM assumption – only ν leave $\mathbf{E_T^{miss}}$

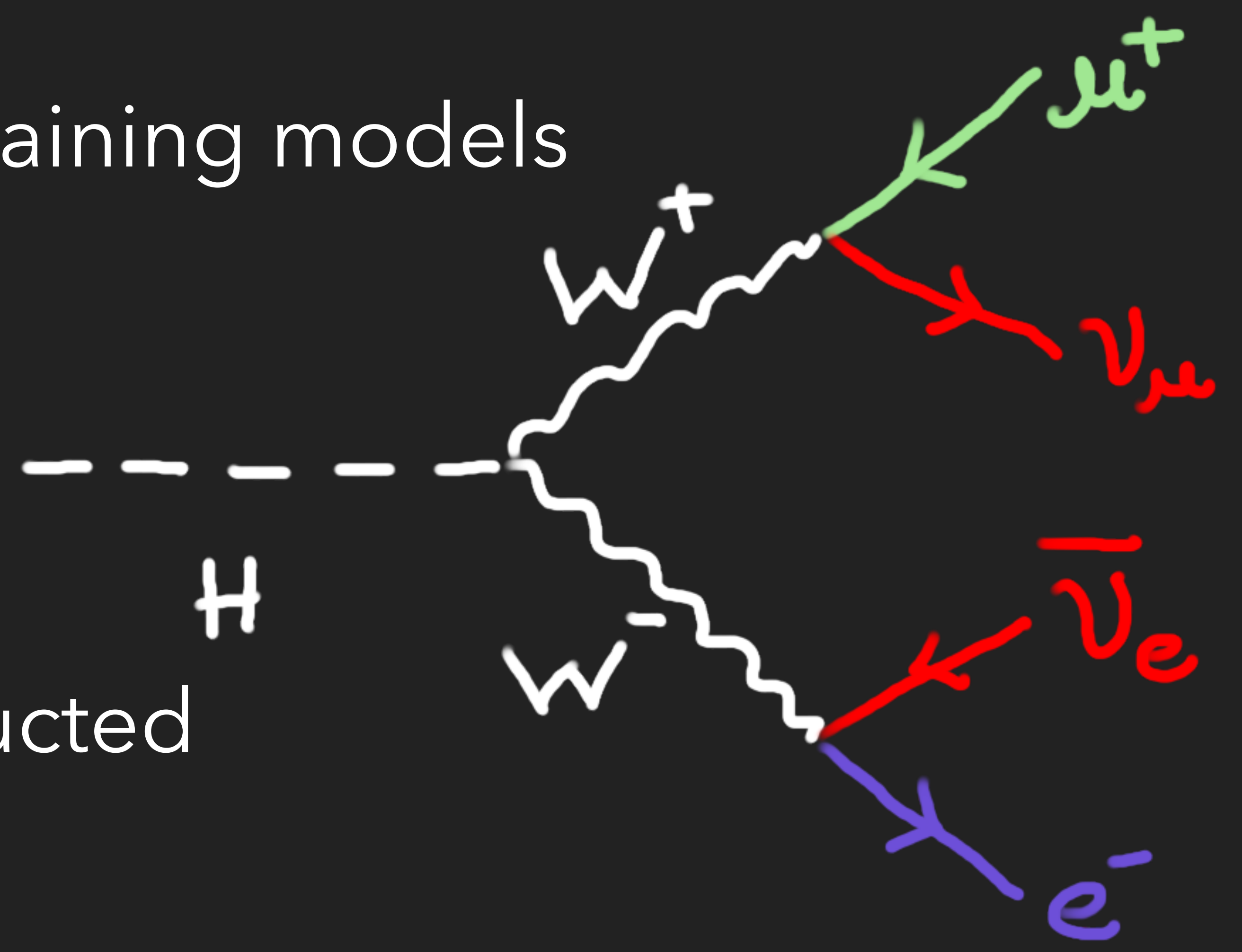

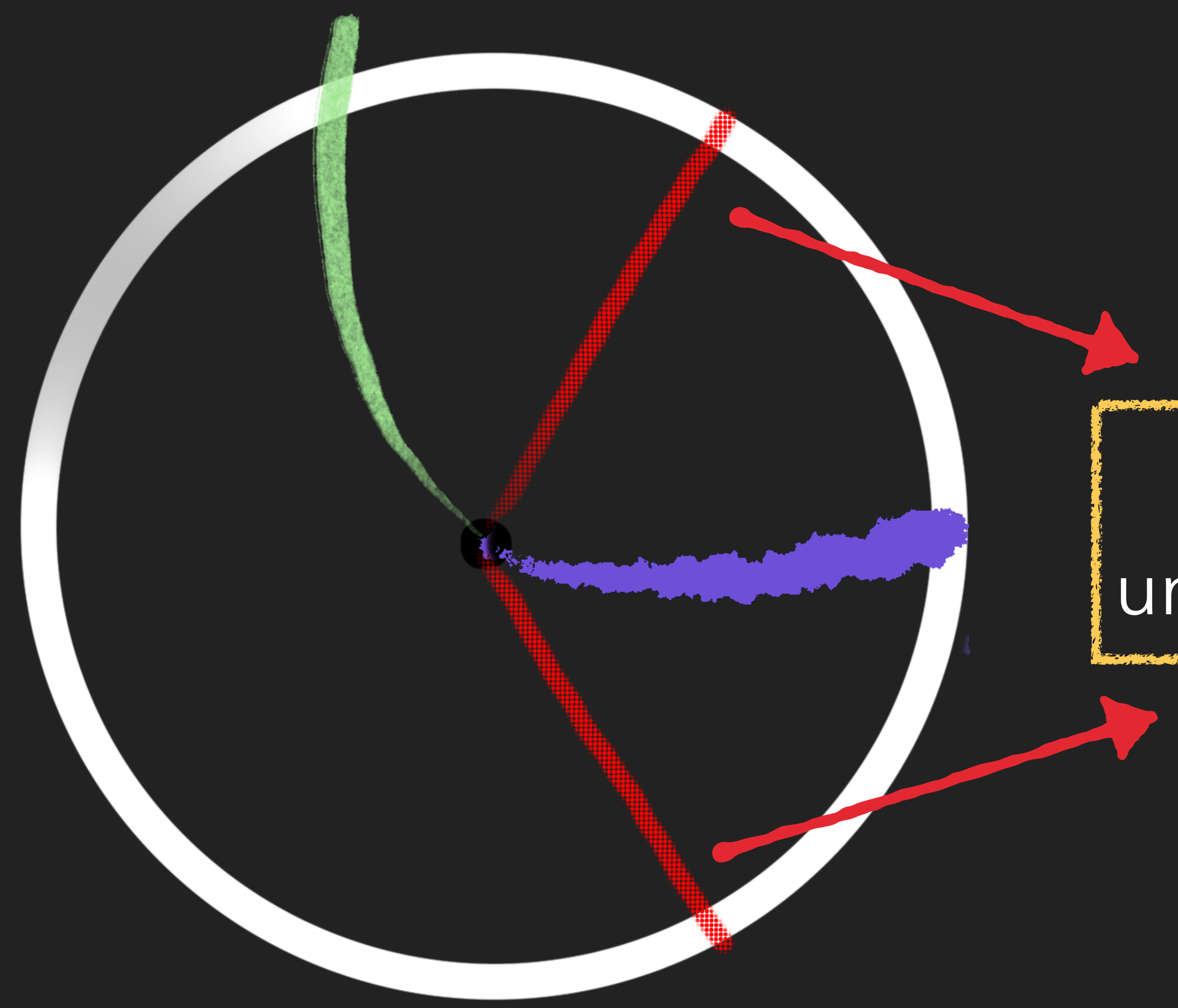

ν pass undetected

Reconstructible **only** in the transverse plane

Learning from previous measurements

VBF H $\rightarrow \gamma\gamma$ (arXiv: 2202.00487)

2022

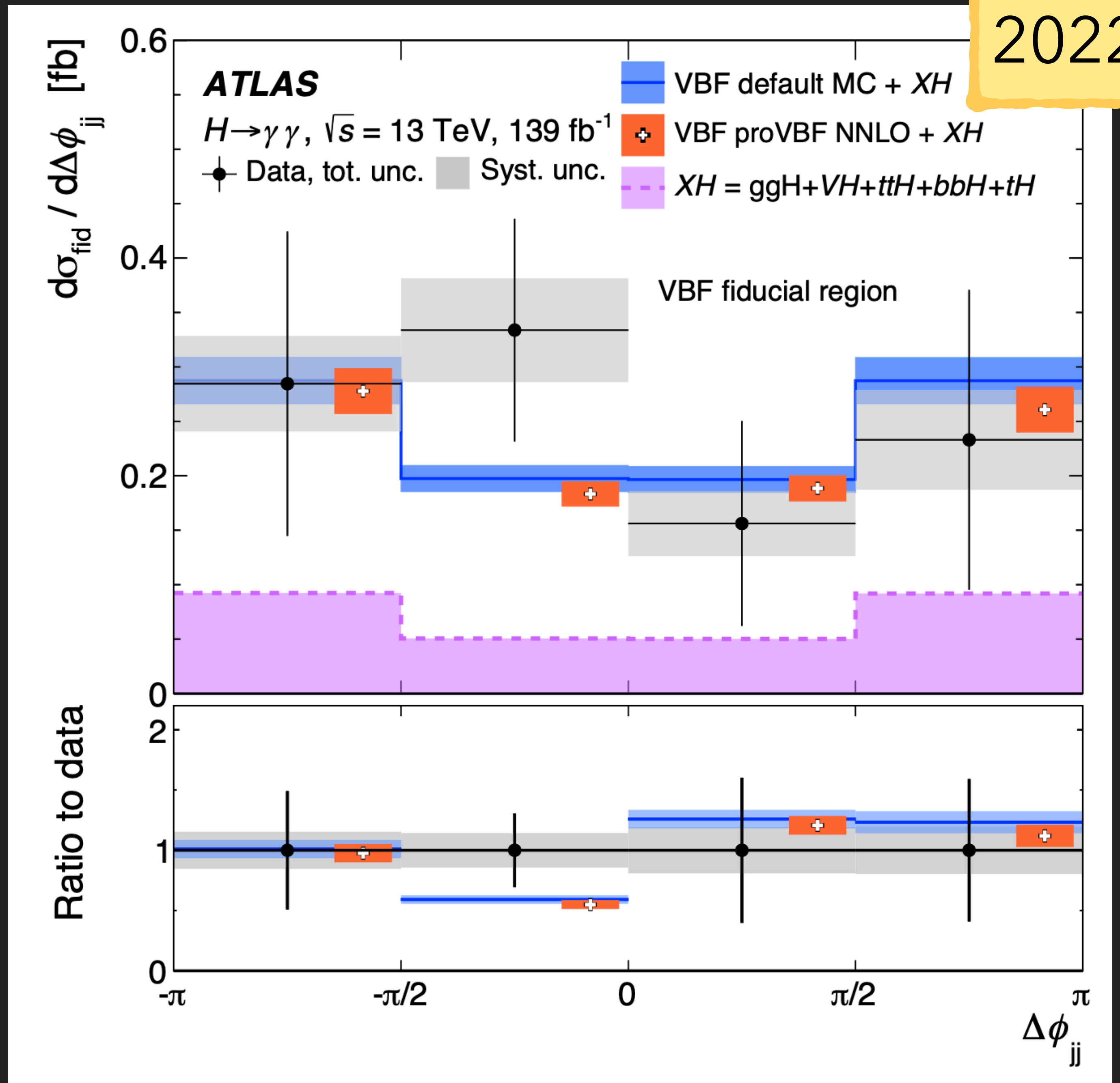

$\gamma\gamma$ fully reconstructible

$H \rightarrow WW$ (arXiv: 2007.01984)

2021

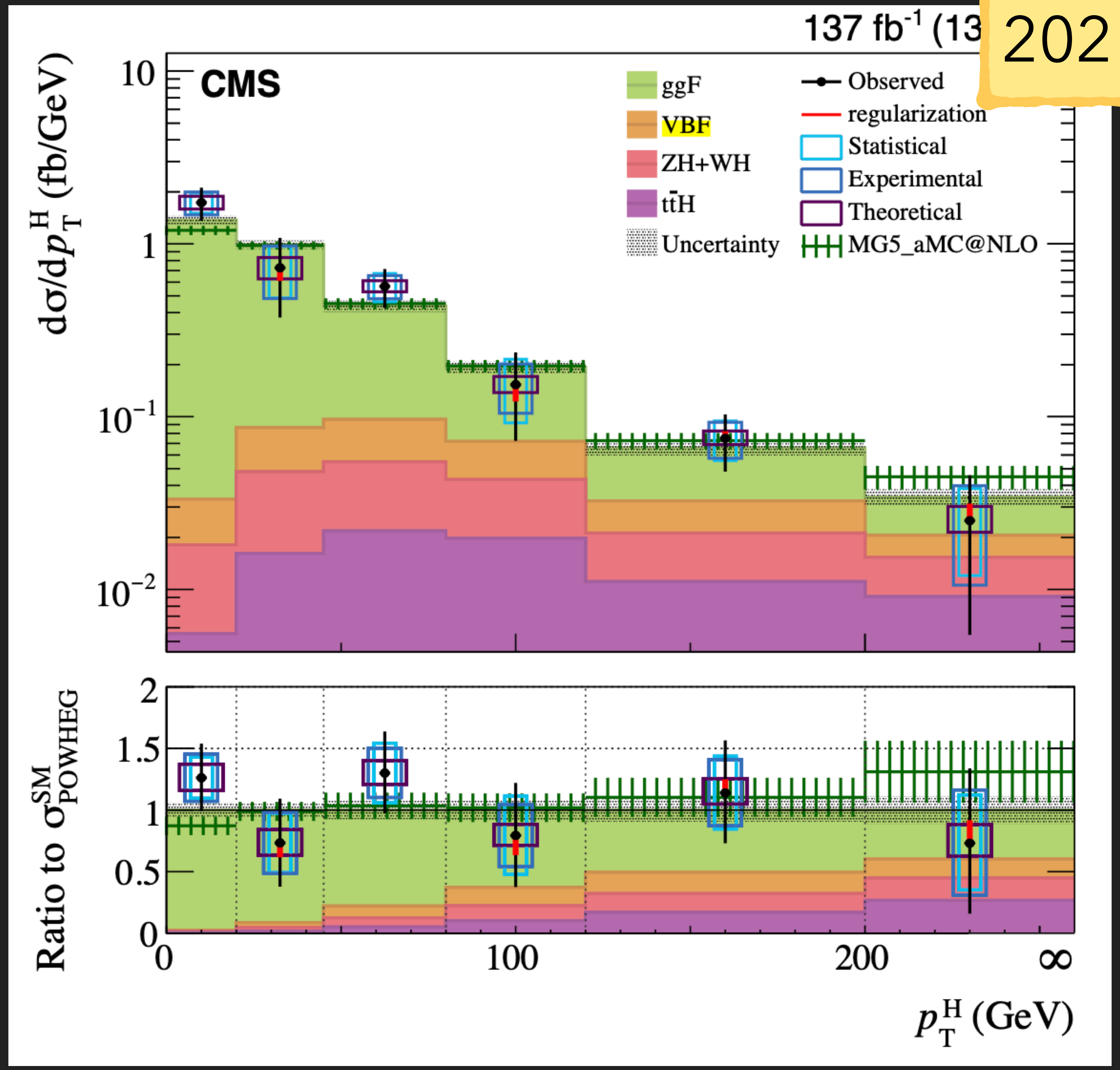

VBF contribution subdominant

STXS $H \rightarrow WW$ (arXiv: 2207.00338)

2023

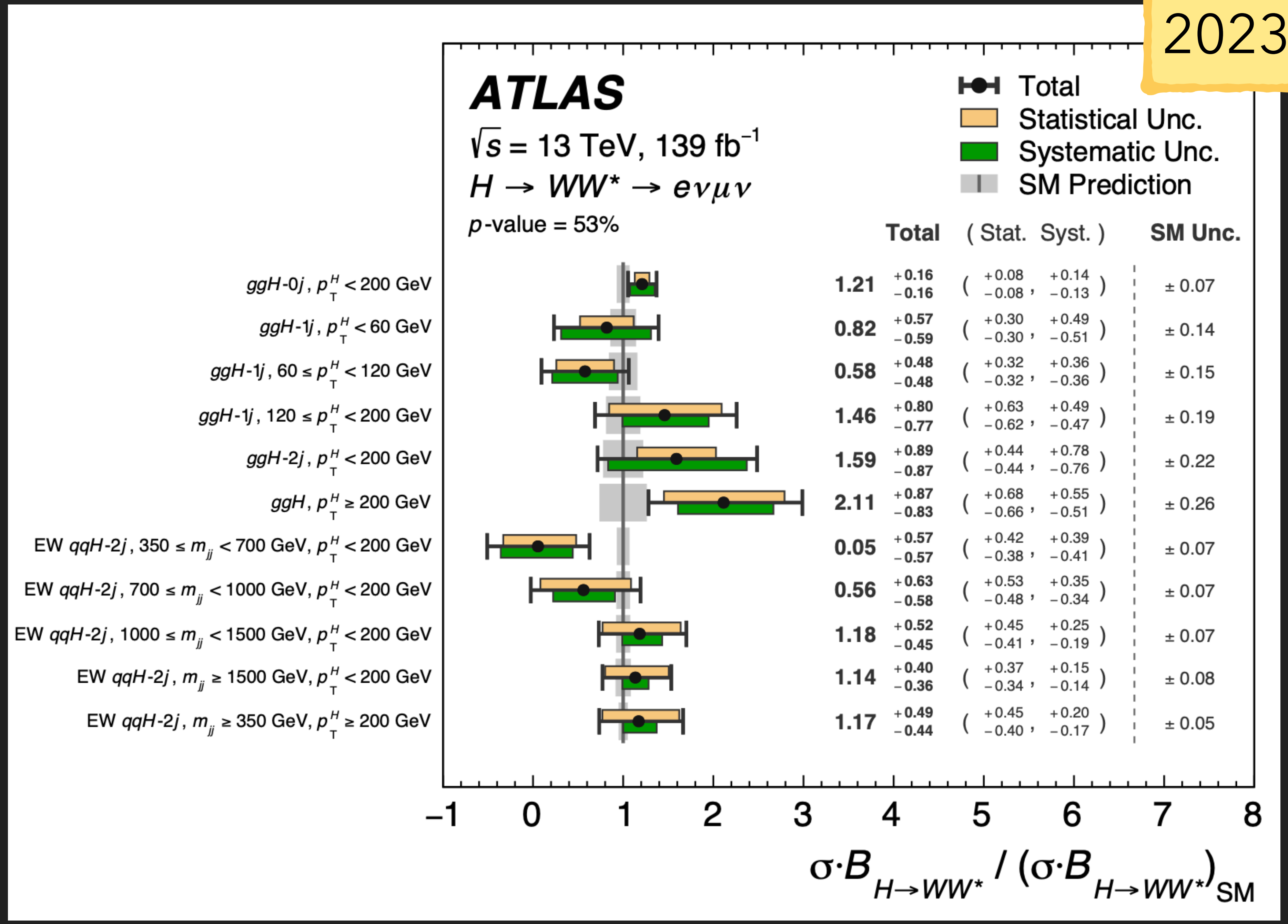

fiducial only in production???

Target Phase Space

$m_{\tau\tau}$	$< m_Z - 25$ GeV
Central jet veto ($p_T > 20$GeV)	yes
Outside lepton veto	yes
m_{jj}	> 450 GeV
$\lvert\Delta y_{jj}\rvert$	> 2.1
$\lvert\Delta\phi_{\ell\ell}\rvert$	< 1.4 rad

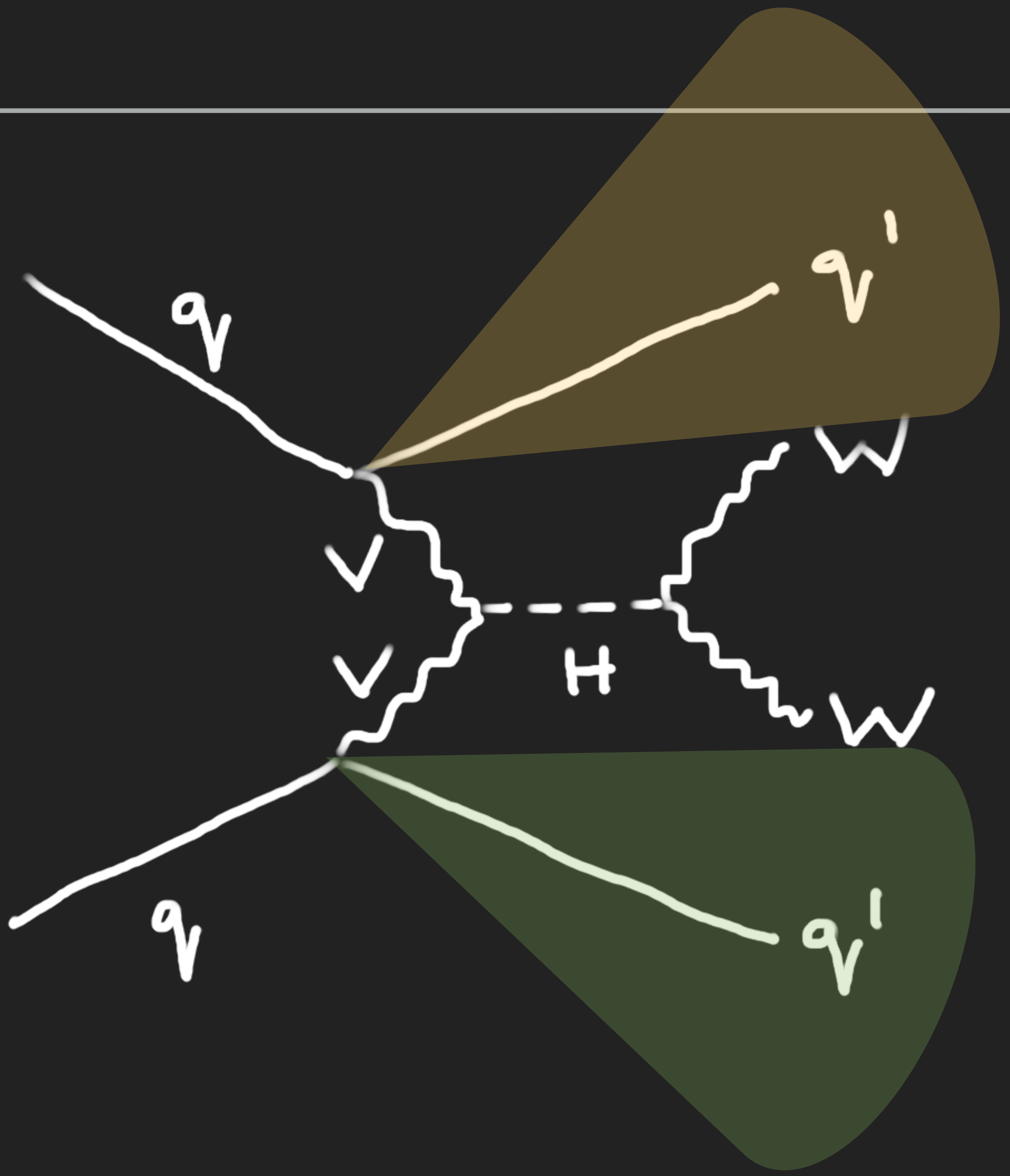

Missing E_T

No high p_T jets between the two leading jets

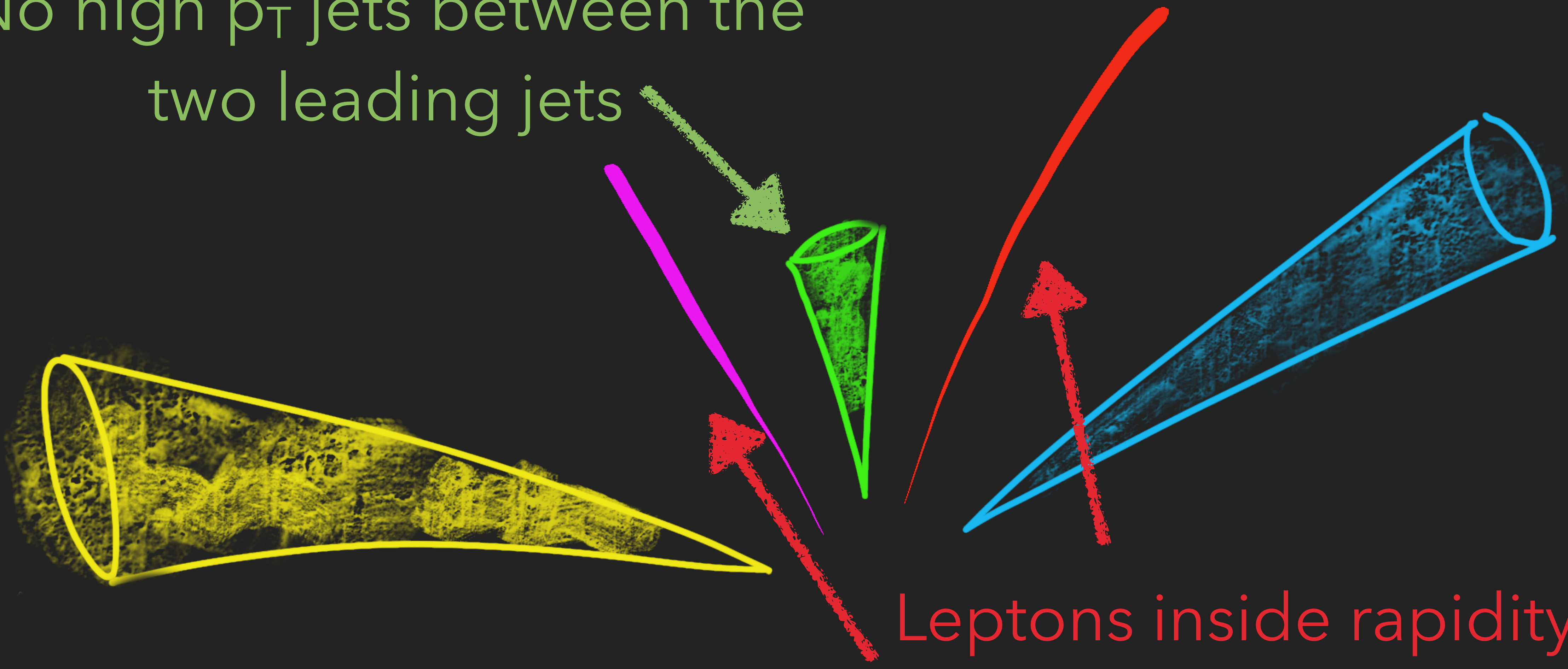

Leptons inside rapidity region spanned by leading jets

Process	# in SR
VBF H	110
VV	280
Top Induced	420
ggF H	39
Z+Jets	79
W+Jets (Mis-Id)	47
$V\gamma$, Htt, VH	16
Total S+B	1000±120
Data	916

$m_{\tau\tau} \rightarrow$ inv mass of $\tau\tau$ system in the collinear approximation (Plehn et al. - arXiv:hep-ph/9911385)

Drell-Yan Background Estimation

$m_{\tau\tau}$	66.2 GeV $< m_{\tau\tau} <$ 116.2 GeV
Central jet veto ($p_T > 20$GeV)	yes
Outside lepton veto	yes
m_{jj}	> 450 GeV
$m_{\ell\ell}$	< 80 GeV

Z/γ^*+jets CR definition

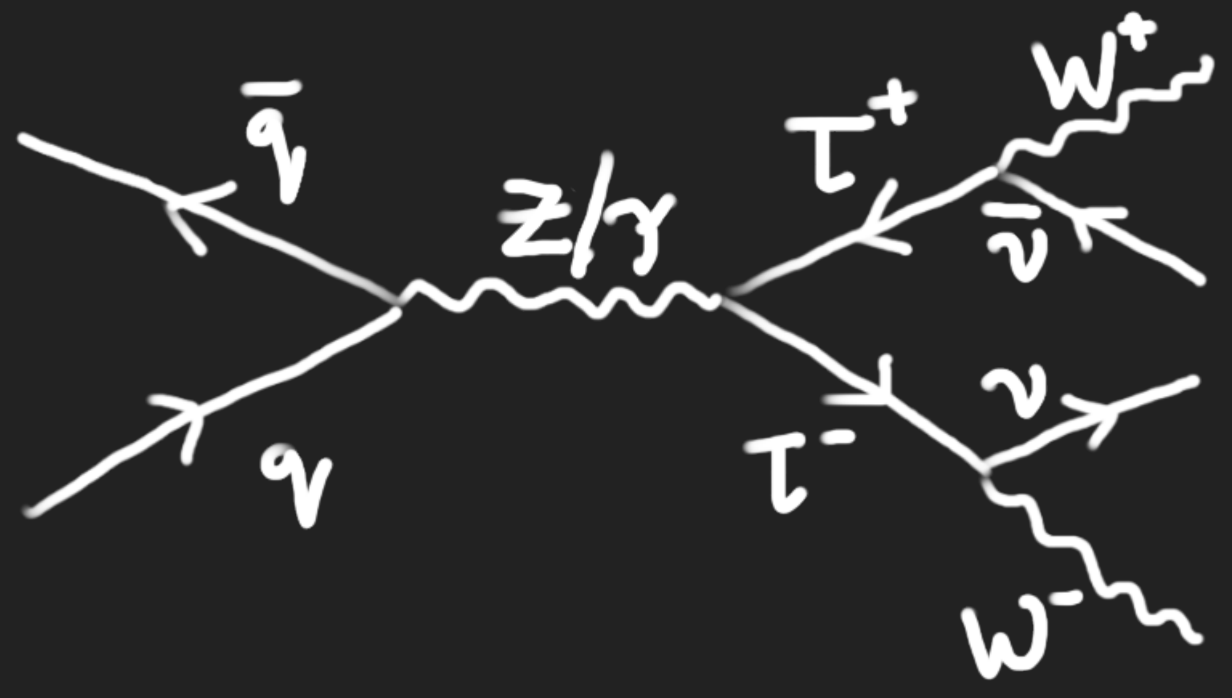

$m_{\tau\tau} \rightarrow$ invariant mass of $\tau\tau$ system in the collinear approximation

75% Z/γ^*+jets purity

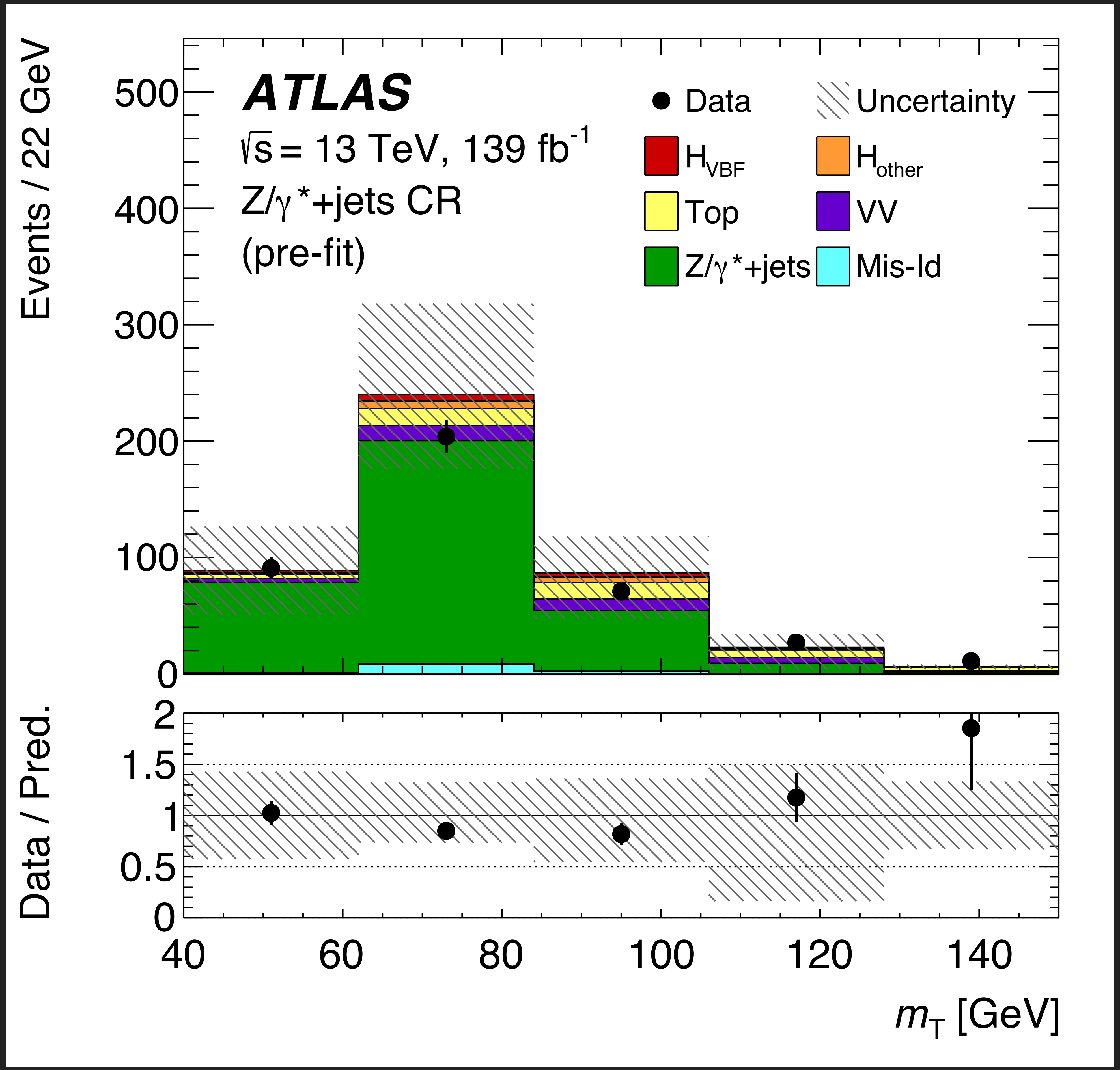

$$m_T = \sqrt{(E_T^{\ell\ell} + E_T^{\text{miss}})^2 - |\mathbf{p}_T^{\ell\ell} + \mathbf{E}_T^{\text{miss}}|^2}$$

gluon fusion Higgs Background Estimation

$m_{\tau\tau}$	$< m_Z - 25$ GeV
Central jet veto ($p_T > 20$GeV) Outside lepton veto	Exactly 1 fails
$\lvert\Delta\phi_{\ell\ell}\rvert$	< 1.4 rad

ggF CR / anti-VBF definition

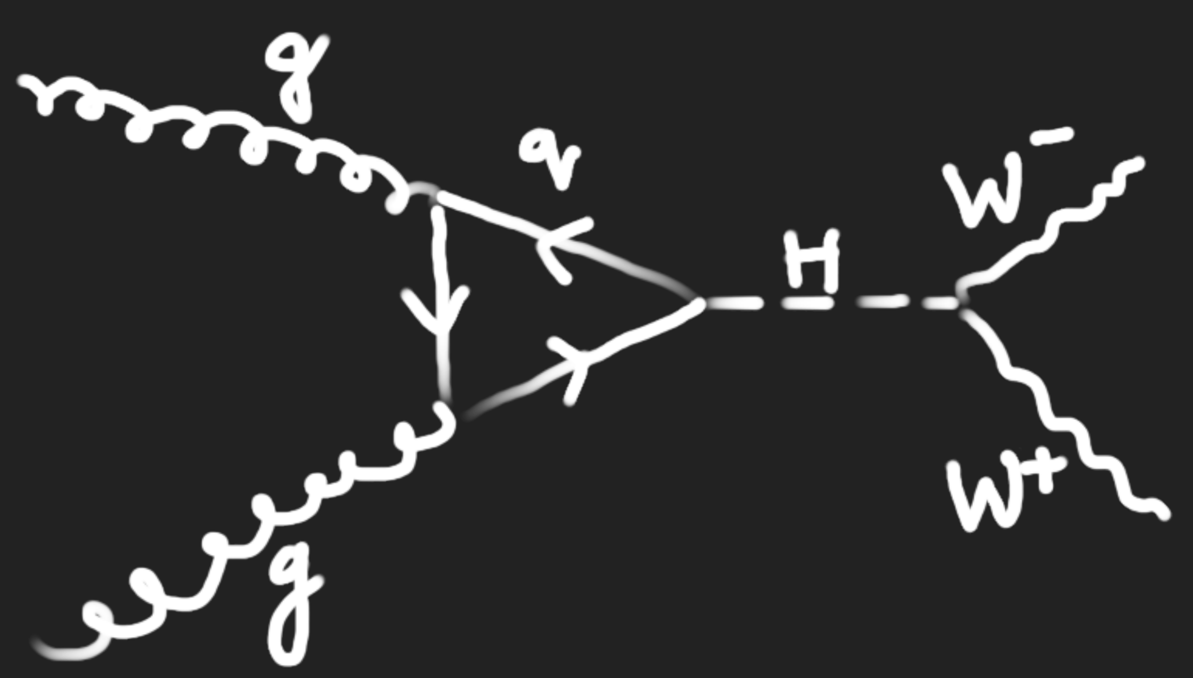

- ggF prediction in the SR needs higher order corrections
- Complementary info with SR – controls modeling uncertainties
- 2% purity – high stat unc on ggF norm factor but low extrapolation unc from ggF-CR to SR

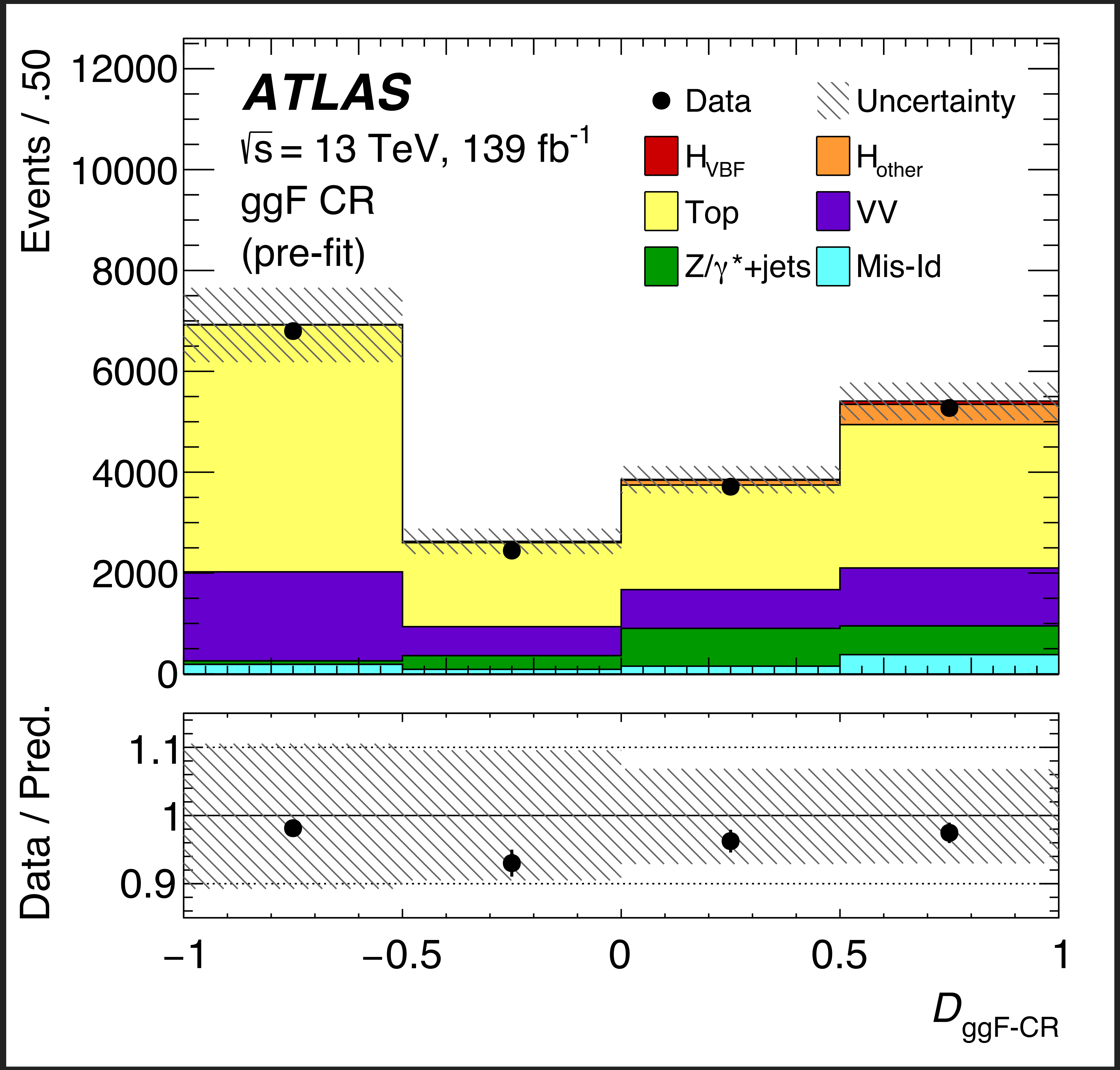

BDT trained to separate ggF from other MC

Mis-identified Leptons

- Impose strict requirements on the isolation and quality of leptons used in the analysis
- 5% mis-ID bkg in the SR – difficult to model
- Using the "fake factor" method to extrapolate from W+jets CR (76% purity of mis-ID bkg) to SR

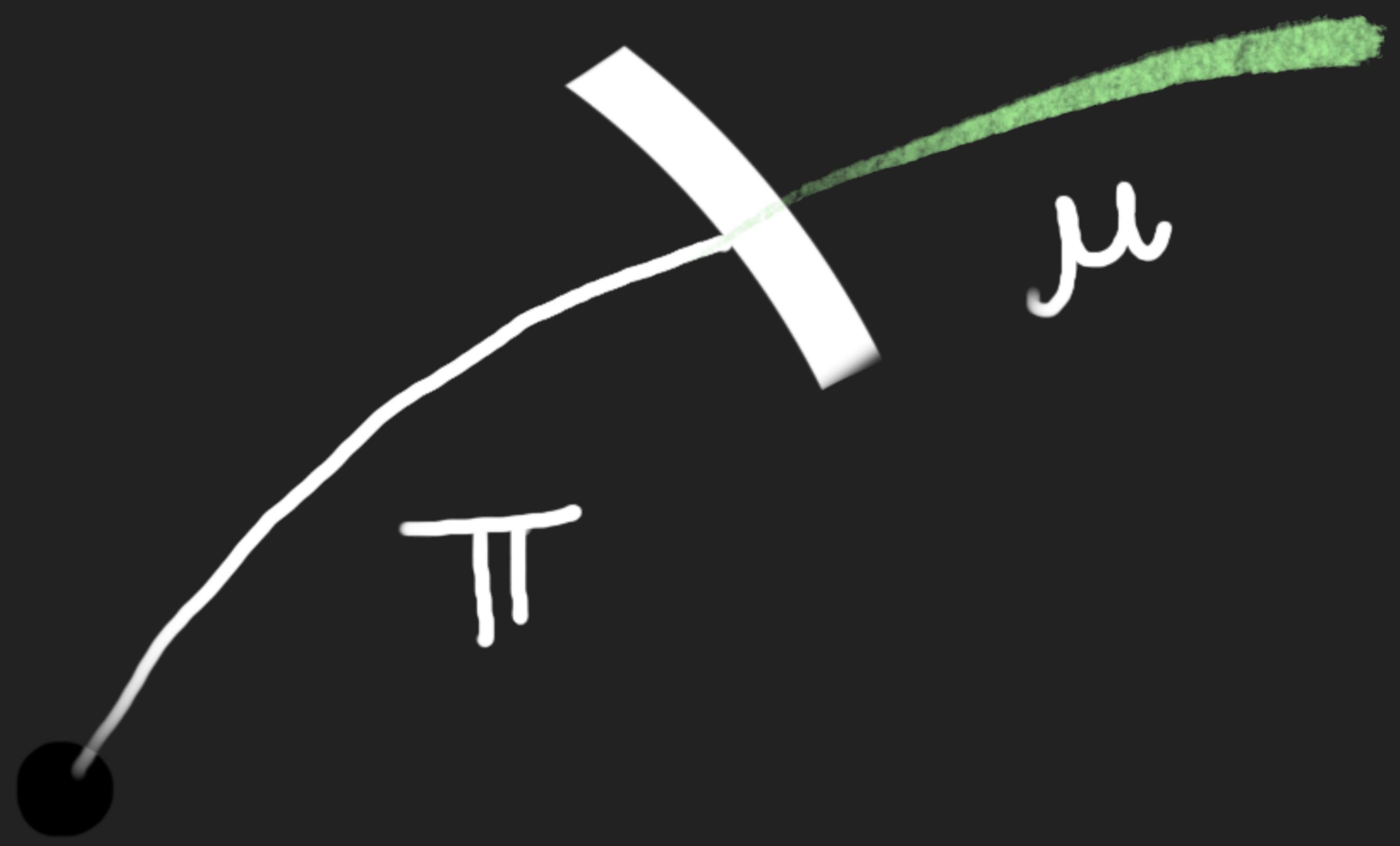

Non-prompt μ

$$F.F. = \frac{N^{\text{i,i,i}} - N^{\text{i,i,i}}_{\text{non-Z+jets}}}{N^{\text{i,i,a}} - N^{\text{i,i,a}}_{\text{non-Z+jets}}}$$

F.F. derived in a Z+jets rich region

$Z \rightarrow \ell\ell$ + recoiling ℓ

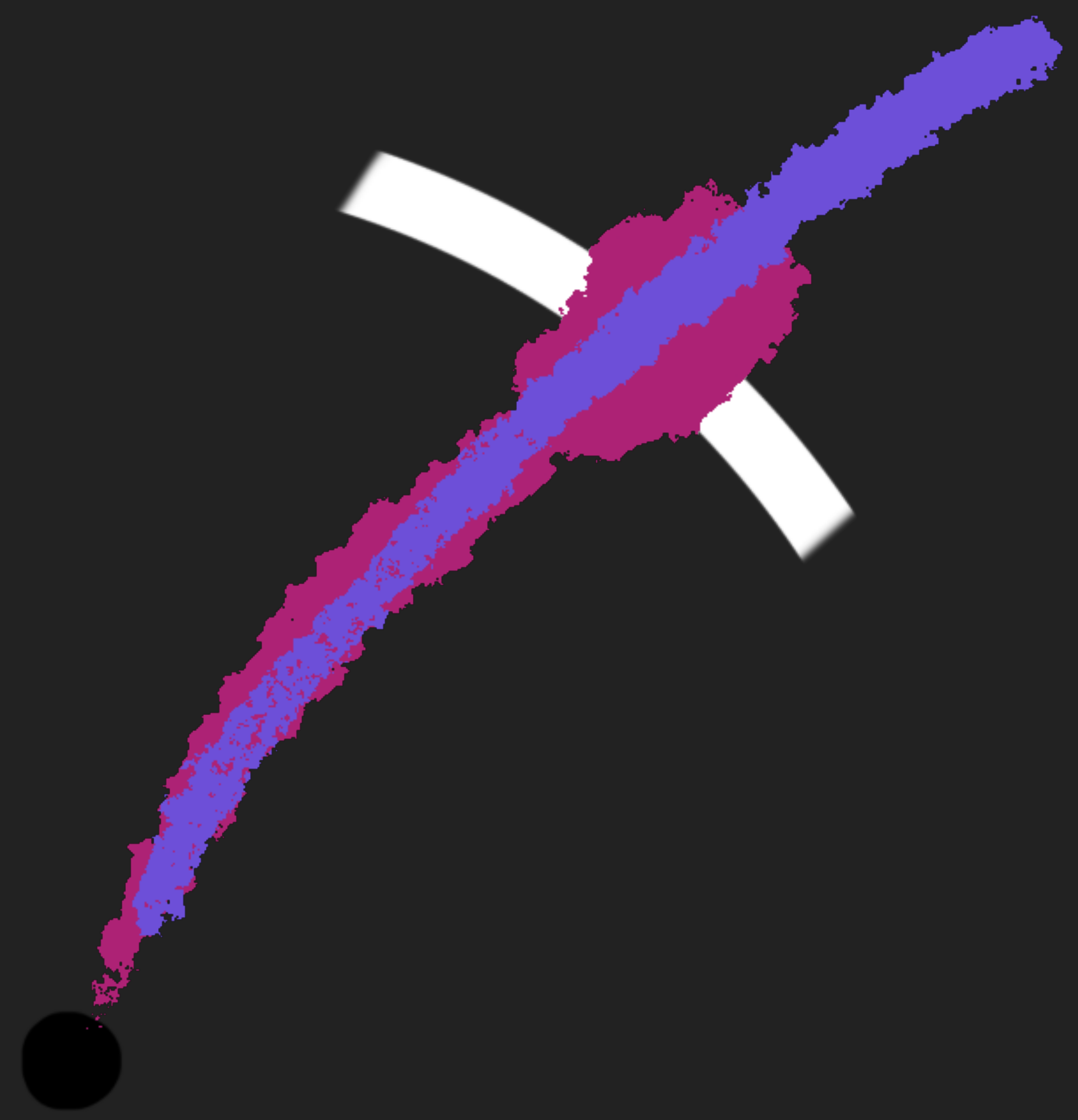

e inside HF jet

Simultaneous Fit

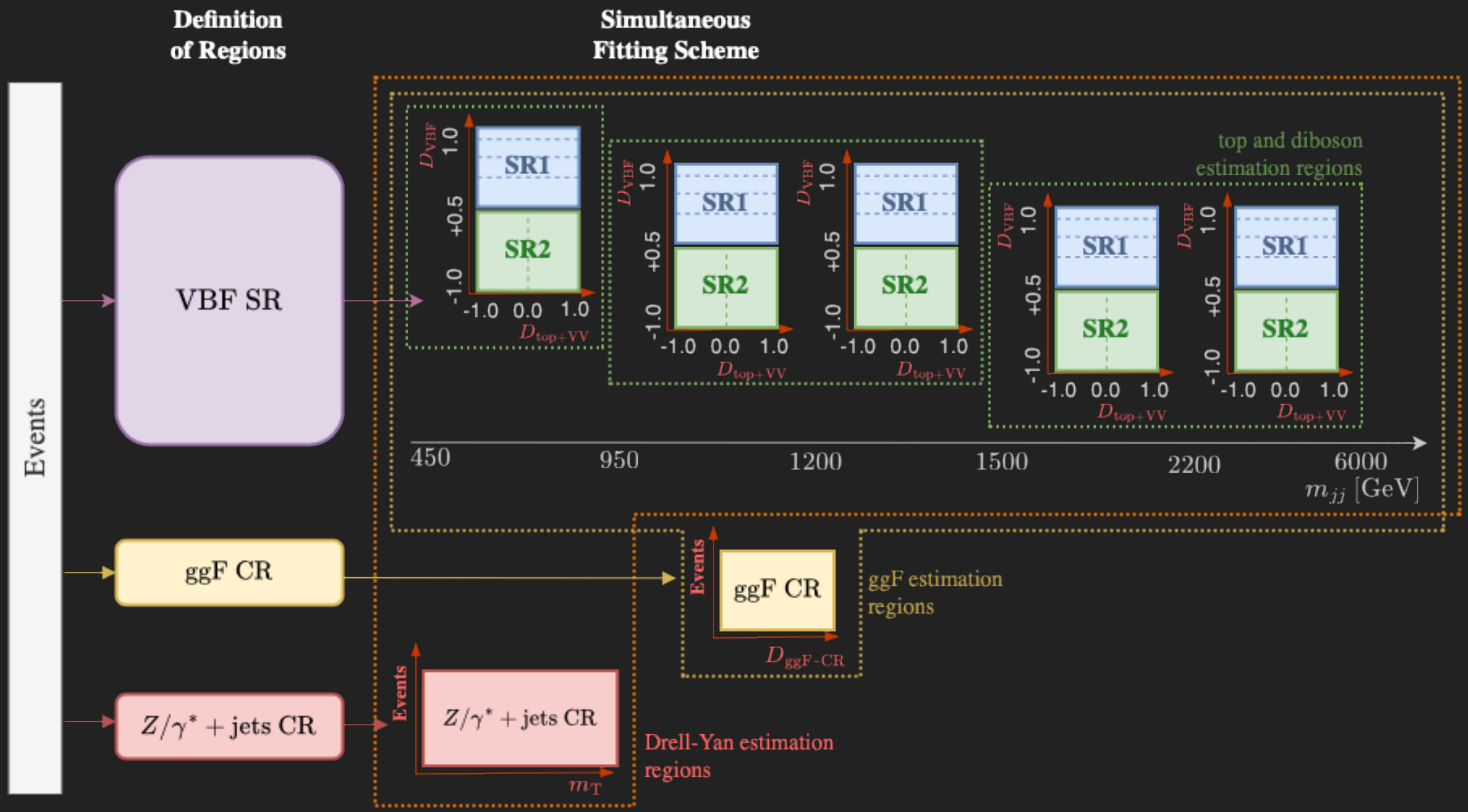

Profile likelihood minimizing fit designed to minimize **total uncertainty** – slight cost of adding stat errors while significantly reducing systematics

The bootstrapping mechanism

- Same data events are used to measure any two differential cross-sections ⇒ measurements are correlated
- We create an ensemble of (pseudo) datasets to evaluate correlations – same data taken in 1000 universes
  1. Weigh data events by Poisson(1)
  2. Binned likelihood minimizing fits for each universe
  3. Statistical covariance between extracted parameters *a* and *b* –

$$\mathrm{COV}(a,b) = \frac{1}{1000}\sum_{i=1}^{1000}\left(a_i - \bar{a}\right)\left(b_i - \bar{b}\right)$$

- Differential XS + correlations = maximal information for theorists! Allows interpretations using more than one distribution

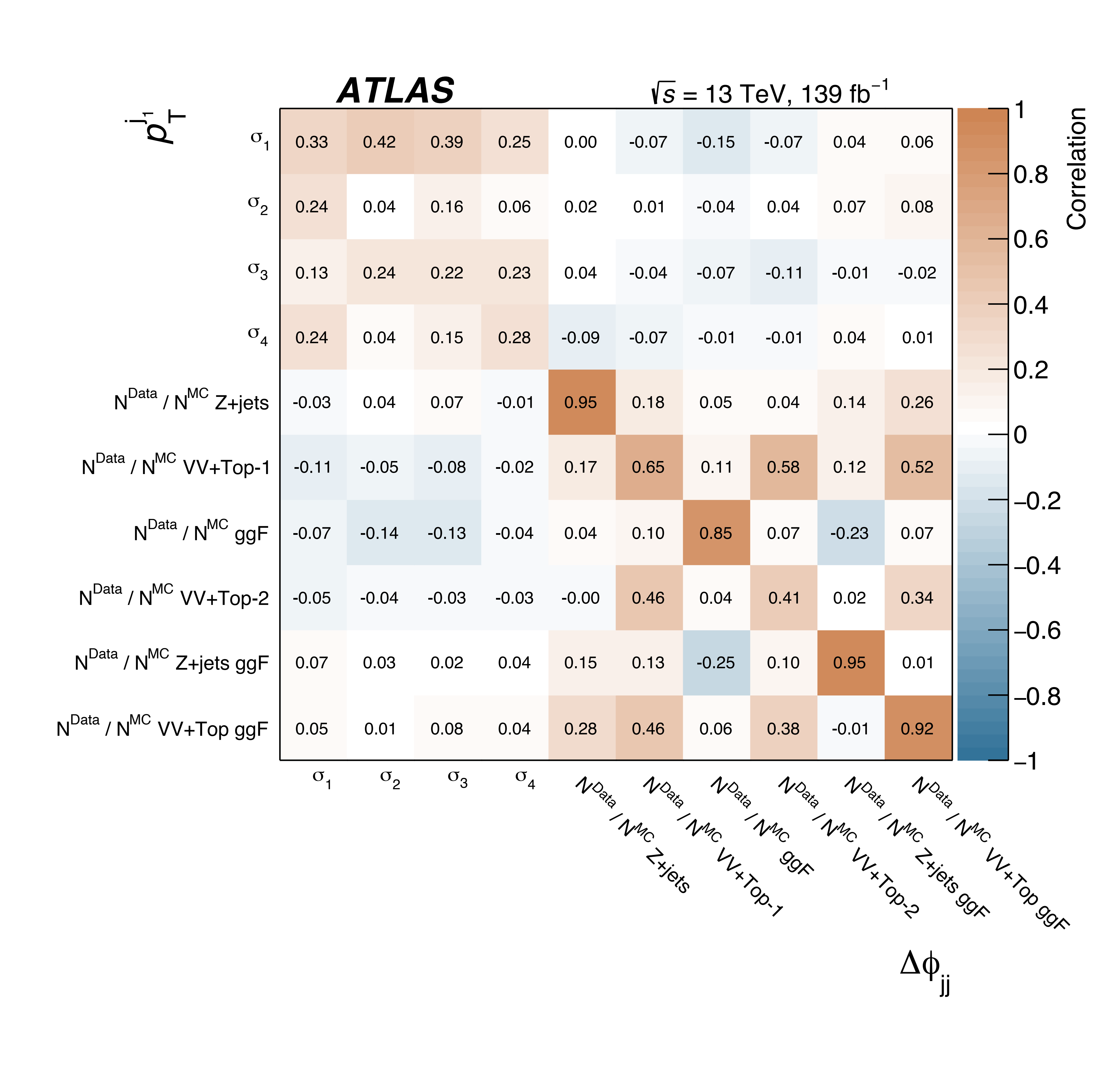

Correlations between measurements

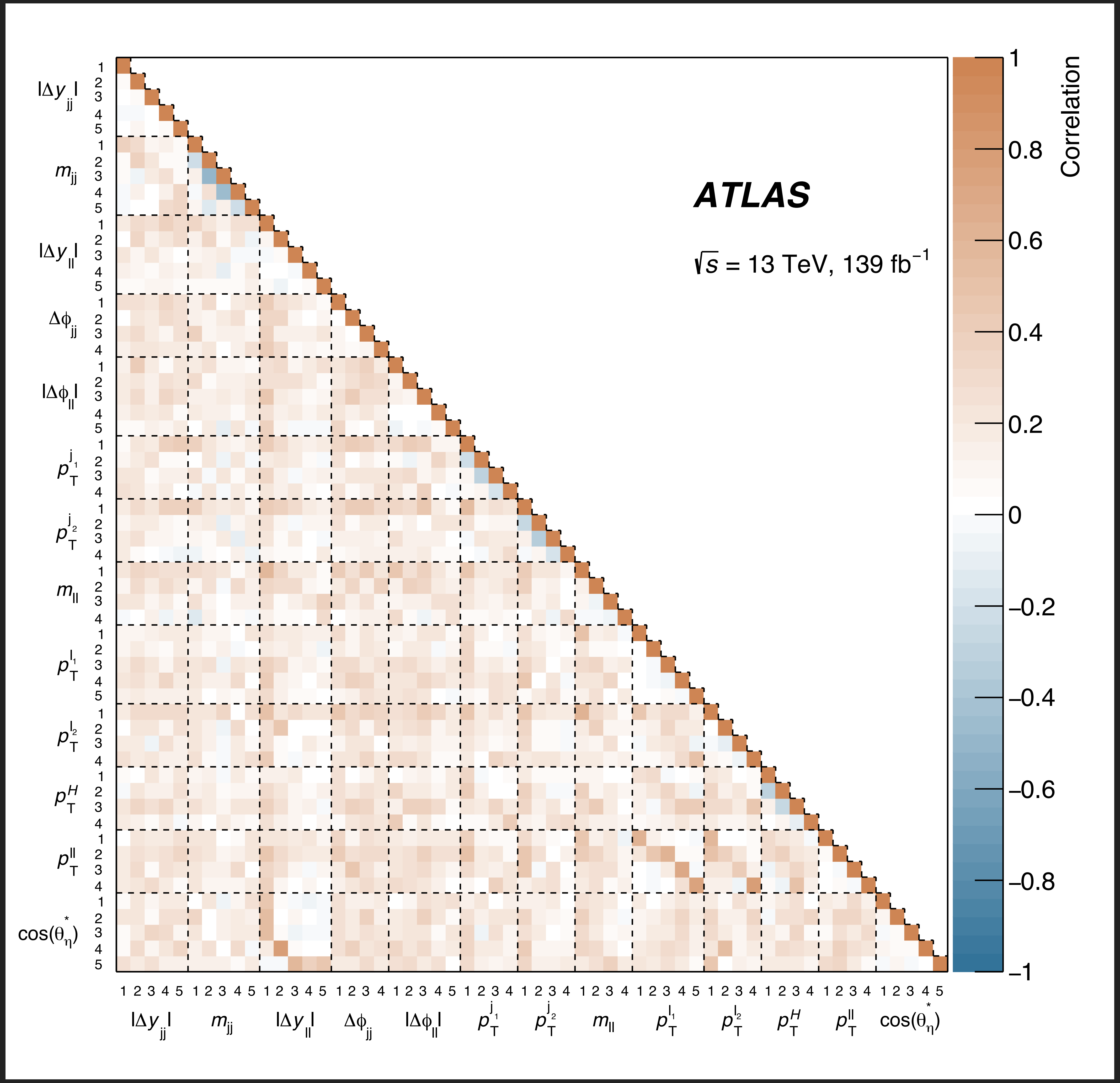

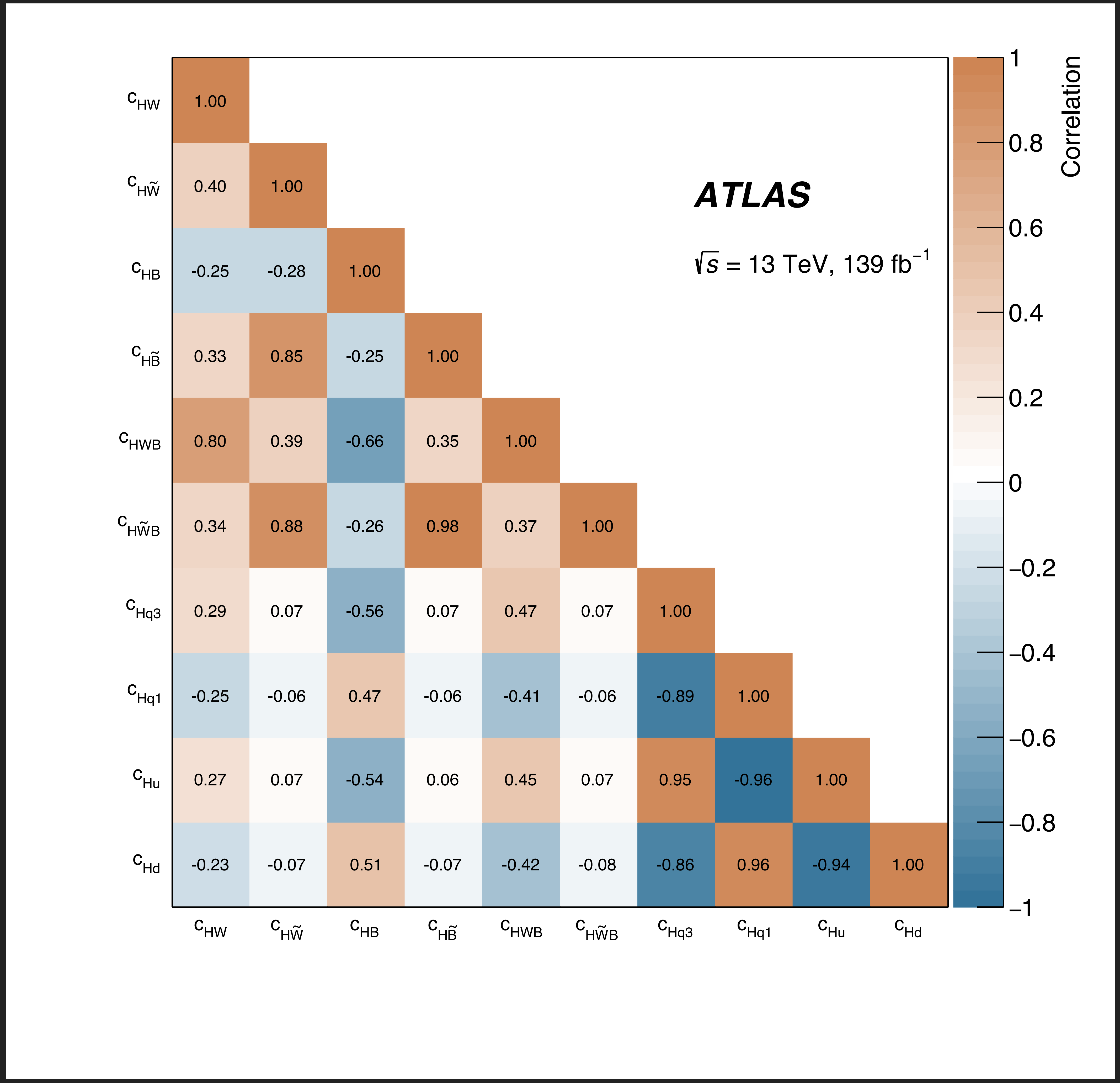

Long Lived Particle searches at ATLAS – A teaser

- LHC Run-3 great time to search for LLPs with the ATLAS detector!
- Major speed-up in standard tracking makes room for reconstruction of high impact parameter objects

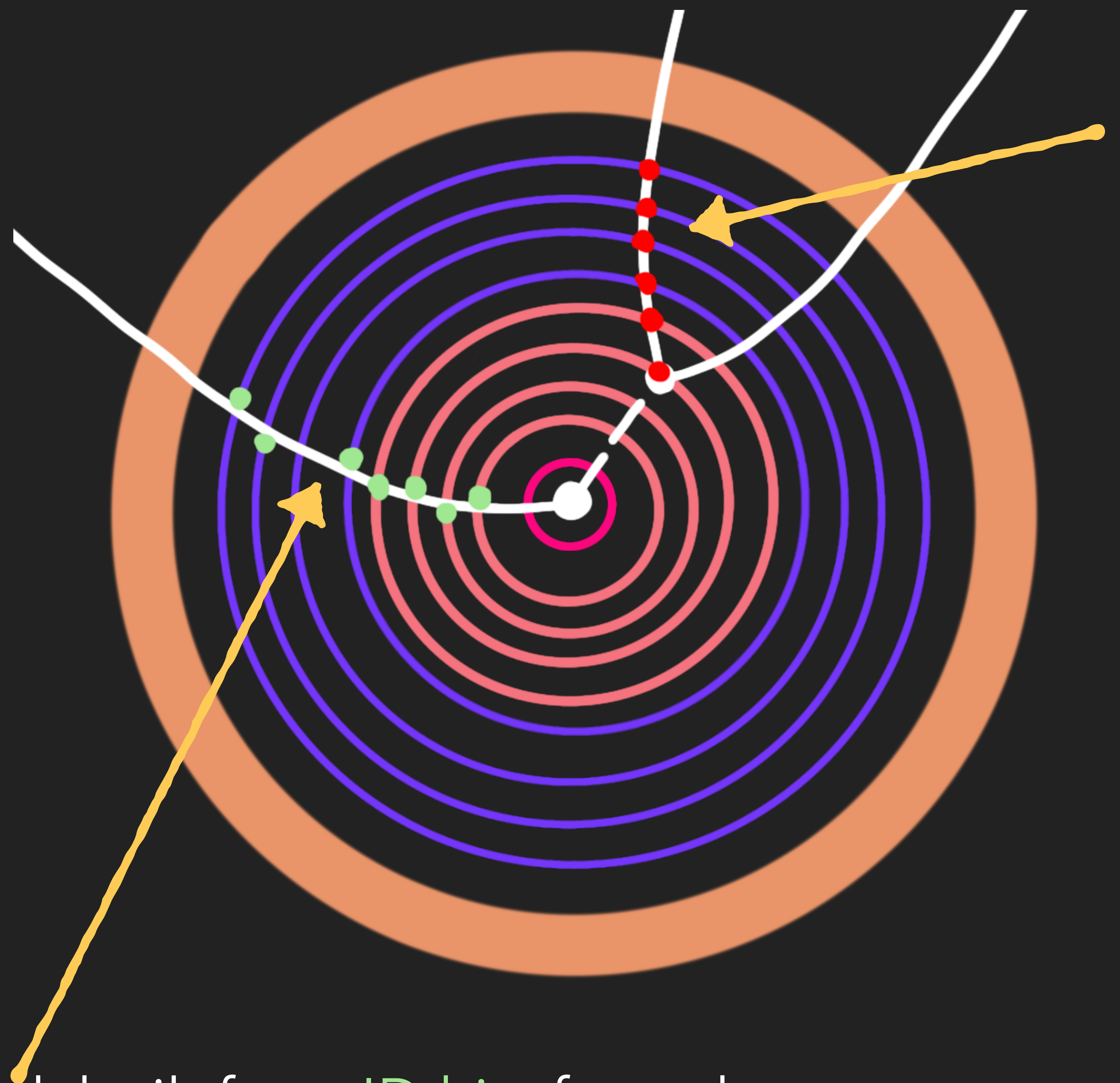

Large Radius Tracking (LRT) used for building tracks with large d_0. Made with leftover hits after prompt pass. Useful for long lived particle searches.

Track built from ID hits from the prompt tracking pass optimised for low-d_0 (< 5 mm) tracks

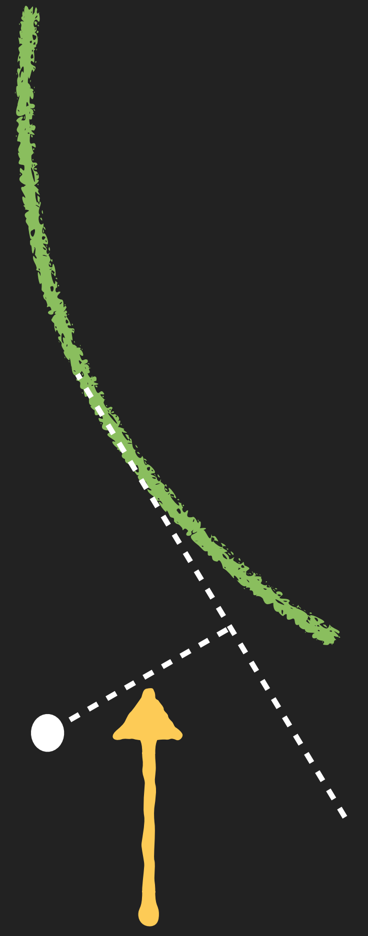

d_0 = Distance of closest approach

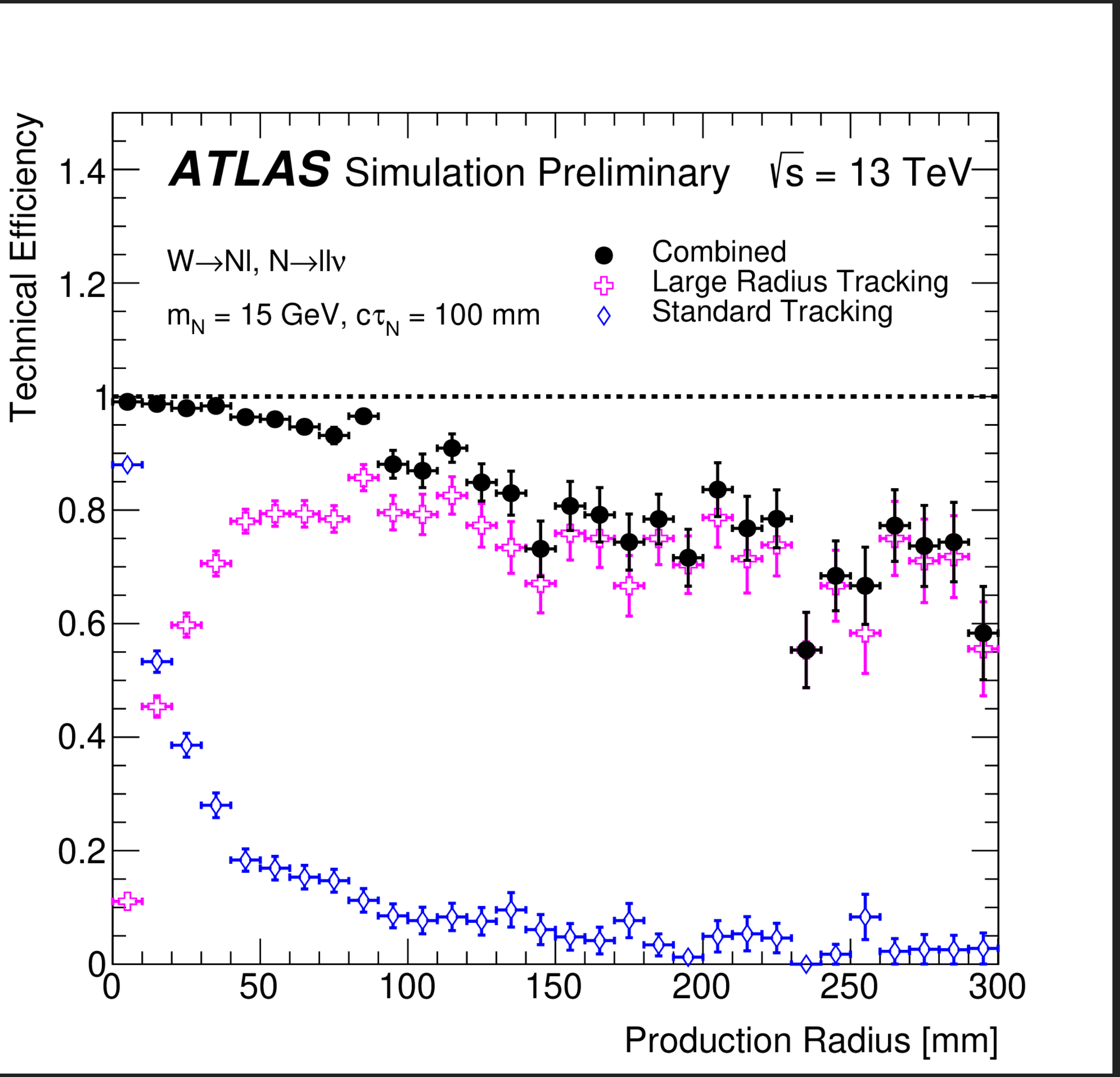

LRT Muon Performance

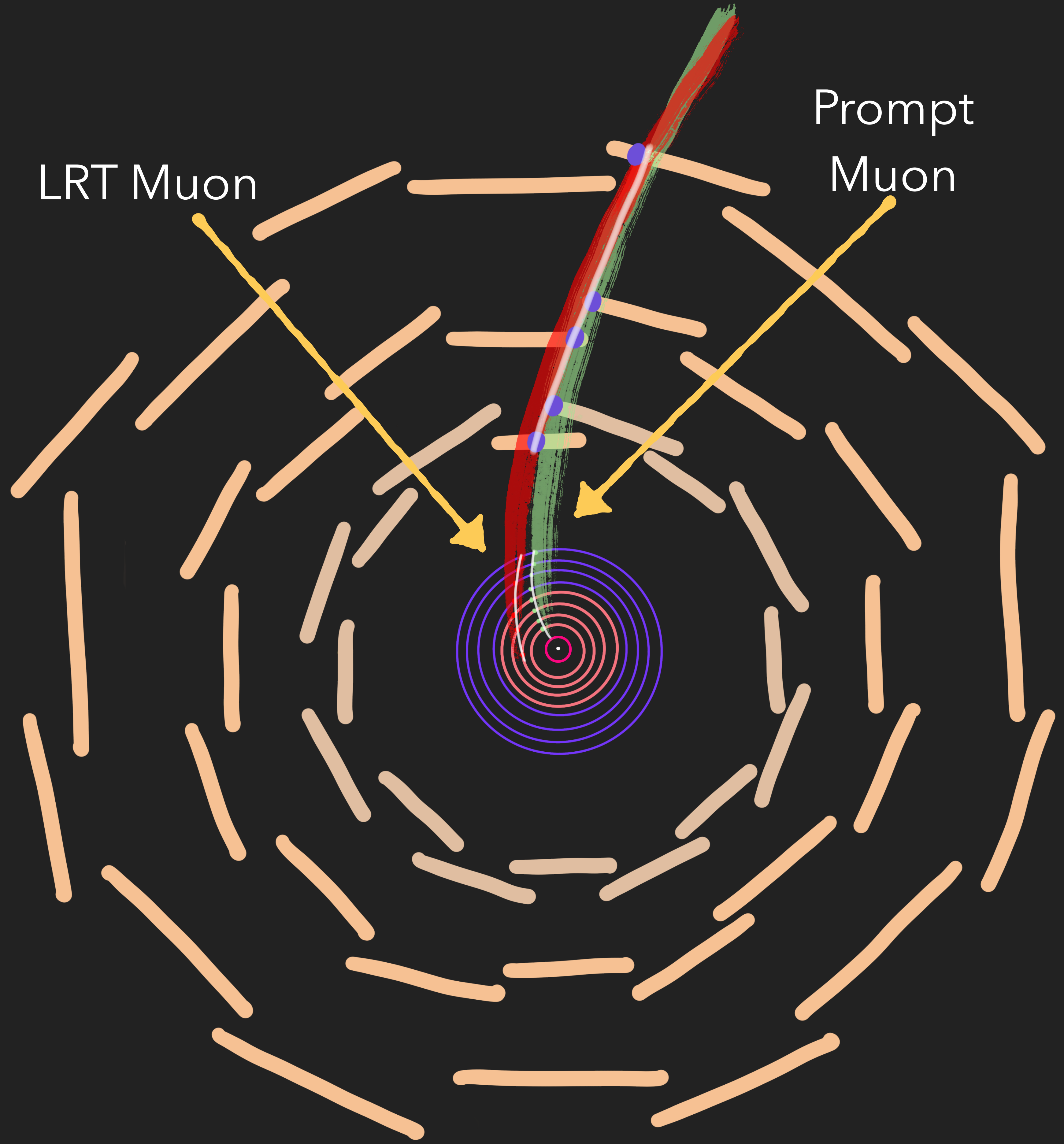

Prompt-LRT muons overlap removal procedure

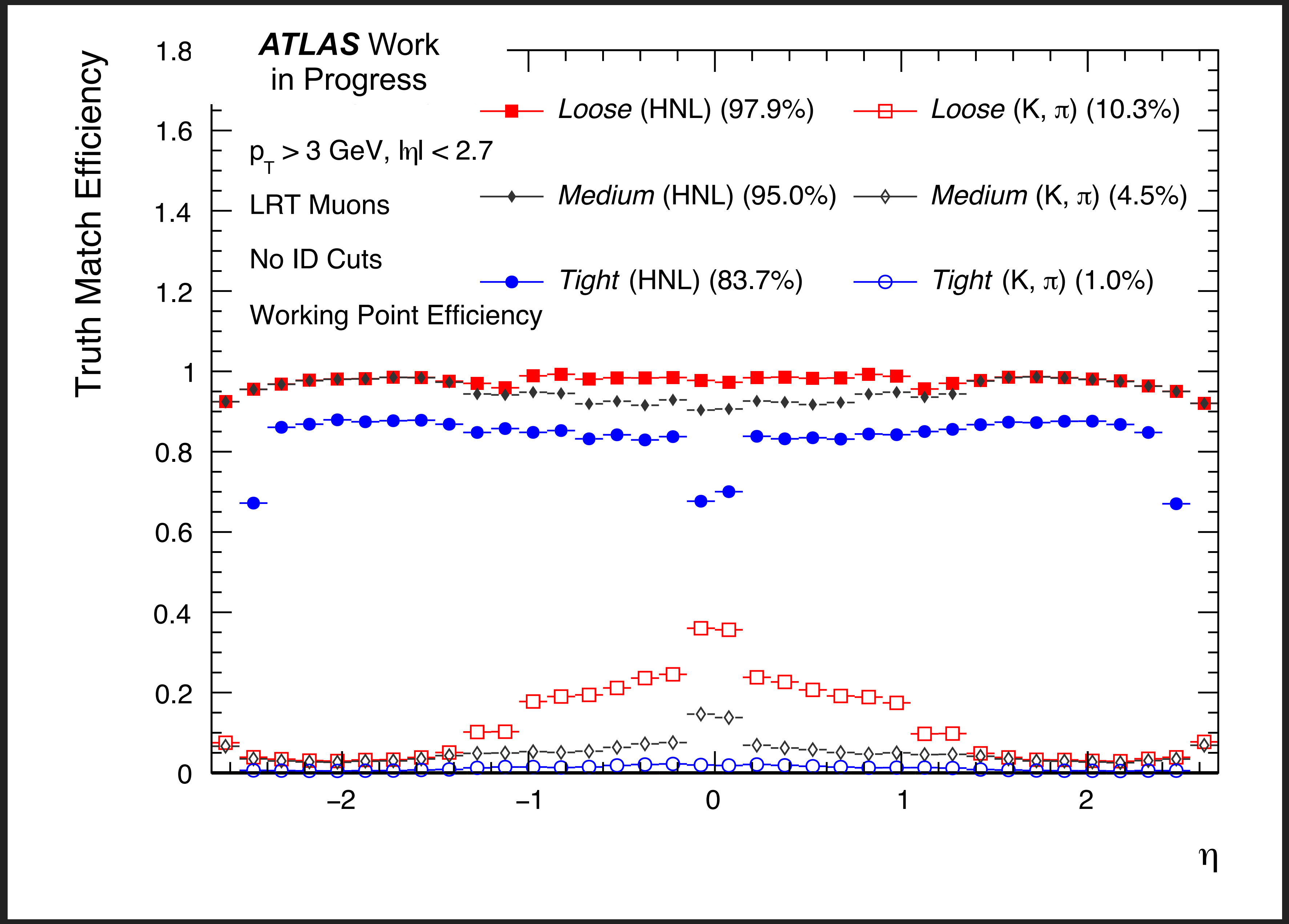

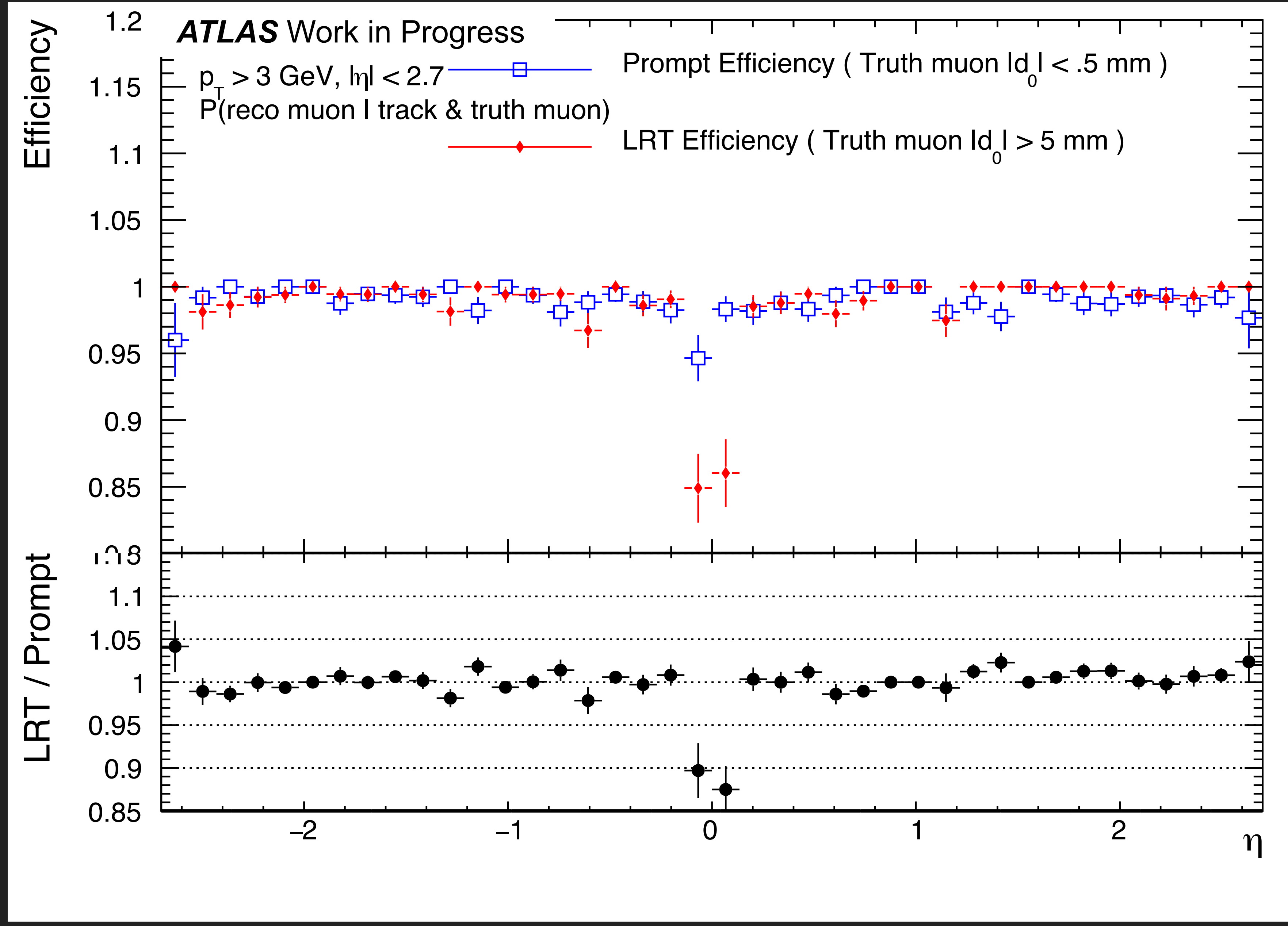

Identification quality / working points (WP) for LRT muons

Calibration of muon WP

Muon spectrometers “far” from the ATLAS tracker – insensitive to mm level displacements at the interaction point

Using Muon Performance

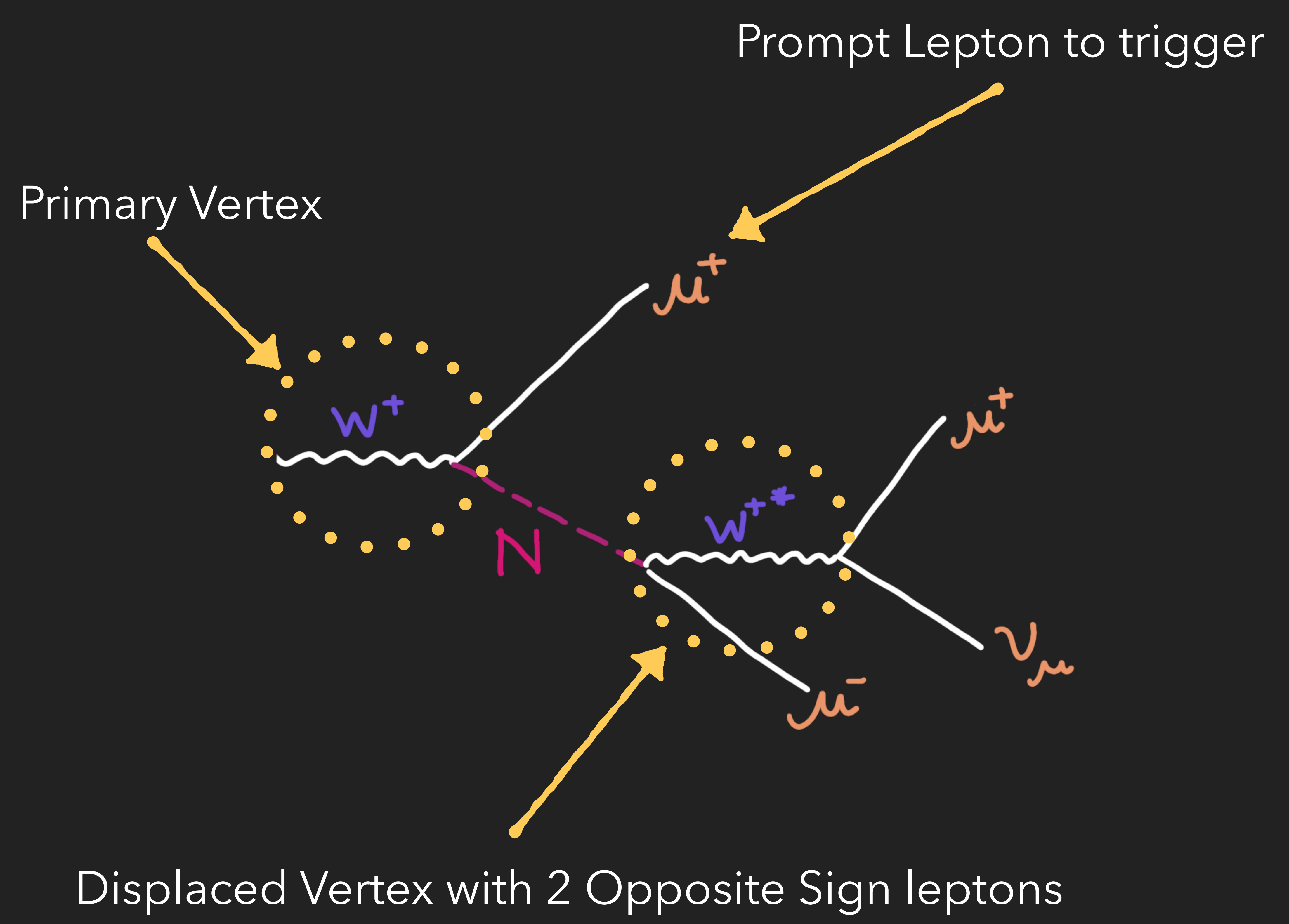

Search for Heavy Neutral Leptons with a displaced vertex

Electrical Testing

Set-up a standalone device to measure the IV response of Silicon sensors. Important quality control step to track the electrical response of the detector to various assembly and testing stages.

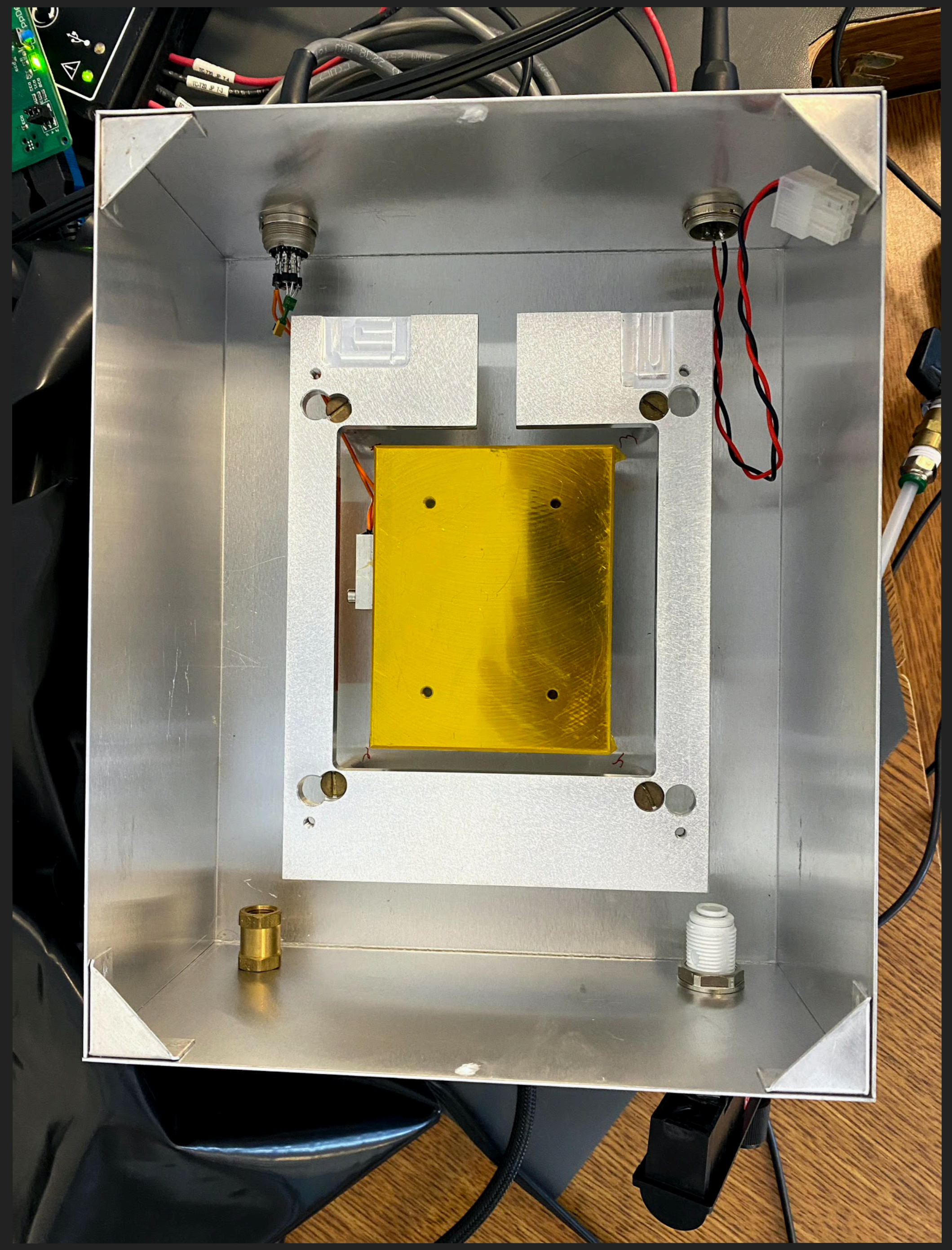

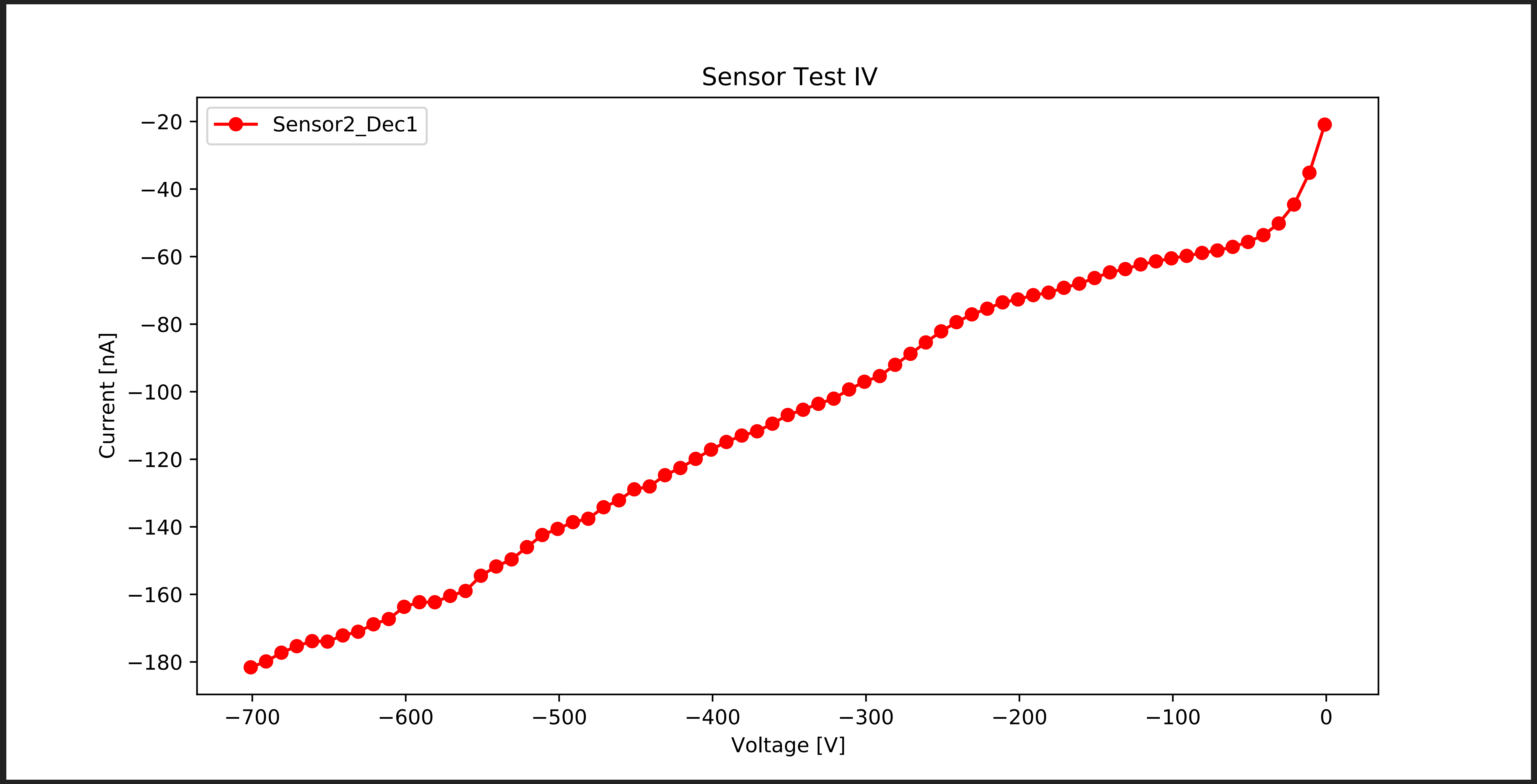

Simplified Template Cross Section Measurements

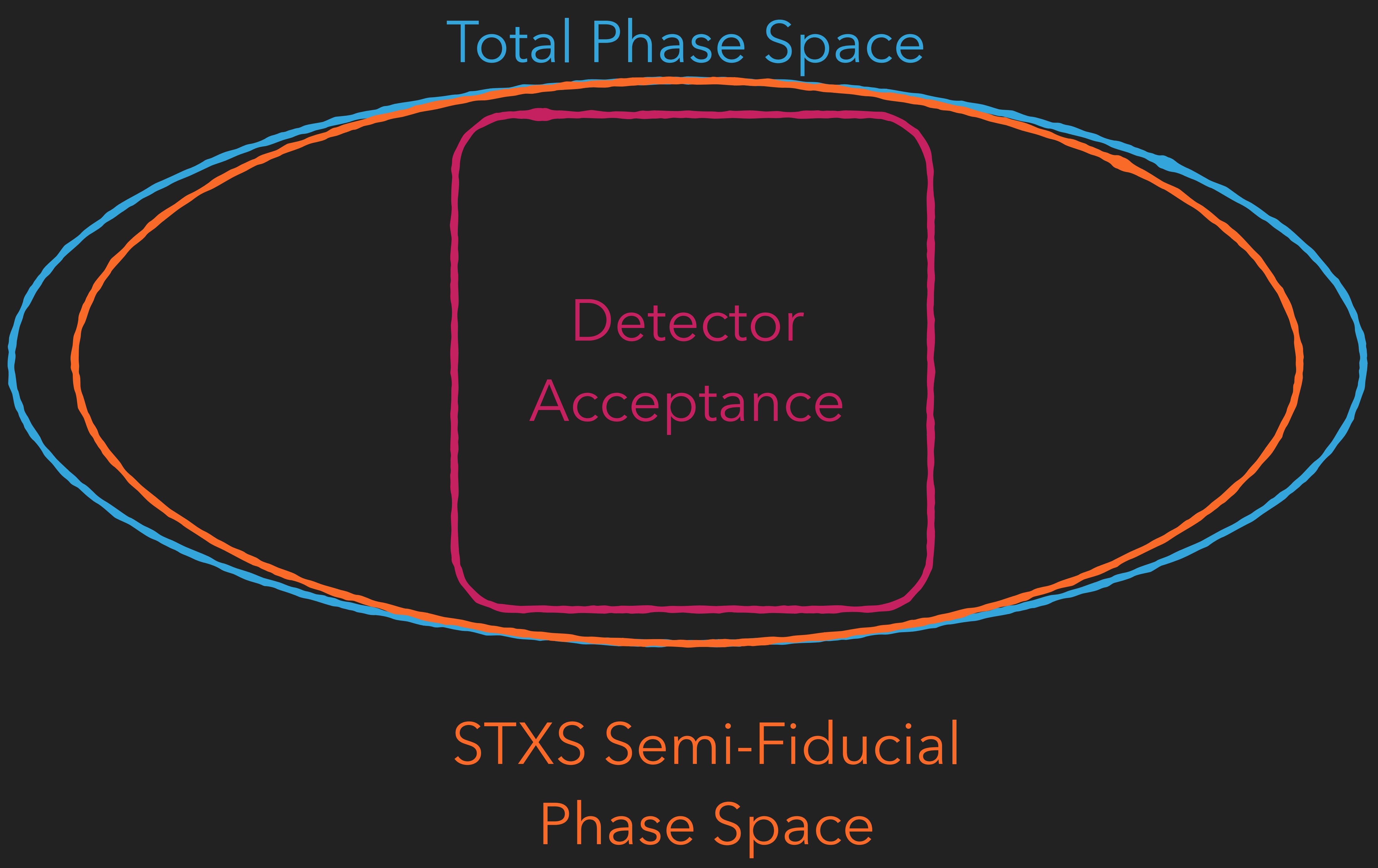

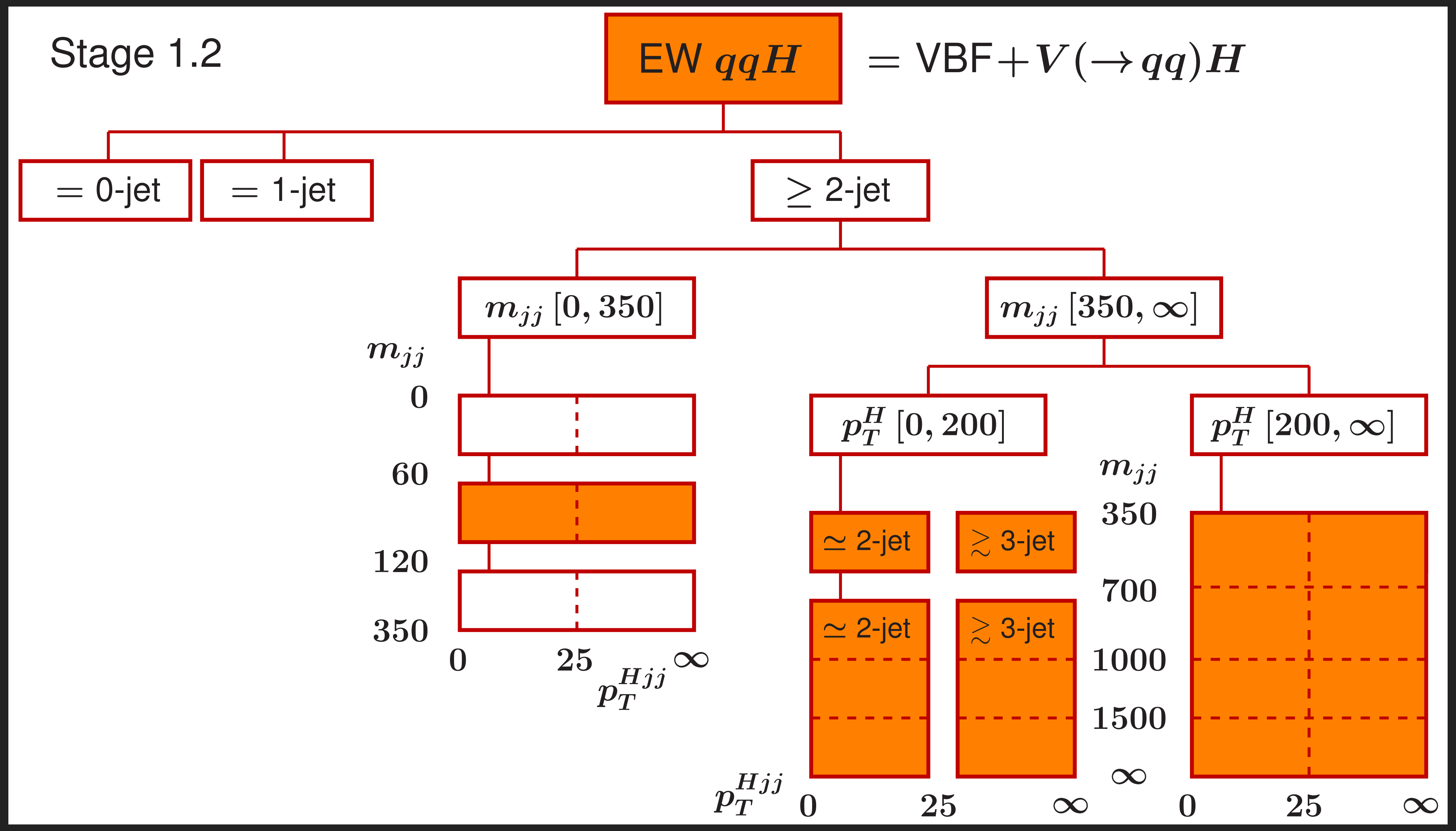

Independent Methods - Adversarial Network with Domain Adaptation

Camaiani et al: Eur. Phys. J. C (2022) 82:921

Fig. 1 Schematic view of the adversarial deep neural network

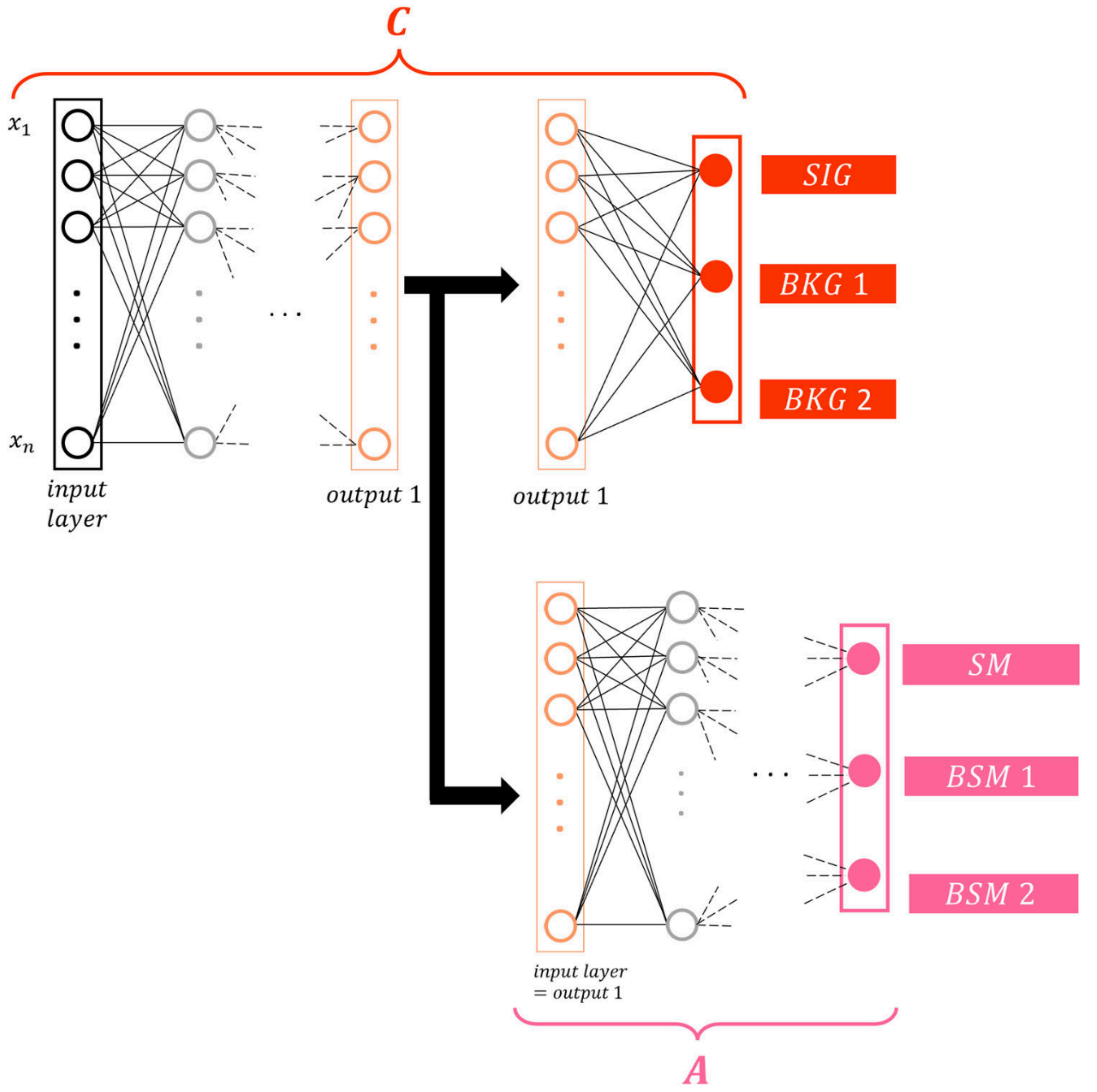

STXS Uncertainties

Source	$\frac{\Delta\sigma_{\mathrm{VBF}}\cdot\mathcal{B}_{H\to WW^*}}{\sigma_{\mathrm{VBF}}\cdot\mathcal{B}_{H\to WW^*}}$ [%]
Data statistical uncertainties	15
Total systematic uncertainties	18
MC statistical uncertainties	4.9
Experimental uncertainties	6.7
Flavor tagging	1.0
Jet energy scale	3.7
Jet energy resolution	2.1
$E_{\mathrm{T}}^{\mathrm{miss}}$	4.9
Muons	0.8
Electrons	0.4
Fake factors	0.8
Pileup	1.3
Luminosity	2.2
Theoretical uncertainties	16
ggF	4.6
VBF	12
WW	5.5
Top	6.4
$Z\tau\tau$	1.0
Other VV	1.5
Other Higgs	0.4
Background normalizations	4.9
WW	0.6
Top	3.4
$Z\tau\tau$	3.4
Total	23

STXS $H \to WW$ (arXiv: 2207.00338)

Fiducial Phase Space Definition

Selection Requirements	Signal Region	Fiducial Region
Lepton pair flavors	e-μ	
Lepton pair charge	0	
Leading (subleading) lepton p_T	> 22 GeV (> 15 GeV)	
Lepton η^ℓ	$\lvert\eta^\mu\rvert < 2.5$	
	$0 < \lvert\eta^e\rvert < 1.37$ or $1.52 < \lvert\eta^e\rvert < 2.47$	$\lvert\eta^e\rvert < 2.5$
No. of additional leptons	0	
$\Delta R(\ell, \ell)$	overlap removal	> 0.1
$m_{\ell\ell}$	> 10 GeV	
$\Delta R(\ell, \text{jet})$	overlap removal	> 0.4
No. of jets ($p_T > 30$ GeV, $\lvert\eta\rvert < 4.5$)	≥ 2	
No. of b-jets ($p_T > 20$ GeV, $\lvert\eta\rvert < 2.5$)	0	
$m_{\tau\tau}$	$< m_Z - 25$ GeV	
Central jet veto ($p_T > 20$ GeV)	✓	
Outside lepton veto	✓	
m_{jj}	> 450 GeV	
$\lvert\Delta y_{jj}\rvert$	> 2.1	
$\lvert\Delta\phi_{\ell\ell}\rvert$	< 1.4 rad	

EFT Operators

Wilson Coeff.	Operator Structure	Fit distr.	Param. Order	95% confidence interval [TeV $^{-2}$] Expected	Observed
c_{HW}	$H^\dagger H\, W^n_{\mu\nu} W^{n\mu\nu}$	$\Delta\phi_{jj}$	lin.	[-1.7, 1.6]	[-2.6, 0.60]
			lin. + quad.	[-1.4, 1.4]	[-1.8, 0.61]
c_{HB}	$H^\dagger H\, B_{\mu\nu} B^{\mu\nu}$	$\Delta\phi_{jj}$	lin.	[-5.9, 6.4]	[-6.7, 4.6]
			lin. + quad.	[-0.59, 0.66]	[-0.60, 0.66]
c_{HWB}	$H^\dagger \tau^n H\, W^n_{\mu\nu} B^{\mu\nu}$	$\Delta\phi_{jj}$	lin.	[-10, 9]	[-14, 5.9]
			lin. + quad.	[-1.2, 1.1]	[-1.2, 1.1]
c_{Hq1}	$(H^\dagger i \overleftrightarrow{D}_\mu H)(\bar{q}\gamma^\mu q)$	p_{T}^{j1}	lin.	[-12, 15]	[-6.9, 22]
			lin. + quad.	[-1.9, 1.7]	[-2.2, 2.0]
c_{Hq3}	$(H^\dagger i \overleftrightarrow{D}^n_\mu H)(\bar{q}\tau^n\gamma^\mu q)$	p_{T}^{j1}	lin.	[-0.56, 0.47]	[-0.74, 0.30]
			lin. + quad.	[-0.43, 1.2]	[-0.56, 0.43]
c_{Hu}	$(H^\dagger i \overleftrightarrow{D}_\mu H)(\bar{u}\gamma^\mu u)$	p_{T}^{j1}	lin.	[-8.3, 6.9]	[-11, 4.2]
			lin. + quad.	[-2.0, 2.6]	[-2.5, 3.1]
c_{Hd}	$(H^\dagger i \overleftrightarrow{D}_\mu H)(\bar{d}\gamma^\mu d)$	p_{T}^{j1}	lin.	[-21, 25]	[-13, 33]
			lin. + quad.	[-3.0, 2.7]	[-3.7, 3.4]
$c_{H\tilde{W}}$	$H^\dagger H\, \tilde{W}^n_{\mu\nu} W^{n\mu\nu}$	$\Delta\phi_{jj}$	lin.	[-1.7, 1.7]	[-1.8, 1.3]
			lin. + quad.	[-1.4, 1.4]	[-1.1, 1.4]
$c_{H\tilde{B}}$	$H^\dagger H\, \tilde{B}_{\mu\nu} B^{\mu\nu}$	$\Delta\phi_{jj}$	lin.	[-28, 28]	[-32, 22]
			lin. + quad.	[-0.62, 0.62]	[-0.63, 0.63]
$c_{H\tilde{W}B}$	$H^\dagger \tau^n H\, \tilde{W}^n_{\mu\nu} B^{\mu\nu}$	$\Delta\phi_{jj}$	lin.	[-15, 15]	[-17, 12]
			lin. + quad.	[-1.2, 1.1]	[-1.2, 1.1]

Uncertainties for Differential Cross Sections

Source	Uncertainty [%]	Uncertainty range [%]				
	σ^{fid}	p_T^H	$p_T^{\ell\ell}$, $p_T^{\ell_1}$, $p_T^{\ell_2}$, $\lvert\Delta y_{\ell\ell}\rvert$, $\lvert\Delta\phi_{\ell\ell}\rvert$, $\cos(\theta^*_\eta)$	$m_{\ell\ell}$	$p_T^{j_1}$, $p_T^{j_2}$, $\lvert\Delta y_{jj}\rvert$, $\Delta\phi_{jj}$	m_{jj}
Signal modeling	5	< 1 – 7	< 1 – 7	< 1 – 19	< 1 – 8	2 – 7
Signal parton shower	< 1	< 1 – 2	< 1 – 1.8	< 1 – 10	< 1 – 1.8	< 1 – 7
$t\bar{t}$ modeling	6	1.7 – 30	3 – 13	3 – 80	3 – 10	1.2 – 70
WW modeling	4	< 1 – 12	3 – 11	2 – 90	3 – 10	3 – 40
Z/γ^*+jets modeling	4	< 1 – 19	2 – 18	4 – 30	3 – 13	2 – 50
ggF modeling	5	4.0 – 28	3.4 – 10	2.6 – 12	2.3 – 9.0	1.4 – 86
Mis-Id background	< 1	< 1 – 12	1.1 – 5	< 1 – 19	1 – 3	< 1 – 40
Jets & Pile-up & E_T^{miss}	5	8 – 60	6 – 30	6 – 120	9 – 30	9 – 130
b-tagging	< 1	< 1 – 9	< 1 – 3	< 1 – 19	1.1 – 3	< 1 – 40
Leptons	1.5	3 – 17	2 – 9	1.2 – 13	1.7 – 7	< 1 – 16
Luminosity	1.5	1.7 – 2	1.3 – 1.9	< 1 – 4	1.5 – 2	< 1 – 1.9
MC statistics	5	10 – 40	6 – 30	6 – 180	8 – 30	7 – 90
Total systematics	13	19 – 90	13 – 60	12 – 180	15 – 50	15 – 200
Data statistics	20	50 – 160	30 – 110	30 – 400	40 – 100	50 – 300
Total uncertainty	23	50 – 190	40 – 120	30 – 500	40 – 100	50 – 400

Lepton Observables

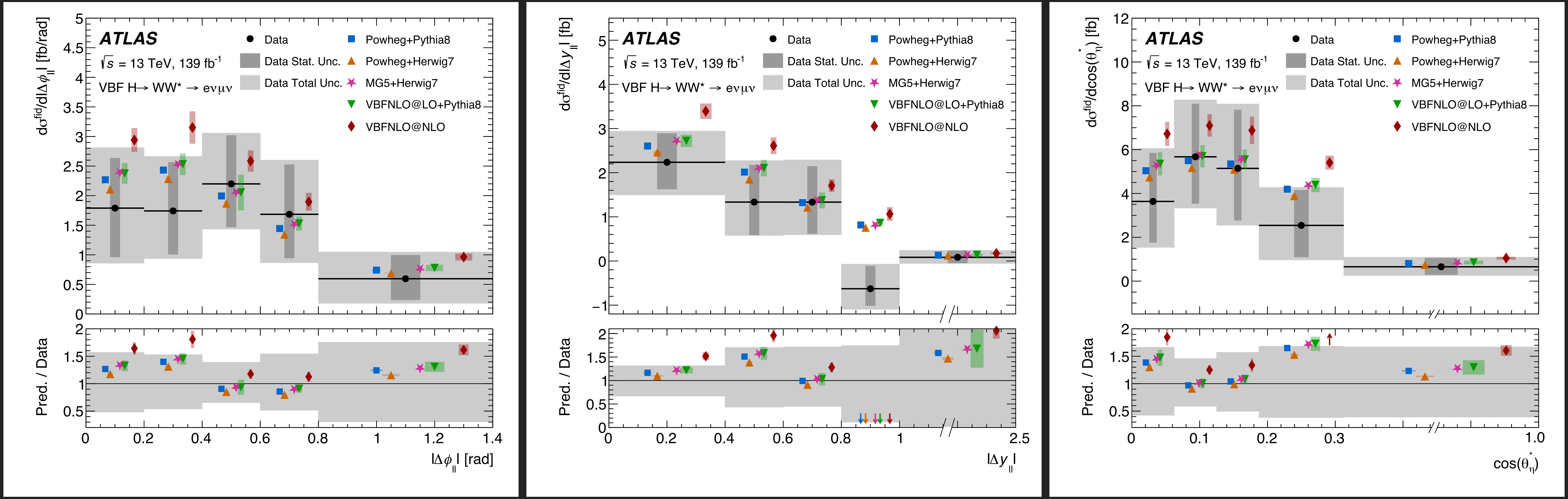

Lepton Observables

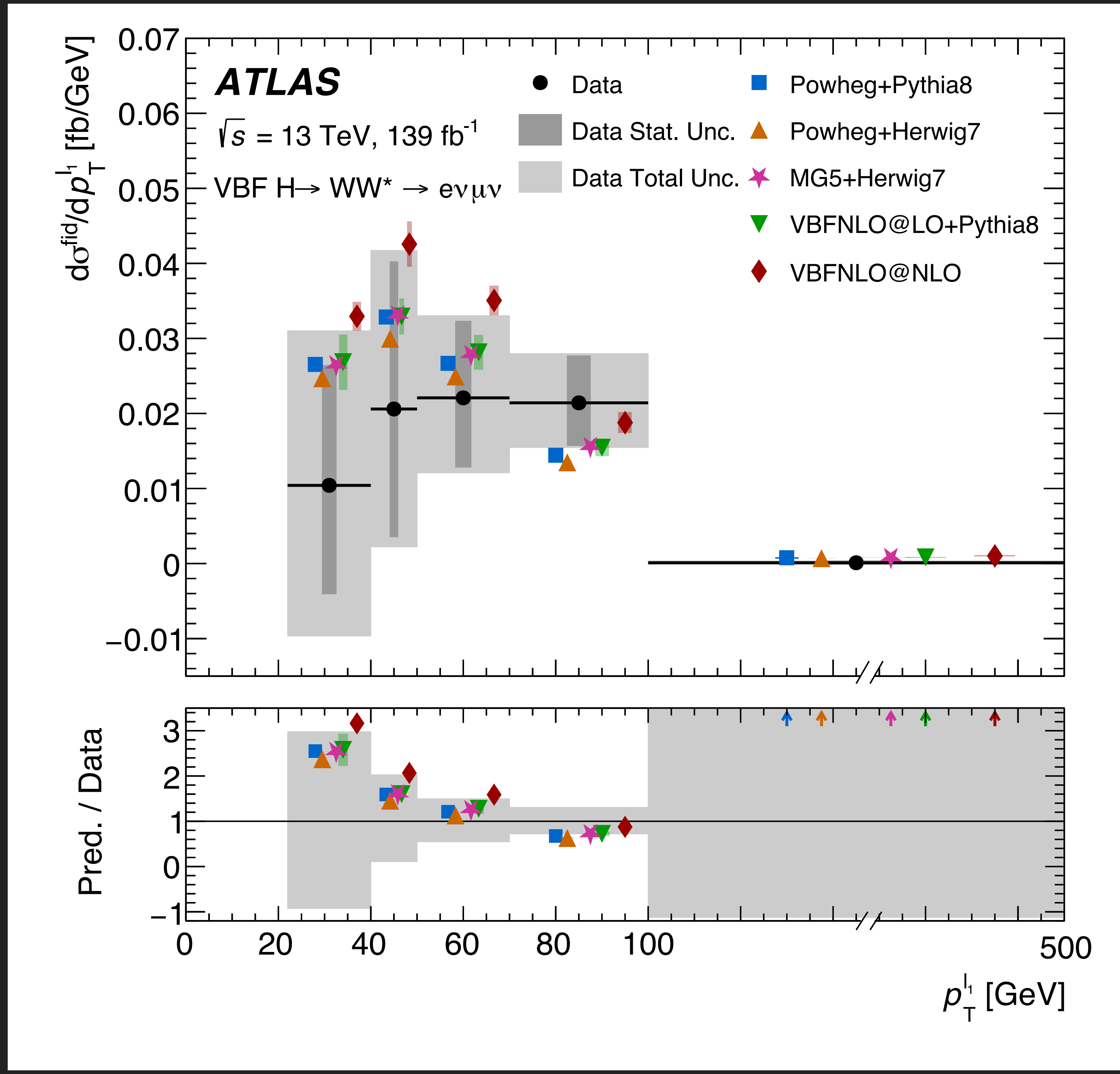

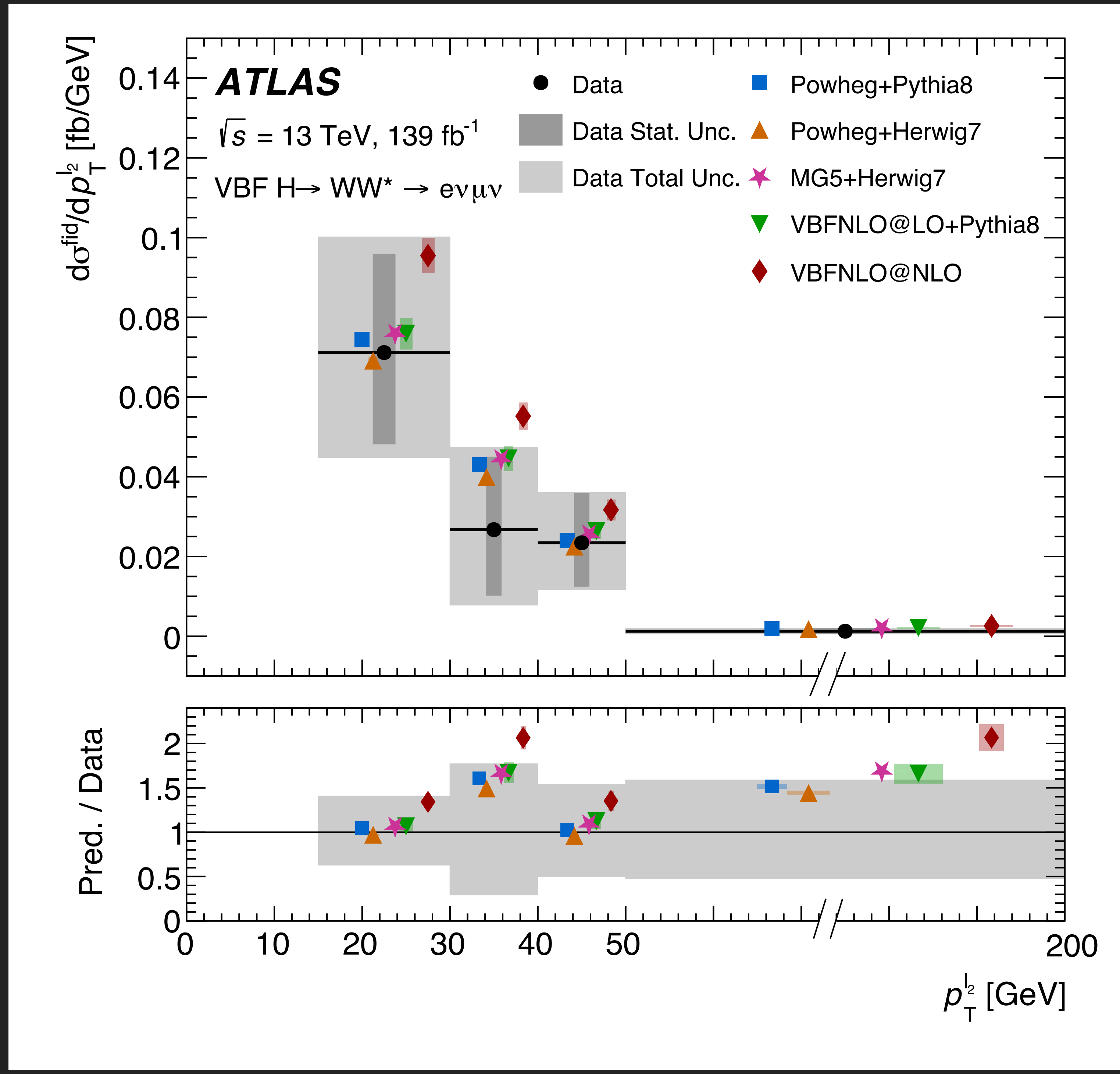

Lepton Observables

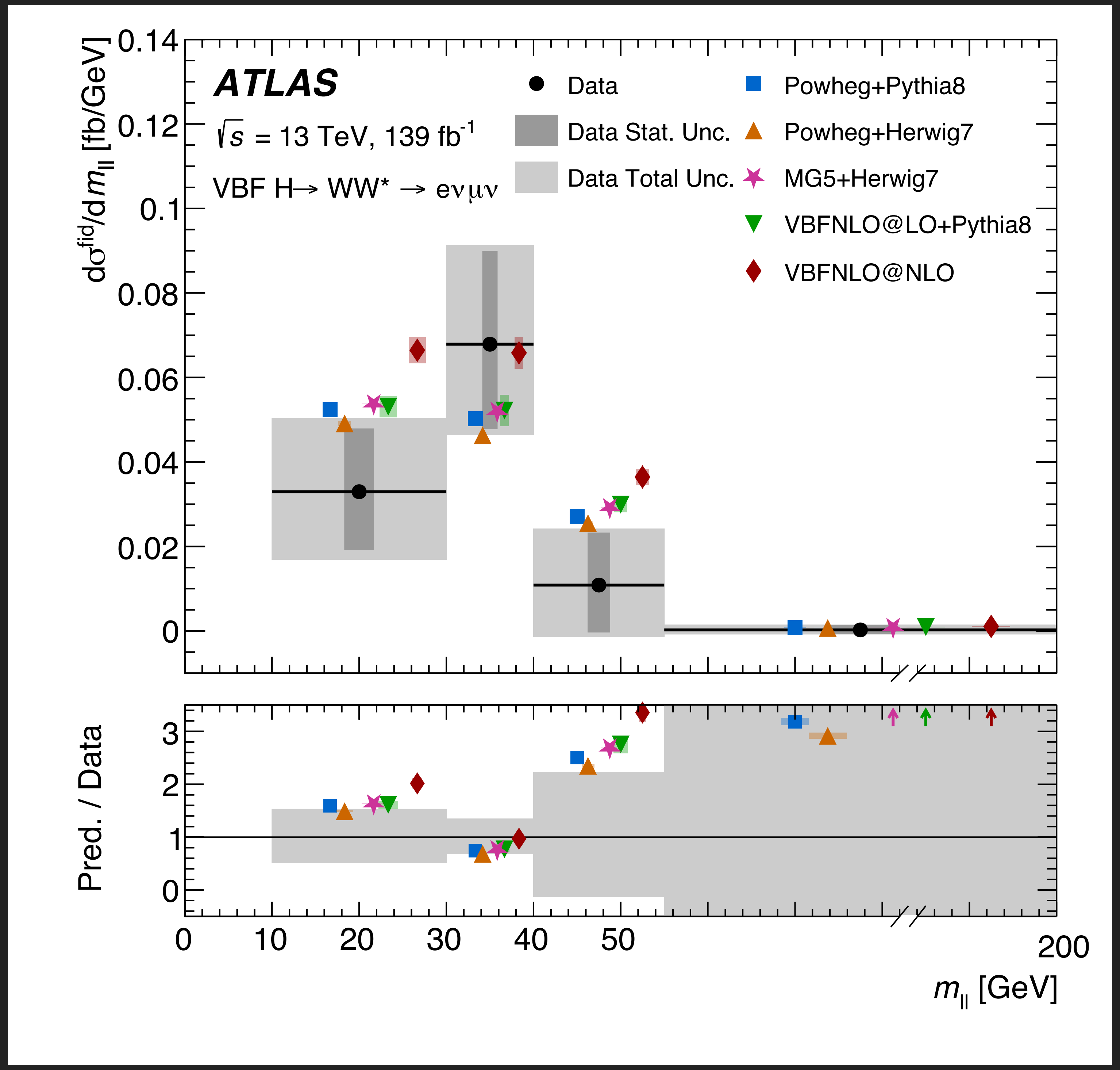

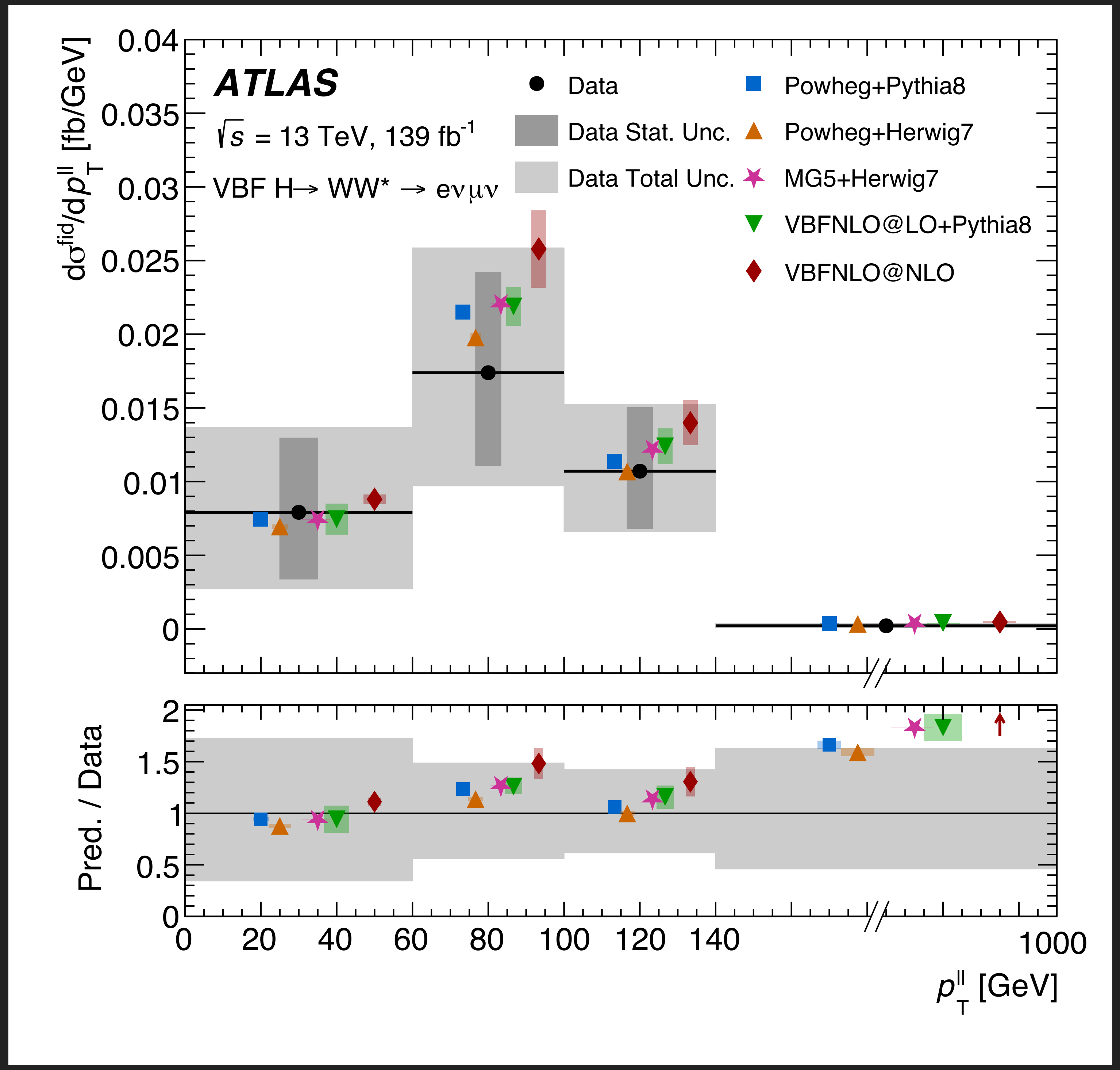

Jet Observables

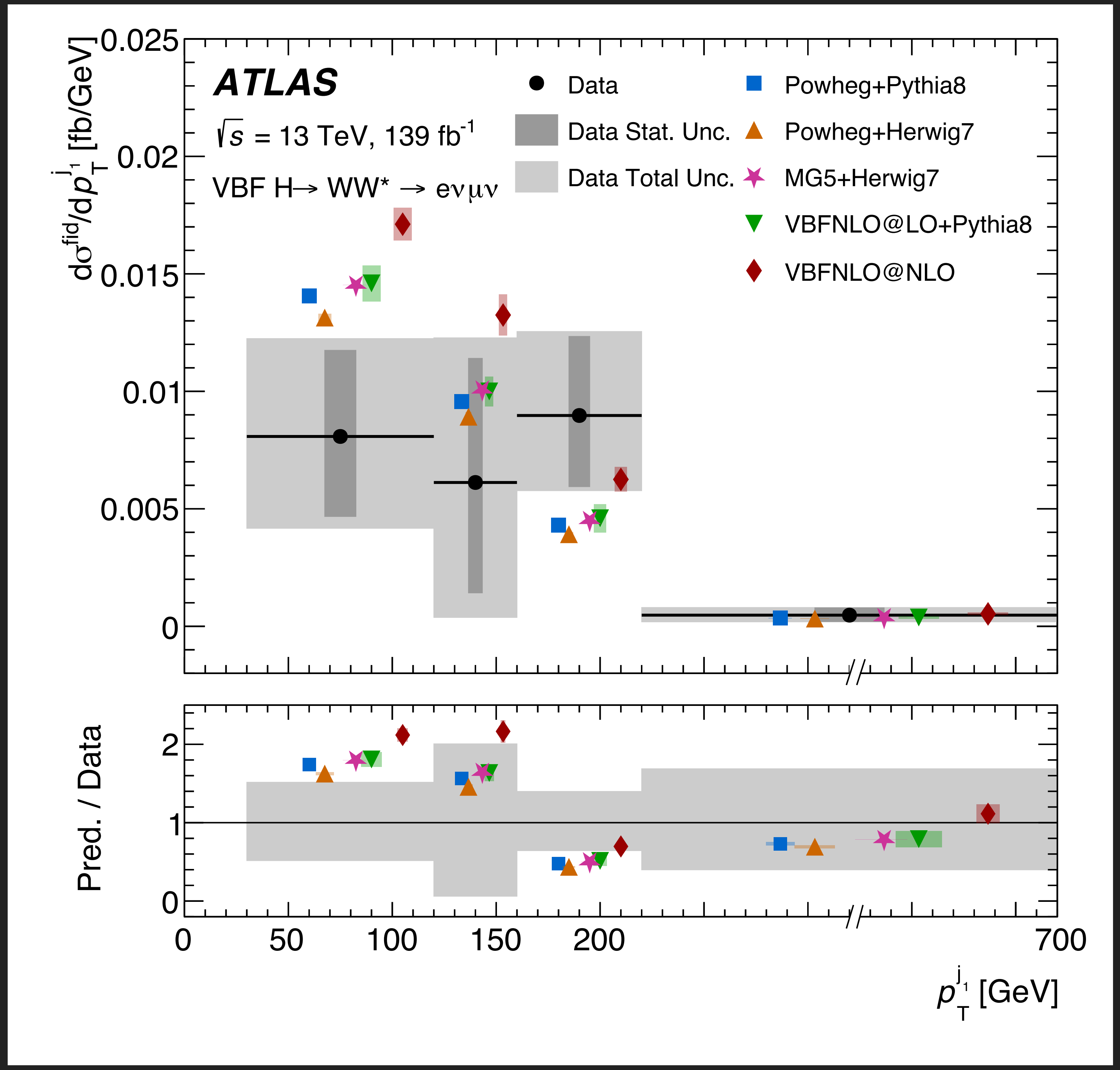

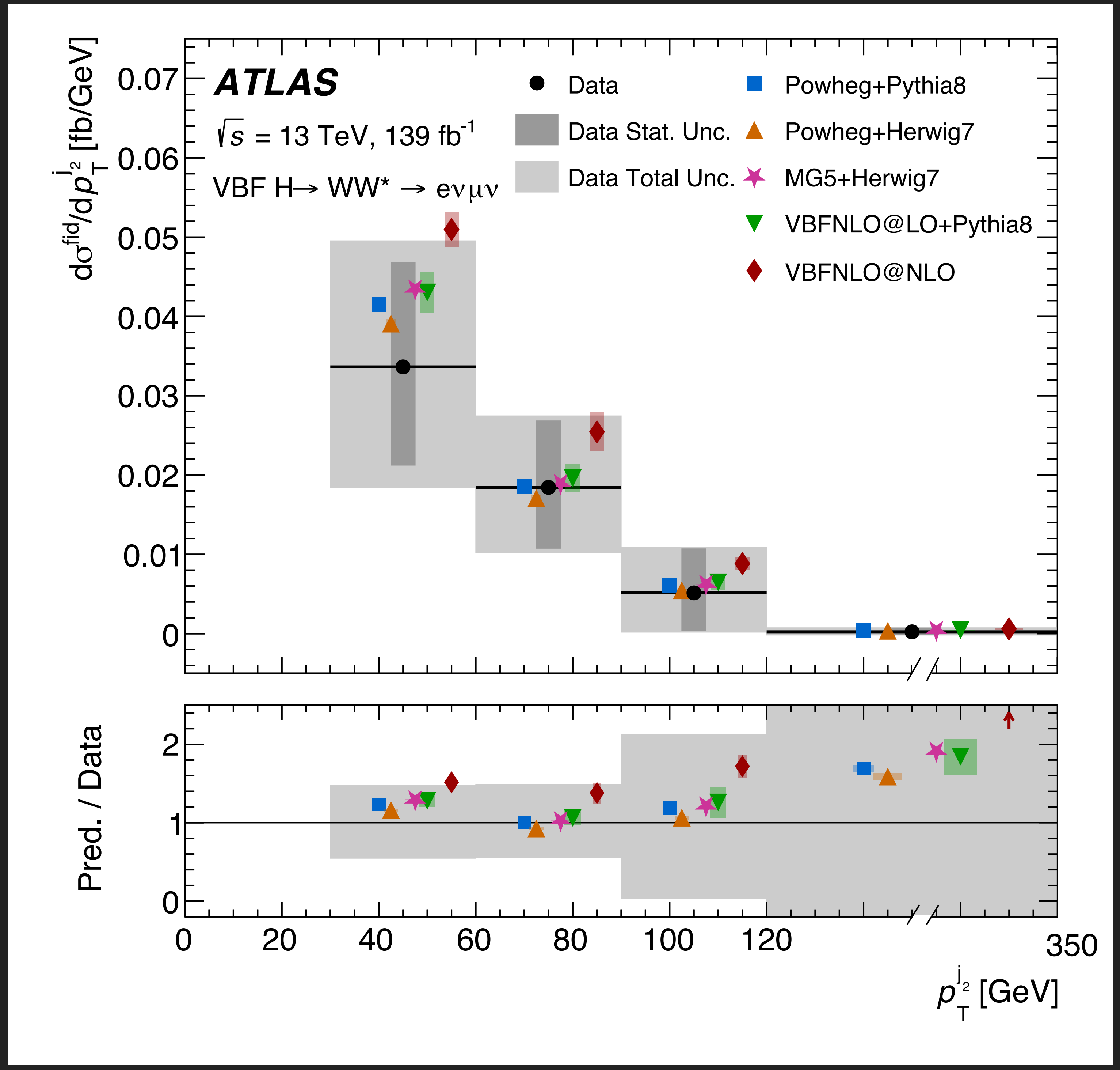

Jet Observables

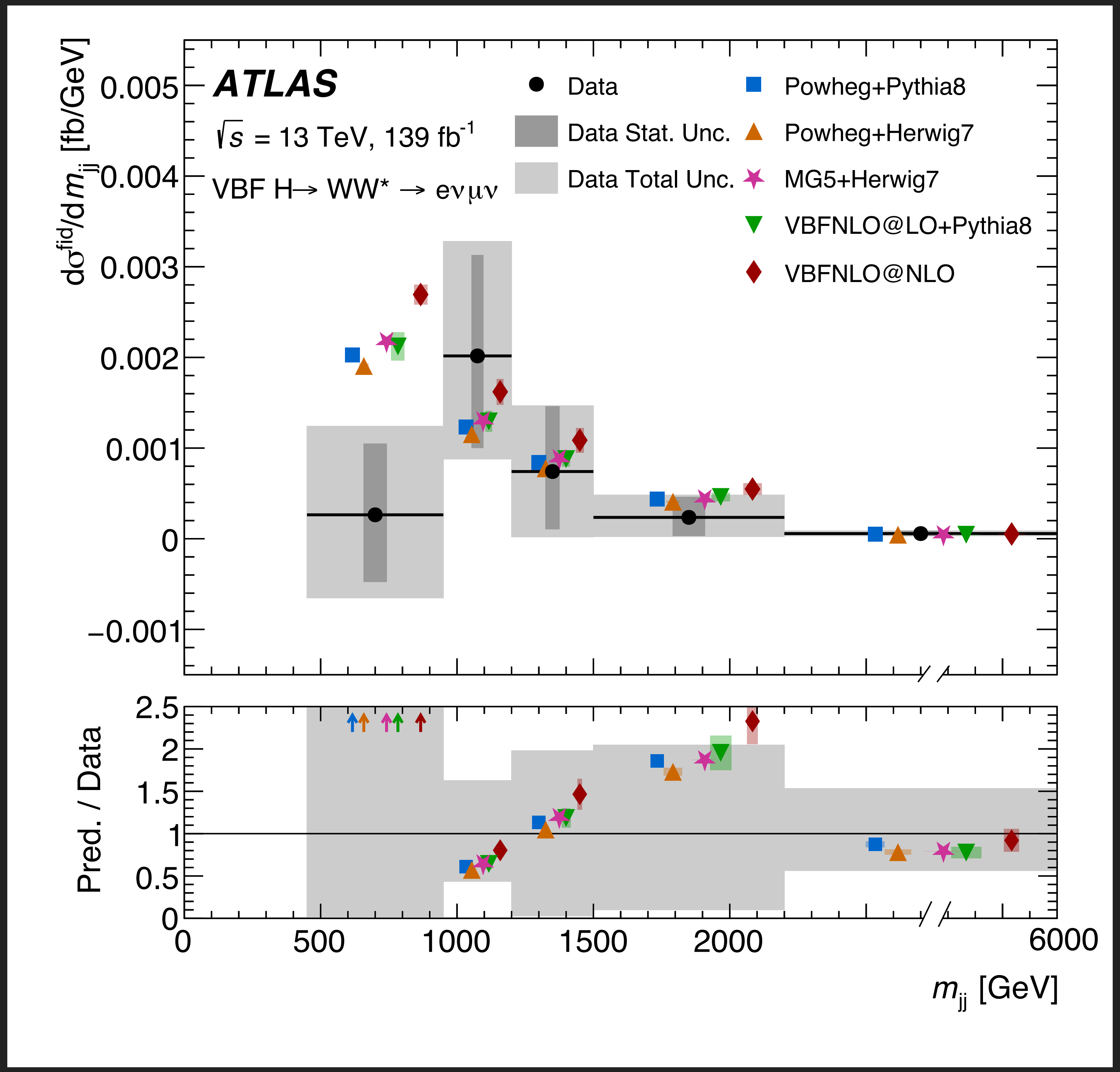

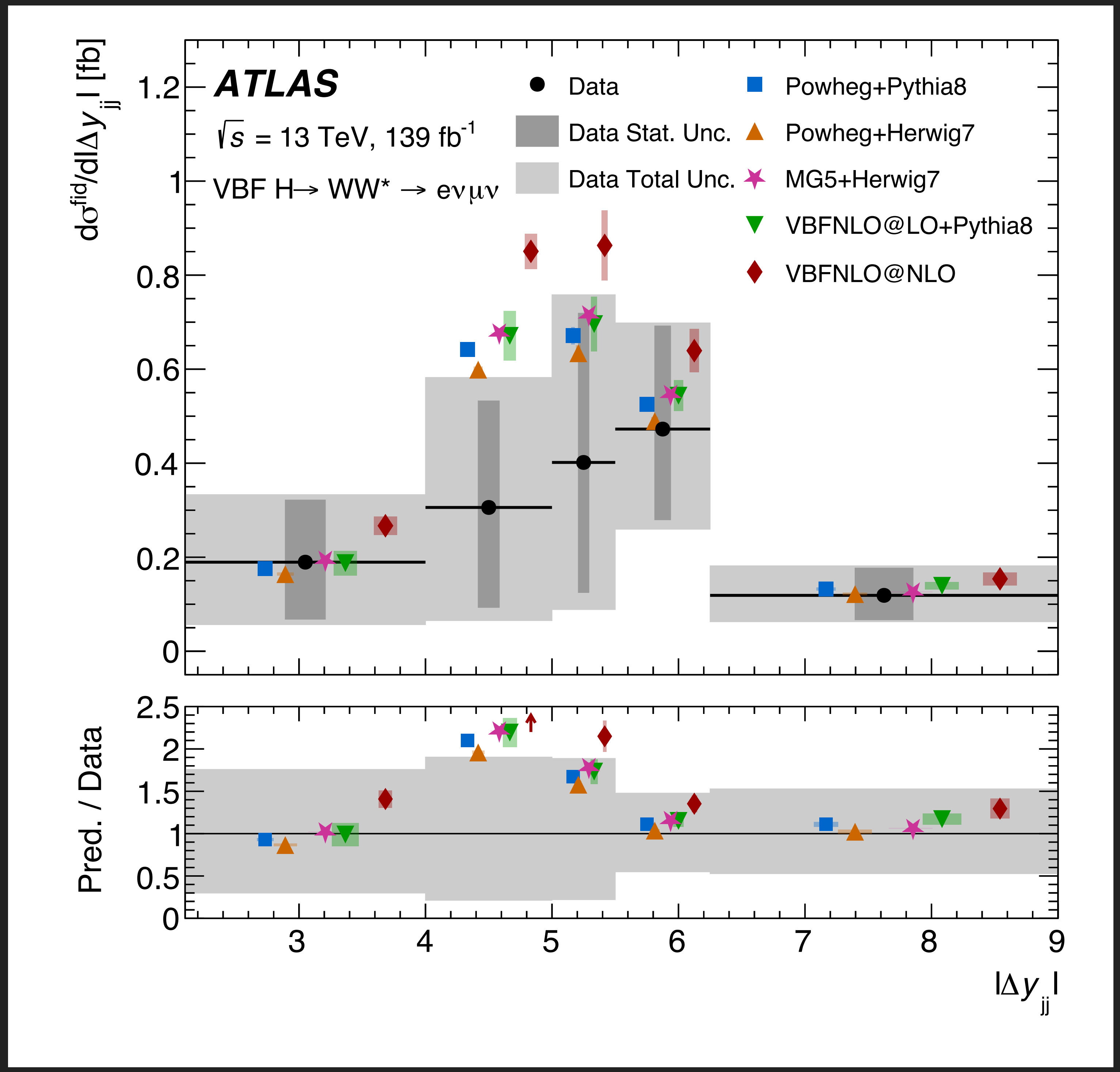

EFT Effects on $\Delta\phi_{jj}$

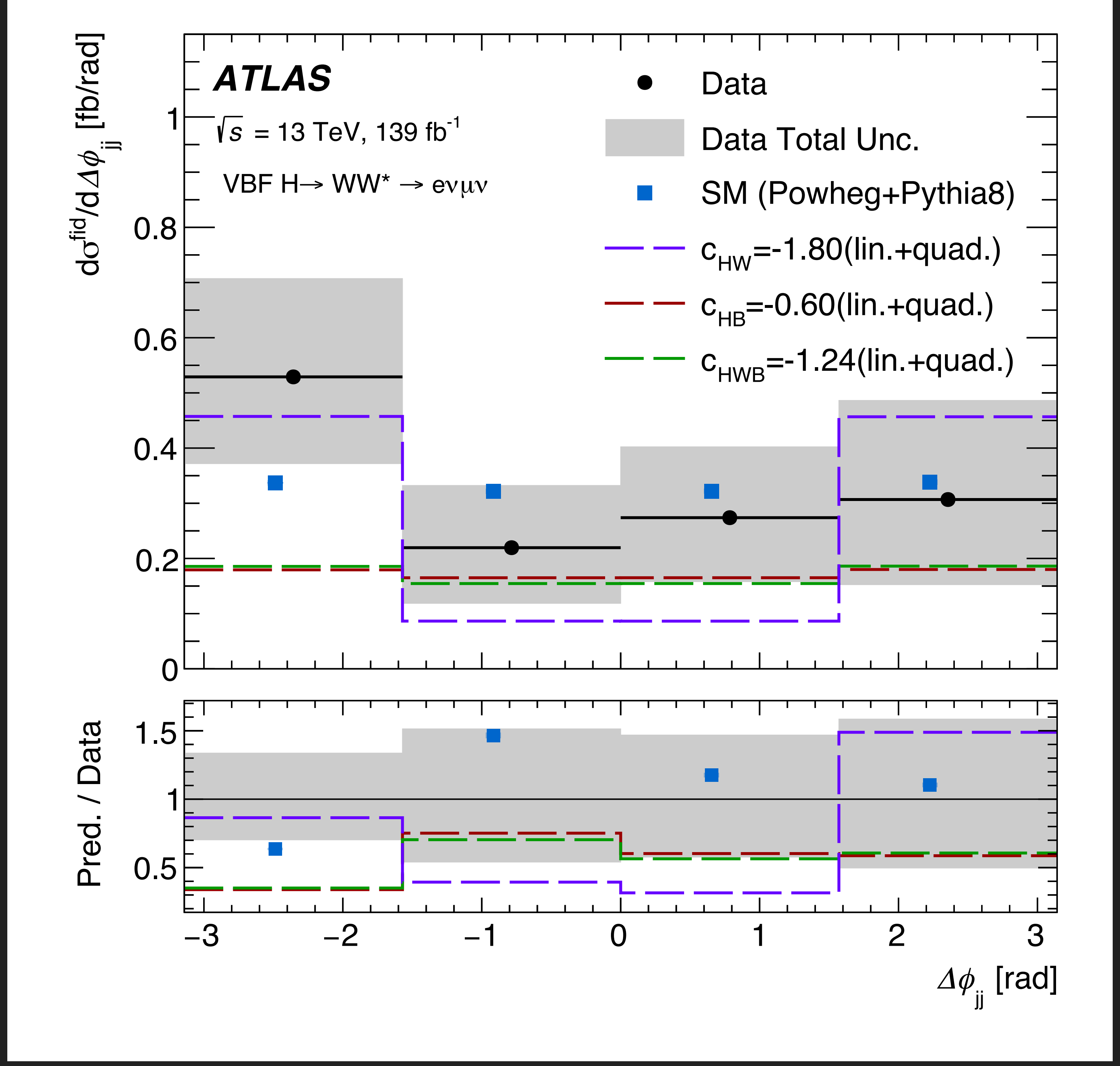

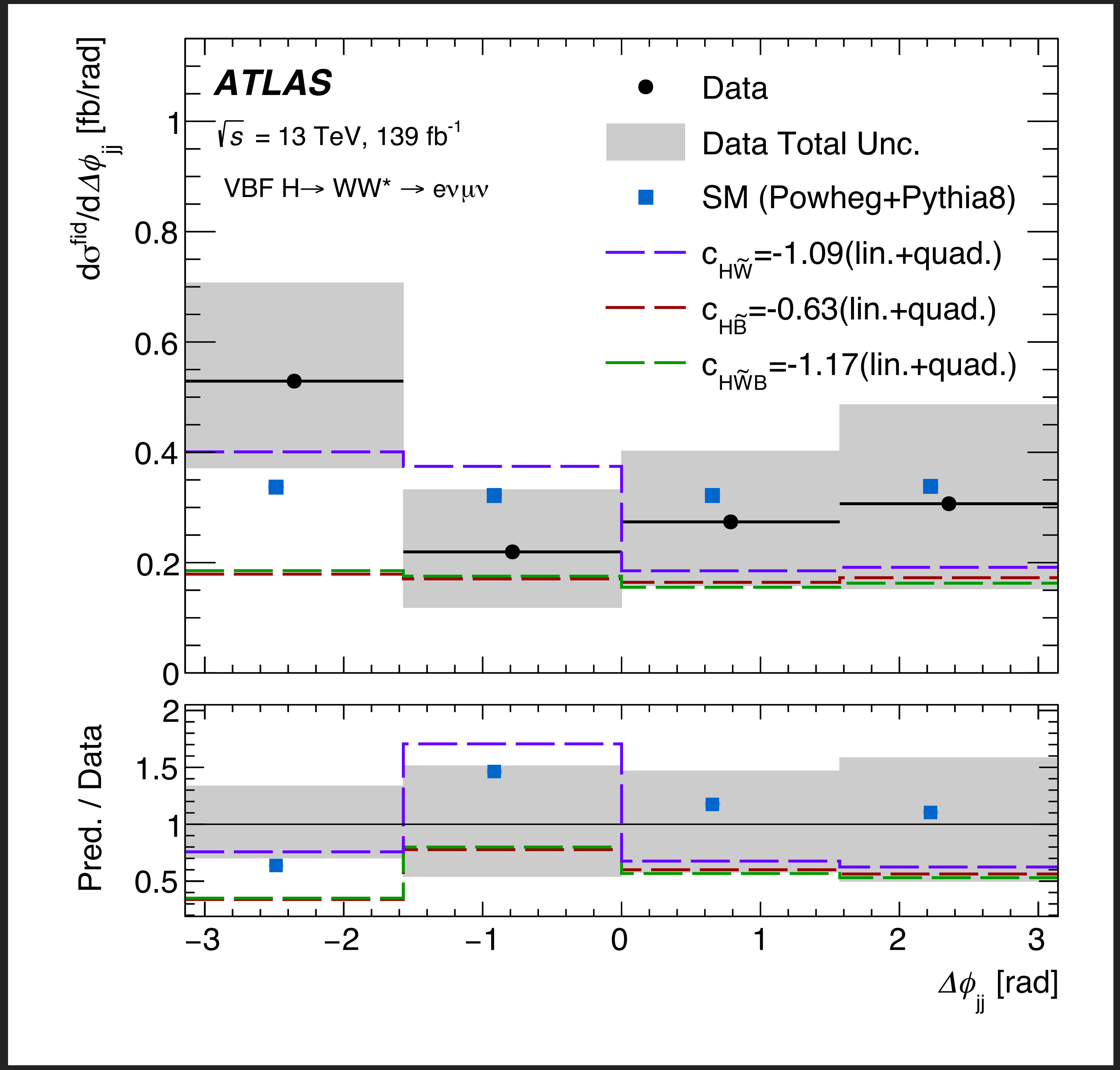

EFT Effects on leading jet p_T

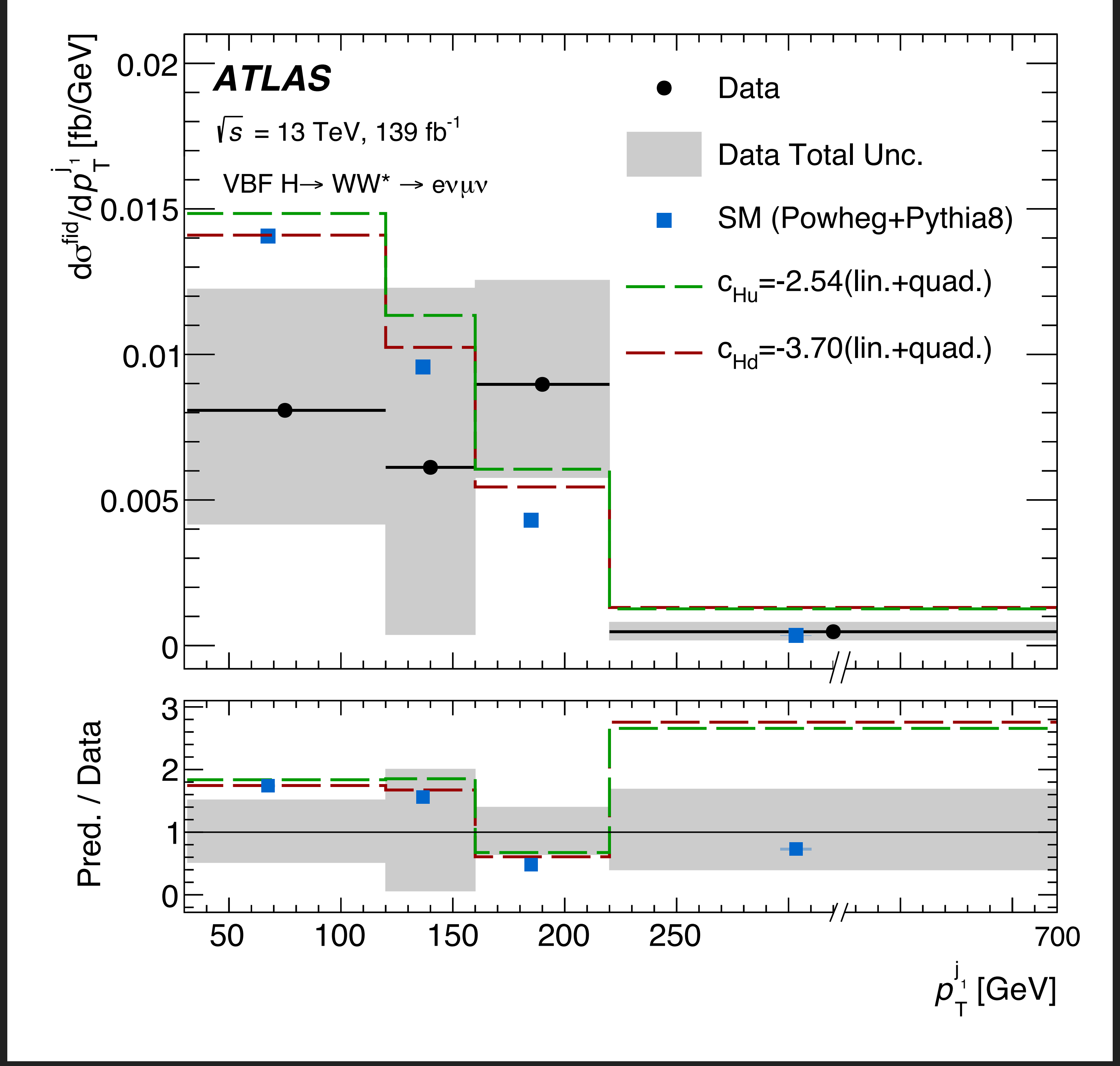

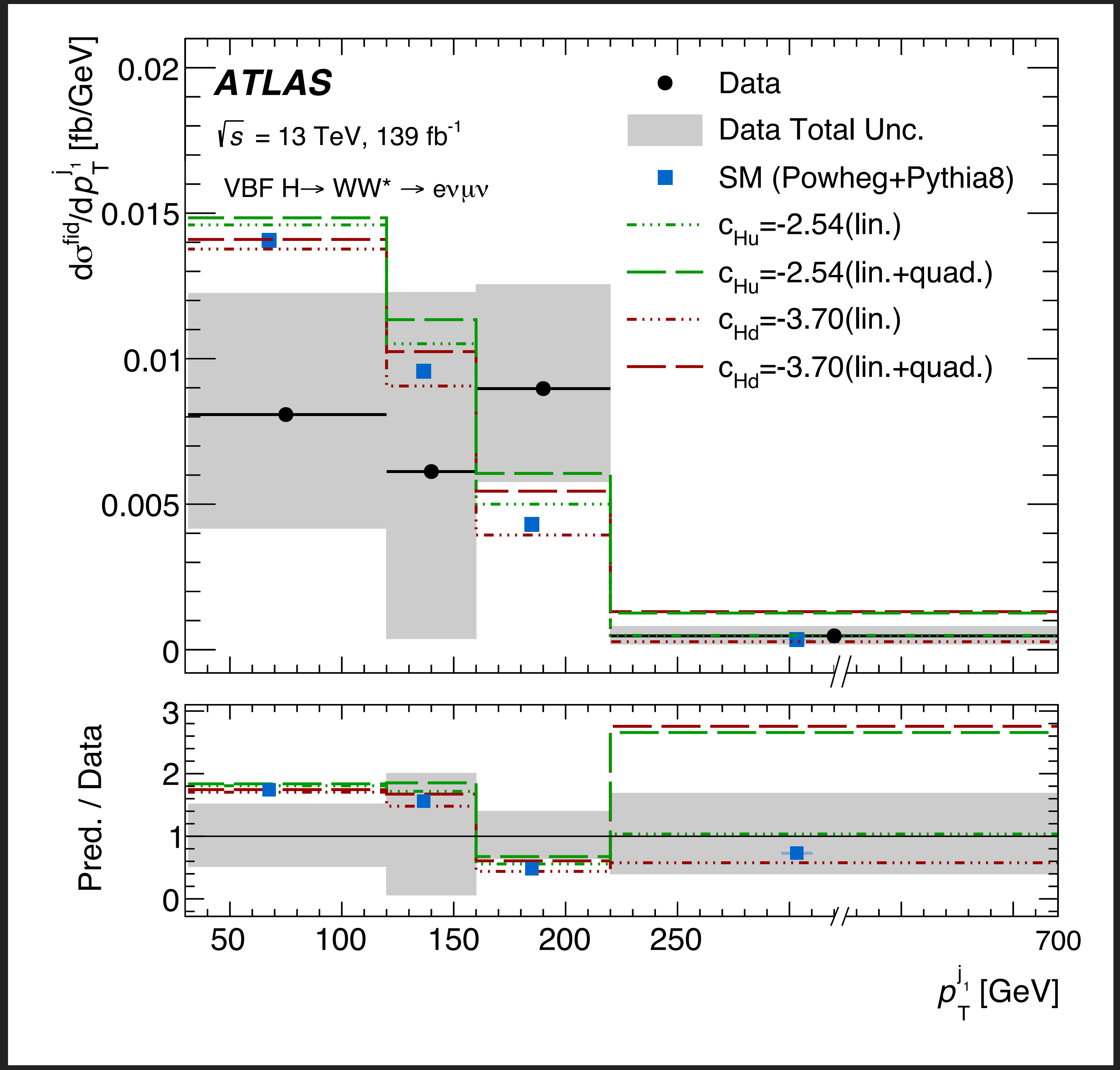

Background Normalizations